UNIVERSITY OF SOUTHAMPTON

FACULTY OF ENGINEERING AND APPLIED SCIENCE

THE EFFECTS OF WHOLE-BODY VIBRATION ON THE PERCEPTION OF THE HELMET-MOUNTED DISPLAY

VOLUME I

by

Thomas Adrian Furness III

A thesis presented for the degree of
Doctor of Philosophy, 1981.

To my Grandfather

Thomas Furness

UNIVERSITY OF SOUTHAMPTON

ABSTRACT

FACULTY OF ENGINEERING AND APPLIED SCIENCE

INSTITUTE OF SOUND AND VIBRATION RESEARCH

Doctor of Philosophy

THE EFFECTS OF WHOLE-BODY VIBRATION ON THE PERCEPTION OF THE HELMET-MOUNTED DISPLAY

by Thomas Adrian Furness III

The purpose of this research programme was to investigate the extent that whole-body vibration degrades the perception of the helmet-mounted display, and to determine the causes of this degradation and develop methods for correcting or improving perception during vibration. Initially, the areas of visual perception, display design, aircraft vibration, and biodynamics were reviewed in the published literature. Vibration and display factors were identified which were relevant to the perception of helmet-mounted displays in a vibration environment. An experimental program consisting of 17 experiments was then conducted to address the specific effects of these factors. Character legibility experiments measured the effects of seat vibration frequency and level, display format, character size, background luminance, and contrast on reading performance. Biodynamic studies measured the movements of the head, helmet, and helmet-mounted display as a function of the vertical Z axis vibration of the seat. Movements of the eye relative to the display were determined using a subjective measurement technique. Field trials in a Sea King helicopter extended and verified the results of the laboratory experiments. Additional experiments were conducted to assess the effects of vibration on the perception of simulated sensor imagery, and the evaluation of a simple image stabilization system.

The main results of the legibility experiments showed that whole-body vibration caused remarkable decreases in display perception. The magnitude and nature of the degradation were functions of the vibration frequency and level and the display conditions under which the visual materials were presented. There were wide variations in the absolute performance of subjects; but generally, vertical sinusoidal vibration of the seat between 4.0 Hz and 5.6 Hz produced the greatest decrements in perception. The biodynamic experiments showed that the vertical motion of the seat induced rotational motions of the head and helmet primarily in the pitch axis. At some frequencies, there were also large motions of the helmet on the head. The rotational motions of the helmet and head also produced displacements of the helmet-mounted display image on the retina causing perception to degrade.

Character reading performance was improved by increasing character size and manipulating background luminances and character-to-background contrasts. Improvements to imagery presentations during vibration were provided by the simple image stabilization system. The overall results of the experimental program were used to establish guidelines for improving the utility of the helmet-mounted display in various flight environments. Areas for additional research were also recommended.

ACKNOWLEDGEMENTS

I would like to thank Dr. M. J. Griffin for the friendly encouragement and direction that he has provided to me during this journey. In addition, I would also like to thank Dr. C. H. Lewis for the inspiration and helping-hand that he has given me and for preparing the way for much of my research by the tools he developed. I am thankful for the friendly and productive working atmosphere of the Human Factors Unit and the Institute of Sound and Vibration Research and for my colleagues who helped me immensely. And, I wish to thank the 16 subjects who gave many hours of their time in performing difficult experimental tasks.

I am grateful to my supervisor, Mr. Charles Bates, Jr., Director of the Human Engineering Division of the USAF Aerospace Medical Research Laboratory for providing this opportunity and for enduring my long absences from duty as I completed this thesis. I wish to thank also Mr. Wayne Martin, my colleague and dear friend, who worked my job in addition to his own during the periods of my absence.

I wish to express my appreciation to my friend Dr. E. Byron Davies of the Royal Aircraft Establishment for his support and constructive criticism of my research and to Dr. John Barrett who graciously provided test equipment and arranged for the flight trials.

I am grateful to Ms. Sharon Seitz, Ms. Susan Poynter, and Mrs. Harriet Stellini for preparing the typed thesis, having worked long hours reading almost illegible manuscripts and for their patience when changes were made. I also would like to thank Dr. Herschel C. Self who graciously consented to critique this document.

Finally, I would like to thank my family, my wife, Linda, and my daughters, Kim and Cindy, for their love, encouragement, and sacrifice over the past four years.

TABLE OF CONTENTS

TABLE OF CONTENTS (continued)

TABLE OF CONTENTS (continued)

TABLE OF CONTENTS (continued)

TABLE OF CONTENTS (continued)

TABLE OF CONTENTS (continued)

TABLE OF CONTENTS (continued)

TABLE OF CONTENTS (continued)

TABLE OF CONTENTS (continued)

Chapter 1
INTRODUCTION

1.1 GENERAL INTRODUCTION

Crews of modern military aircraft perform many complex control and information processing tasks by interacting with a myriad of cockpit controls and displays. For example, a pilot or aircrew member may be required to attend to displayed information from flight systems (e.g., engine/fuel status, attitude, altitude, airspeed, etc.), as well as navigation, communications, threat warning, and sensor systems (such as radar and low-light-level television). Simultaneously, he must make control inputs to direct aircraft weapon systems to accomplish a specific weapon delivery mission. The aircrew must accomplish many of these tasks while rapidly alternating eye direction from conventional instrument displays inside the cockpit to the outside visual scene. Often these tasks must also be performed under high vibration, acceleration, and in some cases, hazardous flying environments. Some automation of these functions has been made by incorporating digital computers into avionics and flight control systems, but these systems have increased the quantity of information and number of control options which are available to the aircrew. Often a consequence of automation has been, therefore, an increase rather than a decrease in task difficulty.

Problems such as these in modern aircraft and their crewstations have stimulated research and development for improving the methods of coupling the visual functions of the crew to cockpit controls and displays. Since 1960, the military services and aerospace industry have investigated head-coupled display techniques as a possible means of enhancing the visual interfaces of the aircrew to various aircraft systems (e.g., Hall and Miller, 1960; Fedderson, 1962; Upton, 1962; Hall and Miller, 1963; Furness, 1969; Birt and Furness, 1974; Furness, 1978).

1.2 HEAD-COUPLED DISPLAY CONCEPT

The function of the head-coupled display is to introduce into the visual pathway of an observer's eye (or eyes) information which has been generated and projected using image sources and optical devices attached to the head. For example, pictorial imagery and/or symbolic information received from aircraft systems can be represented on the phosphor screen of a miniature high-resolution cathode-ray tube (CRT). In this case, the spatial distribution of luminances from the CRT is magnified and collimated by optical elements and projected into the eye of the operator via a partially-reflective optical combiner. As a result, the operator perceives an infinity-collimated and magnified virtual image of the CRT scene. The visual angle subtended by the virtual image is a function of magnification of the head-mounted optics and is, therefore, limited practically by the physical dimensions of the optics and the resolution (size of spatial detail) of the image source (e.g., miniature cathode-ray tube).

In most of the applications of the head-coupled display in fighter aircraft, the image source and optical components are affixed to a flight helmet worn by the aircrew. These systems are termed "helmet-mounted displays."

1.3 ADVANTAGES OF THE HELMET-MOUNTED DISPLAY

The primary advantages of the helmet-mounted display are the following:

1. The helmet-mounted display provides an information display medium which can be viewed continuously, regardless of head position (i.e., the crewmember does not have to shift his head or eyes into the cockpit to see flight instruments or other displays).

2. If desired, the display image can be seen as an overlay on the real world.

3. Computer generated symbols and images from sensors, such as a television camera, can be viewed simultaneously.

4. Since the optics in the helmet-mounted display form a virtual image of the CRT faceplate (or other image source), the subtended visual angle of the resulting image is greater than that which can be achieved with most panel-mounted displays or cockpit-mounted virtual image (head-up) displays. This aspect of the helmet-mounted display is ideal for the display of sensor imagery (which is typically limited by the small image scale when represented on conventional cockpit panel-mounted displays).

5. The helmet-mounted display occupies little panel space in the cockpit making it ideal for incorporation into existing fighter and rotary wing aircraft.

6. The helmet-mounted display can be used with a head position sensing system to align sensors with head movements while viewing the sensor images on the helmet-mounted display, thereby creating a head-aimed sensor for viewing of the outside scene.

7. When used with both eyes, the helmet-mounted display offers the potential for a stereoscopic presentation of information.

Although the advantages noted above are not exhaustive, they represent the unique capabilities of the head-coupled display technology as it might apply to flight operations (Furness, 1969, 1978).

1.4 HELMET-MOUNTED DISPLAYS IN AN AIRCRAFT ENVIRONMENT

Since the early 1960s, helmet-mounted display development programs have concentrated on the development of the hardware technologies and the demonstration of promising applications (e.g., Birt and Task,

1972; Furness, 1978). In spite of the documented efforts to develop this technology, little has been reported in the literature regarding the performance of helmet-mounted displays in a dynamic motion environment. Some human factors studies have been conducted with helmet-mounted or head-coupled displays (e.g., Hall and Miller, 1960; Cohen et al., 1974; Hershberger and Guerin, 1975; Laycock, 1977), but these have been restricted to issues of image quality, display luminance, and binocular rivalry, and have been conducted within a fixed-base environment in the laboratory. The few documented flight test studies (e.g., Abbott, 1969; Jacobs et al., 1971) have been restricted to anecdotal reporting of results and contained no description of the characteristics of the aircraft environment. Although other flight tests of which the author is aware have been conducted with the helmet-mounted display, they either have not been documented or have not been reported in the open literature. Laycock (1978) has been the only investigator to report the effects of whole-body vibration on operator performance using the helmet-mounted display. The results of Laycock's experiment, coupled with those of Benson (1972), Benson and Barnes (1978), and Barnes et al. (1978) regarding the effects of whole-body angular oscillation on the perception of head-stabilized images, provide a preliminary indication that the performance of the helmet-mounted display may be severely compromised by the dynamic vibration motion environment which may be present in operational aircraft. In view of the advantages of the helmet-mounted display for improving the visual interfaces of the aircrew to aircraft systems, there is a special need to resolve those problems which may be caused by environmental factors such as vibration. This need has served as the impetus for this thesis.

1.5 PURPOSE AND ORGANIZATION OF THESIS

The purpose of this thesis is threefold:

1. To investigate the nature and extent of the effects of whole-body vibration on the perception of the helmet-mounted display;

2. To research and identify the mechanisms causing degraded performance;

3. To develop methods for correcting or reducing the deleterious effects of vibration.

The thesis is organized into two volumes comprised of nine chapters, a list of references, and appendices.

A brief description of the contents of the thesis is given below:

Volume I

Chapter 1 - General introduction to thesis and background of the problem.

Chapter 2 - Review of the literature in the areas of visual perception, visual display design, vibration, and biodynamics with the intent of identifying those factors and their interactions which may be relevant to the perception of helmet-mounted displays in an aircraft vibration environment.

Chapter 3 - Introduction to program of experimentation, including description of the apparatus, subjects, experimental methods, and data analysis techniques used in the research.

Chapter 4 - Reports of four experiments to determine the effects of vibration conditions and display characteristics on helmet-mounted display reading performance.

Volume II

Chapter 5 - Reports of eight experiments investigating the dynamic response of the head, helmet, and helmet-mounted display to whole-body vibration inputs.

Chapter 6 - Discussion of the relationships of the reading performance data (Chapter 4) to the dynamic response of the helmet and head (Chapter 5) during whole-body vibration. Reports of additional experiments to measure the movement of the helmet-mounted display image on the retina of the eye.

Chapter 7 - Report of in-flight investigations of helmet-mounted display reading performance and operator dynamic response in a helicopter. Verification of laboratory results from Chapters 4, 5, and 6.

Chapter 8 - Discussion of methods for stabilizing the helmet-mounted display image. Report of experiment to assess the effects of vibration on the perception of pictorial imagery in a target identification task and to evaluate an image stabilization technique.

Chapter 9 - Summary of major findings of experimental program and implications for the flight application of the helmet-mounted display. Recommendations for further experimentation.

References - List of references cited in the chapters and appendices.

Appendices - Special sections on data analysis, equipment description, calibration, and ancillary data, as referenced in the chapters above.

Chapter 2
BACKGROUND AND REVIEW OF THE LITERATURE

2.1 INTRODUCTION

The purpose of this chapter is to review the literature from the standpoint of identifying those factors of visual perception, visual display design, vibration and biodynamics, and their interactions which are relevant to the perception of the helmet-mounted display in an aircraft vibration environment. Unfortunately, much of the empirical data regarding the research and evaluation of helmet-mounted displays does not exist in the open literature; therefore, the greater evidence of the vibration related problems associated with the perception of helmet-mounted displays cannot be cited.

In this chapter, the general topics of visual display systems and vision are introduced first, then followed with specific topics related to helmet-mounted displays and the vibration environment. Terms and relationships will be defined, where needed, to facilitate discussions of relevant literature.

2.2 GENERAL CHARACTERISTICS OF VISUAL DISPLAY SYSTEMS AND THE HELMET-MOUNTED DISPLAY

2.2.1 Introduction to Visual Display Systems

A visual display can be defined as a device or instrument for representing information to the visual sense of the observer. In aircraft, visual displays provide the crew with quantitative and/or qualitative information to operate flight control, navigation, communication, and weapon systems. Electromechanical, optical, or electronic methods can be used for presenting visual information. The most common display source is a cathode-ray tube (CRT), although recent progress has been made in the development of solid state, flat panel displays using arrays of liquid crystal, electroluminescent, and light-emitting diode material (e.g., Scalan and Carel, 1976). Within this review, only visual displays incorporating the CRT will be considered, although

most of the display-observer interactions can be generalized to other methods of display generation.

Information presented on electronic CRT displays can be coded in spatial, spectral, temporal, and luminescence/contrast dimensions. It is most relevant here to address those displays wherein the information is coded into two-dimensional spatial arrangements of luminances, as in the presentation of symbols or sensor images.

2.2.2 Methods for Viewing CRT Images

The two-dimensional image generated on the CRT can be relayed to the eye or eyes of the observer by direct viewing, or through projection optics, as illustrated in Figure 2.2.1. Using the first method, the pilot views a faceplate of the CRT directly or as a real object at its location in the instrument panel of the aircraft. In the second approach, the image source is relayed through optics which magnify, collimate, and project the CRT image via a beamsplitter/combiner which reflects the image into the eyes of the operator. The image is perceived as a virtual image of the CRT scene located at optical infinity. Since the combiner surface can be transparent, the projected image may be superimposed over objects in the real world. The most general form of the projected display is termed a "head-up" display and is commonly used for presenting flight status and weapon aiming information to the pilot of fighter aircraft. The aiming symbols projected on a head-up display permit the pilot to direct various weapons on the aircraft to targets on the outside world. Simultaneously, the presentation of flight status information helps the pilot to fly the aircraft. The helmet-mounted display is a special application of the head-up display wherein the CRT, projection optics, and combiner are incorporated into the flight helmet. Most current helmet-mounted display designs relay the image of the CRT into only one eye of the observer.

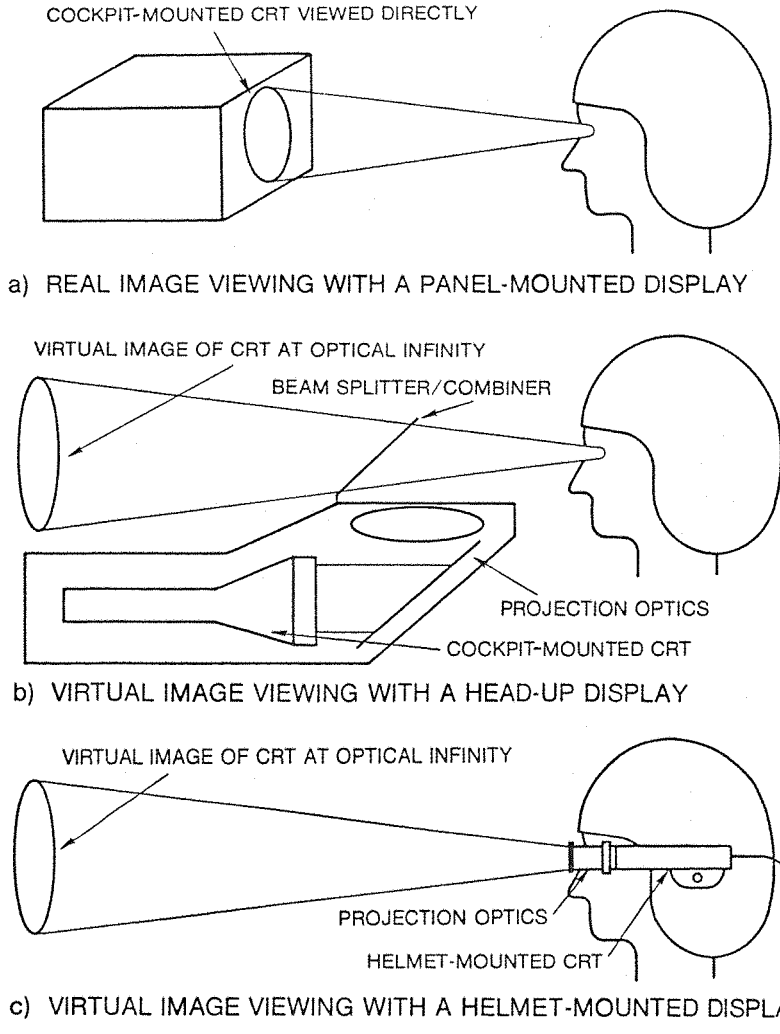

Figure 2.2.1. Typical Methods for Viewing Cathode-Ray Tube Images

2.2.3 General Description of the Helmet-Mounted Display

As shown in Figure 2.2.1, the purpose of the helmet-mounted display is to introduce information in the form of a virtual image in the visual field of the operator. The main components comprising a helmet-mounted display are: (1) a display electronics unit which generates video and deflection signals; (2) a miniature CRT which represents a two-dimensional spatial image; (3) an optics assembly which relays the CRT image into the eye; and (4) a flight helmet platform to which CRT and optical assemblies are affixed. (A detailed description of the configuration and operation of a representative helmet-mounted display is given in Appendix A.3.1.)

The factors relevant to the design of helmet-mounted displays have been discussed by Abbott (1969), Furness (1969), Strother and Upton (1971), Chisum (1975), Task et al. (1980). Self (1972) addressed the design considerations of conventional helmet-mounted display optics, while Kocian and Pratt (1972) and Pratt (1976) discussed reflective optical designs and Lichty (1974) holographic optical designs. Table 2.2.1 gives configuration and performance data of representative helmet-mounted displays which have been developed by the military services over the past 10 years. All of these design systems project a monocular image from a CRT or light emitting diode array and use the helmet as the platform for mounting the display components. Other helmet-mounted displays have been developed which use a coherent fiber optics bundle to relay the image from a CRT located elsewhere to the projection optics mounted on the helmet (e.g., Task and Hornseth, ca 1974).

The optical designs described in Table 2.2.1 use either discrete optical combiners or visor optical combiners. The apparent size of the image (i.e., the visual angle subtended by the virtual image of the CRT faceplate) is a function of the magnification of the optics. Fields-of-view of 10 to 40 degrees have been used. The optical viewing distance or collimation of the display optics has been adjustable typically from 0.5 m to optical infinity.

2.2.4 Applications of the Helmet-Mounted Display

Use of the helmet-mounted display is advantageous in many applications because of its ability to provide a continuous visual presentation of information regardless of head position. This information may consist of simple symbols, complex format of symbols, alphanumeric information, or pictorial imagery (as generated by a television or infrared imaging sensor). The ability to move the direction of the display format by head movement allows the helmet-mounted display, when used with a helmet position sensing system, to have many unique operational applications. Table 2.2.2 lists many of the applications which have been considered or evaluated for the helmet-mounted display. For this thesis, these applications are reduced to three display format/viewing

TABLE 2.2.1. CHARACTERISTICS OF CURRENT HELMET-MOUNTED DISPLAYS (MODIFIED AFTER TASK ET AL., 1980)

	Hughes Side-Mount	Honeywell IHADSS	Honeywell Mod 8	Honeywell Mod 7A	Honeywell Mod 3	Marconi Aviation Mark IV
Weight	530 gms	410 gms	400 gms	570 gms	450 gms	230 gms
Exit Pupil	15 mm	10 mm	13 x 16 mm	15 mm	--	16 mm
Eye Relief	12-18 mm	49 mm	64 mm	50 mm	12-18 mm	64 mm
FOV	30° diag.	30° x 40° (45° diag.)	20° diag.	20° diag.	40° diag.	10°
Transmission Efficiency (before combiner)	0.8	0.75	0.8 est.	0.2 est.	--	0.74
Image Source	CRT	CRT	CRT	CRT	CRT	32 x 32 LED array
Combiner Type	flat	flat	parabolic visor	parabolic visor	flat	spherical
Image Color (Phosphor)	green (P-1, P-31) white (P-4)	green (P-43)	green (P-43)	green (P-43)	green (P-1, P-43)	650 nm, red, narrow band

TABLE 2.2.2. INFLIGHT APPLICATIONS OF THE HELMET-MOUNTED DISPLAY

Application	Purpose
Helmet-Mounted Display (used alone)	
General electronic display	-Provides a substitute for a conventional panel-mounted display with the additional advantages of providing a larger subtended visual angle and image quality than most conventional panel-mounted displays--also display information can be continuously seen regardless of head position. Sensory imagery and/or flight status information can be presented.
Energy management display	-Provides continuous presentation of information to the pilot regarding aircraft potential and kinetic energy. Helpful in managing strategy during air-to-air engagements.
Visual warning display	-Provides a means for input of failure or warning information into the visual sense without having to look into the cockpit at fixed displays.
Helmet-Mounted Display (used in conjunction with a head position sensing system)	
Aiming reticle	-Presentation of a simple reticle to allow observer to align helmet to a specific direction in space, from which the helmet direction can be determined relative to a predetermined boresight using a helmet position sensing system.
Head aimed sensor operation	-Sensor field-of-view is directly aimed by helmet position while imagery from sensor is viewed on the helmet-mounted display.
Stabilized head-up display	-Symbolic information presented on the helmet-mounted display appears at a predetermined location in space or relative to the cockpit--thereby providing the same information as a wide field-of-view head-up display.
Visual cueing	-Using helmet display aiming information (or measured via the helmet position sensing system) can indicate to the crewmember where to direct his visual attention using appropriately placed symbols on the helmet-mounted display.

conditions. These are illustrated in Figure 2.2.2 and discussed below.

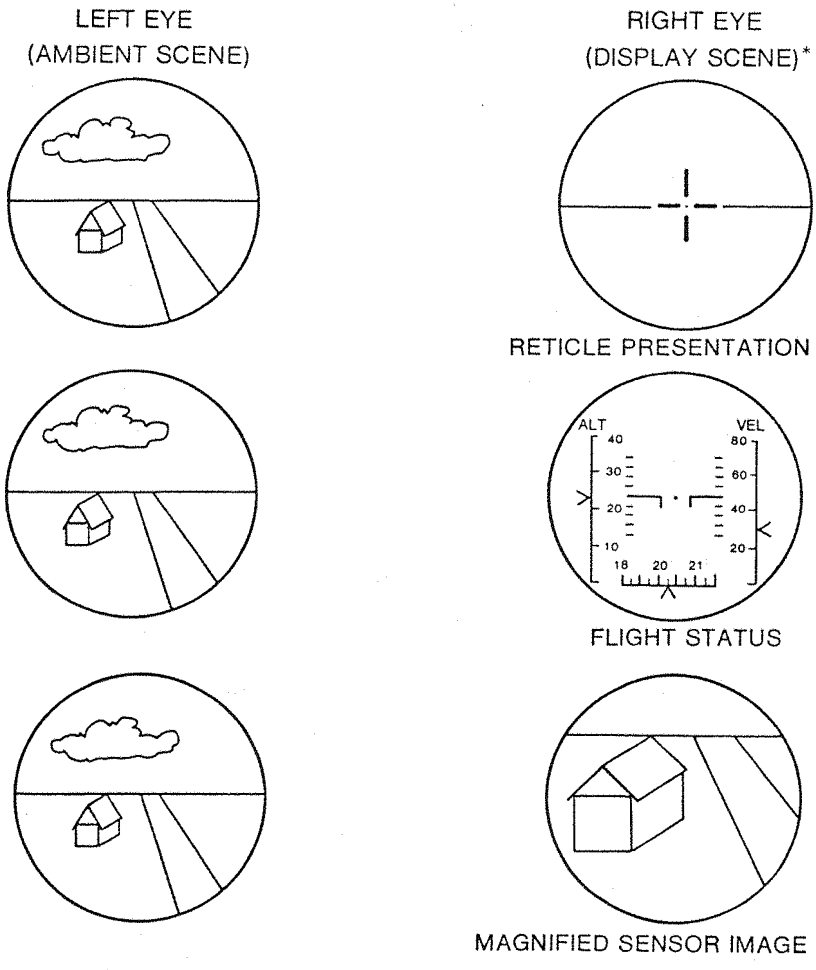

Figure 2.2.2. Representations of Left and Right Eye Visual Fields When Viewing Typical Helmet-Mounted Display Presentations Against an Ambient Background

a) Aiming Reticle. The image introduced into the visual field of the operator by the helmet-mounted display may be a simple symbol such as an aiming reticle. In this application, the task of the operator is to superimpose the symbol over a target within the outside scene. Simple status information may be presented to the operator by flashing or changing the color of the reticle or illuminating discrete status lights around the reticle.

b) Head-Up Display Format. The observer may be presented with complex information in symbolic form. This information may be similar to that viewed on a head-up display, and include weapon aiming information, aircraft system status, or flight status (e.g., altitude, airspeed, vertical velocity, heading information, etc.). Portions of the symbols may be stabilized relative to the airframe or inertial space by using a helmet position sensing system interfaced with a central computer in the aircraft. This information may also be presented so that it can be superimposed over the ambient scene.

c) Sensor Image Presentation. The presentation of information from scanning sensors (such as the low-light-level TV and forward-looking infrared systems) is another typical application envisioned for the helmet-mounted display. Again, when used with a helmet-mounted sight (helmet position sensing system), the optical axis of the sensor may be directed by head position. A scene represented on the helmet-mounted display may have unity magnification with the outside scene or have greater magnification. In this case, the operators task may be to (1) visually acquire a target in the outside scene, (2) aim a small reticle symbol in the helmet-mounted display over the target within the scene to position a separate seeker or sensor, and (3) then by viewing the sensor return on the helmet-mounted display, locate the same target therein.

2.2.5 Summary

The foregoing discussion introduced some of the properties of visual displays and, more particularly, the helmet-mounted display. The next section will review some of the factors involved in the perception of displayed information. Perceptual problems which are unique to helmet-mounted displays are then discussed in Section 2.4. At that time, the implications of helmet-mounted display design factors and applications mentioned above will be discussed in light of their perceptual implications.

2.3 PERCEPTION OF DISPLAYED INFORMATION

2.3.1 Introduction to Visual Perception

Generally, perception involves processes of receiving, selecting, acquiring, transforming, and organizing information through the senses. As shown conceptually in Figure 2.3.1, the human information processing system consists of four basic elements: (1) a sensing subsystem to receive and transduce energy from the physical surround; (2) an information processing system to organize, recognize, and compare the information with (3) stored experience (i.e., storage/memory subsystem) and, based upon some predetermined response criteria, to activate the (4) response subsystem which performs speech and other motor functions. The visual sense modality can be regarded as having optical, photosensitive transduction, conduction, and central physiological mechanisms. It is beyond the scope of this review to address in detail the physiological mechanisms associated with visual perception. Instead, it is more appropriate in this review to concentrate upon the psychological and psychophysiological processes of visual perception especially as they relate to operator performance in viewing electronic displays.

Before proceeding, some concern must be expressed about the variability of human performance research. Although each observer can be viewed as having the same basic elements for processing visual information as shown in Figure 2.3.1, there are unique individual differences due to physical abilities, intellectual capacity, training, and experience of each observer. Psychophysical experimental methods and statistical treatment of data allow "trends" in the intersubject behaviour to be determined, but these data must be interpreted cautiously when applied to a single subject. As one may be reminded: "A statistician can drown in a lake which has a mean depth of 2 inches."

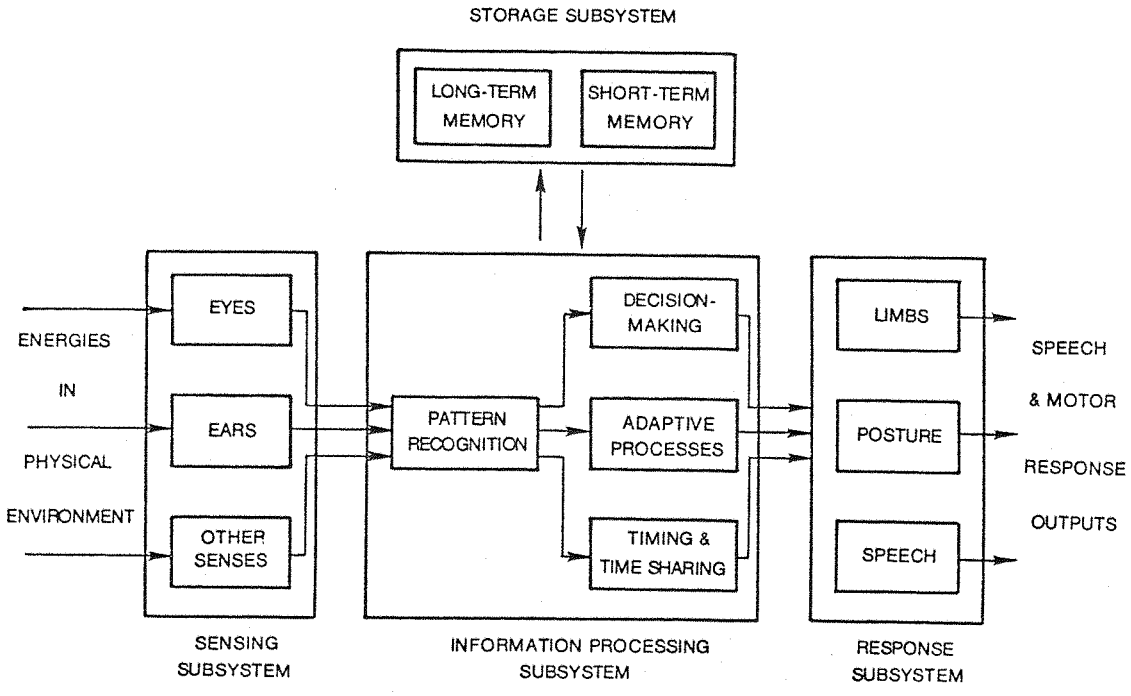

Figure 2.3.1. The Human Information Processing System (after Van Cott and Warrick, 1972)

2.3.2 Sensory Processes

2.3.2.1 Spectral Sensitivity of the Eye

When the line of sight or optical axis of the eye is directed at a CRT display presentation, the light emitted by the phosphor is impressed upon the retina through the optics of the eye, from thence to be conducted and processed at the central level. The stimulation of the photoreceptors (i.e., rods and cones) is a function of the intensity of the light and its spectral characteristics. Figure 2.3.2 shows the spectral sensitivity of the receptors in the retina. The sensitivity to radiated energy is greatest at approximately 550 nm for the cone receptors and approximately 500 nm for the rod receptors. The rods

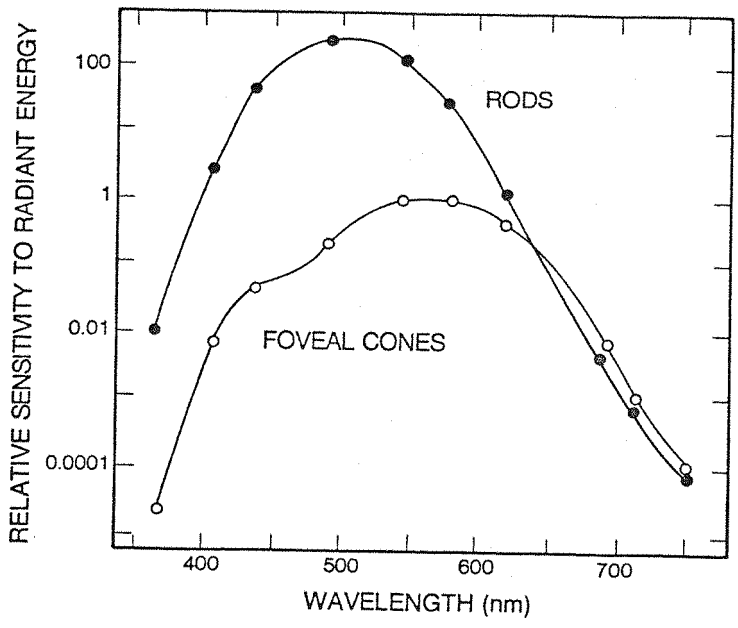

Figure 2.3.2. Spectral Sensitivity of the Retinal Receptors (from Wald, 1945; after Farrell and Booth, 1975)

exhibit about 100 times as much sensitivity to light as the cones. The standard CIE[1] luminosity function was derived from the spectral sensitivity of the eye to describe the contribution of the different parts of the spectrum to the sensation of brightness. Figure 2.3.3 shows the luminosity function defined for the standard observer with the expected range of variation across the subject population.

[1]CIE = Commission Internationale d'Eclairage

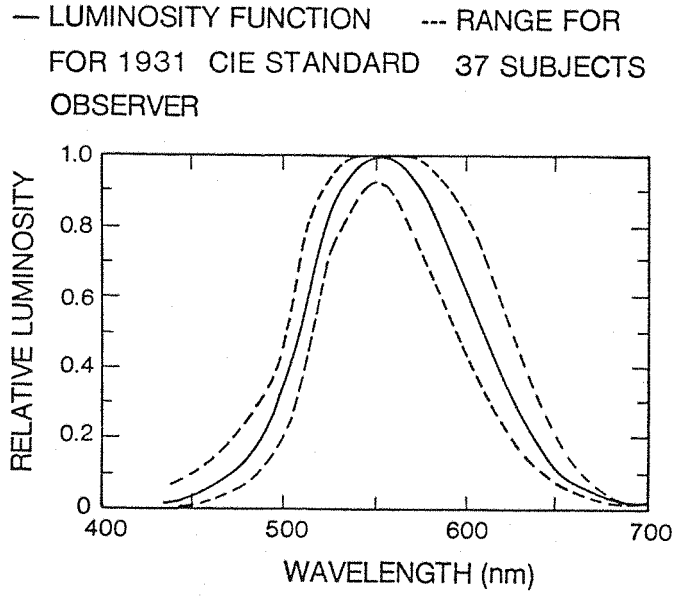

Figure 2.3.3. Relative Contribution of Different Wavelengths to Luminance--The Luminosity Function (from Gibson and Tyndall, 1923; Wyszeck and Stiles, 1967; after Farrell and Booth, 1975)

2.3.2.2 Retinal Illuminance

The passage of light into the eye is controlled by the size of the entrance pupil which is adjusted by circular and radial muscles in the iris. As shown in Figure 2.3.4, the diameter of the pupil is a function of the luminance of the visual field including the display scene. For typical display luminances of 1 to 100 cd/m^2, the mean effective pupil diameter for cone vision, corrected for the Stiles-Crawford

effect[1] is approximately 3 to 5 mm (Farrell and Booth, 1975). The time required to change the exit pupil diameter due to luminance changes is approximately 3 s from dark to light and 9 s from light to dark (Farrell and Booth, 1975).

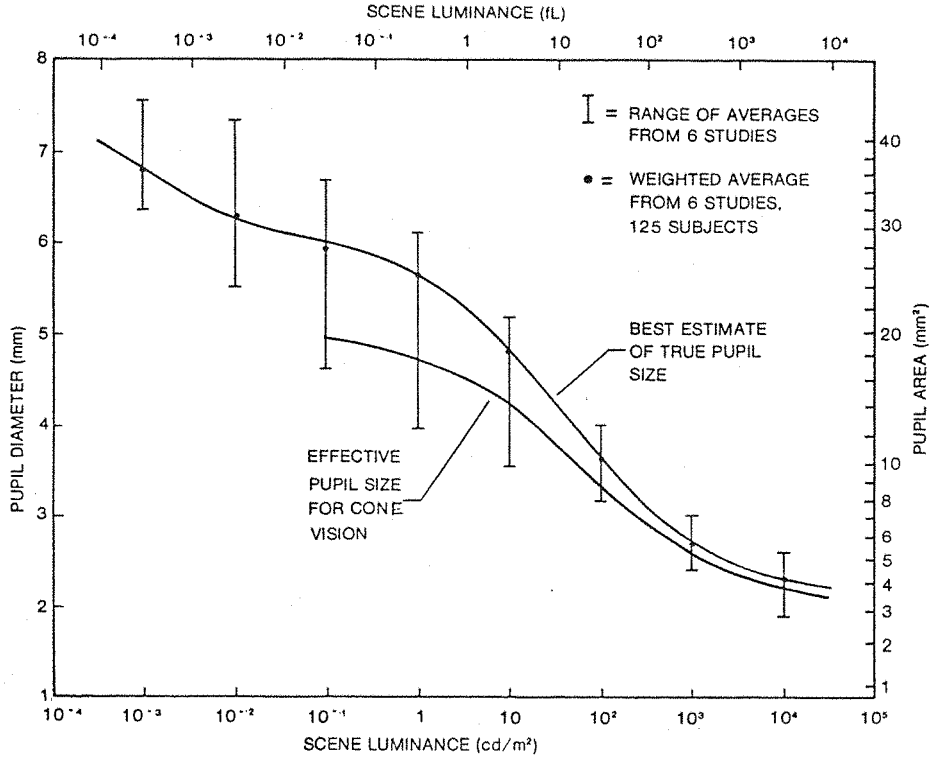

Figure 2.3.4. Eye Pupil Size as a Function of Scene Luminance (after Farrell and Booth, 1975)

[1]Stiles-Crawford effect (Stiles and Crawford, 1933) provides an adjustment to the effective pupil diameter resulting from the relative contribution of light entering various parts of the pupil, thereby evoking different sensations of brightness. The effective pupil diameter is given by the effectivity ratio (ER) where:

$$ER = 1 - 0.0106\ d^2 + 0.0000419\ d^4$$

where d = true pupil diameter in mm. The effectivity ratio accounts for the property that light coming through the center of the pupil is more "effective" than light entering off axis.

The decrease in the sensitivity in the eye, as described by the Stiles-Crawford effect, occurs in the cones and not in the rods.

The quantity of light entering the eye via the pupil is termed retinal illuminance and is expressed in Trolands (Td) according to the expression below:

$$\text{retinal illuminance (Td)} = \text{pupil area (mm}^2\text{)} \times \text{scene luminance (cd/m}^2\text{)} \times \text{effectivity ratio (ER).}$$

2.3.2.3 Photochemical Adaptation

In addition to the pupillary adaptation process described above, the retina in the eye exhibits a remarkable facility for adapting photochemically to the average illuminance. This function provides a gain adjustment of the receptors and extends the dynamic range of luminances over which the eye is sensitive. Generally, the range of luminances to which the receptors are sensitive can be described in three regions (Farrell and Booth, 1975):

Photopic - luminance > 10 cd/m^2
(cone vision with some contribution of rods in the periphery)

Mesopic - luminance of 10^{-3} to 10 cd/m^2
(vision with rods and cones)

Scotopic - luminance $< 10^{-3}$ cd/m^2
(vision with rods only)

The instantaneous sensitivity of the eye to light is, therefore, a function of the state of photochemical adaptation. The degree to which the eye is light- or dark-adapted has been shown in the literature to be a function of: the intensity, spectral characteristics, and duration of the exposure to the preadaptation luminance; the size, shape, contrast of object viewed; the foveal area being stimulated; and individual differences amongst observers (Semple et al., 1971). As shown in Figure 2.3.5, the instantaneous threshold of light sensation is a function of preadaptation luminance and time. Figure 2.3.6

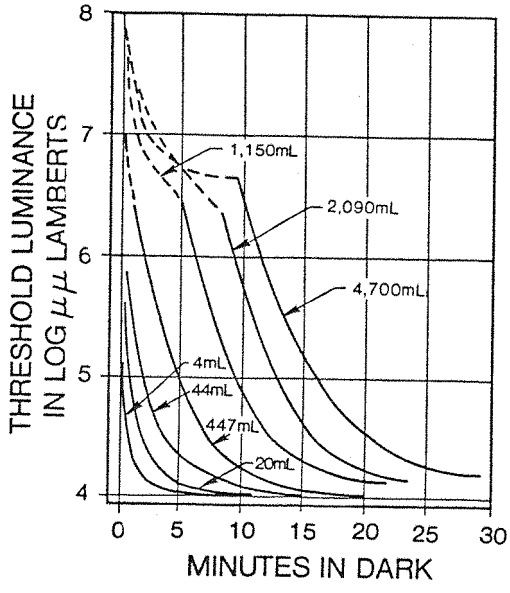

mL × 3.183 = cd/m^2

Figure 2.3.5. Threshold Luminance as a Function of Preadapting Luminance (from Haig, 1941; after Semple et al., 1971)

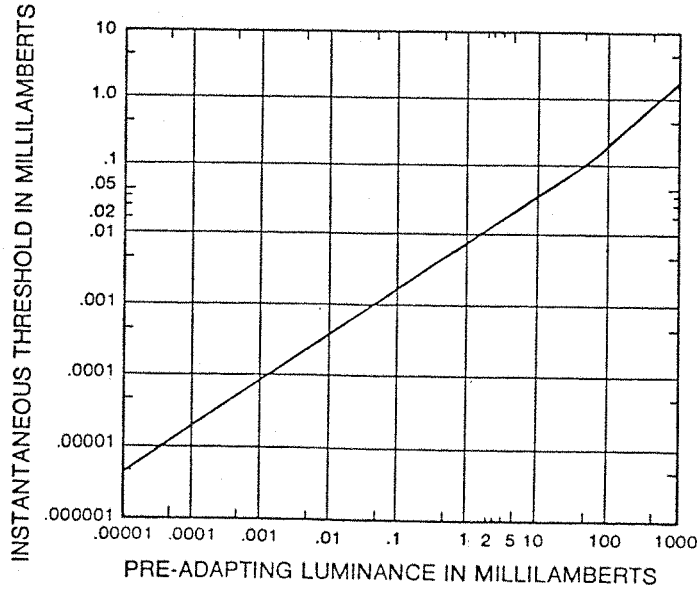

mL × 3.183 = cd/m^2

Figure 2.3.6. Instantaneous Threshold as a Function of Preadapting Luminance Level (from Nutting, 1916; after Semple et al., 1971)

shows the linearity between the logarithm of the threshold sensation of light and the logarithm of the adapting luminance across a wide range of luminances. It follows that threshold is an exponential function of preadapting luminance. Typically, the time to light adapt is less than the time to dark adapt. Semple et al. (1971) stated that, for practical purposes (in the photopic region), exposure to light for approximately 2.5 minutes will create a steady-state adaptation to that level.

2.3.2.4 Sensitivity to Contrast

Contrast is a term used to describe the relationship between areas within a visual field which have different luminance levels. Luminance contrast (C) is usually expressed as the difference of the higher (L_h) and lower luminance levels (L_ℓ) divided by the lower luminance level or:

$$C = \frac{L_h - L_\ell}{L_\ell} \times 100 \text{ percent}$$

The thresholds of perception for differences in luminances (contrast) also vary with the average luminance of the adapting field. This relationship has been expressed in the form of Weber's fraction (1834) (i.e., $\frac{\Delta L}{L}$ is related to log L) as shown in Figure 2.3.7. The region over which the Weber's law holds (i.e., where $\frac{\Delta L}{L}$ = constant) is confined to the region between 0.32 to 3200 cd/m^2, which is also the range of luminances normally observed in CRT displays.

2.3.2.5 Temporal Stimulation

It has been shown that visual sensation resulting from a light stimulus may continue briefly even after the stimulus has been removed. This behaviour and that of temporal summation (i.e., increasing duration of subthreshold stimulus to obtain sensation), indicate that stimulation of the retina causing sensation may result from the integration of light quanta. The temporal properties of vision are vital to the perception of CRT displays due to the intermittent nature of

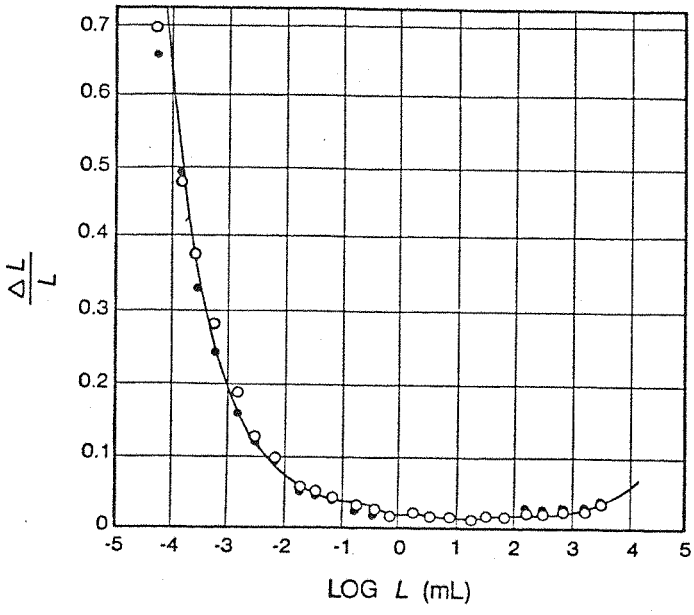

mL × 3.183 = cd/m^2

Figure 2.3.7. Relation Between ΔL/L and Log L (from König and Brodhun, 1889; after Hecht, 1934; after Brown and Mueller, 1965)

the display generation. The temporal properties of the human visual system have been discussed in detail by Brown (1965), Cornsweet (1970), and Semple et al. (1971) and shown to be effected by adaptation state, spatial characteristics of the stimulus, and temporal properties of the stimulus. With caution, Semple et al. (1971) indicated that as a general rule, visual persistence will be about 0.1 s for visual displays not operating in high ambient light environments (i.e., less than 15×10^3 cd/m^2). This temporal behaviour was manifested in results reported by Kelly (1961) and shown in Figure 2.3.8. Kelly used a uniformly illuminated disc which subtended approximately 60 degrees in visual angle and whose intensity varied sinusoidally in time. The independent variables in his experiment were frequency, levels of intensity modulation, and adaptation level. The curves show that for average display luminances between 3.0 and 350 cd/m^2 corresponding to retinal illuminances of 77 to 2300 Td, the critical frequencies wherein flicker of the stimulus would not be observed was between 2 Hz and 50 Hz, respectively, for modulations greater than 20 percent. It follows that a CRT display operating under the conditions above would be seen to flicker or flash to the observer if the interfield luminance (due to phosphor persistence) falls below 80 percent. The critical flicker frequency (CFF) is related to luminance by the Ferry-Porter law for modulations of 10 to 100 percent (Brown, 1965). The law states that the retinal persistence or $\frac{1}{CFF}$ varies inversely with the logarithm of the stimulus luminance (L); therefore,

$$CFF = a \log L + b$$

where a and b are constants.

A similar expression was developed by Granit and Harper (1930), as cited by Brown (1965), describing the approximate relationship between critical flicker frequency (CFF) and the stimulus area (A):

$$CFF = c \text{ Log } A + d$$

where c and d are constants.

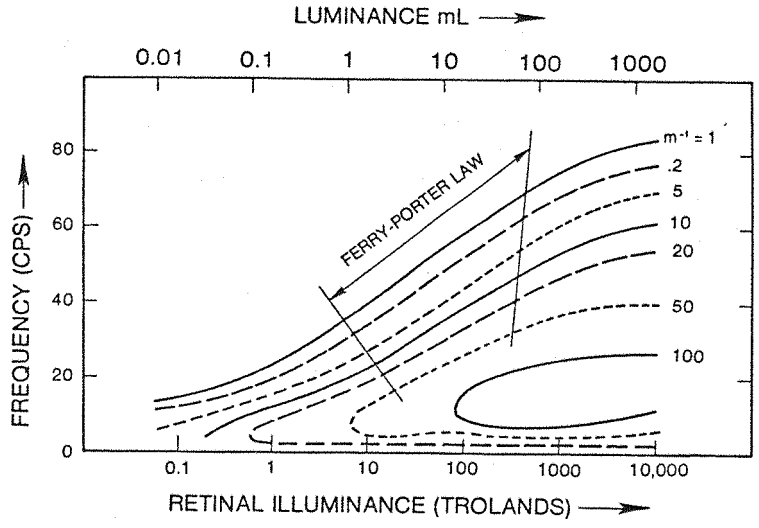

Figure 2.3.8. Flicker Fusion Frequency as a Function of Retinal Illuminance for Each of Seven Amplitudes of Sinusoidal Modulation of a White-Light Stimulus (from Kelly, 1961; after Brown, 1965)

This equation implies that a critical flicker frequency is related to the number of receptors stimulated.

2.3.2.6 Definition of Visual Acuity

Thus far, discussion of the sensory aspects of visual perception has concentrated upon the sensation of light and sensitivity to the intensity, spectral, and temporal properties of the light stimulus. The sensory aspects of vision relative to the perception of the spatial content of stimulus is also very complex. The basic quantity relating the fidelity of spatial vision is visual acuity. Acuity is a measure of how well the eye can resolve spatial detail in the visual scene. The most common measure for visual acuity relevant to a visual display is "minimum-separable acuity." This measure describes the smallest feature or smallest space between the parts of a target that can be detected by the eye, and is expressed as the reciprocal of the size of the smallest resolution element (McCormick, 1976). The Snellen letter test is a commonly used measure of visual acuity in clinical practice. Basically, the Snellen test is a character legibility test (Overington, 1976). Subjects are required to read a specially prepared chart

consisting of rows of high contrast block letters against a white background. The sizes of the letters decrease in each row. The subject reads the chart from a specified viewing distance (usually 6 meters or 20 feet) until an error is made. The acuity of the subject is then determined by the smallest size of the characters before errors are made and expressed as the ratio of the viewing distance to the theoretical viewing distance when the least resolved letter size subtends 1 minute-of-arc or 0.292 mrad, (e.g., 6/x or 20/x). Normal vision is usually considered 6/6 or better corresponding to a minimum-separable acuity of 1 minute-of-arc. Although this approach for measuring the acuity is simple and straightforward, several investigators (e.g., Farrell and Booth, 1975; and Overington, 1976) have criticized this approach because other factors such as contrast, luminance, and target-type also affect visual acuity.

2.3.2.7 Factors Affecting Visual Acuity

Westheimer (1965), Riggs (1965), Overington (1976), Semple et al. (1971), Sekuler (1974), and many others have surveyed the literature concerning the factors affecting visual acuity. Among the factors they report are luminance, contrast, state of adaptation, retinal position, refractive state of the eye (lens accommodation), binocular effects, pupil size, eye and target movements, and characteristics of the target (i.e., orientation, features, etc.). Figure 2.3.9 shows an attempt by Semple et al. (1971) to show how some of these factors may be related to perception of visual displays. Several of these factors are discussed below.

a) Effect of Retinal Position. The effect of retinal position is attributable to the population density of receptors along the surface of the retina. Since cone receptors are responsible for light-adapted vision, the ability to perceive spatial detail is a function of the density of cone receptors in the retina. The optical axis of the eye intercepts the retina at the fovea centralis. Figure 2.3.10 shows the distribution of rod and cone receptors along the horizontal meridian including the fovea centralis. The relative visual acuity is shown to be the

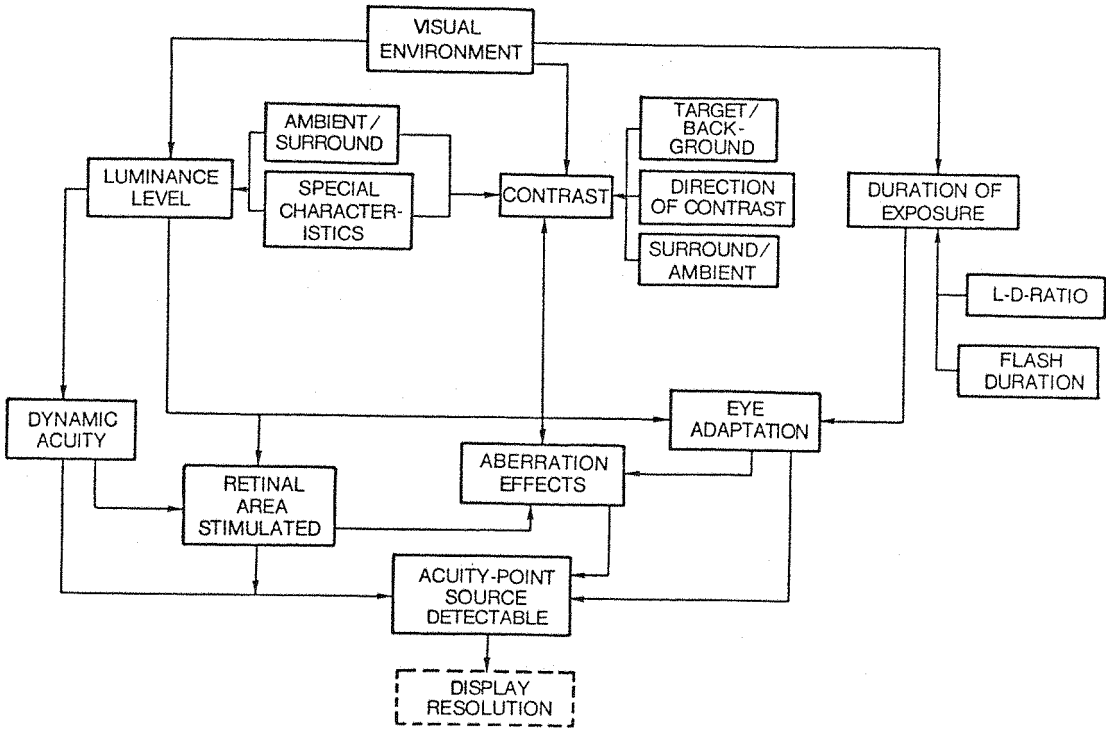

Figure 2.3.9. Factors Affecting Visual Acuity (after Semple et al., 1971)

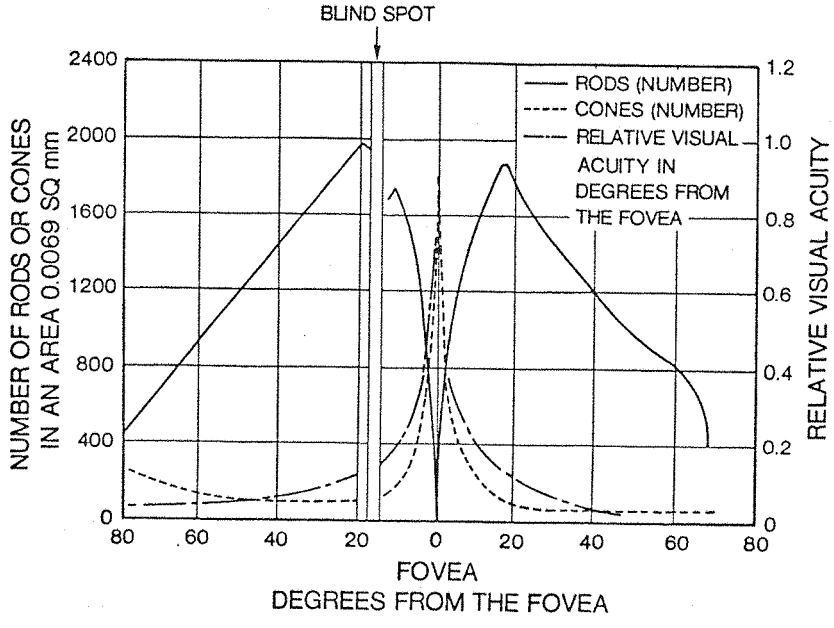

Figure 2.3.10. Distribution of Rods and Cones and Visual Acuity Along a Horizontal Meridian (from Woodson, 1954; after Brown, 1965)

greatest within a region near the fovea within a 2- to 4-degree cone. It is interesting, however, that investigators have shown that the relative acuity very near the fovea centralis is not as much a function of the density of cone receptors as their relative diameter (Westheimer, 1965). As shown in Figure 2.3.11, the main effect of the retinal position is to raise the threshold contrast as the angle of incidence of the target from the optical axis of the eye increases; that is, providing that the background luminance is sufficient to maintain photopic vision. At low luminance levels, the threshold of sensation is lower in the peripheral retina where the rod density is the greatest.

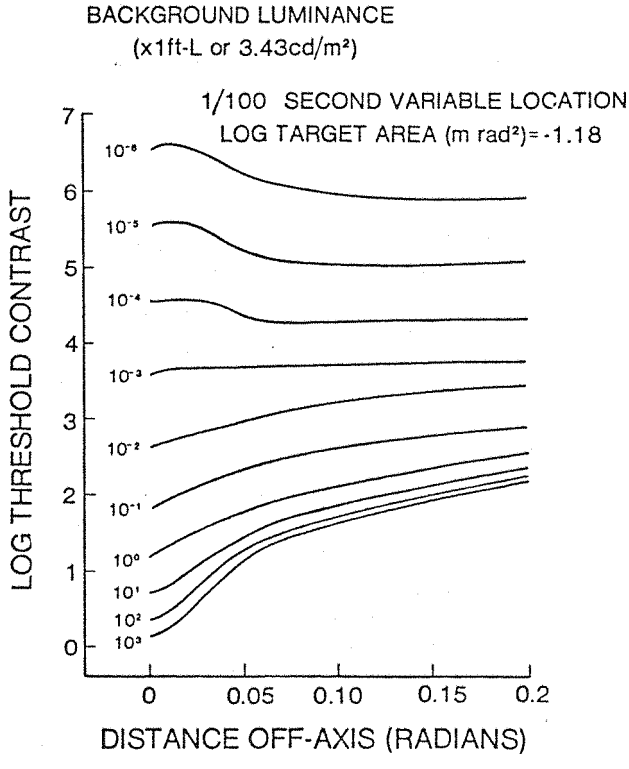

Figure 2.3.11. The Effect of Viewing Position at Various Back-Luminances (from Taylor, 1969; after Overington, 1976)

b) Contrast Sensitivity Function. Although the minimum separable acuity approach for quantifying visual perception is usable for threshold detection tasks, the spatial contrast sensitivity

function is more useful in relating visual perception to displays. The contrast sensitivity function (CSF) is similar to the modulation transfer function (MTF) described for cathode-ray tube displays in Appendix A.3.2. In order to further explain the CSF, a new term, contrast modulation (C_m), is defined:

$$C_m = \frac{|L_t - L_b|}{L_t + L_b}$$

where L_t = luminance of target

and L_b = luminance of background.

The CSF describes the threshold sensitivity of the visual system to contrast modulation (C_m) as a function of average luminance and spatial frequency (expressed as the number of modulation cycles per unit distance). Usually, the spatial contrast sensitivity function has been determined by presenting to subjects visual stimuli consisting of sine wave gratings of various spatial frequencies and average luminances. The subject adjusts modulation until the grating is just perceptible. A representative family of contrast sensitivity curves (for one subject only) determined this way is shown in Figure 2.3.12 for various average retinal luminances. The visual stimulus in this case was a sinusoidal grating with a 30-degree equiluminance surround, reproduced on a CRT with a green (P-31) phosphor and displayed to the single eye of the observer through a 2 mm artificial pupil. At the three higher retinal luminance levels (corresponding to luminances of .77 cd/m^2, 77 cd/m^2, 110 cd/m^2), the contrast sensitivity is a "U-shaped" function with greatest sensitivity (i.e., lowest contrast modulation to perceive), at 4 to 6 cycles per degree. This spatial frequency corresponds to a minimum separable acuity of 5 to 8 minutes-of-arc. The limiting condition for spatial frequency is approximately 50 cycles per degree (or 0.6 minutes-of-arc) for the 110 cd/m^2 luminance condition, which corresponds to the separable acuity measures with high contrast targets (such as the Snellen letter test) discussed above.

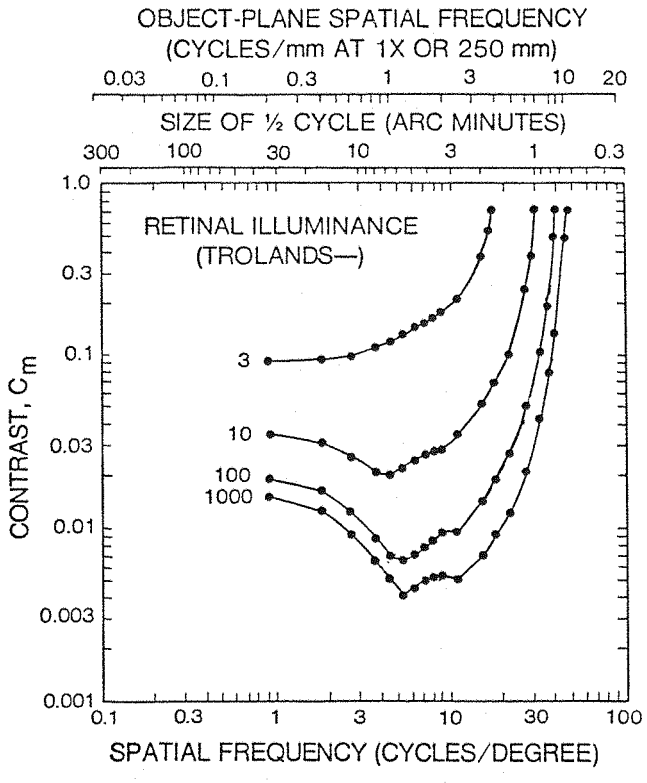

Figure 2.3.12. Contrast Sensitivity at Different Retinal Illuminances (from Patel, 1966; after Farrel and Booth, 1975)

Campbell and Maffei (1974) were amongst the first to employ the contrast sensitivity function. They state that the key advantages of the contrast sensitivity function are that first, it gives a measure of how the eye performs at all spatial frequencies and not just that at limiting acuity, and second, it shows regions of visual scenes which we are unable to see. Overington (1976), Cornsweet (1970), and Sekuler (1974) have indicated, however, that different targets (e.g., sine wave versus square wave gratings) and different methods for determining contrast sensitivity (e.g., direct, contrast matching or threshold), and the field-of-view of the stimulus field can produce entirely different results. Sekuler points out that the effect of field-of-view on stimulus perception probably is due to the heterogeneity of rod/cone distribution in the retinal structure.

Farrell and Booth (1975) summarized several findings in the literature with the CSF curve shown in Figure 2.3.13 which they used as the standard contrast sensitivity curve for the design of image interpretation equipment. Also shown in the figure are the established population distributions of contrast sensitivity functions based upon results of other authors.

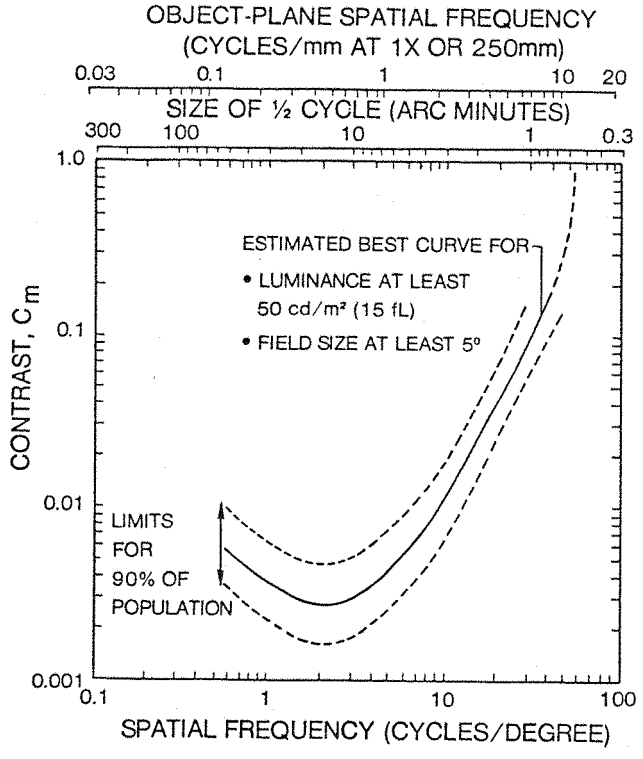

Figure 2.3.13. Average Contrast Sensitivity Curve for the Eye (from Vos et al., 1956; after Farrell and Booth, 1975)

Cornsweet (1970) cautioned that the contrast sensitivity function should not be interpreted as a true transfer function which requires linearity, homogeneity, and isotropy. He proposed, instead, that the contrast sensitivity function be termed a "describing function." Citing research by Davidson (1968), Cornsweet indicated that there were some conditions when the linearity condition was met, especially when the logarithmic response of the receptors has been taken into account. (Indeed,

Davidson showed linearity over a 5:1 range for low spatial frequencies when the logarithmic response of the eye had been compensated.) Cornsweet concluded that, for a CSF determination using threshold techniques and small ranges of contrast modulation, linearity can probably be assumed and the CSF considered to be a transfer function.

c) Effect of Monocular Viewing. Campbell and Green (1965b) demonstrated that, for most spatial frequencies, the threshold level of contrast sensitivity was higher for monocular viewing than for binocular viewing of sinusoidal gratings (e.g., Figure 2.3.14). The results where drawn from an experiment using sinusoidal gratings generated on a CRT which subtended a visual angle of 2 by 1.3 degrees within a 12 degree visual field of average luminance of 80 cd/m^2. The authors indicated that the ratio of monocular to binocular threshold was approximately 1.414. This finding, using the CSF techniques, is in general agreement with the literature when using other techniques such as the Snellen test (Overington, 1976).

d) Accommodation. The perception of detail is greatest when an object in the visual field is focused on the retina. The accommodation reflex adjusts the shape of the lens, via the ciliary muscles, to provide proper focusing on the retina of objects at different viewing distances on the retina. The normal range of the accommodation response is from 0.1 m to 7.0 m corresponding to a lens accommodation of 10.0 to 0.14 diopters (Brown, 1965). An accommodation distance of 7 m or more is considered to be optical infinity. The normal rest state of accommodation in the eye is about 0.8 m (Overington, 1976).

Johnson (1976) has shown that the luminance of the scene being reviewed affects the ability of the accommodation response of the eye to focus the scene on the retina. This aspect of eye accommodation may have a large impact on viewing collimated displays under night conditions. For example, Johnson found that with an

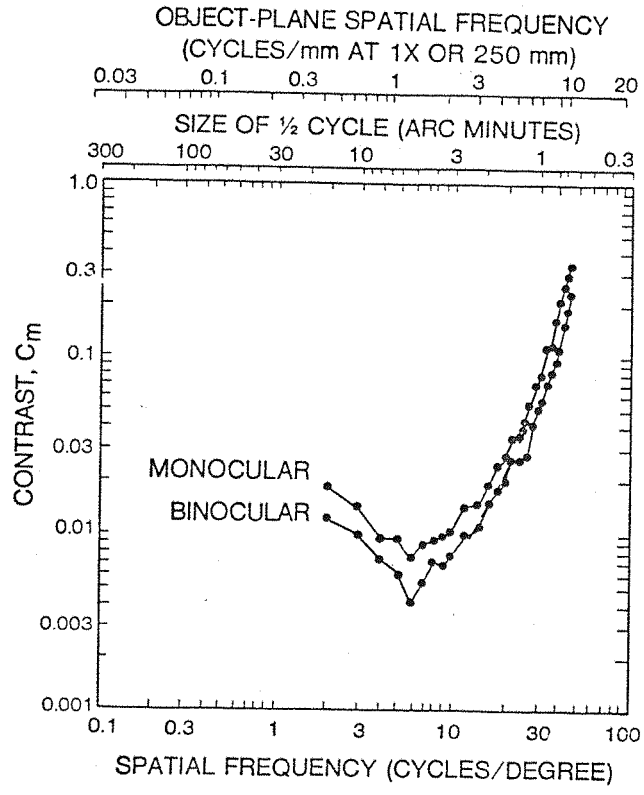

Figure 2.3.14. Contrast Sensitivity for Monocular and Binocular Viewing (from Campbell and Green, 1965b; after Farrell and Booth, 1975)

average scene luminance of 0.5 cd/m^2, an object at optical infinity was viewed with an accommodation error of about 0.8 diopters. At 0.05 cd/m^2 this accommodation error was doubled.

e) Eye Accommodation and Displays. Campbell and Westheimer (1959) have shown that the normal spherical and/or chromatic aberrations in the eye provide some cues to control the accommodative response. It follows from their research that the viewing of monochromatic displays can be compromised by this reflex. If the human visual system is composed of "spatially tuned" receptors/processing components, as Ginsburg (1978) has suggested, then the components of the frequency content in a scene may also be a cue for accommodative response reflex. In any case, Overington (1976) suggested that the poor quality of images often appearing on the visual displays (e.g., smeared edges, low contrast) may

not be conducive to adjusting the optimum accommodation of the eye, thereby causing a further degradation in perception.

Riggs (1965) indicated that the accommodative reflex produced spherical aberrations in the lens causing blurring of the image on the retina; however, the manifestation of these effects was only apparent at large pupil diameters. From these results, it can be assumed that display collimation will probably have little effect on the perception of a high quality image under moderate to high photopic viewing luminances (i.e., for pupil diameters of 4.0 mm or less), but may be a factor in perception of lower quality images under low luminance conditions.

f) Pupil Size and Visual Acuity. Pupil size will also affect visual acuity and the contrast sensitivity function. Apart from the function of the pupil size in controlling retinal illuminance, the primary influence of pupil size on acuity is related to the optical aberrations. Riggs (1965) and Westheimer (1965) presented the findings of several investigators indicating that acuity is maximum for pupil diameters between 2 mm and 5 mm. Visual acuity of the eye for small pupil diameters (i.e., less than 2 mm) is limited by diffraction, whereas larger pupil diameters (i.e., greater than 5 mm) allow optical aberrations of the lens and other elements to degrade the quality of the image on the retina. Campbell and Green (1965a) have shown that pupil diameter influences the contrast sensitivity function. As shown in Figure 2.3.15, the authors observed that increasing the pupil diameter using an artificial pupil from 2.0 mm to 5.8 mm increased the contrast threshold to detect a sinusoidal grating from .005 to .01 at 7 cycles/degree. The data were obtained for one subject viewing a 2 by 1.3 degree sinusoidal grating with a 100 cd/m^2 background produced on a CRT with a P-1 phosphor.

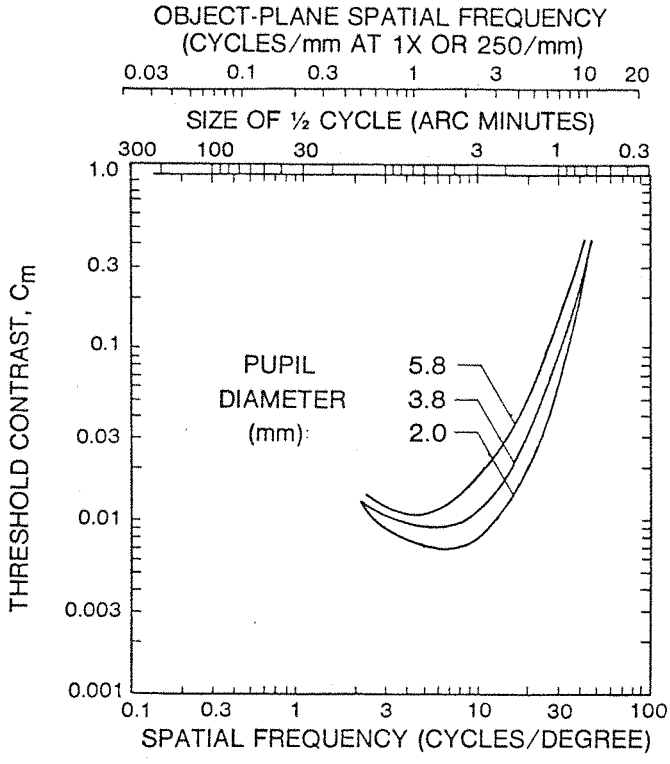

Figure 2.3.15. Effect of Pupil Size on Contrast Sensitivity (from Campbell and Green, 1965a; after Farrell and Booth, 1975)

2.3.3 Interaction of Display Parameters and Sensory Processes

In order to be successfully used by the observer, the display image and viewing situation must be presented with sufficient fidelity that the physical characteristics of the stimuli can be encoded by the sensory processes. As discussed above, the ability of the observer to perceive spatial detail (at threshold) which may be present in a display scene is represented by the contrast sensitivity function. The CSF will be influenced by the luminance, spectral and temporal properties of the stimulus, and its surround. Similarly, as discussed in Appendix A.3.2, the ability of the display to represent visual detail to the observer is manifested in the modulation transfer function. It, too, is affected by luminance and temporal (i.e., bandwidth and refresh rate) properties of the display presentation. Table 2.2.3 summarizes the major interactions of the physical parameters of the display and the sensory aspects of vision. The interactions given in

this table follow from Figure 2.3.9 including the stimulus and environmental conditions which may affect the "acuity" of the operator in a display viewing situation. For viewing a large field-of-view (greater than 15 degrees) monochromatic CRT display, the key factors governing the perceived quality of a display are mainly the average luminance of a display (which also controls adaptation level), the subtended visual angle of the resolution elements, and the modulation contrast of the resolution elements. Using this simplifying approach, the sensory behaviour of the operator, as shown by the contrast sensitivity curve in Figure 2.3.13 and the modulation response of the display (e.g., Figure A.3.2.5 in Appendix A.3.2), provide an overall description of the relationship of the display to the operator.

TABLE 2.2.3a. INTERACTIONS OF DISPLAY AND OBSERVER PARAMETERS

OBSERVER PARAMETERS	Contrast Sensitivity Function	Spectral Sensitivity	Chromatic Aberrations	Pupil Size	Spherical Aberrations	Retinal Illuminance	Dark/Light Adaptation	Accommodation	Viewing Angle	Retinal Area Stimulated	Critical Fusion Frequency
Contrast Sensitivity Function	-	X		X	X	X			X	X	
Spectral Sensitivity	X	-	X				X	X		X	
Chromatic Aberrations		X	-					X			
Pupil Size	X			-	X	X	X				
Spherical Aberrations	X			X	-			X			
Retinal Illuminance	X			X		-	X				X
Dark/Light Adaptation		X					-				
Accommodation		X			X			-			
Viewing Angle	X								-	X	
Retinal Area Stimulated	X	X							X	-	
Critical Fusion Frequency						X					-

TABLE 2.2.3b. INTERACTIONS OF DISPLAY AND OBSERVER PARAMETERS

DISPLAY PARAMETERS / DISPLAY PARAMETERS	Phosphor Color	Phosphor Persistence	Emitted Luminance Intensity	Update/Refresh Rate	Magnification	Viewing Distance	Surround Luminance	Modulation Transfer Function
Phosphor Color	-							
Phosphor Persistence		-		X				
Emitted Luminance Intensity	X	X	-					X
Update/Refresh Rate		X	X	-				X
Magnification					-			
Viewing Distance						-		
Surround Luminance							-	
Modulation Transfer Function			X	X				-

TABLE 2.2.3c. INTERACTIONS OF DISPLAY AND OBSERVER PARAMETERS

OBSERVER PARAMETERS \ DISPLAY PARAMETERS	Modulation Transfer Function	Phosphor Color	Phosphor Persistence	Emitted Luminance	Update/Refresh Rate	Magnification	Viewing Distance	Surround Luminance
Contrast Sensitivity Function	X	X		X				X
Spectral Sensitivity		X						
Chromatic Aberrations		X						
Pupil Size				X				
Spherical Aberrations						X	X	
Retinal Illuminance		X		X				X
Dark/Light Adaptation		X		X				X
Accommodation							X	
Viewing Angle						X	X	
Retinal Area Stimulated						X		
Critical Fusion Frequency			X		X			

2.3.3.1 Modulation Transfer Function Area (MTFA)

Synder et al. (1974), Synder (1976), Task and Verona (1976), and Task (1979) have shown that the area between the modulation response curve of the display and the contrast sensitivity function of the operator is highly correlated with operator performance in a target acquisition and recognition task. The area between these two curves is termed the modulation transfer function area or MTFA. Shown diagramatically in Figure 2.3.16, the MTFA relationship shows the region of spatial frequencies wherein the operator's threshold for contrast at specified luminances is exceeded by the display's capability of producing that contrast. The spatial frequency at which the two curves intersect can be termed the limiting resolution of the display/observer interface. Beyond this point, the threshold contrast to perceive those high spatial frequency resolution elements is greater than the display's ability to produce that contrast modulation; that is, the observer "demand" exceeds the display "supply." Recently, Task (1979) has shown that the subtended angle at target recognition is highly correlated ($r \cong -0.95$) with MTFA. There are limitations to the applications of such a unitary area measure of operator/display quality due to the anisotropic nature of the area between the two curves and the use of threshold data for the contrast sensitivity function. Nevertheless, the MTFA does produce a gross description of the display-operator sensory interface and, more precisely, an indication of limiting performance. Other display/observer describing models have been postulated by Schnitzler (1973), Rosell and Willson (1973), and Task (1979).

2.3.4 Cognitive Processes

As was shown in Figure 2.3.1, visual perception consists of sensory and cognitive processes. Although the consideration of sensory processes is more crucial in this thesis, some concern about cognitive aspects of visual perception is needed, especially since psychophysical experimental methods will be used. In the literature, it is generally agreed that the observer is limited in his ability to receive and process sensory information. Based upon early experiments

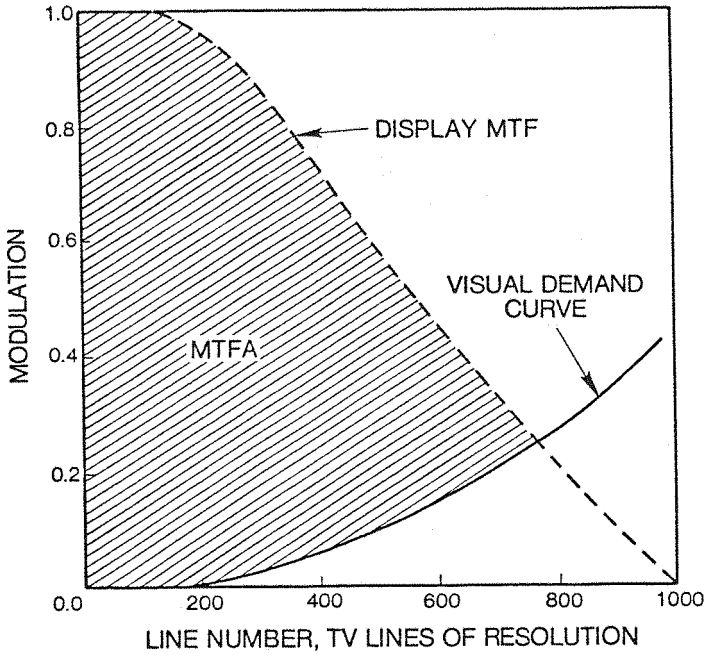

Figure 2.3.16. Representation of Modulation Transfer Function Area (MTFA) Concept. Shaded Area Denotes Capacity of Display to Present Spatial Information Which Can be Seen by the Observer (after Hershberger and Guerin, 1975)

in cognition, Broadbent (1958) proposed a model wherein the sensory organs present a multiple channel input into a single port processor. The rate at which an observer processes visual information (i.e., brings into consciousness an awareness of the input stimuli), has been shown to be a function of physical characteristics of the input signal, the signal rate, response requirements, training, experience, instructions, and individual differences such as age and intelligence. Perhaps one of the greatest factors is learning. Gibson (1965) defines a learning system as "one that optimizes performance based upon the recognition and use of familiar features in a present situation." The aspect of learning can introduce problems in psychophysical experiments involving cognitive processes, such as target recognition tasks, and can become a significant factor contributing to experimental variance. For example, Fleishman and Hempel (1955) have shown several ways that the composition of experimental variance can change due to learning during the course of an experiment involving a

visual discrimination recognition task. They found that, as proficiency increases, different combinations of sensory and cognitive factors interact, and there appears to be a shift from the variance attributable to cognitive processing to that associated with motor control functions.

Martin et al. (1976) reported an experiment involving a target recognition task wherein they investigated effects of training and instruction set. Recognition error rate and the subtended visual angle at recognition were dependent variables. They used pilot studies to determine the effects of instruction set on learning (repetition of trials) and found that there was a rapid decrease in the subtended angle needed to recognize targets (response time) which began to asymptote after two replications of the stimulus conditions. Thereafter, additional replications produced only small additional decreases of reaction time (i.e., 10 percent after nine replications). Likewise, in another pilot experiment, the authors found that when they changed the criteria in the instruction set for recognizing targets from "as soon as possible" to "when virtually certain," the number of errors in recognition decreased from 25 percent to 4 percent. The authors eventually used the latter instruction in the main experiment so that subtended visual angle at target recognition would be the most sensitive independent variable.

2.3.5 Interaction of Cognitive and Sensory Processes

The discussion of visual perception above presumes, erroneously, that perception is composed of monodirectional (i.e., input, processing, output) and autonomous sensory and cognitive processes. The enormous body of literature in cognitive psychology shows that, at least in the case of the control of eye movements, this is not the case. For example, Adam and Just (1976) have proposed that for tasks involving visual input, the rapid mental operation of the central processor may be reflected in eye movement behaviour and that separate mental operations may be dependent upon, or at least compatible with, the ability to make separate fixations in a scene being searched. In this situation, the optical axis of the eye is directed to a location within the

display field in order to acquire information for the processor which is needed to meet a response criterion. This behaviour may also modify peripheral control of eye movement, such as the smooth pursuit and vestibular-ocular reflex. The nature of the eye fixation and movements have been related also to the stimulus parameters and the type of visual task (e.g., Williams, 1966, 1967; Luria and Strauss, 1975; Just and Carpenter, 1976).

2.3.6 Image Quality and Display Perception

Numerous studies have been conducted to attribute character legibility and target acquisition performance to the spatial, contrast, and luminance parameters of the display/observer interface. (For a summary of this research, see Semple et al., 1971.) Typically, these studies show that increasing the number of resolution elements, the subtended angle of the target, and target-to-background contrast also increase the probability and accuracy of target recognition and decrease the reaction time to recognize a target.

2.3.6.1 Legibility of Symbols

A representative study involving the recognition of geometric forms on a CRT display was reported by Hemingway and Erickson (1969) wherein the angular subtense of the symbol and the number of resolution elements per symbol height were manipulated independently. The summary data from their experiment are shown in Figure 2.3.17. The data indicated interacting effects of resolution and subtended angle. Within the range of the independent variables investigated, performance tended to follow the relationship:

$$P \propto \frac{a}{x^2} + \frac{b}{y^2}$$

where P = probability of correct recognition,
x = number resolution elements per symbol height,
y = angular subtense of the symbol,
and a and b are constants.

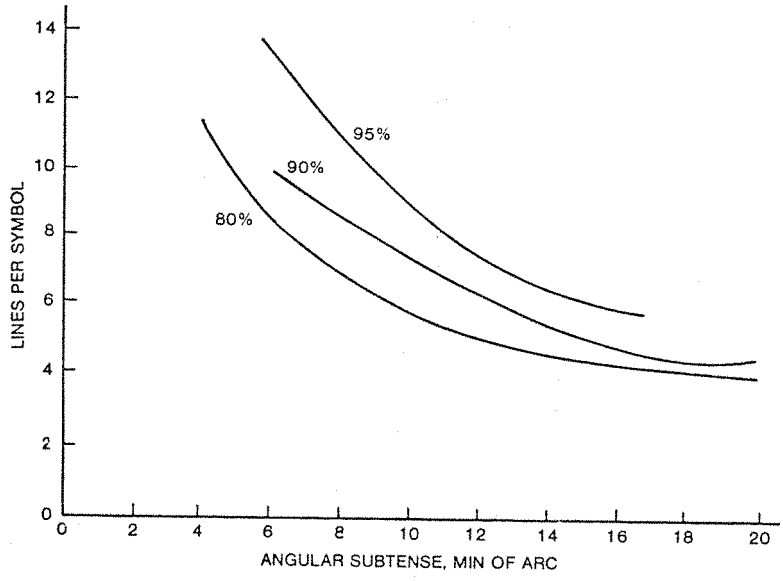

Figure 2.3.17. Interaction of the Number of Scan Lines and Angular Subtense of Symbols to Produce 80, 90, and 95 Percent Levels of Correct Response (after Hemingway and Erickson, 1969)

For low angular subtenses (i.e., 4 to 6 minutes-of-arc), the sensitivity to changes in resolution were greater than at 16 minutes-of-arc where performance begins to asymptote regardless of the number of lines per symbol height. Performance can be maintained by trading-off resolution for an increased symbol height and vice versa. Similar results were obtained by Shurtleff (1974) for alphanumeric characters.

2.3.6.2 Target Recognition from Imagery

Erickson and Hemingway (1970), Lacey (1975), and Erickson (1978), have also studied the effects of the number of scan lines and subtended angles on target recognition performance using pictorial visual targets. Some of the results obtained by Lacey are shown in Figure 2.3.18. His data indicated similar trends as those discussed above for symbolic targets (i.e., interaction of scan lines and subtended angle). Also, it was noted that increasing the number of scan lines (number of vertical resolution elements) had little effect except for the larger subtended angles. This effect was primarily due

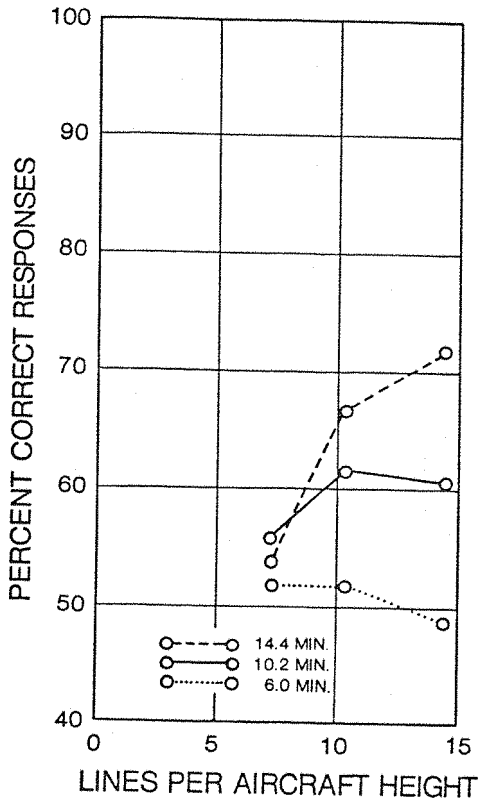

Figure 2.3.18. Target Recognition Performance as a Function of Subtended Visual Angle and the Number of Scan Lines Across Pictorial Targets (after Lacey, 1975)

to the need for making the visual angle subtended by each resolution element large enough so that it can be perceived by the observer. Erickson and Hemingway (1970) showed that the interaction of the number of scan lines and subtended visual angle to produce equal recognition probabilities was shifted by the type of background (plain, foliage, sandy) upon which the target was viewed. Other studies have shown considerable influence on the probability of recognition, reaction time, and accuracy of response due to target type and complexity (e.g., Scott and Hollanda, 1970).

2.3.6.3 General Display Quality Requirements

Burnette (1971) suggested that alphanumeric and pictorial targets should subtend a visual angle of at least 15 minutes-of-arc in order to achieve a high probability of identification (.99). He qualified

this suggestion by indicating that, for displays used in an airborne environment, the minimum visual angle should be increased to 24 minutes-of-arc. At the same time, alphanumeric symbols should contain at least 10 resolution elements per symbol height and pictorial targets 16 elements per target height. This assertion agrees with the criteria originally established by Johnson (1958) that, for low contrast targets, identification will occur (with 50 percent probability) when the angular width of the target is approximately 6.5 times the highest detectable spatial frequency of a periodic test pattern.

As was the case for the determination of the contrast sensitivity function in Figure 2.3.12, target legibility performance is influenced also by the luminance and contrast of the information on the display (e.g., Semple et al., 1971). Generally, for a particular probability of recognizing numeric characters, the character-to-background contrast can be reduced as long as the display luminance is increased. (This behaviour tends to follow a Weber's law wherein $\frac{\Delta L}{L}$ = constant.) The effect of luminance on contrast sensitivity is describable as the shift in the contrast sensitivity function as retinal illuminance changes (i.e., greater average luminance lowers modulation contrast thresholds or sensitivity to contrast increases with increased luminance).

2.3.7 Perception of Dynamic Visual Information

The discussions to this point have been concerned with visual perception when there is little or no motion of the displayed information or observer. When information on the display is moving or the observer is moving relative to the display, the basic aspects of visual acuity and the contrast sensitivity function discussed for static images must be altered. Prior to continuing the literature review in this area, it is appropriate to address the nature and role of eye movements in the maintenance of vision for static and moving visual fields.

2.3.7.1 General Nature of Eye Movements

Because the field-of-view of the high acuity visual field of the eye is small (i.e., 2 to 4 degrees as shown in Section 2.3.2.6), movements of the eyes are required to orient the foveal field-of-view over the targets of interest. This process also occurs when there are relative movements between the target and observer. Rapid, ballistic-type movements of the eye take place when searching a visual field to position objects of interest over the foveal retina. These eye movements are called saccades. Smooth pursuit movements of the eyes are used to track moving targets within a stationary visual field. In both cases, the eyes move together (conjugate movement). Involuntary movements of the eyes consist of physiological, optokinetic, and vestibular nystagmus. Aspects of these movements will be discussed below, except for vestibular nystagmus which will be discussed in Section 2.5.5.2. Vergence is another type of eye movement wherein the eyes move differentially and is related to the binocular perception of depth or stereopsis. Aspects of the vergence system will not be discussed, since it will not be a factor in the perception of a monocular helmet-mounted display.

a) Saccadic Eye Movements. For a display field larger than 2 to 4 degrees, visual information is obtained by voluntarily positioning the optical axis of the eyes over features within the field. This function places the object of interest over the high acuity portion of the retina. When the visual field and targets of interest within the visual field are not moving, the position fixation of the eye usually occurs by a sequence of discrete high velocity movements termed saccades. Saccadic eye movement has been shown to be a function of both sensory and cognitive processes. The probability of making a particular eye fixation, the duration of that fixation, and the rate of other fixations have been shown to be related to the properties of the stimuli (e.g., color, shape, size) and/or cognitive properties, such as the similarity with a prebriefed target, instruction set, training,

and experience. Typical fixation durations for target recognition tasks have been shown by Gould (1976) and Gutmann et al. (1979) to be approximately 300 ms. Fuchs (1971) presented findings from several investigators which indicated that the duration of movement and the maximum velocity of the eye during a saccade increase with the magnitude of the angular displacement of the eye due to the saccade. Typically, a 5 degree saccade required about 13 ms to achieve. The duration continued to increase at a 7 ms per degree rate up to 80-degree angular movements. The practical maximum velocity of the eye during saccadic eye movements has been shown to be about 700 degrees per second. Saccadic eye movements generally observed in searching a visual field are in the range of 30 to 120 ms (Young and Sheena, 1975). The saccade will usually position a target of interest within 0.3 degree of the fovea centralis. Similarly, saccades do not occur when discrete target displacements are less than 0.3 degree. Random step displacements of the target in the visual field at angles greater than 0.3 degree are usually followed by step saccades after a latency period depending upon the target displacement. Reporting from the literature, Fuchs (1971) concluded that the average latency or reaction time before a 5 degree saccade was about 200 ms, but for a 40 degree saccade was about 250 ms. If the target motion was predictable (e.g., a periodic square wave), latency can be reduced to zero with the observer tracking in a phase-locked mode relative to the moving stimulus.

b) Saccadic Suppression. There is a considerable body of evidence that saccadic movements of the eyes are accompanied by an elevated threshold of vision during the movement process (Westheimer, 1965). Bridgeman et al. (1975) were able to show that detection of target displacements during saccadic movements was strongly suppressed. The amount of suppression increased as a function of the ratio of eye movement to target movement magnitudes. In almost all cases of target movement, suppression occurred before saccadic eye movement (up to 50 ms in some cases). These findings added to the body of literature supporting a central basis for saccadic suppression of vision often called "corollary

discharge." Richards (1969), on the contrary, attributed the saccadic suppression effect to mechanical properties of the retina. Regardless of the mechanism supporting saccadic suppression one cannot, when looking in a mirror, see ones eyes move.

c) Physiological Nystagmus. During the fixation periods between saccades, small involuntary eye movements continue to occur. These movements, called physiological or normal nystagmus, are usually less than 0.3 degree. These very small angular movements are characterized by small flicks (microsaccades), slow drift, and high frequency tremor. The slow drifts are probably due to instability in the neuromuscular system of the eye and occur in the range of 2 to 3.5 minutes-of-arc per second (Cornsweet, 1970). Microsaccades correct for the drift at a 3 to 10 Hz rate with an average movement of 5 to 10 minutes-of-arc occurring from 3 to 10 times a second. The residual tremor in eye movement occurs at frequencies of 30 to 80 Hz (Robinson, 1968) with an angular displacement on the order of the angular size of a cone receptor in the fovea (i.e., approximately 20 seconds-of-arc).

It is thought that the involuntary movements of the eye (physiological nystagmus) were necessary to maintain vision (Robinson, 1968, Fuchs, 1971, Festinger, 1971) since removal of these small movements via retinal image stabilization techniques caused a loss of visual sensation after several seconds. Because of this phenomenon, it was proposed that the visual system transmits information about changes in the visual scene (e.g., color, intensity, etc.), which are promulgated by micromovements of the eye. Tulunay-Keesey and Jones (1976) have shown that there was little relationship between micromovements of the eye and contrast sensitivity function for fixation durations less than 1 second.

d) Pursuit Eye Movements. While the saccadic eye movement system uses high velocity discrete steps to place the fovea of the eye over targets of interest in the visual field, the pursuit system

functions to stabilize the image of moving targets on the retina. The pursuit system performs this function by slewing smoothly the optical axis of the eye at a velocity and direction which matches that of the target. It is thought that the target velocity is measured by the sum of the eye velocity and the retinal slip velocity. Unlike saccadic eye movements, there is some question as to whether the smooth pursuit system is under voluntary control since it is very difficult for an observer to cause smooth "pursuit-type" movements of the eye without a moving target (Young and Sheena, 1975; Robinson, 1976). Research on the pursuit system has shown that the angular velocity of the eye and target are equal up to a target angular velocity of 15 deg/s. At target velocities at about 30 degrees per second, eye velocity is slightly less than the target, causing a residual retinal slip error which is corrected by high velocity saccades. The maximum tracking velocity of the smooth pursuit system appears to be about 30 to 40 deg/s. Beyond 40 deg/s, tracking is accomplished primarily by saccadic movements. At velocities beyond 100 deg/s, there appears to be no attempt to track the target (Young, 1971).

As in the case of the saccadic eye movement system, a delay time exists in the pursuit system between the time that the target begins a smooth pursuit movement and the initiation of the smooth tracking response. This latency was measured to be between 125 ms and 134 ms (Young, 1971; Robinson, 1976). After the response begins, the eye then accelerates to match the angular velocity and direction of the target under the limitations above.

The behaviour of the pursuit tracking system is also influenced by the predictability of target motion. Young (1971) has shown that targets with predictable smooth motion (e.g., smooth sinusoids) were tracked with apparently higher gain than those targets with unpredictable movement. The gain/phase response of the eye under these conditions are shown in Figure 2.3.19. Young reasoned that the smooth pursuit tracking system attempts to predict the future movement of the target up to 300 ms ahead. This behaviour reduces the phase lag which normally would be

inherent with the latencies above. According to Figure 2.3.19, the open loop bandwidth limit of the pursuit tracking system with nonpredictable target motion is 1.5 to 2.0 Hz (i.e., when open loop gain is -3 dB).

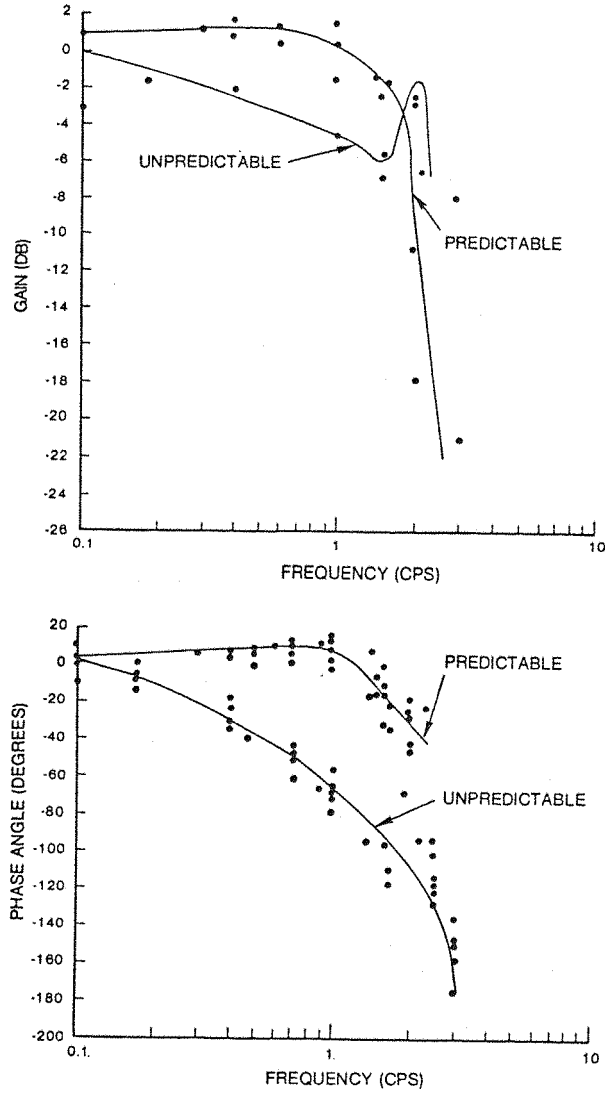

Figure 2.3.19. Frequency Response of the Eye Following Predictable and Unpredictable Targets (after Stark et al., 1966)

e) Maintenance of Visual Space Perception. Even though the eyes perform saccadic and smooth pursuit movements, the visual world is perceived as remaining stationary. Since the displacement of the stimuli is physically occurring on the retina, the orientation of this visual space must be accomplished centrally. There is some controversy as to whether the stabilization of visual space results from centrally derived efferent signals driving the extra-ocular muscles or proprioceptive feedback signals from the muscles themselves. Festinger (1971) asserted that an "efference copy" is probably used for spatial orientation during saccadic eye movements, since the efferent program initiating the saccade must take into account the precise present and future eye positions due to the saccade, whereas the smooth pursuit system provides only a direction and velocity of movement which matches that of the target. Festinger also points out from other results that egocentric localization is more accurate after a saccade than after a pursuit movement.

f) Optokinetic Nystagmus. When the entire visual field of an observer is translation in one direction, an involuntary or automatic movement of the eyes termed the optokinetic nystagmus (OKN) usually results. This behaviour is often called "train nystagmus" because of the association of looking out a train window at a passing scene. The movement of the eyes during OKN has a characteristic "sawtooth" pattern, with slow phase "pursuit-type" movements following objects in the scene, interspersed with fast phase or "saccadic-type" movements to reset the eye direction to a new point in the scene so that tracking can resume. Young and Sheena (1975) reported that the amplitude of the fast phase OKN movement may be from 1 to 10 degrees with a minimum time interval between fast phases of 0.2 second (or a maximum frequency of 5 Hz). It can be observed that the OKN response is difficult to suppress against a moving visual world unless a fixation point (static or moving) is provided. Robinson (1976), citing the research of others, noted that the OKN could be produced by stimulation of the peripheral retina only. He reasoned that there are perhaps two mechanisms involved in the OKN, a

foveal/centrally-mediated system which provides tracking of specific targets and a peripheral/subcortically-mediated reflex response to help stabilize the eyes (reduce retinal slip) when the entire field moves. The observation that the OKN can be suppressed with foveal fixation at a static target he attributed to the dominance of the foveal fixation over the subcortical or peripheral stimulation. He added that the purpose of the peripheral eye tracking system was probably not to move the eye as much as to keep the image still. Robinson concluded his treatise with the hypothesis that the development of such a redundant peripheral fixation/tracking system was due to the need to provide some stabilization of the eye movements at low luminance levels when the normal foveally-mediated response by the cone receptors is inoperative.

2.3.7.2 Dynamic Visual Acuity (DVA)

The ability of the eye to perceive detail within a moving visual field is termed dynamic visual acuity (DVA), or vision during ocular pursuit. Dynamic visual acuity has been shown to be a function of the angular velocity of the image, the direction of movement relative to the observer (i.e., horizontal, vertical, oblique, or circular), the characteristics of the stimulus (e.g., illumination, contrast), exposure time and practice affects (i.e., transfer and retention of learning). Many of these factors have been summarized by Miller and Ludvigh (1962).

a) Effect of Target Velocity. The general findings of laboratory experiments show that dynamic visual acuity deteriorates as the angular velocity of the image relative to the observer increases. As a general rule, the degradation becomes readily apparent at an angular rate of about 50 deg/s (Ludvigh and Miller, 1953). They described the form of the decrease in dynamic visual acuity using the following equation (to fit their mean data):

$$Y = a + bx^3$$

where Y = minimum separable acuity (minutes-of-arc),
a = static visual acuity (minutes-of-arc),
b = coefficient of dynamic visual acuity (minutes-of-arc/deg/s),
and x = angular velocity of the image at the eye (deg/s).

The mean data from their experiments using 18 naval aviation cadets with good static visual acuity yielded a model with a = 2 and b = 3.46×10^{-6}. The authors found a wide variation in dynamic visual acuity across subjects. For example, for a threshold acuity measure at 110 deg/s, one group of subjects (separated by dynamic visual acuity performance) had a DVA of 11 minutes-of-arc whereas another group had a DVA of 3.75 minutes-of-arc. The static visual acuity of both groups was 2 minutes-of-arc. The authors noted that they could find no consistent correlation between static and dynamic visual acuity in any of their experiments. Even with the wide variation in DVA between subjects, the within subject means were found to be reliable over a time period of up to 10 months.

b) Effect of Direction of Movement. In other experiments, Miller and Ludvigh (1953) found that DVA, using a test object moving in a vertical plane relative to the observer, was consistently better than DVA in the horizontal plane. The mean data show that a 1 to 2 minutes-of-arc acuity degradation in horizontal movement was present across a range of object velocities from 20 to 140 deg/s. Miller (1956) also found that DVA deteriorated most rapidly when the target was moving in a circular path. In a later experiment, Miller (1958) observed that DVA in the horizontal plane was no different for angular movement of the target versus the angular movement of the observer, providing the vestibular effects of accelerating the subject had subsided.

c) Effect of Stimulus Characteristics. As was shown for static visual acuity, stimulus characteristics also affect DVA. Citing experiments by Van Den Brink and Ludvigh and Miller, Miller and Ludvigh (1962) concluded that increasing the luminance of a test

object will improve dynamic visual acuity. Barnes (1979) has also found that the luminance, character-to-background contrast, and size of the character pattern also affected character legibility in a dynamic visual legibility task.

d) Effect of Learning. Miller and Ludvigh (1962) cited experiments by themselves which showed that practice and/or learning affected DVA. Among a selected group of subjects, they found that mean DVA (measured at 100 deg/s) improved from approximately 10 minutes-of-arc to 2 minutes-of-arc after ten trials. They noted, however, that the improvement varied widely across subjects. Using the data of 200 subjects, they modeled the effect of learning using the equation:

$$Y = 5.0 + 6.91\ e^{-0.178t}$$

where Y = dynamic visual acuity (minutes-of-arc)
and t = number of trials.

This model shows that a substantial amount of learning takes place in the first few trials, if it is going to occur at all. Miller and Ludvigh observed that this training or learning effect was retained for at least 7 months.

e) Mechanisms of Dynamic Visual Acuity. The differences and lack of correlation between static and dynamic measures of minimum separable acuity indicate that perhaps two mechanisms are involved. In the case of the moving target, ocular movement behaviour involves a combination of pursuit and saccadic eye movements as discussed in Section 2.3.7.1. The general deterioration in dynamic visual acuity beyond 40 to 50 deg/s occurs because of the inability of the eye to keep using pursuit movements thereby causing eye movements to be punctuated with saccades. As image velocity continues to increase, almost all movement is saccadic causing observers to obtain only the briefest glimpse of the target.

Visual acuity under dynamic viewing conditions degrades because the target image moves on the retina, either due to the failure of the pursuit system to keep up (i.e., match the velocity and direction of the target), or perhaps the inaccuracy of the saccades to obtain a precise registration of each glimpse during high target angular rates. These results are consistent with the findings of Hoffman and Greening (1967) who found that in the case of image blur using Landolt "C" targets in a photographic media, performance measured in accuracy and time to recognize targets was unaffected as long as the ratio of the target critical dimension to the size of the image smear was less than 2. If the ratio were greater than 2, the performance decreased rapidly to a chance level.

The effect of learning can probably be attributed to the enhancement of pursuit eye tracking behaviour when target movement is predictable. In these cases, the generation of tracking error signals from retinal slip may be eliminated, being replaced by some central process which matches eye motion with target motion.

f) Effect of Image Motion on Retina. Since the receptors in the retina exhibit a finite integration time and persistence (see Section 2.3.2.5), relative motion of the display image on the retina can cause a smearing of the image. Recently, Barnes and Smith (1980) have shown that even small retinal velocities can dramatically reduce the legibility of small characters. They found that retinal image velocities less than 3 deg/s were needed to recognize characters (with a 90 percent accuracy) subtending a visual angle of 18 minutes-of-arc and presented with a 8 cd/m^2 luminance and on a background of 0.5 cd/m^2. The characters were exposed to subjects for 80 ms. The limiting velocity to achieve 90 percent accuracy decreased as character size, luminance, and character-to-background contrast also decreased, but increased as exposure time decreased.

2.3.8 Summary of Perceptual and Display Interaction

The visual factors involved in the perception of the displays are very complex and are related to both the content and context within which the information is presented to the operator, as well as a priori factors, such as learning, which may affect the cognitive processing of visual information. The key factors influencing sensory processes were shown to be luminance, contrast, and spatial frequency of the information presented on the display. The general descriptors of modulation transfer function and contrast sensitivity function can be used together to describe the usable image quality or the sensory channel capacity of the display and observer. Eye movements in the pursuit of moving targets were shown to be a major factor affecting dynamic visual acuity. The variation across subjects and the confounding effects of learning have also been shown to be important. In short, all of these factors must be considered and controlled in any psychophysical experimentation involved with visual display systems.

2.4 SPECIAL PERCEPTUAL PROBLEMS ASSOCIATED WITH THE HELMET-MOUNTED DISPLAY

2.4.1 Introduction

The purpose of the helmet-mounted display is to introduce visual information into the visual field, without disrupting the normal function of perceiving the outside or nondisplay world. As will be seen, the degree to which this goal is achieved is a function of the information which is presented on the helmet-mounted display, the display mechanization, and the nature of the outside scene. A simplified configuration representative of helmet-mounted displays was introduced in Section 2.2.3, along with illustrations of some of the ways the helmet-mounted display may be used in an operational setting. A detailed consideration of all of the design factors and their impact on the perception of the helmet-mounted display is beyond the scope of this review. Instead, it is intended here to select key factors associated with the perception of the helmet-mounted display and highlight those aspects which are unique to a monocular presentation

of a virtual image scene. Many aspects of the sensory processes, other than those addressed for electronic displays, are a function of the mode of operation of the helmet-mounted display. The three operational applications discussed in Section 2.2.4 bring some of the perceptual problems to light. These applications prompt the question: Can the human visual system process, simultaneously, two independent channels of visual information?

2.4.2 Perceptual Conflicts in Monocular Helmet-Mounted Displays

There are three main factors involved in the perception of the helmet-mounted display and real-world scene: (1) the nature of the ambient scene; (2) the nature of the helmet-mounted display scene; and (3) the optical interaction of the ambient and helmet-mounted display scenes. As shown in Figure 2.4.1, the design of the helmet-mounted display provides multiple elements which independently control or can change the transmission of the light to each eye of the observer, either from the display image source or the outside world scene. This unique design of the helmet-mounted display optics can cause the following unnatural viewing situations to occur:

1. The average luminance entering the two eyes may be different. Because the light transmissivity of the visor and combiner elements may be different for each optical path to the eyes, the light entering either eye from the outside scene may be adjusted independently from a completely opaque or zero light transmission level to an almost unattenuated see-through or partially see-through condition.

2. The display image is impressed or presented into one eye of the observer, whereas the outside scene may be available to both eyes simultaneously. The luminances from the outside and the display scene are additive. The luminance at the eye due to the display is a function of the CRT luminance, transmissivity of the optics, and reflectivity of the combiner, whereas the luminance due to the outside scene is a function of the visor and combiner transmittances.

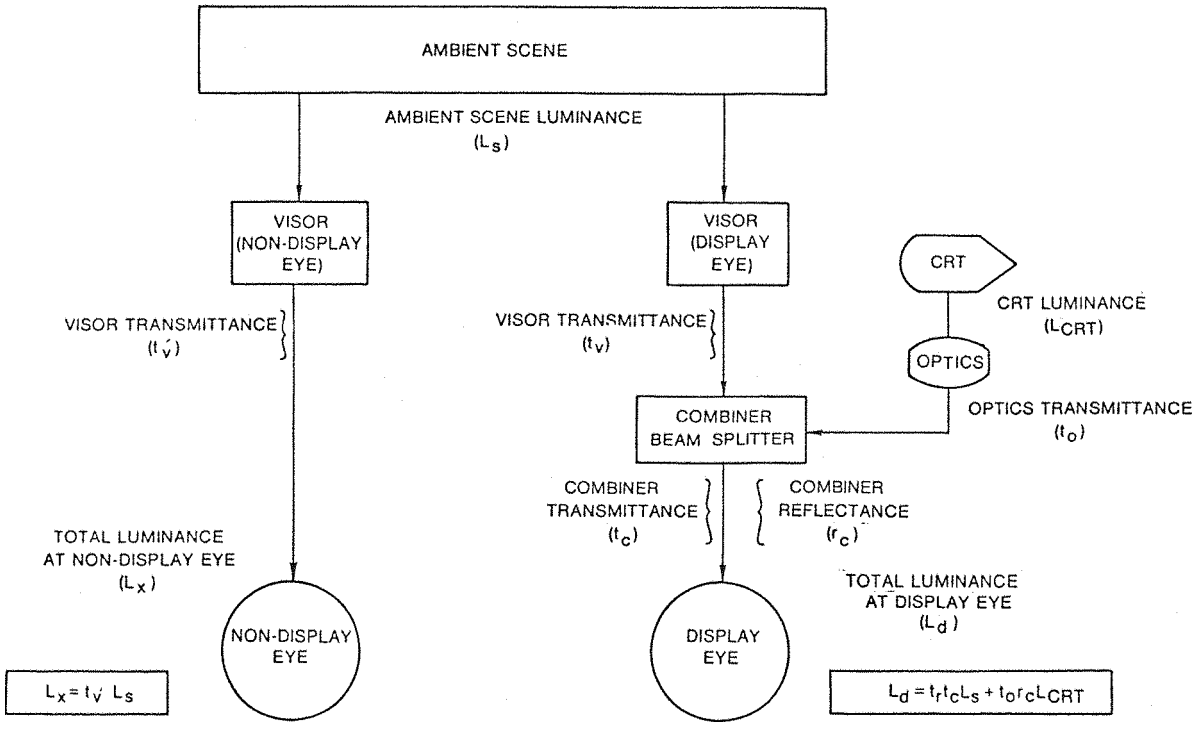

Figure 2.4.1. Diagram of the Optical Pathways in a Monocular Helmet-Mounted Display

3. The scale or spatial features of the scene within the helmet-mounted display presentation may be different from the outside world due to magnification or minification of the helmet-mounted display scene.

4. The color of the display may be different from that the outside scene due to the spectral characteristics of the CRT phosphor and any color selective filtering which may be present in the optical combiner.

5. The viewing distance of the display scene versus the outside scene may be different. Assuming the outside scene is located at optical infinity, the apparent viewing distance of the display scene may be variable or adjusted to a fixed distance anywhere between 0.5 m and optical infinity.

6. The resolution of spatial detail in the display scene may be different from that of the outside scene as viewed by the observer.

7. The contrast contained in the display scene may be different from that of the outside scene.

8. Movements of the images within the display scene and outside world scene may be different.

9. The display scene moves with the head, whereas the outside world is stabilized in space, and cockpit instrumentation is oriented with the vehicle.

Perceptual factors which are unique to a monocular helmet-mounted display interrelate with how the human visual system processes the two independent channels of visual information. Some of the perceptual processes and problems encountered when disparate visual information is presented to each eye has been addressed in literature reviews by Shontz and Trumm (1969), Hughes et al. (1973), Hershberger and Guerin (1975), and Laycock (1976). Some of the factors addressed by these authors include monocular versus binocular vision, brightness disparity, binocular rivalry, image luminance/contrast, eye dominance, accommodation, and image interference or shifting of attention. Each of these factors is discussed in more detail in the following sections.

2.4.3 Monocular Versus Binocular Vision

As discussed in Section 2.3.2.6, visual acuity has been shown to be greater for binocular than for monocular viewing. For visual threshold tasks, binocular viewing usually improves performance by a factor of $\sqrt{2}$ or less. The data from experiments by Campbell and Greene (1965), shown in Figure 2.3.14, also indicated this overall trend. Overington (1976), however, suggested that for visual target acquisition tasks, the difference between monocular and binocular viewing may not be as marked. Quoting from an experiment by Spicer in 1973, using

low and high contrast Snellen letters, Overington stated that observers exhibited only marginal improvement in performance when viewing with both eyes rather than with either eye monocularly. This finding was supported by an experiment reported by Task and Hornseth (ca. 1974) who found very little difference in the target detection performance for subjects using a panel-mounted display viewed with both eyes versus a helmet-mounted display viewed with the right eye only.

Although little degradation in target acquisition performance may be expected with monocular viewing of the helmet-mounted display, there may be some effect on size and distance judgments. Quoting from the research by Fried in 1964, Shontz and Trumm (1969) indicated that the perceived length of a straight line was shorter when viewed monocularly than binocularly. In several of the flight trials using the helmet-mounted display reported by Upton (1962), subjects reported an apparent reduction in size of the helmet-mounted display scene over the real-world scene even though targets within both scenes subtended the same visual angle. This finding was also apparent from other flight tests which have not been reported in open literature but of which the author is aware. Shontz and Trumm (1969) reported several sources from the literature which indicated that the reaction time to visual stimuli was longer under monocular viewing conditions than binocular viewing conditions, and that this difference was accentuated when the eyes were differentially light or dark-adapted. Also, reaction time increased when one eye was suppressed under conditions of binocular rivalry, as discussed in Section 2.4.8 below.

2.4.4 Luminance/Contrast

It has been shown in previous sections that the luminance and contrast of display scenes affects the visual perception of those scenes. In the special case of the helmet-mounted display, the luminance of the CRT at the eye or L_d(CRT) is a function primarily of the CRT luminance

(L_{CRT}), the transmittance of the optics (t_o)[1] and the reflectance of the combiner (r_c) and is given by the expression:

$$L_d(CRT) = r_c t_o L_{CRT}$$

Similarly, the luminance entering the display eye from the outside world or $L_d(scene)$ is a function of the ambient scene luminance (L_s), the transmittance of the visor (t_v) and the transmittance of the combiner (t_c), and is given by the expression:

$$L_d(scene) = t_c \; t_v \; L_s$$

(Note that for a partially silvered beam splitter combiner, $t_c \cong 1 - r_c$.) If the combiner is a bandwidth selective filter, as in the case of a trichroic or dichroic coating, the interaction of the spectral characteristics of the CRT and the combiner must be taken into account. Since the luminances from the outside scene and the display scene are additive, the total luminance available to the display eye is:

$$L_d = L_d(CRT) + L_d(scene)$$

$$= r_c \; t_o \; L_{CRT} + t_c \; t_v \; L_s$$

The contrast (C_d) of HMD scene is usually expressed as the increase in luminance contributed by the figure relative to the background or:

$$C_d = \frac{L_{figure} - L_{background}}{L_{background}}$$

[1]The light transmission properties of the optical components will be sensitive to the wavelength of light; therefore, discrete values for the transmittances and reflectances of the optics may be valid for only one wavelength.

(Note that this is similar to the same method for computing contrast in Section 2.3.2.4.) Contrast modulation (C_m) is expressed as the difference of the maximum to minimum luminance over their sum by the equation below:

$$C_d = \frac{L_{max} - L_{min}}{L_{max} + L_{min}}$$

L_{max} and L_{min} are the highest and lowest luminance values of the display. The contrast modulation, or C_m, is related to the expression for contrast by the equation below:

$$C_d = \frac{2\ C_m}{1 - C_m}$$

Since the total CRT luminance available to the display eye will always be greater than the ambient scene (i.e., the ambient scene luminance adds to the display luminance), another relationship is defined for describing the maximum figure to background contrast modulation (C_{max}) which can be made available to the display eye:

$$C_{max} = \frac{1}{1 + \frac{2\ t_v\ t_c\ L_s}{t_o\ r_c\ L_{CRT}}} \quad \text{for } L_{CRT} \neq 0$$

From the equation above, it can be seen that, as the ambient luminance approaches zero, C_{max} approaches 1.00 or, conversely, as ambient luminance becomes greater, C_{max} approaches zero. In other words, the ambient luminance limits the maximum contrast which can be presented via a see-through combiner into the display eye, the actual value being a function of the combined CRT and ambient luminances.

Based upon a review of the literature related to head-up virtual image displays, Cohen (1973) proposed a maximum value of $C_{max} \geq 0.23$ as acceptable for visual performance. This value was later confirmed by

Cohen et al. (1974) in a laboratory study. In this study, Cohen et al. presented a tribar resolution target to the display eye and a random-generated reticular pattern (noise) as the ambient scene to both eyes. Simulated CRT luminance (L_{CRT}) was varied from 42 to 792 cd/m^2, visor transmitted light (i.e., $t_v \times L_s$) was varied between 2.5 and 3344 cd/m^2 and combiner transmittances (t_c) of 0, 4, 10, and 25 percent were used. Data from this study are shown in Figure 2.4.2. The data show that at high contrast ($C_{max} > .40$) the minimum resolvable detail on the helmet-mounted display was less than 2 minutes-of-arc. However, if C_{max} falls below approximately 0.25, the smallest resolvable detail on the display increases in size, causing overall visual performance in perceiving the display to decrease. If the visual scenes were reversed (i.e., the tribar resolution target used as the ambient scene and the noise target used as a display scene), the outside scene would be perceived through the masking of the noise pattern until $C_{max} = 0.98$ as shown in Figure 2.4.3. It can also be seen from this figure that the variation in mean resolvable detail in the ambient scene varies inversely with C_{max}; however, the impact of C_{max} on the outside scene does not become significant until very high display luminances (relative to the ambient scene) are reached.

In the studies reported by Cohen et al. (1974) above, the visual material was generated by photographic slides consisting of high contrast tribar targets. The mean resolution data presented must be interpreted as minimum separable acuity which can be achieved by observers against high contrast targets. Electronic imaging displays, such as cathode-ray tubes, do not necessarily produce high contrast images. The contrast or modulation of the picture elements is a function of spatial frequency and is described by the modulation transfer function. The modulation transfer function for typical helmet-mounted display is described in Appendix A.3.2. Using the MTF concept, the effect of varying the optical parameters in the luminance transfer equations can be computed and a visual performance measure, such as MTFA (Section 2.3.3.1), used to relate the display performance to operator performance. Hershberger and Guerin (1975) have shown the relationship between the MTF and visual acuity threshold for various

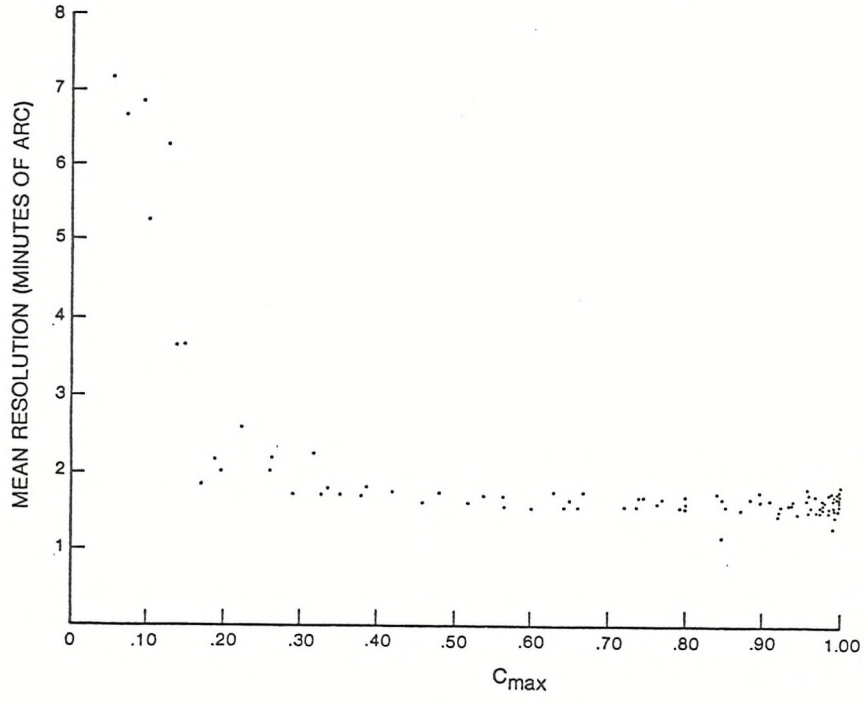

Figure 2.4.2. Mean Resolution as a Function of C_{max} for Imagery Presented on a Helmet-Mounted Display (after Cohen et al., 1974)

values of ambient luminance, display luminance, and combiner transmittance. Shown in Figure 2.4.4 is a family of curves relating the MTF of a typical helmet-mounted display with a limiting resolution of 740 TV lines per display width (370 cycles per display width at 10 percent modulation contrast for an average CRT luminance of 50 fL). Different MTF curves are shown for display luminances of 50, 100, 500, and 1000 fL due to the growth in the spot size with increasing luminance. The loss of modulation at the lower spatial frequencies is due to the interaction of the ambient light at 500 fL with the display luminances through the 10 percent transmittance visor. Three sets of visual demand curves (contrast sensitivity curves), are shown for theoretical subtended visual angles of the display of 15, 30, and 45 degrees. The four curves within each family are for different eye adaptation levels due to the ambient light, as shown. Again, the crossover between the MTF and the visual demand curve is the practical resolution limit of the display/observer interface, in that the operator's demand for

contrast information is beyond that which can be provided by the display at that spatial frequency.

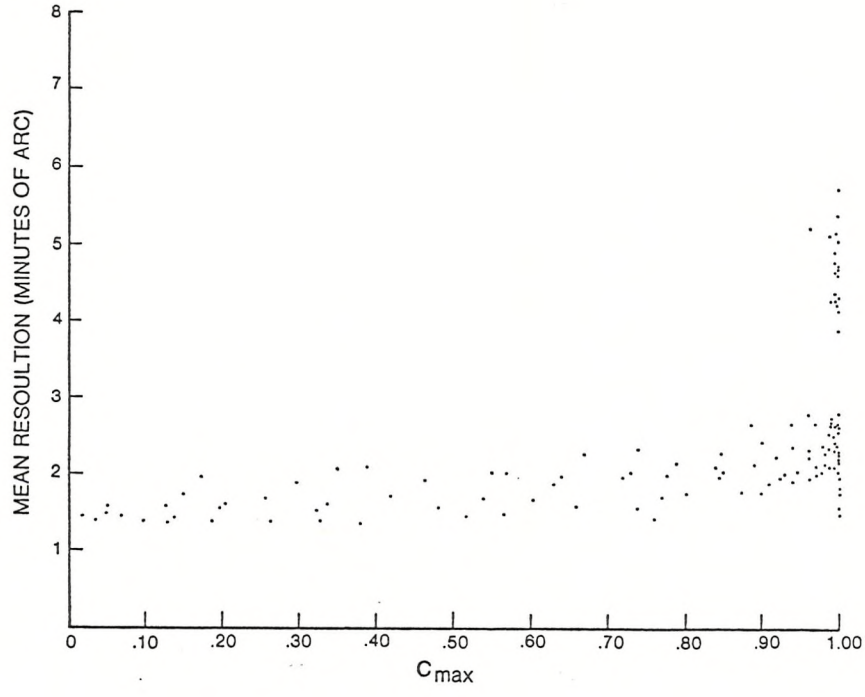

Figure 2.4.3. Mean Resolution as a Function of C_{max} for Background Imagery Observed Through the Helmet-Mounted Display (after Cohen et al., 1974)

As discussed in Section 2.3.3.1, the area between the MTF and visual demand curves, or the MTFA, has been correlated with visual performance. The theoretical MTFAs for some of the data in Figure 2.4.4 are shown in Figure 2.4.5. As can be seen, the MTFA is reduced by the ambient luminance for low display luminances and by the decrease in resolution at the high display luminances (10.0 percent transmittance combiner). To achieve the optimum performance (i.e., maximum MTFA), it would appear that either the average display luminance or combiner transmittance could be adjusted. Assuming that a visor transmittance of 0.10 is required to perceive the outside scene, then the display luminance should be adjusted to approximately 200 fL or at least 40 percent of the ambient. (Remember that the display and ambient luminance are additive.)

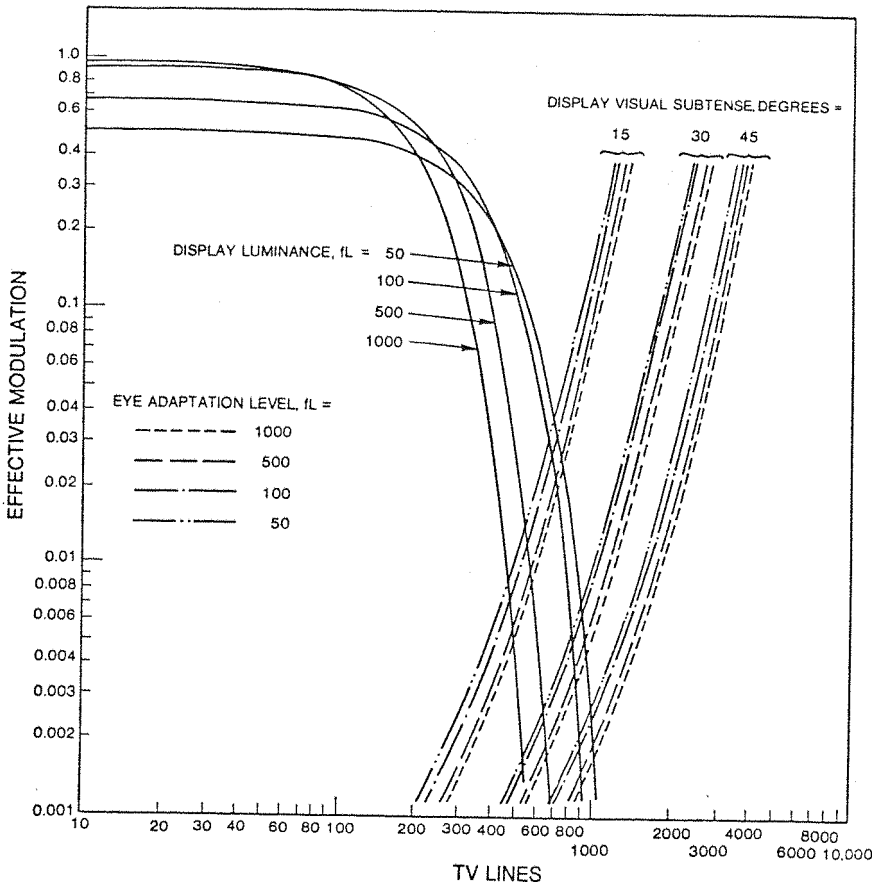

Figure 2.4.4. Modulation Transfer Function and Visual Threshold Function and Visual Threshold for 10.0 Percent Transmittance See-Through Display and a 500 fL Ambient (after Hershberger and Guerin, 1975)

The dynamic range of the display can be stated in terms of the number of steps of luminances which can be provided within the total range of minimum to maximum luminances. The commonly used measure for a grey step (GS) is given by the equation below for $\sqrt{2}$ grey steps.

$$\frac{L_{max}}{L_{min}} = (\sqrt{2})^{GS-1}$$

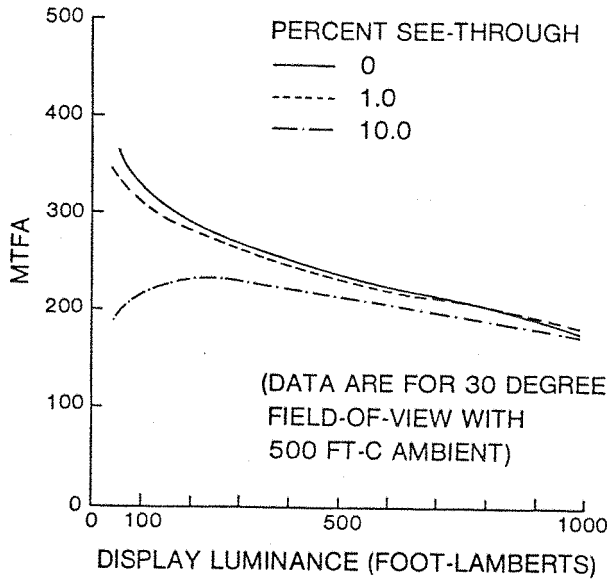

Figure 2.4.5. Estimated MTFA as a Function of Display Luminance for a 30 Degree Field-of-View Helmet-Mounted Display at Three Combiner Transmittances. (Plotted from Data from Hershberger and Guerin, 1975)

The number of grey shades (GS) is the number of $\sqrt{2}$ changes in luminance which are available within the total luminance range of the display. The number of grey shades can be determined from contrast modulation (C_m) using the equation below:

$$GS = \frac{2 \log \left(\frac{1 + C_m}{1 - C_m} \right)}{\log 2} + 1$$

Figure 2.4.6 shows a reinterpretation of the MTF curves from Hershberger and Guerin's (1975) data in Figure 2.4.4 in terms of grey shades. As can be seen, increasing the luminance causes an increase in grey shade rendition capability of the display, but at the same time, as shown in Figure 2.4.4, causes a fall off in resolution. Task et al. (1980) have suggested that the presentation of symbols on the helmet-mounted display requires only a one grey shade luminance change above the background luminance (i.e., C_d = 0.3 to 0.4), whereas pictorial imagery requires far more shades of grey to produce reasonable performance (i.e., C_d = 0.8 to 0.9). This statement implies that in

order to perceive high quality imagery. almost all of the ambient scene must be attenuated.

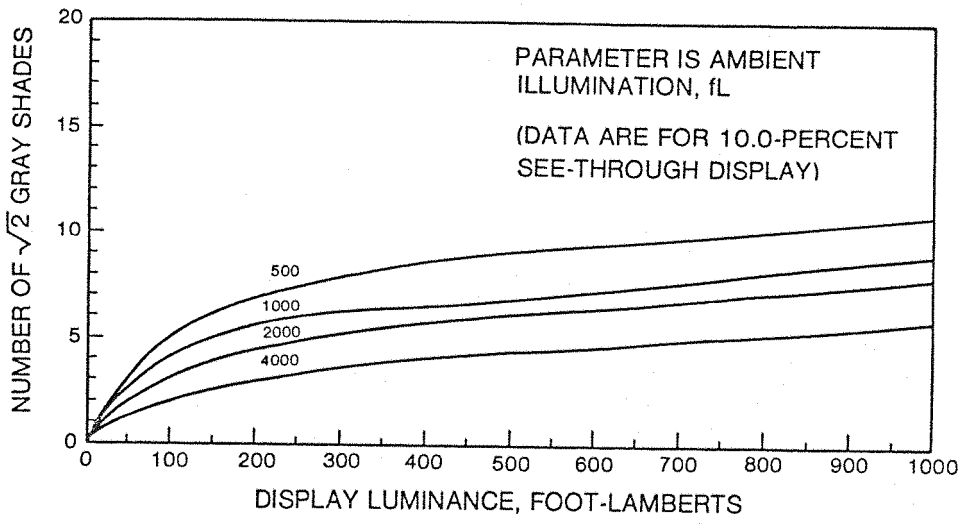

Figure 2.4.6. Number of $\sqrt{2}$ Grey Shades as a Function of Display Luminance and Ambient Luminance for a 10 Percent Transmission See-Through Display (after Hershberger and Guerin, 1975)

2.4.5 Brightness Disparity

As can be seen from the optical schematic in Figure 2.4.1, unequal amounts of luminance energy may be received by the two eyes due to the differences in the transmittances of the optical paths. The disparity in brightness between the two eyes can affect vision. One major effect, termed binocular rivalry, is discussed in Section 2.4.7. Hughes et al. (1973) argued that adverse perceptual effects due to brightness disparity in helmet-mounted displays may extend beyond the production of binocular rivalry. They cited a study by Gassowski (1941) wherein the discrimination of information presented to one eye was reduced when the other eye viewed a surface of different brightness. Jacobs et al. (1970) reported subjective flight trial data which may also support this finding. Observers viewing an occluded helmet-mounted display with the right eye (ambient light was excluded from entering the helmet-mounted display on the right eye) had great difficulty viewing the display image when the left eye was exposed to

high ambient luminances. Task and Hornseth (ca. 1974), whose experiment was cited in Section 2.4.3, admit that their findings for the helmet-mounted display were made under ideal conditions where no external light or scene was presented to the nondisplay eye.

One effect of the disparity of brightness between the two eyes is termed the "Fechner paradox" (1861) wherein a low intensity light seen by one eye reduces the perceived brightness of a more intense light seen by the other eye. More recently, Levelt (1968) has shown that the eyes have complimentary shares in the production of constant binocular brightness in that the increase in luminance in one eye leads to an equal decrease of the contribution of the other eye. Levelt described this effect by the linear relationship $e_\ell + e_r = c$, where for constant perceived brightness, the algebraic sum of the luminance of the left field (e_ℓ) and the right field (e_r) is some constant (c) which itself is a nonlinear function of stimulus energy.

Other studies have shown that the visibility of the helmet-mounted display scene is not completely dependent on the luminance in the display eye, but is also affected by the difference in luminances between the two eyes (e.g., Laycock, 1977). In order to consider the effects of differential eye luminance levels, Cohen (1973) defined interocular difference ratio (L_Δ) as an expression of the ratio of the average luminance of the display eye (L_d) to that of the nondisplay eye (L_x):

$$L_\Delta = \frac{L_d}{L_x}$$

Here the luminance transmitted to the nondisplay eye (L_x) is given by the equation:

$$L_x = t'_v L_s$$

where t'_v is the visor transmittance over the nondisplay eye, and L_s is the ambient scene luminance.

It may be recalled from Figure 2.4.1 that the transmittance of the visor over the display eye, t_v, is not necessarily equal to the transmittance over the nondisplay eye t'_v. It is reasonable to assume that, in order for both the display scene and ambient scene to be visible, L_Δ would have to lie within some reasonable range. In the same experimental study related above in Section 2.5.4, Cohen et al. (1974) determined empirically that the mean perceived resolution of a tribar target presented on the display with the noise scene as the ambient background (and in reverse) was a function of L_Δ. Data are shown in Figure 2.4.7 for the display scene, and in Figure 2.4.8 for the ambient scene, for various values of L_Δ. The authors concluded that, if L_Δ falls below 0.3, the visibility of the helmet-mounted display scene deteriorates and, conversely, if L_Δ is greater than 10, the display scene will interfere significantly with the ambient scene.

The findings above lead to the conclusion that in the absence of any consideration of image characteristics (i.e., contour, color, complexity, etc.), the interaction of the luminance transmitted by the optics of the helmet-mounted display to the left and right eye may seriously degrade the perception of either the outside or display scene. This effect could be pronounced if the luminance to either eye caused a concomittant lowering of the contrast sensitivity of the other eye to the extent that the distribution of luminances and spatial detail could not be perceived. The two criteria proposed by Cohen (i.e., $C_{max} \geq 0.23$ and $0.3 < L_\Delta < 10.0$) can be considered as approximate windows for adjusting the values of t_o, t_c, r_c, and t'_v, depending upon the expected ambient luminance levels and optimum CRT operating luminances.

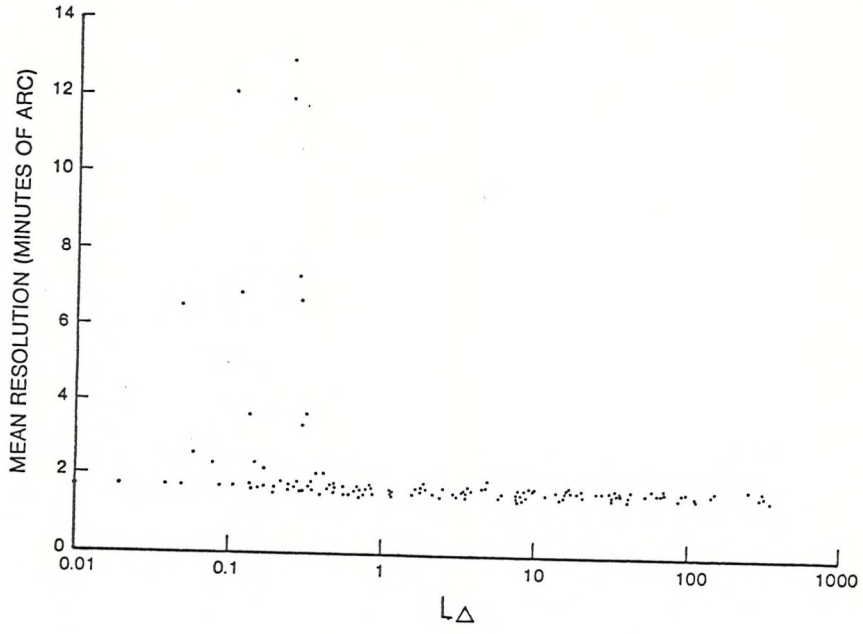

Figure 2.4.7. Mean Perceived Resolution as a Function of L_Δ for Imagery Presented on the Helmet-Mounted Display (after Cohen, 1973)

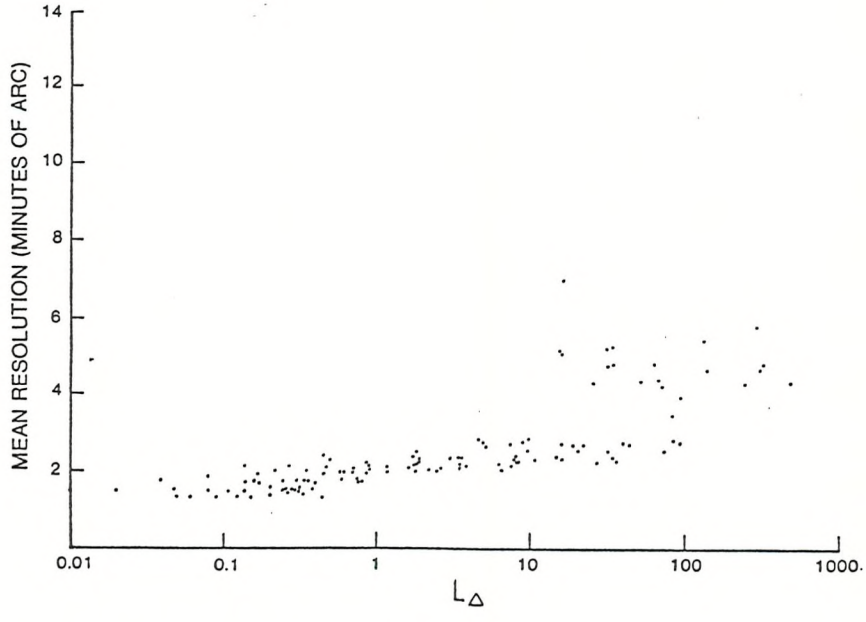

Figure 2.4.8. Mean Perceived Resolution as a Function of L_Δ for Background Imagery Observed Through the Helmet-Mounted Display (after Cohen, 1973)

2.4.6 Differential Eye Adaptation

Cornsweet (1970), amongst others, has described the process of photochemical adaption of the eye. Light quanta causes pigment in the retina to bleach (both rods and cones). The rate of the bleaching of the cone pigments (since mainly photopic vision is considered here) is a function of the integrated light energy at the retina. The threshold sensitivity of the eye to light is proportional to the fraction of the pigment in the bleached state or:

$$\log_{10}\left(\frac{\Delta L}{\Delta L}\right) = aB$$

where ΔL is the threshold intensity,

ΔL_0 is the threshold intensity after complete adaptation,

B is the fraction of rod or cone pigment in the bleached state

and $a_1 = 20$ for rod adaptation or

$a_2 = 3$ for cone adaptation

It follows from the relationship above that an adapting field of light which is different for each eye will cause a differential state of light adaption between the two eyes which, in turn, causes a difference in light sensitivity. Hughes et al. (1973) suggested that the differential adaptation of the eyes probably reduces somewhat the effects of brightness disparity (over the long term), even though a transient increase in luminance to the eye viewing the outside scene will cause some consensual pupillary constriction to the display eye thereby reducing the luminance to the retina. This action would cause perhaps the same perceptual effect as the brightness disparity noted above.

Although the differential adaptation state of the two eyes may not affect significantly the perception of the helmet-mounted display image, which is viewed monocularly, some abnormalities in depth perception of the outside scene may result. The Pulfrich effect is an apparent displacement in depth as an object moves in a plane normal to the line-of-sight when the light into the two eyes is considerably

different, or when the adaptation levels of the two eyes differ considerably. Using several sources from the literature, Shontz and Trumm (1969) and Hughes et al. (1973) suggested that the "Pulfrich effect" can be evoked by the differences in retinal illuminances between the display and nondisplay eyes. This may be produced either by the optics of the helmet-mounted display or by the differences in the adaptation state of each eye.

2.4.7 Binocular Rivalry

As discussed above in Section 2.2.4, the helmet-mounted display can be used to introduce supplemental information which the operator is required to integrate or use in conjunction with an outside scene. In some special circumstances, the helmet-mounted display scene may be used exclusively while ignoring the outside scene. The two sources of information (i.e., the display scene and outside world scene, may or may not differ). The helmet display scene may vary in complexity from a simple symbol to a pictorial image. At the same time, the outside world scene may be a homogeneous background, as in the case of the clear sky or night time scene, or may be complex with terrain features or aircraft cockpit structures and instruments. Depending upon the content of the helmet-mounted display and outside world scene and the luminance and contrast conditions under which they are presented, one of three possible perceptual states may be elicited:

1. The helmet-mounted display image may be superimposed on the real-world image and become a part of the real-world scene, both being clearly and simultaneously perceived.

2. A partial fusion of the images may occur in that a portion of the helmet-mounted display image may be inserted or imbedded in the outside world scene or vice versa.

3. The two scenes may appear to alternate between each other, one or other of the scenes temporarily dominating (being perceived) while the second scene is suppressed (not seen).

These affects appear because of the perceptual organization of the human visual system. As discussed previously, the human information processing system can be thought of as having several sensory organs interfaced through a multiplexing filter to a central processor. At any one time, the central processor processes the inputs from only one sensory modality. In the case of the visual sense organs, normally the scenes received by the two eyes are highly correlated and can be processed together. Some of the disparity information in the two scenes is used to compute depth (i.e., stereopsis or perhaps motion). With the introduction of the helmet-mounted display scene into the optical path of one eye, more disparity is introduced into the sensory organs. Depending upon the magnitude and nature of the disparity, the sense organ outputs may compete for access to the central processor, causing the central processor to interpret and/or process the disparate sensory returns to produce the perceptual effects above. In general, these perceptual effects can be categorized under the overall heading of binocular or retinal rivalry.

2.4.7.1 Observation of Binocular Rivalry in Helmet-Mounted Displays

Hughes et al. (1973) have defined binocular or retinal rivalry as the "irregular alternation of colors or figures when the two eyes gaze upon different fields that cannot be given unitary interpretation." Early investigators of the helmet-mounted display concept were keenly aware that a monocular helmet-mounted display could produce binocular rivalry with perhaps degrading effects on the perception of the outside world and/or the display scenes (e.g., Hall and Miller, 1960, 1963; Brown, 1964; Abbott, 1968; Furness, 1969; Jacobs et al., 1971). Early practical experiments with helmet-mounted displays, however, were inconclusive in assessing the incidence and effect of rivalry. Rivalry was reported to have occurred in some situations and not in others. For example, Hall and Miller (1963) observed no evidence of binocular rivalry during their experiment which involved the presentation of simple symbols on a monocular see-through display with a pictorial background.

Brown (1964) stated that viewing alphanumeric information on a see-through helmet-mounted display became difficult when superimposed on a complex background when both scenes had the same average luminance and viewing distance. Performance improved, however, when the apparent viewing distance of the virtual image plane of the helmet-mounted display was set at a different viewing distance from the outside scene. The observer could then focus on either scene, making the other scene out of focus or blurred. Jacobs et al. (1971) also concluded, from their qualitative laboratory and flight evaluation of occluded and see-through monocular helmet-mounted displays, the following:

1. Binocular rivalry was greatest when the two eyes were accommodated to the same distance.

2. Helmet-mounted display imagery information was degraded when viewed against a background consisting of a structured field or scene.

3. Rivalry was greater when the nondisplay eye was exposed to high ambient luminances.

4. Rivalry did not occur when simple symbolic information was presented on the helmet-mounted display.

In each case, the evidence above can be corroborated with the findings in the general literature. The lack of rivalry when simple symbols are presented on the helmet-mounted display was also documented by Cohen and Markoff (1972). This finding, and that of Jacobs et al. above, agrees with nonobservance of rivalry in the original experiments of Hall and Miller (1963).

2.4.7.2 Factors Affecting Binocular Rivalry

The general mechanisms and observed effects of binocular rivalry are extremely complex. The literature is replete with studies investigating the various factors affecting binocular rivalry. Shontz and

Trumm (1969) and Hughes et al. (1973) performed limited reviews of the literature in their treatments of the perceptual processes surrounding the perception of the helmet-mounted display. More recently, Laycock (1976) published a comprehensive review of 108 documents from an original bibliography of 133 addressing those binocular rivalry research findings most germane to helmet-mounted display design and application. The general trends in the literature, as surveyed by these authors, seem to apply in the case of binocular rivalry in helmet-mounted displays investigated experimentally by Cohen and Markoff (1972), Hershberger and Guerin (1975), and Laycock (1977).

The factors affecting binocular rivalry fall into two general categories: the attributes of the stimulus presentations and the characteristics of the observers. Table 2.4.1 lists some of the attributes of the stimuli and subjects which have been reported in the literature as affecting binocular rivalry.

2.4.7.3 General Conclusions About Binocular Rivalry in the Helmet-Mounted Display

From the discussions of binocular rivalry in the general literature, as well as the specific experiments by Cohen and Markoff (1972), Hershberger and Guerin (1975) and Laycock (1977), the following conclusions can be drawn regarding the impact of binocular rivalry on helmet-mounted display use:

1. It is apparent, generally, that the operator cannot process information from two conflicting visual fields simultaneously due to the alternation or dominance of one scene or the other.

2. Binocular rivalry has been shown to be a complex phenomenon involving a myriad of factors which can be related to the characteristics of the stimulus presented to each eye and to the individual characteristics of the operator. Rivalry will most likely occur when different complex images are presented to each eye with approximately equal contrast and

TABLE 2.4.1. FACTORS AFFECTING BINOCULAR RIVALRY

Attributes of the Observer	Attributes of the Stimulus Fields*
Ocular dominance	Sensory factors
Sensory dominance	Complexity of the stimuli
Motor dominance	Contour strength
Intelligence	Density
Visual acuity	Closure
Arousal	Continuity
Voluntary control	Viewing distance (accommodation)
Learning	Motion
	Luminance (interocular)
	Resolution
	Color
	Cognitive factors
	Semantic content
	Stimulus meaning
	Instruction set

*For competing visual fields

luminance. The literature indicates that the time for the operator to switch attention between scenes may vary from 1 s to 7 s for simple scenes.

3. The scene which has the greater contour or stimulus strength, (i.e., contours, luminances, contrast) tends to dominate.

4. Some voluntary control has been shown to affect binocular rivalry, especially in those situations involving differing instruction sets and learning; but under no experimental conditions have subjects been able to exert complete voluntary control over which of two conflicting scenes is processed.

5. Effects of binocular rivalry which may be detrimental to flight operations are:

   a. Increased response time in switching attention between different displays.

   b. Increased probability of missing information in the suppressed visual field.

   c. A lack of complete voluntary control of the scene which is selected by the observer for viewing from conflicting scenes in each eye.

6. The process of shifting attention is enhanced when the display scene is presented at a different viewing distance from the real-world scene.

7. Presentation of simple symbolic information on the helmet-mounted display with a see-through combiner/visor can be performed with little or no binocular rivalry.

8. The removal of one of the conflicting stimulus fields via occlusion or visual fixation will eliminate binocular rivalry.

9. The helmet-mounted display with a depressed optical axis as described by Hershberger and Guerin (1975) as a "bifocular display" eliminated the effects of binocular rivalry.

2.4.8 Image Interference

The experiments of Laycock (1977) suggested that a special case of rivalry of visual scenes occurs when the light transmission of the optical combiner of the helmet-mounted display is sufficiently high to allow the external scene to appear through the combiner along with the display scene. If the viewing distances are the same (i.e., the focal distance of the virtual image equals the viewing distance of the

outside field), the display scene may appear to overlay the outside scene. If one of the two scenes is simple, as in the case of an aiming reticle, then the two images may appear to be superimposed or a part of each other. If the two scenes are complex, then a conflict in processing the information of the two overlayed scenes can occur, causing an image interference or monocular rivalry condition. This condition may be lessened if the helmet-mounted display scene moves with the head. Depending upon the input into the other eye, the conflict may have to be resolved by the central processor using information from the nondisplay field (i.e., image separation and binocular rivalry). Jacobs et al. (1971) observed in their laboratory and airborne evaluations of the helmet-mounted display that rivalry (binocular or monocular) did not occur when symbolic information was presented on a see-through helmet-mounted display. Further research is required to determine the threshold of scene complexity and other stimulus characteristics that cause monocular rivalry.

2.4.9 Summary of Helmet-Mounted Display Perceptual Problems

The special perceptual problems associated with the helmet-mounted display can be attributed mainly to presenting a display scene to one eye and a separate scene to the other eye. Other perceptual problems, such as eye fatigue and space disorientation problems, may also exist, but as yet are undocumented. The motion of the display with the head can cause additional perceptual conflicts due to the vestibular control of eye movements. Some aspects of this problem will be discussed in Section 2.5.5.2.

Other problems of a perceptual nature may be caused by the mechanical interface of the exit pupil of the display optics with the entrance pupil of the eye. Sufficient personal adjustment ranges must be available in the helmet-mounted display design to provide for the centering of the exit pupil of the display optics over the entrance pupil of the eye. Furthermore, the exit pupil size should be sufficiently large to accommodate for any relative movement of the helmet on the head. The aspects of helmet to head movement will be discussed

later in Sections 2.5.3.12 and 2.5.6. Image distortion in some display optical designs, especially at the extremes of the exit pupil, may cause eye strain and headaches especially during large excursions of the helmet on the head. Similarly, improper focusing or collimation of the display image may also cause perceptual problems.

2.5 VISUAL PERCEPTION IN A VIBRATION ENVIRONMENT

2.5.1 Characteristics of Vibration

Within this thesis, the term "vibration" is defined as a sustained mechanical oscillatory disturbance applied to the body and/or to a display object. The nature of the oscillatory motion is deterministic if the motion is predictable at any point in time based upon a prior time history (e.g., sinusoidal or simple harmonic motion). Simple harmonic motion can be described by the frequency, amplitude, and direction of the motion. The frequency is the number of complete cycles of oscillation per unit time. The amplitude is the extent of the oscillation motion and is expressed relative to the maximum displacement from the equilibrium position, as peak, peak-to-peak (double amplitude), or root mean square values of displacement. The direction of the vibration is the vector direction of the applied oscillatory force. Vibration amplitude can also be expressed as velocity and acceleration, the first and second derivatives of the displacement with respect to time. Acceleration amplitude is expressed as distance per time squared (m/s^2) or in terms of the standard measure of gravity (g), where one g equals 9.81 m/s^2. It is often desirable to express the quantity of vibration displacement, velocity, and/or acceleration in terms of the root mean square (rms) value which has a direct relationship to the energy content of the vibration. The rms value (X_{rms}) of a time varying vibration quantity [x(t)] (i.e., displacement, velocity, or acceleration) is given by the expression:

$$X_{rms} = \frac{1}{T} \int_0^T x^2 (t)\, dt$$

where T is the period of time (t) over which the quantity is calculated.

For pure harmonic motion (i.e., motion at a single sinusoidal frequency), the relationships between displacement, velocity, and acceleration are described by the expressions:

$$\text{velocity (m/s)} = 2\pi \times \text{frequency (Hz)} \times \text{displacement amplitude (m)}$$

$$\text{acceleration (m/s}^2\text{)} = 4\pi^2 \times (\text{frequency})^2 \times \text{displacement amplitude (m)}$$

$$\text{acceleration (m/s}^2\text{ rms)} = \frac{\sqrt{2}}{2} \text{ acceleration (peak m/s}^2\text{)}$$

Vibration motion, which is periodic and can be defined mathematically by a time-varying function and whose waveform exactly repeats itself at regular intervals, is also classified as a deterministic motion (Bendat and Piersol, 1971). This type of complex, periodic motion can be represented by expansion into a Fourier series giving the combinations of discrete sinusoidal frequencies (and phases) which can be added together to produce the same waveform.

Nondeterministic vibration motion is aperiodic or random and can be described using statistical techniques based upon the Fourier transform and correlation analysis. In this case, the vibration motion can be expressed as the time-averaged estimate of the mean-squared value of the true amplitude as a function of frequency over a continuum of vibration frequencies (e.g., power spectral density). The analysis of vibration motion using statistical techniques is discussed further in Appendix A.5.1.

Other terms and definitions regarding the application of vibratory motion in this thesis will be used in accordance with the International Organization for Standardization, ISO 2041-1975 (E/F): Vibration and Shock Vocabulary and ISO 2631-1974 (E): Guide for the Evaluation of Human Exposure to Whole Body Vibration.

2.5.2 Nature of the Airborne Vibration Environment

The vibration forces in aircraft are complex, consisting of an admixture of deterministic and random components acting in three orthogonal axes with 6 degrees of freedom: three translational--X axis, Y axis, and Z axis; and three rotational--pitch, roll, yaw. These axes of motion follow the convention in Figure 2.5.1. These forces can be attributed to internal and external influences. Internal sources of vibration include the rotating components of the engine, aeroelasticity of the structure, and the dynamic response characteristics of the flight control system. External influences result from the interaction of the aircraft and the atmosphere in which it flies and include factors such as atmospheric turbulence. (For a more thorough discussion of the causes of vibration in aerospace vehicles, see Guignard and King, 1972.)

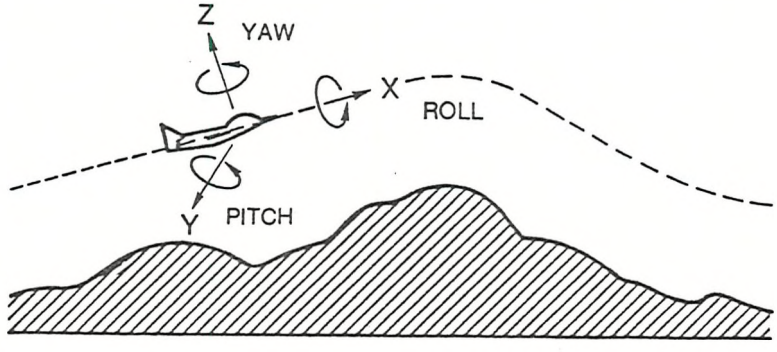

Figure 2.5.1. Axes of Translational and Rotational Vibration in Aircraft (after Speakman et al., 1971)

Rotary-wing and fixed-wing aircraft have different vibration characteristics due to differences in the nature of their propulsion systems and the way they interact with the atmosphere. Figure 2.5.2 shows typical power spectral densities (PSD) of translational accelerations in the X, Y, and Z axes and rotational accelerations in the pitch, roll, yaw axes for the F-4C "Phantom" fighter aircraft. The curves were computed by analyzing a vibration time history record of 120 seconds obtained while the aircraft was flying at a velocity of 1,110 ft/s

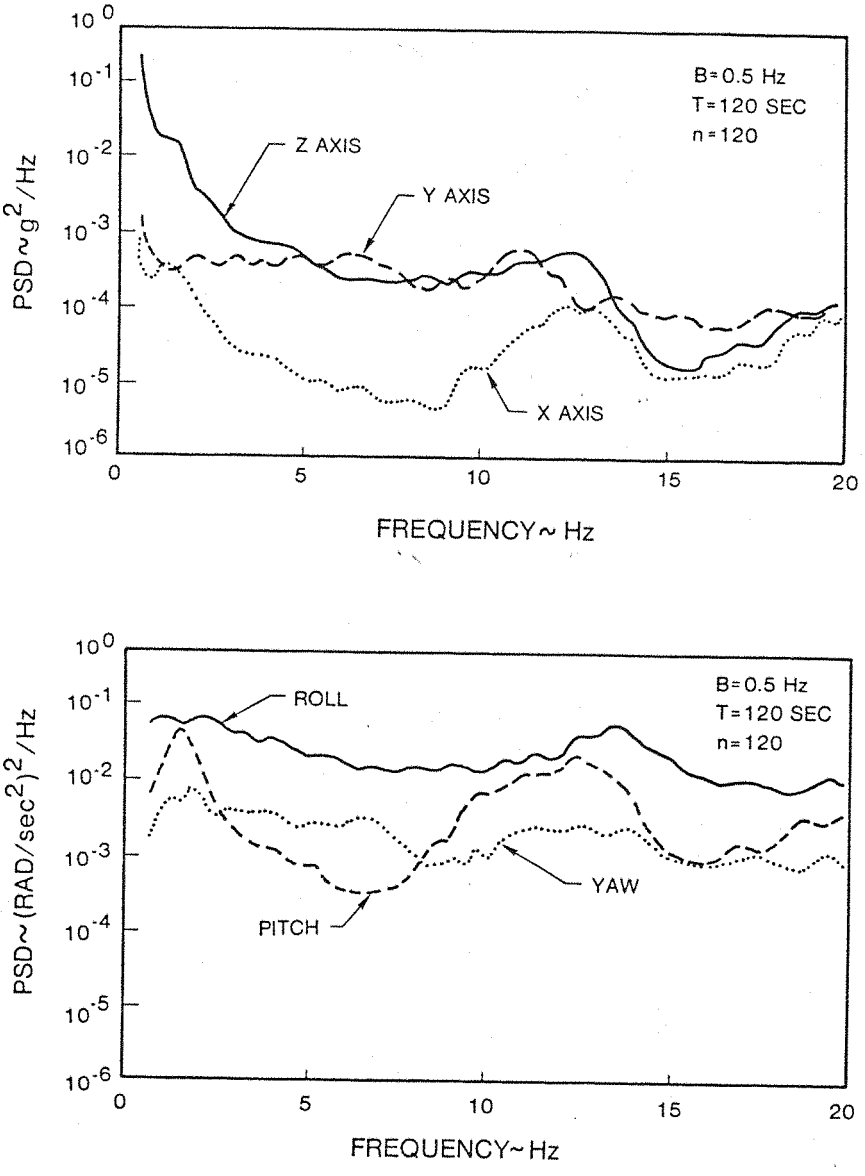

Figure 2.5.2. Power Spectral Densities for Vibration Acceleration in Six Axes Obtained from a F-4C Phantom Aircraft During Low Altitude, High Speed Flight (after Speakman et al., 1971)

(0.91 mach) over mountainous terrain with altitudes varying between 100 and 1000 feet. Vibration energy below 5 Hz was predominantly in the Z axis, decreasing by approximately 5 db/octave until about 8 Hz. X axis vibration followed the same trend, but with power levels approximately one order of magnitude lower. Rotational motion was greatest for the roll axis, with the greatest amount of energy between 1 Hz and 5 Hz and between 12 Hz and 14 Hz. Pitch motion peaked at 1.5 Hz and 13 Hz. The roll-off of pitch motion followed the trends observed for the Z and X axis translational motion. Figure 2.5.3 shows a composite of PSD curves for Z axis vibration over a range of flight conditions (altitude: 100 to 1000 feet; velocity: 0.73 to 1.1 mach) and over a variety of terrains (mountains, deserts, rolling fields, flat lands, and plains). As can be seen, the general forms of the PSDs were the same for most of the flights; however, the rms vibration levels at each frequency varied by a factor of 3 to 1. Speakman et al. (1971) attributed these differences to the variations in flight conditions, with perhaps the terrain features being the most important factor in causing variability of the vibration level.

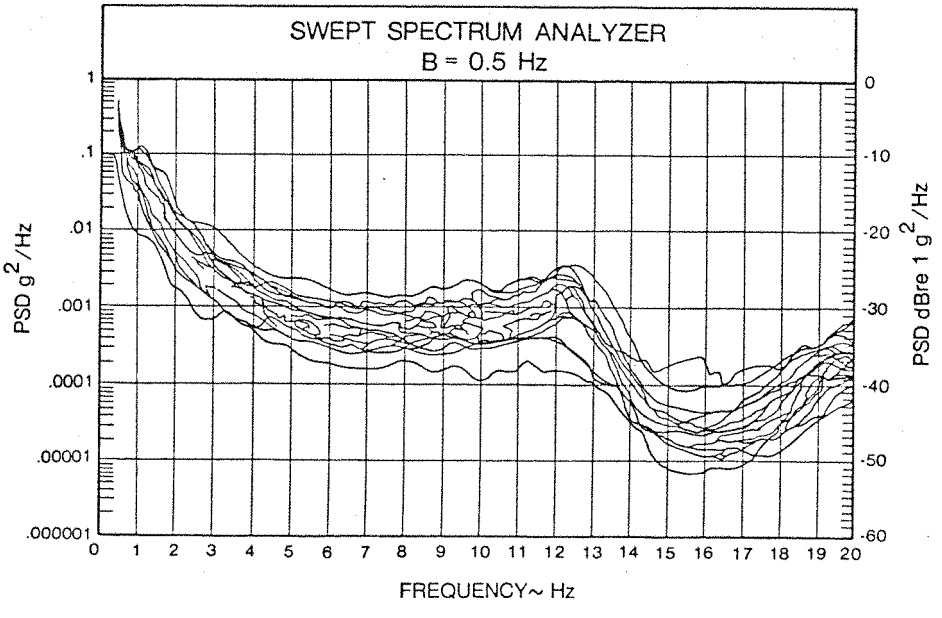

Figure 2.5.3. Composite of Power Spectral Densities of Z Axis Vibration Acceleration Obtained During 24 Flights of a F-4C Phantom Aircraft (after Speakman et al., 1971)

In a separate report, Speakman (1971) compared the vibration of the B-52 and B-58 aircraft with the F-4C. He observed that both the magnitude and frequency distribution of the power within the PSDs were different for each aircraft, with the average magnitude of the B-52 and B-58 about ten times less than that of the F-4C. He attributed these differences to the greater size and weight of the larger bomber aircraft. Also, the flight trials of the F-4C were made at very low altitudes and high speeds; therefore, it was more susceptible to high gust inputs and the introduction of pilot induced manoeuvres.

The power spectral density curves shown above often do not adequately provide a realistic representation of the vibration behaviour of fixed-wing aircraft. For example, inspection of time history records of a fighter aircraft flying at low altitude and high speeds generally show that there were frequent "quiet" periods with low amplitude broadband vibration interspersed with large amplitude "bumps" or "shudders."

In contrast to the fixed-wing aircraft, the vibration experienced in a rotary-wing (helicopter) aircraft is more deterministic. Figure 2.5.4 shows the PSDs of vibration acceleration in three translational axes obtained by Griffin (1972a) at the floor of the "Scout" helicopter during forward flight at 100 knots and at an altitude of 1000 feet above the ground. Griffin ascribed the peaks in the vibration spectra to sources such as multiples of the main rotor frequency (7, 14, 28, and 56 Hz) and the tail rotor frequency (33 Hz). He found that vibration levels were greatest in the vertical axis (Z axis) for all peaks associated with the main rotor frequency, and least in the lateral axis (Y axis) (with exception of 28 Hz). Vibration in the fore-aft (X axis) direction was greatest at the frequencies associated with the tail rotor. Although the levels of vibration changed for different flight conditions (e.g., ground-rotors turning, hover, forward flight at 60 knots, 100 knots, 115 knots at 1000 feet above the ground), the relative changes were similar in all three axes of vibration.

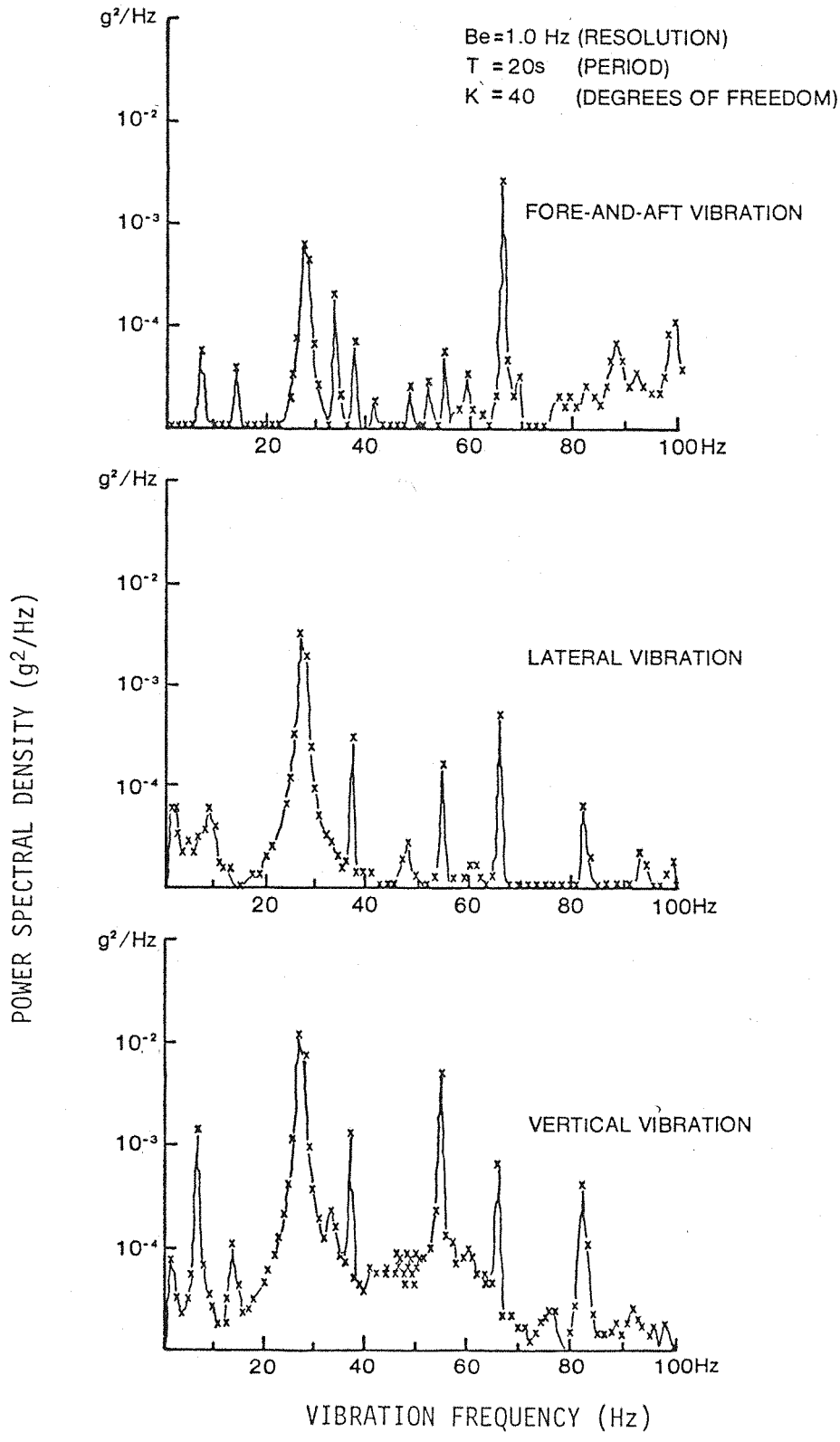

Figure 2.5.4. Vibration Acceleration Spectra at the Floor of a Scout Helicopter during 100 kt Forward Flight at 1000 ft Above Ground Level (after Griffin, 1972a)

Although some trends in the nature of vibration in aircraft can be observed, it should be cautioned that vibration may vary widely across the type of aircraft and the conditions under which each aircraft is flown. Aircraft type, flight parameters, terrain, weather, fuel load, and individual pilot control characteristics are among the factors which have been shown to affect the vibration characteristics of these aircraft.

For further information regarding the factors causing aircraft vibration and the characteristics of vibration, the reader is referred to Guignard and King (1972), AGARD-AR-82 and AGARD-CP-145. (For the full references regarding AGARD reports, see References).

2.5.3 Biodynamic Response to Whole-Body Vibration

The manner in which the body responds to forced oscillations, such as those described for aircraft, is also complex. From a mechanical standpoint, the human body cannot be treated as a simple mass or a combination of masses, but instead as an intricate structure incorporating structural members (skeleton) and masses (organs, head, limbs) which are supported and coupled by visco-elastic soft tissues. Some tissues can also change their mechanical properties by voluntary control, such as increasing muscle tension. Von Gierke and Clark (1971) have summarized the effects of vibration on the body as follows:

> ". . . the body when exposed to mechanical forces or motions does not react as a solid mass but is deformed and undergoes elastic changes in shape. Reactive, elastic, and viscous forces in the tissue result in stress distributions which depend on these properties, the geometric shape, and the time course or frequency of the load applied. When excited with certain input frequencies, resonances of body parts can occur, i.e., the deformation or displacement of the organ is much larger at the resonance frequency than at the other frequencies. For large masses combined with very soft elastic structures, these resonances are at low frequencies; for smaller masses or stiffer suspension, they shift to higher frequencies. The biologic effects of mechanical forces are to a large extent dependent upon this dynamic response of the system, which makes the effect of an input force dependent on its time course or frequency. All biologic reactions are mediated first through such mechanical

reactions; namely, through displacement of some tissue areas relative to adjacent areas or, in other words, through tissue stress. Small deformation of tissue can result in the stimulation of receptors; larger deformation of body segments or organs can influence their functional capacity. These larger deformations, such as head or eye motions or arm or hand vibrations, are also the ones the that interfere with normal task performance." [Von Gierke and Clarke (1971), p. 204.]

2.5.3.1 General Factors in Vibration Transmission to the Body

The vibration motion exhibited by the aircraft discussed in Section 2.5.2 is transmitted or coupled to the observer or aircrew member primarily by the main supporting structures of the seat, seat back, and headrest. Secondary means of vibration conduction include harnesses, lap belts, or other restraint mechanisms and/or man-mounted equipment (such as the oxygen mask), which have mechanical connections to the airframe for life support and communication. The use of head-coupled displays also provides an additional pathway for vibration conduction via the electronics cable leading to the helmet-mounted equipment. The mechanical properties of these supporting structures and conducting paths have a great influence on the perception and effect the vibration on the body. The factors discussed above can be classified as "extrinsic" factors, or those having to do with the system to which the operator is interfaced. Other extrinsic factors associated with the transmission of vibration to the body include: the direction or axis and area over which the vibration is applied to the body via the primary and secondary conducting media; the intensity of vibration and its frequency characterictics; the distribution of weight, mass, and dynamic properties of man-mounted equipment; and the characteristics of the conducting media, especially the dynamic interactions between the body and seat through the cushions.

Body weight, height, size, etc. also affect the biodynamic properties of the operator. Other factors, such as muscle tension, posture, and the position of the limbs and head which are under voluntary control, can change the coupling and distribution of vibration forces. These factors can be classified "intrinsic" factors, or those which are

related to the properties of the human being exposed to the vibration. [The reader is referred to Guignard and King (1972) and Griffin et al. (1978) for a summary of the intrinsic and extrinsic properties affecting biomechanical behaviour under vibration.]

2.5.3.2 Methods of Describing Vibration

The direction that the vibration force is applied to the body follows the convention established by ISO 2631-1974 (E) as shown in Figure 2.5.5. Following this convention, the direction of the vibration force will be given relative to the gravity vector (e.g., "vertical Z axis seat vibration" indicating that the vibration force is applied in a direction parellel to the gravity vector and along the longitudinal direction of the spine in a seated observer). Conventions for rotational movements of the load are given in Section 5.1.

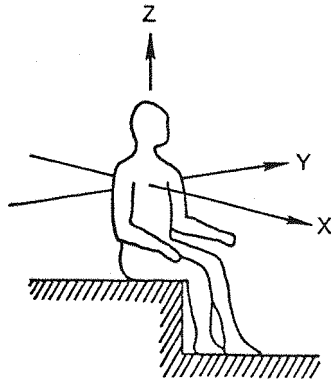

Figure 2.5.5. Directions of Coordinate System for Mechanical Vibration Influencing Humans [From ISO 2631-1974(E)]

"Transmissibility" is defined as the quantity of vibration transmitted from the seat to the body and is expressed in terms of the ratio of the amplitude of oscillation motion at some point on the body (e.g.,

head, shoulder, legs) to the amplitude of the source of excitation (the seat structure), when the body is undergoing some steady-state forced vibration [ISO 2041-1975 (E/F)]. The transmissibility or amplitude ratio is nondimensional and can be a ratio of forces, displacements, velocities, or accelerations. Typically, the vibration motions are measured with accelerometers. If the relationship of the output to input motion is linear (as defined in Appendix A.5.1), then the system response can be related to the input vibration as a transfer function. Depending upon the analysis procedures used (and described in Appendix A.5.1), the transfer function can relate, as a function of frequency, both the modulus or amplitude response and the phase response of the site being measured relative to the excitation input. Mechanical impedance is another measure of system behaviour during simple harmonic motion. It is a complex ratio of force and velocity taken at the same or different points in the system [ISO 2041-1975 (E/F)]. Mechanical impedance is probably most useful in developing models or analogues of the biomechanical system, whereas transmissibility is most useful for describing biodynamic behaviour in terms which can be related to visual performance in head-coupled systems.

2.5.3.3 Transmissibility of Vibration to the Head

Since in most aircraft the aircrew are seated in an upright position and the predominant vibration force is acting in the Z axis direction (as discussed in Section 2.5.2), it is most appropriate to focus the review of head transmissibility on those situations where vertical vibration has been applied to the Z axis direction of seated subjects. The transmissibility of vertical vibration from the seat to the head has been measured by numerous authors (e.g., Guignard and Irving, 1960; Pradko et al., 1965; Griffin, 1975a; Griffin and Whitham, 1978; Lewis, 1979). Seat-to-head transmissibilities obtained by these authors are compared in Figure 2.5.6. Although these data were obtained for vertical sinusoidal vibration under different seating and instrumentation conditions, there is agreement in the form of the data. Generally, the amplitudes of head-to-seat movement are greater than 1 for vibration frequencies between 2 and 7 Hz, indicating that

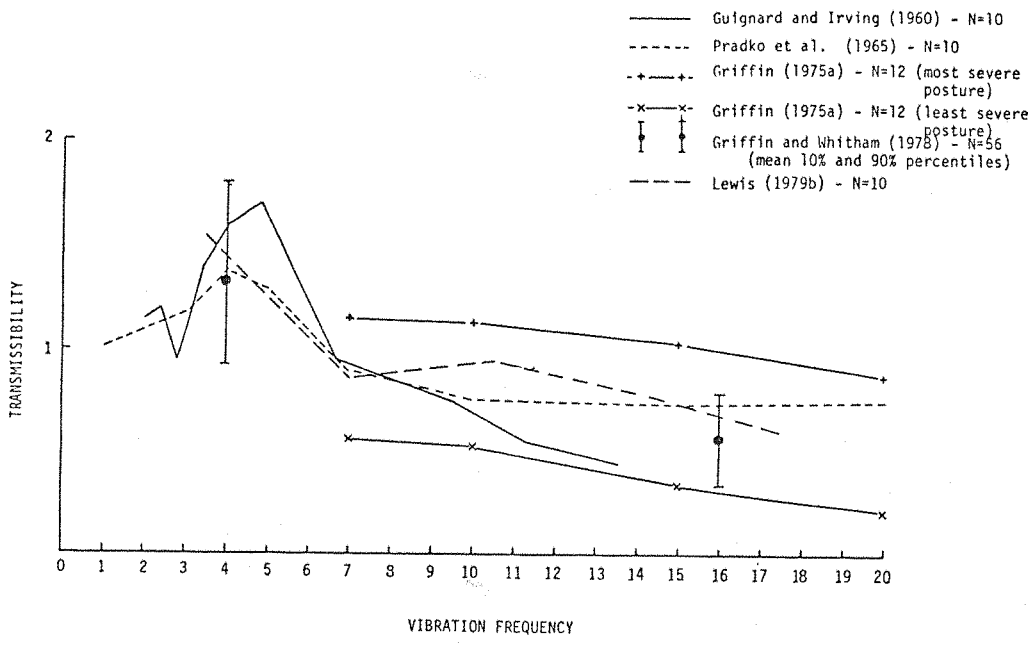

Figure 2.5.6. Comparison of Seat-to-Head Vibration Transmissibilities

the mechanical system of the body is amplifying the motion of the head. Almost all experimenters have identified a resonance frequency between 4 and 6 Hz. There seems to be general agreement that this behaviour is associated with major body resonances of the upper torso and shoulder girdle (Guignard and King, 1972), although Von Gierke and Clark (1971) have indicated that, within this frequency range, the abdominal viscera also have been observed to resonate in and out of the rib cage. The resonance effects in this frequency range are probably a combination of the individual resonances in the pectoral girdle, thorax, and abdominal regions. Guignard and Irving (1960), using high speed cinematography, also showed that nodding of the head (pitch-axis) and interior-posterior flexion of the upper spine accompanied the resonance at 5 Hz. At frequencies below 1 to 2 Hz, there are no significant resonances (Z axis) and the body behaves as a single mass (Guignard, 1965).

The rapid roll-off of transmissibilities above a vibration frequency of 6 to 8 Hz is probably due to the absorption of vibration in the thoraco-abdominal cavity. Guignard (1965) and Guignard and King (1972) identified a second and possibly a third resonant mode at

frequencies between 11 to 14 Hz and 17 to 25 Hz, respectively. They postulated that the second resonance was due to an axial compression of the torso accompanied by a bending moment of the spinal column, while the third resonance was probably that of the head relative to the trunk through a compression and/or flexion of the cervical spine.

2.5.3.4 Effect of Posture, Muscle Tension, and Seating Condition

The second and third resonances of seat to head transmissibility discussed above do not appear in the data shown in Figure 2.5.6. A possible reason for their observation may be due to the seating configuration used in the respective vibration transmissibility experiments. Rowlands (1977), Griffin et al. (1978) and Lewis (1979b) were able to show a dramatic increase in the transmissibility of vertical Z axis vibration to the head in the frequency region of 12 to 20 Hz when subjects were restrained against seat backs or when required to increase muscle tension voluntarily by setting in an "erect" rather than a "slumped" posture. Representative data from the experiments by Rowlands (1977) are shown in Figure 2.5.7. The data was for one subject who, according to the author, exhibited average characteristics. Rowlands used a hard seat back and seat base and subjects were restrained at the lap, but not at the shoulders. Subjects were presented with a vertical Z axis sinusoidal vibration at a level of 2.0 m/s^2 (peak) swept from 1 to 25 Hz. It can be seen that, between 10 Hz and 20 Hz, the "erect" posture (i.e., sitting at attention with back against back rest) increased the transmission of vibration to the head by 200 percent over the condition where the subject removed his back from the seat back. The "slumped" position was an intermediate position wherein the back was in light contact with the seat back. Even though the seat back contact and erect posture increased transmissibility above 10 Hz, it tended to lower the transmissibility below 10 Hz. Perhaps the stiffening of muscles in the thoraco-abdominal area and spinal areas changed the stiffness and subsequently the damping ratio of the resonance within the 4 Hz to 6 Hz frequency range. Similar results were obtained by Griffin et al. (1978) and Lewis (1979b) when comparing seat-to-head transmissibilities with a flat seat versus a hard helicopter-type seat with a seat back. These

results indicate that the seat back can provide a significant secondary conducting path for vibration to the head, especially at frequencies greater than 10 Hz.

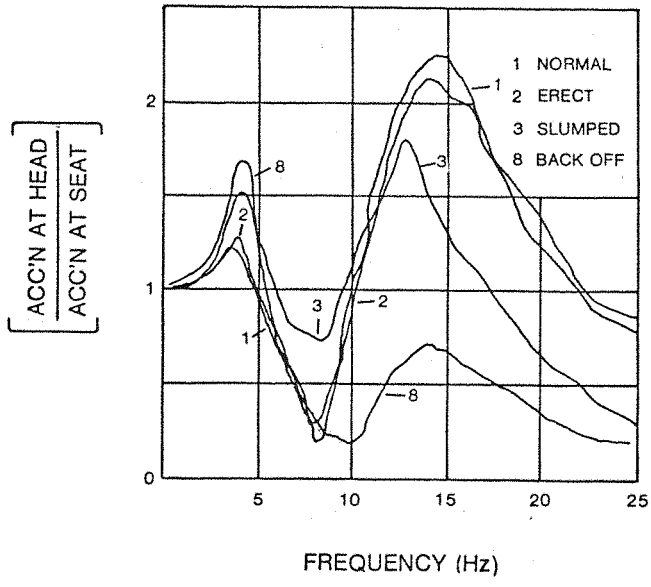

Figure 2.5.7. The Effect of Posture on the Transmission of Vibration from the Seat to the Head (after Rowlands, 1977)

Griffin (1975a) also found that subjects could voluntarily control seating posture to maximize or minimize the sensation of vibration at their heads. The ratio of the transmissibilities of the "most severe" posture (i.e., greatest vibration transmitted to the head) to the "least severe" posture, was 2.07 at 7 Hz, increasing to 4.0 at 20 Hz and up to 6.66 at 45 Hz. During all of these conditions, the subject sat on a flat hard seat with no backrest and, therefore, could easily change his sitting posture. Griffin's findings emphasized the need to control postural and muscle tension variables by seating configurations and by appropriate instructions.

2.5.3.5 Effect of Head Position

Guignard and King (1972) observed that when subjects sat erect and looked upward by head rotation, there was an increase in the vertical

seat-to-head vibration transmissibility. Griffin et al. (1978) also found that the position of the head affected transmissibility, as can be seen in Figure 2.5.8. These data indicated (for one subject) that looking up at 25 to 50 degrees above the horizontal tended to increase seat-to-head transmissibility, while looking down by the same amount decreased transmissibility. The magnitude of these effects were frequency dependent, with the greatest effect (800 percent) occurring between the 50 degree upward to the 50 degree downward positions at 16 Hz. Again, this behaviour may result from the way that the muscles in the neck are stiffened and by the orientation of the vertebrae in the cervical spine.

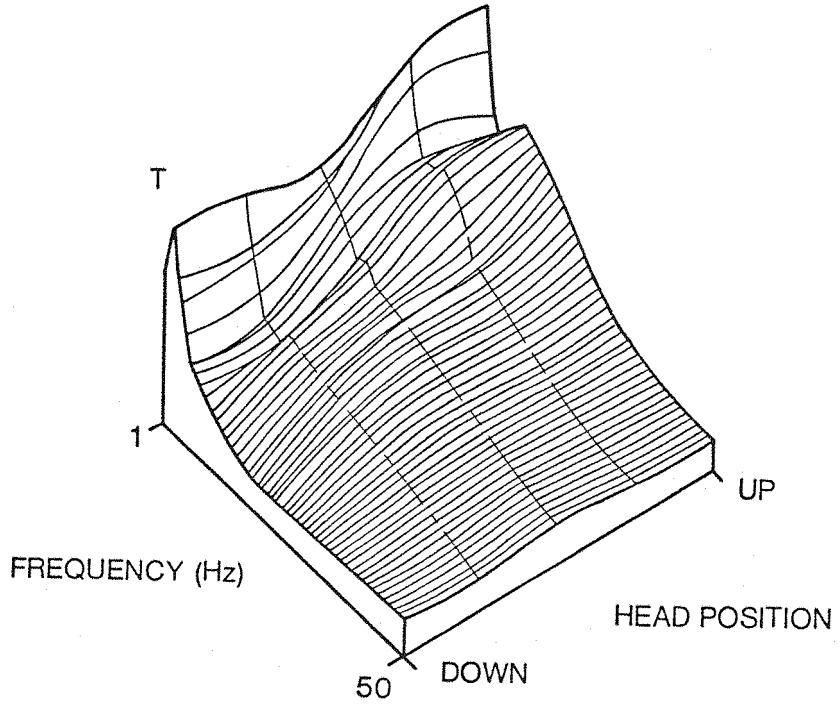

Figure 2.5.8. Transmission of Vertical Z Axis Vibration of the Seat to the Head for One Subject with Five Head Positions: Horizontal, 25 Degrees, and 50 Degrees Above and Below the Horizontal (after Griffin et al., 1978)

2.5.3.6 Individual Differences

Under experimental conditions wherein posture was a controlled variable, there was still a large intersubject variation in vibration transmissibility to the head. Griffin and Whitham (1978) measured the seat-to-head transmissibilities of 56 men, 28 women, and 28 children using vertical Z axis vibration at 4.0 Hz and 16.0 Hz (1.0 m/s^2 rms). They found that the data assumed (after logarithmic transformation) a normal distribution, with a mean transmissibility of 1.35 at 4 Hz and 0.58 at 16 Hz for the adult male subjects. About 20 percent of the population had transmissibilities either less than 1.0 or greater than 1.8 at 4.0 Hz and less than 0.4 or greater than approximately 0.8 at 16 Hz. The authors could find no significant differences between the distributions across populations due to sex or age, but did find a significant correlation ($p < .05$) between body weight and vibration transmissibility at 16.0 Hz for both men and women. (Generally, across the literature surveyed, there does not seem to be any consistent correlation between the reported physical characteristics of the body and the transmission of the vibration to the head.)

The wide population variance described by Griffin and Whitham and others reinforces the need to be judicious in analyzing and presenting transmissibility data across several subjects. Often the mean or median data and its distribution as a function of frequency does not reflect the behaviour of any one subject in form or magnitude, since averaging the data can obscure resonant peaks due to individual differences in frequency and amplitude of resonance. For these reasons, several authors have elected to present individual subject data along with the averaged data.

Griffin et al. (1978) were able to show that within subject variability was less than between subject variability, providing that seating condition, posture, and muscle tension were the same. They presented data for the vertical Z axis seat to head transmission for one subject over a 1 Hz to 100 Hz frequency range at a 1.0 m/s^2 rms vibration level. The data were obtained during 21 runs over a 2 week period and indicated a consistent location of resonant peaks at

2.0 Hz, 5.0 Hz, and 12 Hz with 80 percent of the transmissibility measurements being within ±20 percent of the median transmissibility. By contrast, the data obtained by Griffin and Whitham (1978) showed that 80 percent of the transmissibilities measurements for 56 men were within approximately ±33 percent of the mean transmissibility.

2.5.3.7 Rotational Movements of the Head

Several authors have indicated that the vertical Z axis vibration applied to seated subjects causes oscillatory movements of the head in directions other than vertical. Guignard and Irving (1960) observed from cinematographic records the nodding of the head (in the pitch axis) at the 5 Hz resonant frequency. Griffin (1975a) measured translational movements in the X, Y, and Z axis and rotational movements in the pitch axis of the head during vertical (Z axis) seat vibrations. He found that vibration of the head in the lateral (Y axis) was approximately 10 to 20 percent of vertical (Z axis) head motion. Postural variables (i.e., adopting the most severe versus the least severe postures) also had a significant effect on lateral (Y axis) head transmissibility. Fore-aft (X axis) motion of the head was up to 95 percent of the level of the vertical seat movement following the same transmissibility versus frequency roll-off as the vertical (Z axis) head vibration. Griffin noted that the transmissibilities of vertical vibration to the fore-aft (X axis) of the head was highly nonlinear at 7 Hz and contained frequency components twice the input vibration frequency (i.e., 14 Hz) which were 20 to 50 percent of the magnitude of the fundamental vibration level. There was little effect of posture on the fore-aft (X axis) transmissibilities below 15 Hz, but changes in posture did cause transmissibilities to vary more than a factor of 2 to 1 at 40 Hz. Mean peak pitch motion of the head at 7 Hz was ±10 minutes-of-arc per m/s^2 rms of vertical seat motion, with a steep roll off of 20 db/octave up to 40 Hz.

Rance (1978) and Lewis (1979b) also measured rotational motions of the head in pitch, roll, and yaw axes due to vertical Z axis sinusoidal seat motions. Rance (1978) found that the maximum amplitude for head rotational motion in pitch, roll, and yaw occurred at about 5 to 7 Hz

when vertical Z axis vibration of 7.85 m/s^2 (peak-to-peak) produced a 12 rad/s^2 rms, 5 rad/s^2 rms, and 3 rad/s^2 rms oscillation of the head in the pitch, roll, and yaw axes, respectively. Rance's data also indicated that the rotational motions of the head contained second harmonic components with amplitudes up to 50 percent of the fundamental. Lewis (1979b) found that subjects seated in a helicopter-type seat with hard seat and seat back surfaces (instead of cushions), and restrained with a lap and shoulder harness, demonstrated a significantly greater amount of pitch rotational movement of the head than if seated on a hard flat seat with no backrest. The mean data from his experiment are shown in Figure 2.5.9. Although the head pitch motion for the helicopter seat was greater over the total frequency range of 2 to 50 Hz, it was especially dramatic (up to a 400 percent change) beyond 14 Hz. Lewis argued that the flat seat vibration was attenuated by the body before reaching the head, but was allowed to be transmitted directly to the shoulders and upper back by the helicopter seat via the seat back and harnesses. The direct transmission of vibration by the seat back thereby caused the increased head pitch motion.

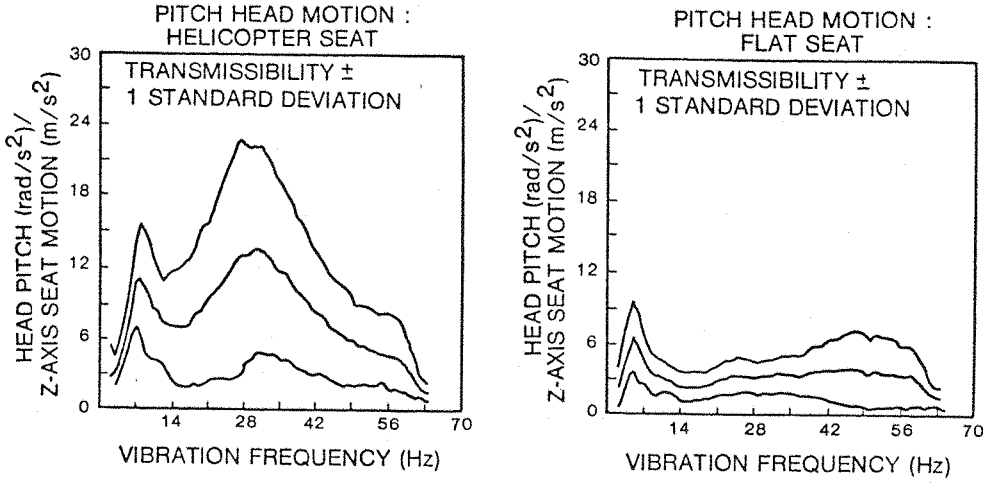

Figure 2.5.9. Mean and ±1 Standard Deviation of Head Pitch Motion of 10 Subjects in Response to Vertical (Z Axis) Seat Motion of 1.6 m/s^2 rms with Simulated Helicopter and Flat Seats (After Lewis, 1979)

Barnes and Rance (1974, 1975) found that rotational oscillations of the body induced rotational motions of the head. The gain and phase relationships which they determined for the transfer of rotational vibration are shown in Figure 2.5.10 for the roll, pitch, and yaw axes with subjects restrained by shoulder and seat harnesses. Again, the maximum gain was observed at about 4 Hz for the roll and pitch axes but there was a smooth roll off (approximately 3 db/octave) with a slight dip at approximately 6 Hz for the yaw axis. The authors noted that the motion of the seat in one axis tended to also induce some motion of the head in the other axis. Cross-coupling of roll and yaw motion of the seat to the pitch axis of the head was typically 5 times lower than that of the head pitch motion exhibited due to pitch motion of the seat. Also, the motion cross-coupled to the pitch axis of the head from roll or yaw motion of the seat had a second harmonic content between 1 and 6 Hz, which was approximately equal to the fundamental frequency.

The rotational motions of the head due to translational and rotational oscillating forces applied to the body will probably have a great influence on the perception of helmet-mounted displays, since the rotation of the head stimulates the semicircular canels, thereby eliciting the vestibulo-ocular reflex. This aspect of the relationship of biodynamic and visual performance will be discussed in Section 2.5.5.2.

2.5.3.8 Linearity

In order for the biomechanical system to exhibit linearity, the ratio of head motion to seat motion should remain constant over a range of seat vibration amplitudes (at one frequency). Pradko et al. (1965) found that for vertical Z axis sinusoidal vibration of the seat, head Z axis acceleration was reasonably linear for vibration amplitudes from 0.1 to 0.8 g_z (rms) at discrete frequencies of 3 Hz to 60 Hz. Guignard and King (1972) cited the results of seven investigators indicating that the vertical Z axis response of the head at 5 Hz was linear up to acceleration amplitudes of about 0.5 g, but at greater levels, the transmissibility tended to decrease. Griffin (1975a)

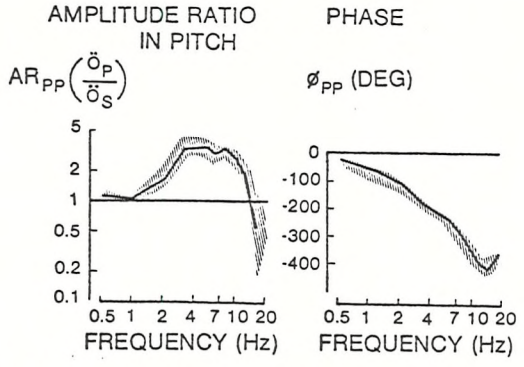

A(PITCH AXIS - 8 SUBJECTS AT 5 rad/s^2 PEAK
(AFTER BARNES & RANCE, 1975)

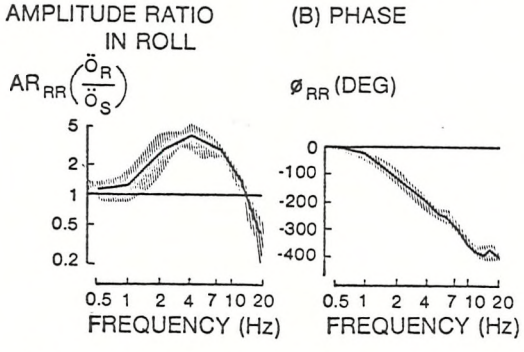

B) ROLL AXIS - 8 SUBJECTS AT 10 rad/s^2 PEAK
(AFTER BARNES & RANCE, 1975)

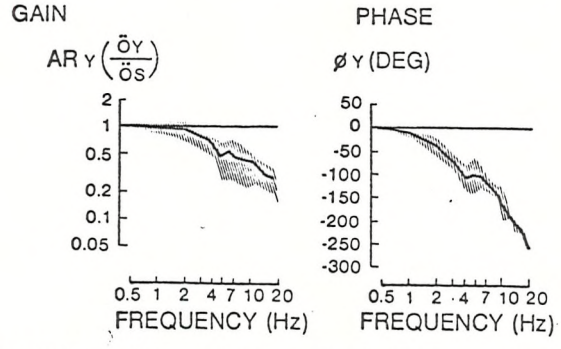

(C) YAW AXIS - 8 SUBJECTS AT 70 rad/s^2 PEAK
(AFTER BARNES & RANCE, 1976)

Figure 2.5.10. Mean and ±1 Standard Deviation of Modulus and Phase of Head to Seat Rotational Vibration Transfer Functions in the Pitch, Roll, and Yaw Axes

found that the effect of vibration level on head to seat transmissibility was statistically significant and that, for the "least severe" posture condition, the interaction of vibration level and frequency was also highly significant. Inspection of Griffin's results show that the nonlinearity tended to occur at frequencies less than 20 Hz and at vibration levels less than 1.0 m/s^2 rms. Rowlands (1977) also found that vibration level (2.0, 2.8, 4.0 m/s^2 peak) affected transmissibility, depending somewhat upon seating conditions. However, the differences were not greater than 15 percent and were not consistant across subjects. Griffin et al. (1978) found that for a 7 to 1 change in vertical Z axis vibration level at the seat (0.4 to 2.8 m/s^2 rms), there was little change in the seat to head Z axis transmissibility when the vibration frequency was swept from 1 Hz to 50 Hz, except at some lower frequencies (less than 10 Hz) when the maximum variation due to vibration level was about 30 percent. Guignard and King (1972) and Griffin (1975a) postulated that these nonlinearities may be caused by voluntary muscle tensing and/or control of posture to "tune out" unpleasant sensations due to the vibration. This hypothesis was the subject of other experiments by Griffin et al. (1978). In one experiment, they found that when a single subject was exposed to three different vibration spectra of vertical Z axis random vibration (using a hard flat seat), the seat to head transmissibilities reflected only small changes above 9 Hz (where vibration transmission was inherently lower), but below 9 Hz (viz. between 4 Hz and 8 Hz), they observed that the transmissibility was inversely proportional to the amount of low frequency energy in the spectra. This finding suggested that although the subject attempted to maintain the same posture during the three vibration spectra conditions, he may have changed his posture or muscle tension unconciously to reduce the transmission of vibration through the body at those frequencies that caused the most discomfort. In another experiment, Griffin et al. (1978) observed that sinusoidal vibration frequency sweeps of long duration tended to produce lower seat to head transmissibilities than those of shorter duration. The authors speculated that the shorter sweep periods did not allow enough time for the subject to change to a posture that reduced transmissibility. Even though nonlinearities have been observed in their experiments and those by others, Griffin et al. (1978) argued that the

magnitude of the nonlinearities were really insignificant when compared to the variabilities due to the other factors, such as intersubject differences. In any case, large interactions between postural and muscle tension variables and the linearity of vibration transmission in the body have been demonstrated.

2.5.3.9 Effects of Vibration in Other Axes

When vibrated in the X axis (fore-aft) and Y axis (lateral), major body resonances have been observed in seated subjects between 1.5 Hz to 2.5 Hz. These resonances have been associated with flexion of the lumbodorsal spine and/or articulation (fore-aft) of the hip joints (Guignard, 1965). The increased sensitivity of the body to vibration motion at low frequencies in the horizontal plane is reflected in ISO 2631-1974 (E) wherein the 8-hour fatigue decreased proficiency boundary level at 1 Hz to 2 Hz is approximately 0.22 m/s^2 rms, whereas for the vertical Z axis motion, the same boundary is approximately 0.32 m/s^2 rms for the frequency range of 4 Hz to 8 Hz. Rance (1978) and Lewis (1979) have shown that seat motions in the horizontal plane also produce rotational head motions in pitch, roll, and yaw axes. Again, peaks in the amplitudes of these motions occurred at frequencies between 4 Hz and 8 Hz, but also there may be low frequency head resonances in roll and yaw. During X axis (fore-aft) movement of the seat, the pitch motion of the head predominanted, whereas for Y axis (lateral) motion, roll, and yaw motion of the head predominanted.

As shown in Figure 2.5.11, Lewis (1979b) found that the ratio of the pitch motion of the head to seat fore-aft (X axis) motion was of the same order as that of head pitch to seat vertical (Z axis) motion (Figure 2.5.9) as long as the subjects were restrained in a seat with a seat back. Unrestrained motions using a flat seat are also shown. Head roll motion due to seat lateral (Y axis) motor is also shown in Figure 2.5.11.

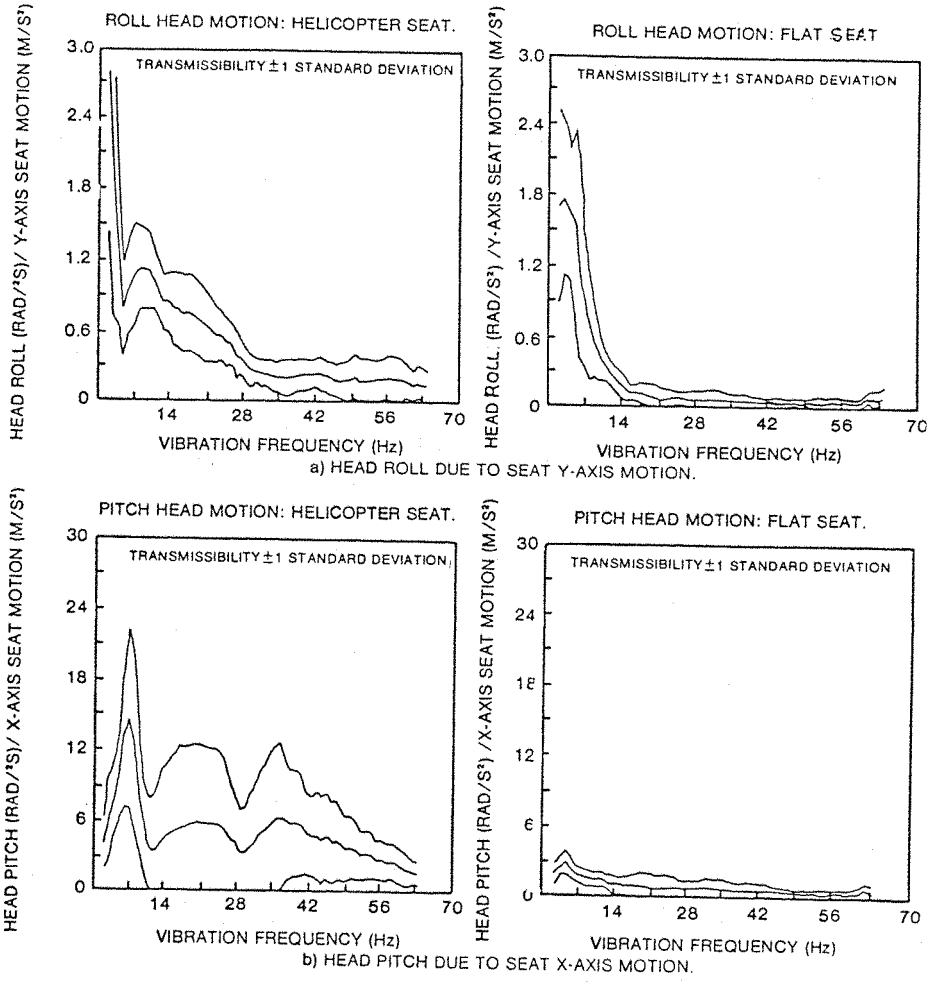

Figure 2.5.11. Mean and ±1 Standard Deviation of Rotational Head Motions in the Roll and Pitch Axes due to the Translational Vibration of the Seat in the Y Axis and X Axis, Respectively--Two Seating Conditions, 10 Subjects at 1.6 m/s^2 rms (after Lewis, 1979b)

2.5.3.10 Effects of Random Motion

Biodynamic responses to vibration thus far have been discussed only for sinusoidal motion occurring in one axis and primarily one frequency at a time. Aircraft vibration has been shown to be multiaxial and depending upon aircraft type, either random motion or a combination of deterministic and random motion. Unfortunately, there is very

little useful biodynamic response data for multiaxial broadband vibration other than that measured under operational settings (Section 2.5.3.11). Guignard and King (1972) cite some references that indicate that the multiaxial biodynamic response can be derived by combining the intensity and phase relationships of the component motions in each individual axis.

If the mechanical system undergoing forced oscillation is truly linear, then the response of the system should be the same for random oscillation as for a combination or composite of discrete sinusoidal oscillations which have the same energy distribution across frequencies. Pradko et al. (1965) found this ostensibly to be the case when they exposed observers to vertical Z axis seat vibration created by a broadband white noise source filtered by bandpass filters with a central frequency of 5.0 Hz and bandwidths of 2 Hz and 10 Hz. They observed that the transmissibility of rms head to seat motion due to the 2 Hz bandwidth filtered random motion was almost equivalent to that of a pure 5 Hz sinusoidal vibration input. The mean transmissibility for this condition was 1.5. The transmissibility of the 10 Hz bandwidth filtered motion was reduced somewhat (amplitude ratio = 0.88) for the same rms vibration levels. (Intuitively, this situation would result since for a given rms level, the concentration of vibration energy within the high gain response region of seat-to-head transmissibility is greater for the 2 Hz bandwidth centered at 5 Hz band than for the 10 Hz bandwidth centered at 5 Hz.) Levison (1978) also demonstrated the linearity of biodynamic response characteristics of the observer in a series of experiments using complex (sum of single sinusoidal frequencies) and random vibration motion with amplitudes of 0.15 to 0.3 g rms in the Z axis. He found that he could predict the biodynamic response of subjects to complex vibration spectra by cascading the response data derived for single frequency components. There was a 20 percent maximum error following such a procedure.

These findings are consistent with the application of ISO 2631-1974 (E) which recommends that the effects of narrow band random vibration (i.e., within 1/3 octave at a given center frequency) be

evaluated the same as the vibrating level for the center frequency. For vibration frequencies separated by more than one octave band, the same levels can be applied to each frequency. As a general rule, Von Gierke and Clarke (1971) recommended that broadband rms levels be reduced by a factor 0.6 (or subtraction of approximately 5 dB) to obtain equivalence with the narrowband application of ISO 2631. [Note that this difference is approximately equivalent to the Pradko et al. (1965) finding for differences in transmissibility for broadband versus narrow random vibration.] Griffin (1976c) cautioned that, at least for subjective comfort data, the simple application of ISO curves to random vibration can lead to errors in establishing the appropriate boundary levels. Based on experimental results, he proposed a frequency weighting paradigm which predicted contours of equal comfort for broadband vibration using findings for either sinusoidal single frequency or 1/3 octave random vibration. He added that the weighting function still may not be appropriate for random vibration with occasional high peak accelerations.

2.5.3.11 Head Vibration in Aircraft Environment

As discussed in Section 2.5.2, Griffin (1972a) found the vibration of the floor (under the seat) in a Scout helicopter was mostly deterministic with the predominant frequencies being generated by the main and tail rotors. Figure 2.5.12 shows the vibration behaviour of the head in the X axis (fore-aft), Y axis (lateral), and Z axis (vertical) directions Griffin obtained under flight conditions similar to those for the floor vibration in Figure 2.5.4. Comparison of the two figures shows that the peak amplitudes of vertical head motion generally occurred with those of the floor vibration, but the relative amplitude of the peaks in head vibration appear to be greater for low frequencies and decrease with increasing frequencies. Griffin used four flight conditions while evaluating head vibration: ground (rotor turning), hover at 10 feet above the ground, 100 knots, and 115 knots forward flight at 1000 feet above the ground. The ranking of the magnitudes of head vibration in the three axes tended to correlate with the rankings of floor vibration in the same axes, at least for the 7 Hz and 28 Hz frequencies. Generally, the magnitude of head

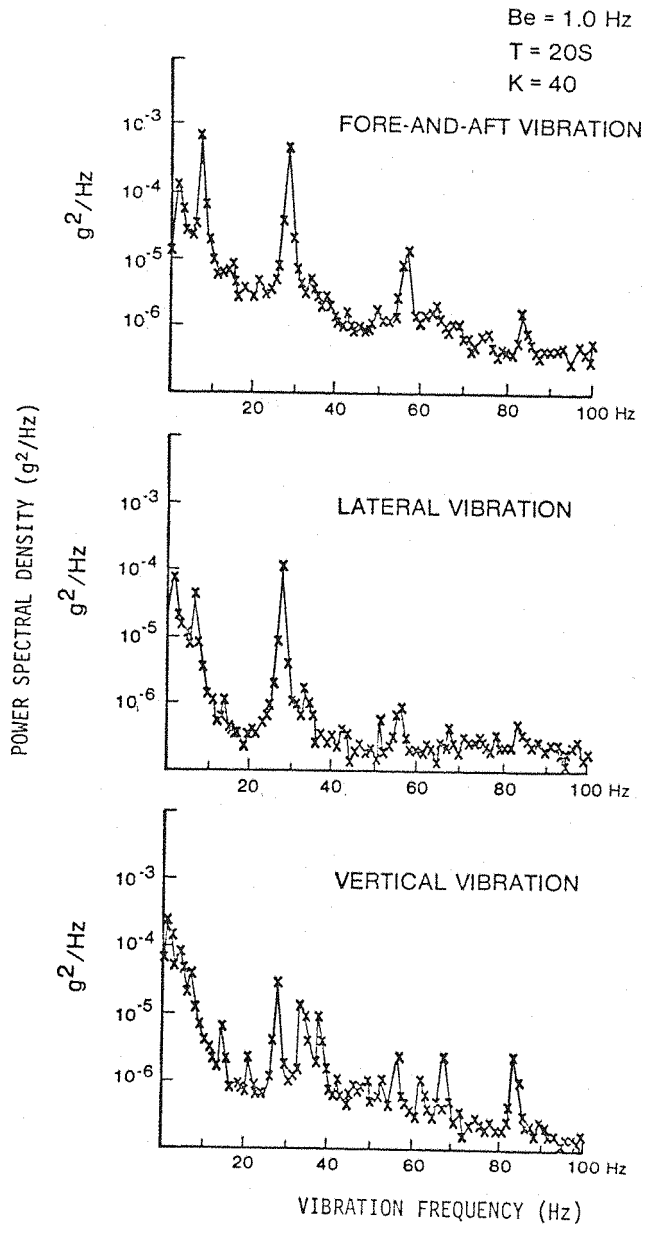

Figure 2.5.12. Vibration Acceleration Spectra at the Head of a Pilot in a Scout Helicopter During 100 kt Forward Flight at 100 ft Above the Ground Level (after Griffin, 1972a)

vibration was least for the X axis (lateral) and greatest for the Z axis (vertical) at almost all frequencies. The X axis (fore-aft) vibration had a magnitude similar to the Z axis (vertical). Griffin noted that head vibration behaviour of all eight pilots was similar in form across all flight conditions, but with a between subjects variability of up to 10 to 1. Using rank order correlation analyses,

Griffin was able to show that Z axis (vertical) head vibration at 7 Hz was negatively correlated with hip circumference during the 115 knot flight condition but positively correlated with hip circumference in the hover condition. This meant that at 115 knots the head vibration was significantly less for pilots with the largest hip circumference, but greater than other pilots for the hover condition. Griffin conjectured that this finding reflected changes in the triaxial characteristics of the seat vibration (as a function of flight condition); and because of the dual nature of the seat and seat back vibration conduction paths, large pilots responded in an opposite manner to small pilots for the two flight conditions.

In a separate experiment, Griffin (1972a) simultaneously measured the triaxial vibration of the seat-pilot interface and the head during a hover manoeuvre. As can be seen in Figure 2.5.13, the mean rms Z axis (vertical) vibration transmitted to the head was greater than the seat vibration between 2 Hz and 10 Hz. The transmissibility of the head to the seat vibration using the ratios of the square roots of the power spectral densities (1.0 Hz resolution) is shown in Figure 2.5.14, along with the mean and standard deviation of transmissibilities across the eight subjects during the hover manoeuvre. The mean transmissibility follows the general form of the data discussed previously in Section 2.5.2 and Section 2.5.3.3. Between 2 Hz and 10 Hz, the Z axis (vertical) vibration of the head was greater than that of the seat, peaking at 5 Hz, with a mean transmissibility of 2.16 and a standard deviation of 0.62. The mean and standard deviation of the data in Figure 2.5.14 hint that there may have been resonances between 14 Hz and 18 Hz, but these were obscured by the averaging of the data. The lack of a significant peak in the data between 14 Hz and 18 Hz is surprising, considering findings of Rowlands (1977) and Lewis (1979b) wherein observers were either sitting erect or restrained to seat backs. The frequency response of the seat cushions may account for this discrepancy. Griffin estimated that the transmissibility of the seat cushions in this experiment was 0.84 at 7 Hz and 0.25 at 14 Hz. The reduced transmissibility of the vibration through the seat cushions to the buttocks and backs of the pilots within the 14 Hz to 18 Hz region may, therefore, have greatly attenuated the peaks

observed by Rowlands and Lewis for seating conditions without cushions.

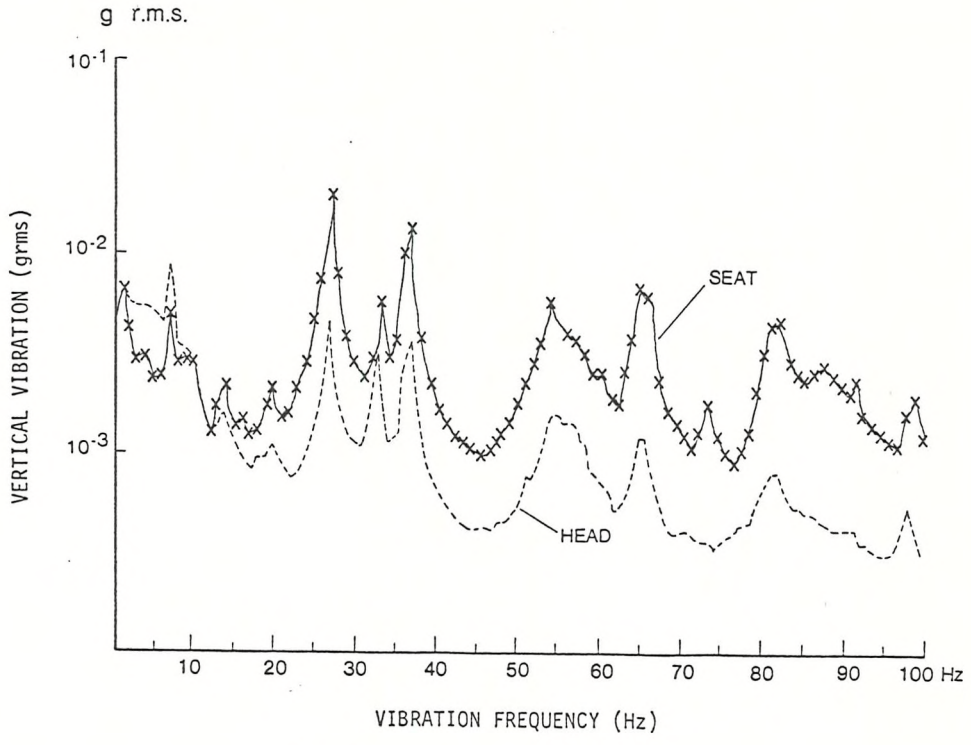

Figure 2.5.13. Mean Vertical (Z Axis) Vibration Acceleration of the Head and Seat of 8 Pilots During Hover in the Scout Helicopter at 10 ft Above the Ground Level (after Griffin, 1972a)

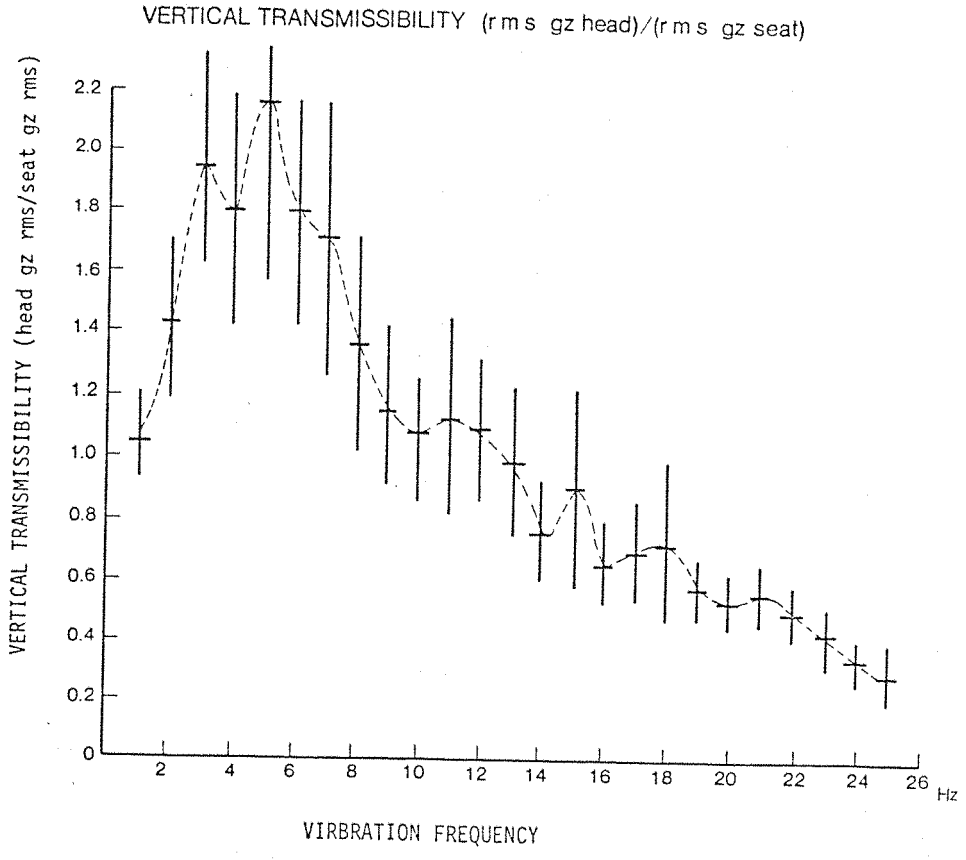

Figure 2.5.14. Mean and ±1 Standard Deviation of the Seat to Head Transmissibility of Vertical Z Axis Vibration for 8 Pilots in the Scout Helicopter During Hover at 10 ft Above the Ground (after Griffin, 1972a)

2.5.3.12 Effect of Flight Helmet

Lewis (1979b) found that, depending on the vibration frequency, wearing a flight helmet affected the transmissibility of vibration to the head. Figure 2.5.15 compares the mean Z axis (vertical) transmissibility for 10 subjects with and without wearing of a representative flight helmet. For vertical (Z axis) seat motion between 7 and 20 Hz, Lewis found that the flight helmet caused the transmissibility to increase (up to 30 percent at 14 Hz), but to decrease at frequencies greater than 20 Hz. There was otherwise little effect of the helmet on the vertical motion of the head induced by X axis motion. The helmet also affected rotational motions of the head in pitch due to Z axis and X axis seat motions. For vertical Z axis (vertical) input motion, the helmet attentuated head pitch motion between 7 Hz and 14 Hz, but greatly increased motion (up to 200 percent) between 14 Hz

and 16 Hz (Figure 2.5.16). Similar behaviour was observed for pitch motion due to X axis (fore-aft) seat motion. At frequencies below nominally 7 Hz, the helmet had little effect on head motion.

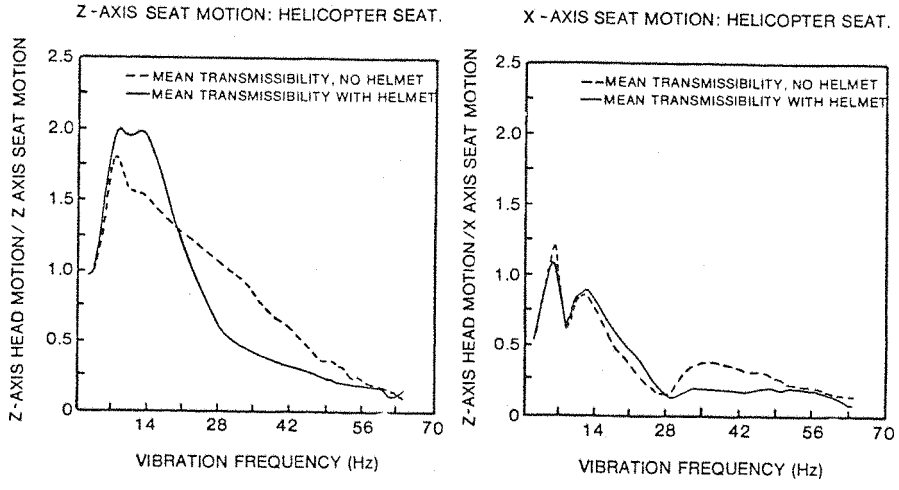

Figure 2.5.15. Mean Vertical Motion of the Head in Response to Vertical (Z Axis) and Fore-Aft (X Axis) Motion of the Seat at 1.6 m/s^2 rms for 10 Subjects With and Without an MK 1A Flight Helmet (after Lewis, 1979)

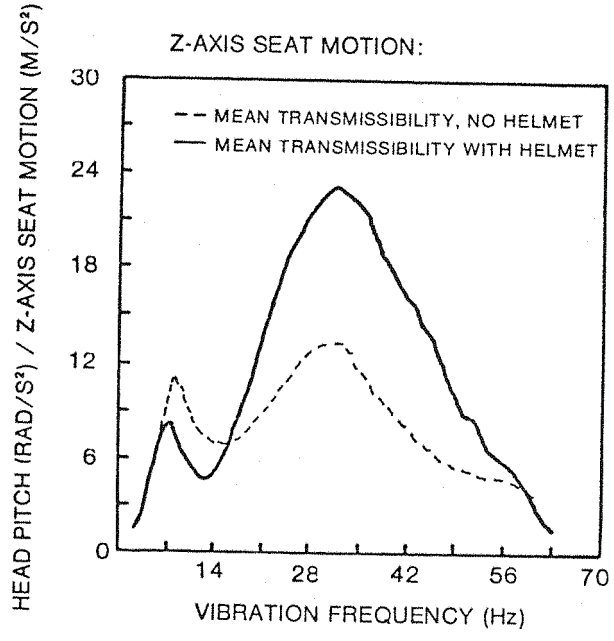

Figure 2.5.16. Mean Pitch Axis Motion of the Head in Response to Vertical (Z Axis) and Fore-Aft (X Axis) Motion of the Seat at 1.6 m/s^2 rms for 10 Subjects With and Without the MK 1A Flight Helmet (after Lewis, 1979)

Since the helmet serves as the platform upon which the helmet-mounted display is affixed, the dynamic behaviour of the helmet on the head may be relevant to the determination of the visibility of the images presented on the helmet-mounted display. Kennedy and Kroemer (1973) and Kroemer and Kennedy (1973) found that vertical Z axis acceleration in a centrifuge caused a rotational displacement of the helmet on the head in the pitch, roll, and yaw axes. The magnitude of the rotational displacement was a function of the mass and location of the mass loading on the helmet and the acceleration level. The mean displacement in the pitch axis increased linearly from 0 degrees at 1 g_z to -4 degrees (rotation back to front) at +6 g_z.

In a series of static and vibration experiments using several helmets (with and without a helmet-mounted dislay) and helmet suspension techniques, Jarrett (1978) found that relative motion of the helmet on the head occurred during simulated aircraft Z axis and Y axis vibration conditions. In his experiments, Jarrett used vibration recorded from a Canberra and a Phantom aircraft during low altitude, high speed flight. The recorded vibration levels were 0.25 g_z rms and 0.1 g_y rms for the Canberra and 0.18 g_z rms and 0.1 g_y rms for the Phantom. The recorded vibration time histories were reproduced by a dual-axis vibrator with the subject seated and restrained in a Canberra ejection seat. Two pilots were used as subjects. One of Jarrett's experimental conditions included the use of a USAF helmet with a helmet-mounted display affixed and a custom fit liner. (Note: The helmet display used in Jarrett's experiment was similar to that used by the present author in the experiments reported in this thesis.) During the simulated flight conditions, the displacement of the helmet on the head was measured relative to the eye. For the Canberra flight conditions, helmet to head displacements were about 0.45 mm rms in the vertical direction and 0.2 mm in the horizontal direction. The vibration displacements decreased by a factor of about 2.5 in the Phantom. When the subjects were asked to move their heads to simulate a visual searching task, the helmet to head displacement in the vertical axis doubled, while that in the horizontal axis increased from 7 to 15 times, depending upon the aircraft vibration spectra. The author noted that the maximum displacement was always less than 2 mm from the

center in the vertical axis and 10 mm for the horizontal axis. (Based upon the dimensions of the helmet and head reported by Jarrett, and assuming the center of rotation of the helmet on the head to be at the center of the head volume, it can be estimated that a 1 mm displacement is equivalent to an angular displacement of about 0.4 degrees.) Jarrett also found that the helmet suspension technique had little effect on the relative head to helmet movement.

In a separate study conducted under no vibration conditions, Jarrett measured the amount of helmet-to-head displacement while applying tangential and radial loads to the helmet. He observed that a force of 1 kg acting vertically downward produced a displacement less than 0.5 mm of the helmet on the head as measured at the eye. However, a forward tangential force applied at the top of the helmet of 1 kg produced a 5 mm displacement. While applying different loads in the tangential direction, the rotational displacement of the helmet on the head was separated into two components as shown in Figure 2.5.17: one due to the rotational compliance of scalp and the other due to the slip of the helmet relative to the scalp. These data led Jarrett to conclude that the displacement of the helmet on the head was largely rotational due to the oscillatory rotation of the head induced by the input vibration during the dynamic experiment.

Tatham (1976) provided some indication of the amount of overall helmet pitch and yaw motion which may be encountered in an operational aircraft. Tatham used a helmet position sensing system to measure the angular deviation of the subject's helmet line-of-sight against a collimated (earth referenced) target located straight ahead and at a fixed line-of-sight. The subject's task was to superimpose a helmet-mounted collimated reticle over the target while being presented with whole-body vibration in Z axis (vertical) and X axis (lateral). The same vibration equipment and spectra from two aircraft were employed as used by Jarrett (1978) above. The vibration spectra for the Canberra aircraft is shown in Figure 2.5.18. Shown in Figure 2.5.19 are the tracking errors in the vertical (azimuth) and horizontal (elevation) directions as a function of the rms vibration input from the Canberra spectra. As can be seen, the rms variation in the helmet

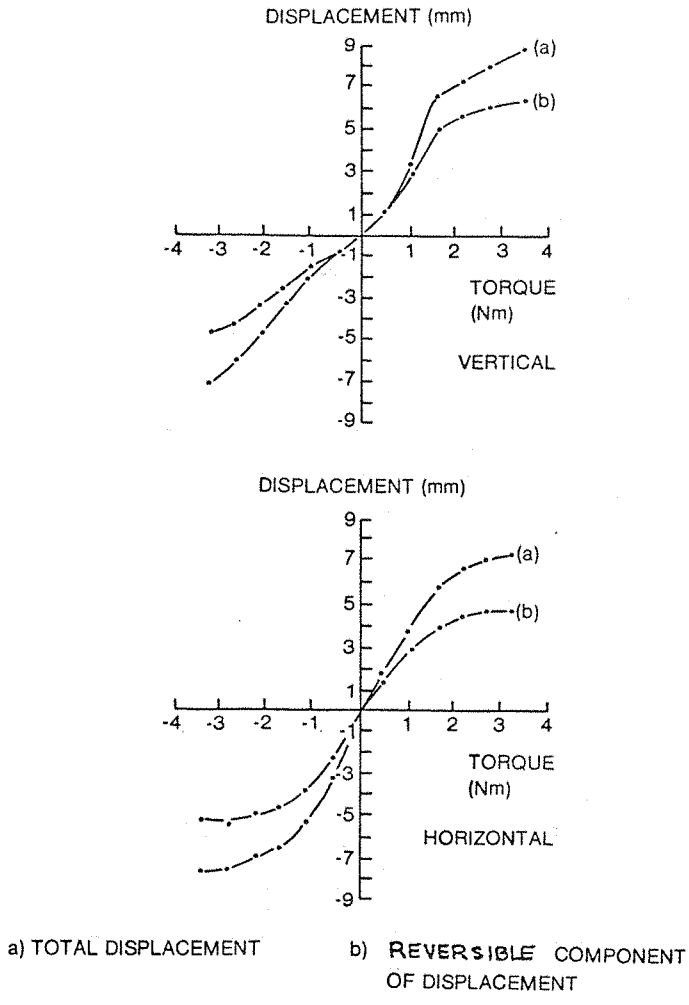

Figure 2.5.17. Vertical and Horizontal Displacements of the Helmet on the Head Due to the Application of a Tangential Force to the Helmet, 1 Subject, USAF Flight Helmet With Custom Fit Liner (after Jarrett, 1978)

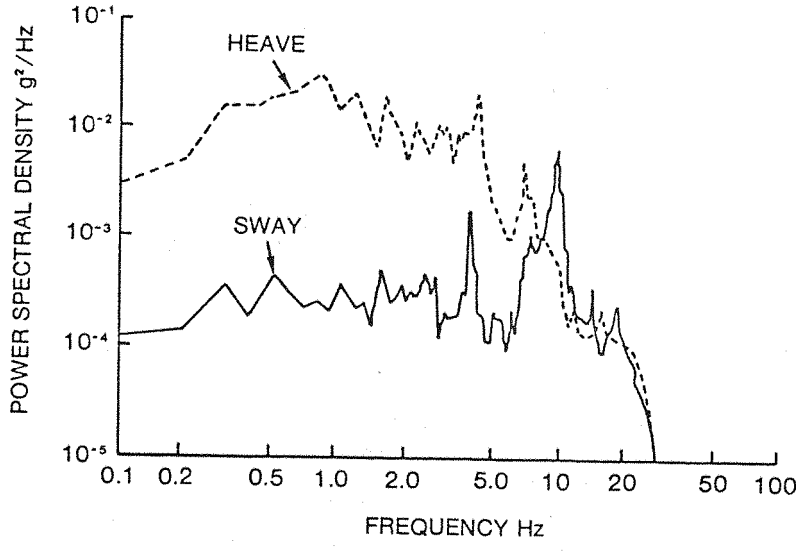

Figure 2.5.18. Power Spectral Densities for Vibration Acceleration in the Vertical "Heave" (Z Axis) and Lateral "Sway" (Y Axis) of a Canberra Aircraft Flown at 450 kts at 250 ft Above the Ground Level, $B_e \approx 0.1$ Hz (after Jarrett, 1978)

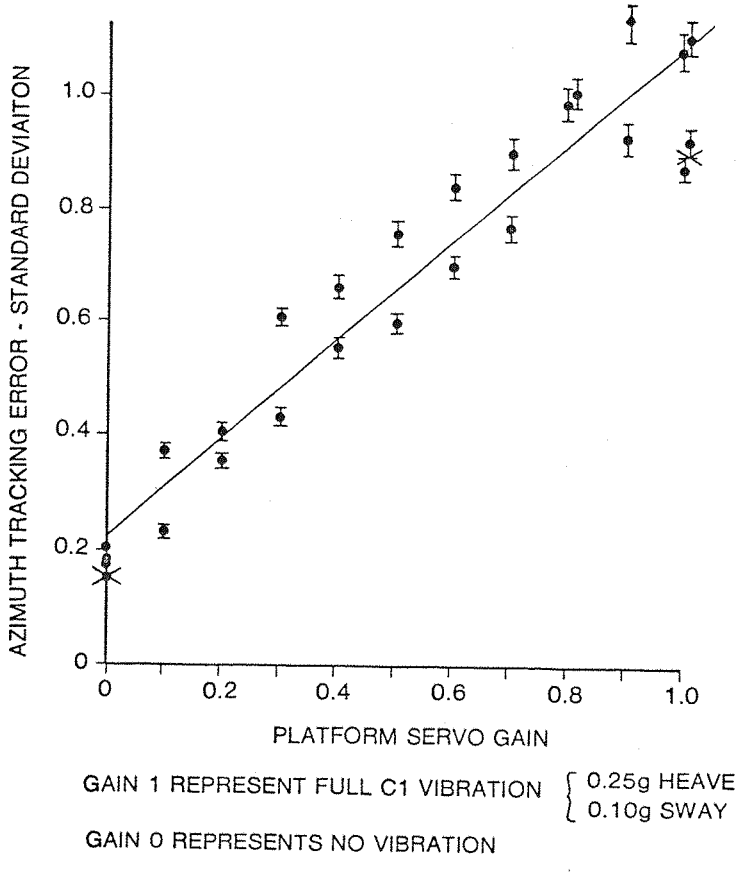

Figure 2.5.19. Helmet Tracking Error in Azimuth (Yaw Axis) and Elevating (Pitch Axis) for Various Levels of Dual Z Axis and X Axis Canberra Vibration, 1 Subject Showing 80 Percent Confidence Limits (after Tatham, 1976)

line-of-sight versus the target line-of-sight was linearly related to the rms vibration level. For vibration levels simulating actual flight conditions (i.e., 0.25 g_z rms, 0.10 g_y rms), the angular displacement tracking errors were about 1.0 rms in azimuth and 2.0 rms in elevation. The power spectral densities of the tracking errors in the azimuth and elevation axis are shown in Figure 2.5.20. The greatest power in the error was concentrated in the frequencies between 0.7 Hz and 2.0 Hz. From the PSDs, the rms angular tracking error as a function of frequency can be estimated as shown in Table 2.5.1. Assuming the deviations from the target line-of-sight were involuntary and due to the vibration input, then the data in Table 2.5.1 can be interpreted as the helmet rms rotational displacements in the pitch and yaw which can be expected in flight.

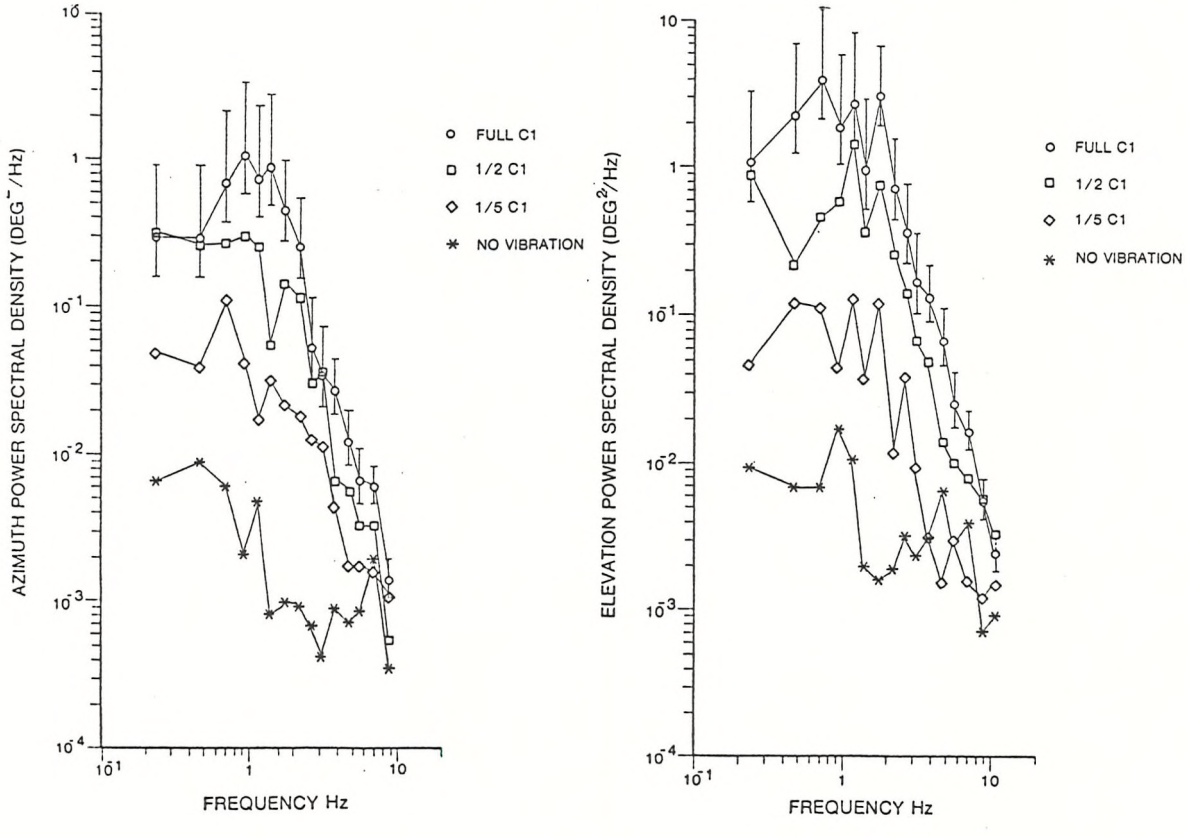

Figure 2.5.20. Mean Power Spectral Densities of Helmet Tracking Error in the Pitch (Elevation) and Yaw (Azimuth) Axes Due to Simulated Vertical (Z Axis) and Lateral (X Axis) Motion From a Canberra Aircraft at Three Levels, 4 Subjects, $B_e \approx 0.2$ Hz (after Tatham, 1976)

TABLE 2.5.1. ESTIMATED HELMET ROTATIONAL TRACKING ERRORS DURING AIRCRAFT VIBRATION CONDITIONS (DERIVED FROM TATHAM, 1976)

Frequency Band (Hz)	Tracking Error (deg rms)	
	Azimuth	Elevation
.23	.21	.48
.45	.21	.70
.67	.39	.94
.89	.49	.65
1.11	.41	.77
1.33	.43	.44
1.7	.31	.66
2.15	.23	.39
2.7	.10	.28

2.5.4 Vibration of the Object

The effect of object vibration on visual perception has been studied by Crook et al. (1947a, 1947b, 1948, 1949, 1950), Drazin (1962), Dennis (1965a, 1965b), Huddleston (1970), O'Hanlon and Griffin (1971), Alexander (1972), Meddick and Griffin (1976), and others. (For a recent summary of this literature the reader is referred to Griffin and Lewis, 1978.) These researchers have found that vibration frequency, amplitude, axes of vibration, stimulus size, stimulus luminance, and learning affect the perception of a vibrating visual scene. Many of these factors have been associated with dynamic visual acuity discussed in Section 2.3.7.2. All of the authors above have used sinusoidal target motions or combinations of single sinusoidal frequencies (e.g., Alexander, 1972). Dependent measures of performance have been acuity discrimination and reading tasks (Landolt "C" or Snellen letters) or, in the case of Huddleston (1970), a compensatory manual tracking task. Surprisingly, the results of these studies generally agree as to the nature of visual performance at various vibration frequencies. In particular, the following trends have been observed for the three vibration frequency ranges discussed below.

2.5.4.1 Effect of Object Vibrating Frequency

a) Object Vibration at Frequencies Less Than 1 Hz. Researchers generally agree that for target sinusoidal oscillatory motion of 1 Hz or less, the smooth pursuit movements of the eye are adequate to match the angular velocity and direction of the target movement, thereby stabilizing the image of the target on the retina and permitting good visual performance. Drazin (1962) suggested that, for large visual fields, eye movements at these frequencies may be considered to be "reflexive" or "compulsive" in nature. These eye movements may be similar to the slow phase optokinetic nystagmus discussed in Section 2.3.7.1. Huddleston (1970) referred to these eye movements as a psycho-optical reflex based upon an original term defined by Westheimer in 1954. The psycho-optical reflex, however, is due to an oscillatory motion as opposed to the OKN which is a reflexive counterpart due to linear motion. In either case, the involuntary response attempts to stabilize the moving visual field on the retina by the appropriate oculomotor commands. Drazin supported this hypothesis by showing that eye movements measured by an electro-oculographic eye movement recording technique (EOG) required progressively longer times to suppress voluntarily as frequency of oscillation decreased from 4.0 Hz to 2.5 Hz. The mean time to suppress the reflexive action of the eye at 4 Hz was 1 s whereas at 2.5 Hz the suppression was rarely achieved even after 15 s. Even though Drazin noted that the frequency response of the eye in pursuit falls off rapidly after 1 Hz, he suggested that the involuntary nature of the pursuit reflex may possibly exist up to 3.0 Hz, although with a low amplitude response.

b) Object Vibration at Frequencies Between 1 Hz and 5 Hz. The research results consistently have shown that the greatest degradation in visual performance will occur when the object is vibrating in the range of 1 Hz to 5 Hz. Drazin (1962), using a dial reading task and exposure times of 1 s, found that maximum reading errors occurred at 3 Hz to 4 Hz for vibration double

amplitudes of 1 degree, 2 degrees, and 4 degrees. Over a vibration frequency range of 1 Hz to 3 Hz, the magnitude of the error varied directly with vibration amplitude. Huddleston (1970) also found that compensatory tracking error, when zeroing a vibrating zero reader display, was greatest at vibration frequencies between 3 Hz and 5 Hz for a 2 degree and 4 degree double amplitude vibration. Alexander (1971) observed that for vibration frequencies less than 5 Hz, an increase in vibration amplitude was accompanied by a similar decrease in the frequency of greatest error. This trend can also be observed in the results of Drazin and Huddleston. Both Drazin and Huddleston explained their results in terms of the frequency response of pursuit eye movements, indicating that the increasing error with increasing vibration frequency and amplitude reflects the progressive attenuation of the gain of the pursuit response. Huddleston (1970), also using an EOG, measured angular eye movements at 2 Hz which were 63 percent of the angular movement of the object and which lagged by 18 degrees. At 3 Hz, he measured a 16 percent eye-to-object amplitude which lagged by 36 degrees. These observations were in good agreement with the data presented by Young (1971) in Figure 2.3.19, and those of Guignard and Irving (1960). Huddleston noted that sinusoidal movements of the eye were observable up to 3 Hz, but at 4 Hz the eye remained directed somewhat at the center of the object excursion with some wandering (perhaps saccadic) motion. At 5 Hz, however, he observed that all subjects tended to fixate at the maximum excursion of the object most of the time (still with some saccadic behaviour). Again at 6 Hz, the subjects fixated only upon the upper excursion of the image. Huddleston explained that this behaviour between 3.0 Hz and 5.0 Hz occurred because the limits of the oculomotor pursuit system (i.e., 30 to 60 degrees per second) had been exceeded. Therefore, the smooth pursuit movements became more interrupted by saccades (as shown in Section 2.3.7.1). Eye position errors and visual suppression which accompanies the saccadic eye movements probably produced the degraded and somewhat unstable movement behaviour of the eyes between 3.0 Hz and 5.0 Hz until the images of the object became defined at the maximum excursion or nodal points.

c) Object Vibration at Frequencies Between 5 Hz and 20 Hz. Perception of objects vibrating at frequencies greater than 5 Hz are probably facilitated by the formation of nodal images on the retina. Griffin and Lewis (1978) defined nodal points as the "...extremities of the [oscillatory] motion where the velocity is zero and the displacement is at its maximum." Drazin (1962) observed that at frequencies greater than 3 Hz to 4 Hz (where the greatest scale reading errors occurred), the effects of vibration frequency and amplitude on reading performance were opposite to that observed at frequencies lower than 3 Hz to 4 Hz. Instead of increasing error with increasing object vibration amplitude, the increased amplitude caused a decrease in error rate. Drazin attributed this behaviour to the tendency of the observers to fixate on the nodal images. He reasoned that as long as the distance separating the nodal images (i.e., the double amplitude of vibration) was less than the visual angle subtending the object, an apparent overlap of the upper and lower nodal images occurred, causing confusions between the two images and, subsequently, higher error rates. Increasing the amplitude of vibration (in this case beyond the 2 degree double amplitude), caused the upper and lower nodal images to become separate and distinct so that they could be readily perceived. Huddleston's (1970) tracking performance also showed some increase in performance (decrease in tracking error) above 3 Hz to 5 Hz, but the effects of changes in amplitude (between the 2 degree and 4 degree double amplitude) were not as marked as Drazin's. This finding probably resulted because even at the 4 degree double amplitude, the overlap of the nodal image was present in Huddleston's display.

2.5.4.2 Effect of Object Vibration Frequency and Amplitude

O'Hanlon and Griffin (1971) have studied the effects of vertical vibration frequency and amplitude under nodal image viewing conditions wherein the nodal image elements of the visual scene were always separated and did not overlap. For these studies, they used Landolt "C" targets with gap sizes conforming to static Snellen acuities of 6/4, 6/5, 6/6, and 6/9 when presented at a 1 m viewing distance. The

authors conducted three experiments. The first experiment showed that the number of reading errors, reading time, and the subjective rating of difficulty increased with increasing vibration frequency from 5 Hz to 40 Hz and with double amplitude from 1.27 mm to 5.08 mm. The second and third experiments investigated the form of the error in more detail. In the second experiment, a double amplitude of 1.27 mm to 7.62 mm was used at a constant vibration frequency of 16 Hz. The authors found that the reading errors produced by these conditions were proportional to the square root of the double amplitude of object motion. In the third experiment, the vibration frequency was varied from 5 Hz to 30 Hz at a constant amplitude of 2.54 mm. In this case, there was a linear increase in the number of errors with increasing frequency. Generally, the number of reading errors, reading rate, and subjective rating of difficulty were linearly correlated. A small change in the size of the Landolt "C" (6/4 to 6/5 with corresponding gap widths from 0.170 mm to 0.215 mm) reduced the number of errors by 75 percent and reading time by 20 percent. The authors explained these results by reasoning that the perceptibility of detail in an object, such as the gap in a Landolt "C," is proportional to the time for the image of the detail to pass over some group of receptors in the retina. Since this time is longer at the nodal point of the vibration motion, an image is most likely to be perceived at that position. The duration of the image at some critical region on the retina (T) would then be inversely proportional to the vibration frequency (f) and the square root of the vibration amplitude (a); hence:

$$T \left[\frac{1}{f}, \frac{1}{\sqrt{a}} \right]$$

Since the number of errors (E) is inversely proportional to image duration on the retinal area (T),

$$E \quad f, \sqrt{a}$$

The authors demonstrated that, at least for the threshold 6/4 size, the relationship above predicted their data results. This relationship was later verified by Alexander (1971).

2.5.4.3 Axis of Vibration

Drazin (1962) postulated that the reason a nonoverlapping nodal image was not perceived as clearly as a static image was probably due to the diminished contrast of the nodal image caused by the apparent mixture of luminance from background areas which were projected on the same region of the retina during the greater part of the cycle. This hypothesis may be supported by Krauskopf (1957) who found that when targets oscillated on the retina at frequencies greater than 10 Hz, threshold contrast increased with increasing frequency and vibration amplitudes. Here the mechanics for the contrast reduction proposed by O'Hanlon and Griffin (1971) are reasonable.

Meddick and Griffin (1976) combined horizontal and vertical vibration motions of the stimulus to achieve a circular motion. In a numeric reading task with characters subtending 0.66 minutes (or an equivalent Snellen size of 6/4), the authors found that when they increased the object vibration frequency from 5 Hz to 10 Hz and the amplitude of vibration from 4.7 mm to 8.7 mm, reading errors and reading time also increased for motions which were horizontal, vertical, and circular. The errors produced by the circular motion were greater than either the horizontal or vertical motions. The increase in errors for the circular motion, when compared to the translational motions, were highly significant ($p<.005$) at 6 Hz, 8 Hz, and 10 Hz vibration frequencies. The differences in linear motion (between the vertical and horizontal axes) were not significant, except at the 8 Hz and 10 Hz frequencies ($p<.05$), being slightly greater for the vertical motion. The authors concluded that the higher error rate for the circular object movement was due to the absense of nodal images, as would be predicted by their model.

2.5.4.4 Object Characteristics

As has been shown previously for visual performance under static and dynamic pursuit conditions, some characteristics of the stimulus object will also affect the visibility of the object when it is vibrating. O'Hanlon and Griffin (1971) found that relatively small

increases in object size (Landolt "C") resulted in large improvements in performance. Crook et al. (1950) also found a large effect of character size, especially under low luminance conditions of less than 3.4 cd/m^2 and vibration amplitudes of greater than 0.02 mm. The authors also found that there was an interaction effect between the illumination of reading material and vibration amplitude in producing reading error.

The shape and form of the object may cause a directional sensitivity relative to the axis of object vibration. Drazin (1962) observed that the variation in reading errors on a circular scale (vibrating vertically) was greatest when the indicator was horizontal. O'Hanlon and Griffin (1971) were careful to orient the gap in the Landolt "C" (which they used as a stimulus object) either to the right or left of the vertical axis of vibration in order to avoid the gap appearing as a streak. Meddick and Griffin (1976) noted that reading errors for some numeric characters (e.g., 6, 9, and 5), were greater than for others (e.g., 1 and 7), and that different patterns in the confusions of numeric characters emerged as a function of the axis of vibration of the object (horizontal, vertical, or circular). The authors concluded that probably the errors which resulted were confusions between other alternative characters rather than total illegibility of any one character.

2.5.4.5 Object Vibration at Multiple Frequencies

Alexander (1972) investigated the effects on reading performance of combined sinusoidal vertical vibrations on an object at two frequencies in the range of 3 Hz to 20 Hz. Her results were complex, but showed that, depending upon the relevant amplitudes, multiple frequency motion either increased or decreased errors produced by either of the single frequency components alone. The findings of Alexander indicate problems of describing and/or predicting performance with other than simple sinusoidal motions.

2.5.5 Vibration of the Observer

The open literature contains numerous sources addressing the effects of whole-body vibration on visual perception. This literature has been reviewed by Dennis (1963), Guignard (1965), Guignard and Guignard (1970), Grether (1971), Von Gierke and Clark (1971), Guignard and King (1972), Shoenberger (1972), Collins (1973), Griffin (1973, 1976a), and Griffin and Lewis (1978). Most recently, Griffin and Lewis (1978) reviewed and summarized the results of approximately 50 studies in this area.

2.5.5.1 A Historical Perspective

From a historical standpoint, several investigators have addressed the differences in whole-body vibration versus object vibration on visual perception. Guignard and Irving (1960) found that the mean frequency response of eye movements for a vibrating subject viewing a static target was approximately 2.8 Hz (i.e., the frequency at which eye movements were one-half of the relative movement of the head to the target), whereas for a static subject viewing a moving target with the same relative angular movement (i.e., 0.8 degree peak), it was approximately 1.7 Hz. The authors attributed the difference to the stimulation of the otoliths eliciting a compensatory reflex during whole-body vibration. During the experiment, the head was restrained to reduce rotational movements.

Using a numeric reading task, Dennis (1965a) found that subjects incurred more reading errors and produced longer readings times when the object was vibrated at 6 Hz than when the subject was vibrated at 6 Hz; however, the reverse was true at 19 Hz. At 6 Hz, the mean number of reading errors was up to 81 percent greater for the moving object than the moving subject (when both the head and object were caused to have the same equivalent vertical displacements). Dennis also noted that the peak-to-peak motion of the head had to be increased to 2.2 mm (subtended visual angle of 2.32 minutes-of-arc) to give approximately the same mean error as when the object vibrated

with 1.3 mm displacement (1.45 minutes-of-arc subtended visual angle). On the other hand, at 19 Hz, vibration of the object with a peak-to-peak displacement of 0.3 mm caused only very slight increases in error (i.e., less than 5 percent greater than the static condition), whereas the vibration of the subject with a peak-to-peak displacement of 0.18 mm at the head produced a 90 percent increase of reading error over the static error. Dennis concluded that the different behaviour of the subjects between the object versus subject vibration at frequencies of 6 Hz and 19 Hz was due to the compensating movement of the eyes elicited by stimulation of the "labyrinth" which was present in whole-body vibration, but absent in object vibration. He continued, however, that although compensating eye movements did improve performance, it was limited, since at 19 Hz such a small head movement created errors much larger than equivalent object displacement. Dennis conjectured that this factor was probably due to eye resonances or contributions due to local resonances of facial tissues.

Unfortunately, neither Dennis (1965a) nor Guignard and Irving (1960) took into account the rotational movement of the head which, in conjunction with eye rotation, would produce angular oscillation of the target which was an admixture of that due to head translation. Drazin (1962) did mention that nodding movements of the head which had been observed during vertical vibration of the body would stimulate the vestibular organs causing compensatory eye movements. However, he discounted any effect of the compensatory reflex beyond 1 Hz to 2 Hz because overall the frequency response of the reflex which had not been investigated up to that date.

Rowlands and Allen (1969), in a theoretical treatment of the subject-eye motion relative to visual perception, noted that perhaps the variation in performance observed in prior experiments was due to the rotational movement of the head rather than translational. Since translatory motion of the body usually produced both translation and rotational movements of the head, it was the rotational movements of the head that caused more impairment of vision and required more compensatory movements of the eyes than that due to translatory motion (especially in longer viewing distances or when collimated displays

were used). Griffin (1976b) later verified this hypothesis by showing that the minimum vertical Z axis seat vibration levels which produced a perceived blur in a target at 7, 15, 30, and 60 Hz frequencies concurrently produced head motions which were predominantly rotational rather than translational in nature. The rotational movement of the head and decrement in visibility of visual material could readily explain the large errors produced by relatively small head translational motions observed by Dennis at 19 Hz. Since Dennis used a long viewing distance (i.e., 3.2 m), the effects of translational motion were minimal even at 6 Hz, and performance was most sensitive to rotational movements of the eye. Since large head pitch motions have been observed in the 4 Hz to 8 Hz frequency range (e.g., Rance, 1978; Lewis, 1979b), it must be concluded that the rotational movement of the eye was relatively stable in space regardless of the magnitude of the head pitch motion, at least at 6 Hz, but the eye stabilization had degraded by 19 Hz. It was not until the experiments of Benson (1972) that the true nature and extent of the compensatory eye movements in terms of the vestibulo-ocular reflex began to emerge.

2.5.5.2 Nature of Eye Movements During Whole-Body Vibration--The Vestibulo-Ocular Reflex

Perhaps the greatest factor inhibiting the understanding of compensatory eye movements during whole-body vibration has been the lack of a suitable technique for measuring eye movements (e.g., Young and Sheena, 1975). Although electro-oculographic methods had been used by experimenters, these techniques were usually limited to a maximum eye oscillation frequency of 2.0 Hz. Lee and King (1971) implemented a unique method of measuring the amplitude and phase of eye-to-head movements by having subjects "tune" the gain and phase of a stabilized target presented at different viewing distances. In order to obtain eye-to-head transmissibility data, the eye motion deduced from the gain and phase adjustments for the moving display target was compared to head Z axis motion. Unfortunately, the head Z motion data was confounded with head rotational data as well, thereby compromising the accuracy and validity of the data.

As a means of overcoming this obstacle, Benson (1972) used pure rotational movement of the head/body and a numerical reading task to determine the bandwidth aspects of the stabilization or compensatory reflex of the eyes. He compared reading performance when the target was undergoing rotational oscillation in the yaw axis (±20 degrees per second at a frequency of 0.5 Hz to 10 Hz) to that when the subject was oscillated (under the same conditions). As shown in Figure 2.5.21, reading performance degraded quickly when the object was oscillated even at frequencies below 1.0 Hz. At 1.0 Hz, the number of reading errors increased by 10 percent over static conditions, and the number of characters which could be read in 10 seconds decreased by 67 percent. On the other hand, during the viewing condition wherein the target remained static and the subject oscillated, a 10 percent error rate did not occur until approximately 8 Hz. The differences in visual performance under the two vibration conditions led Benson to deduce that rotational motion of the head can cause a compensatory reflex in eye movement which enhances the visibility of objects in space. As a check to verify that the vestibular mechanism mediated this behaviour, Benson presented data for one subject who did not have a normal vestibular function. In this case, there was no significant difference between the two target viewing conditions. Later, Benson and Barnes (1978) reported that they observed similar decrements in visual performance between the yaw and pitch movements of subjects with targets moving with the subjects (no relative movement of the head to the target), but that for a given target stimulus condition, the decrement developed more rapidly and was detected at a lower frequency with pitch motion than with yaw motion of the subject. (These results will be discussed in more detail later.)

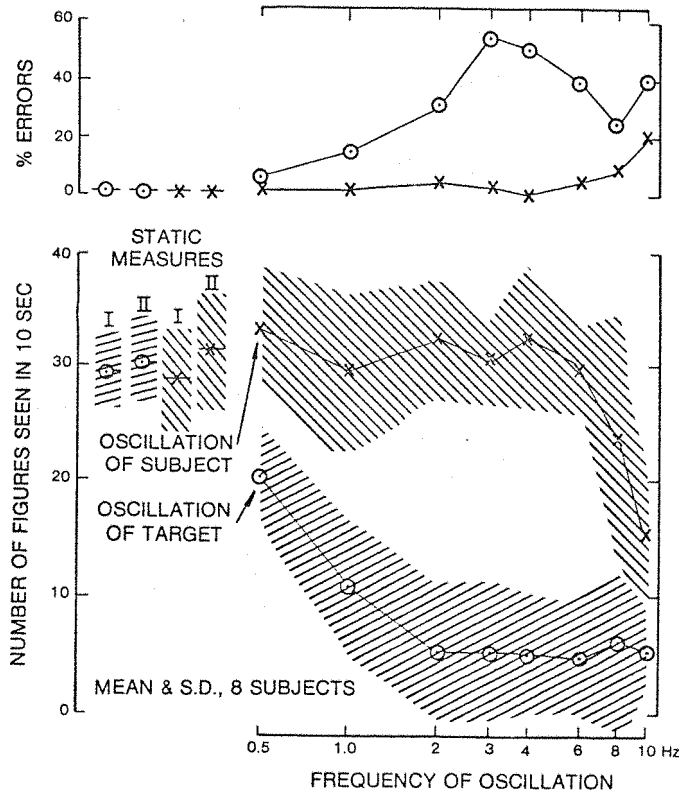

Figure 2.5.21. Effect of Rotational Oscillation in the Yaw Axis on Visual Performance--Mean ±1 Standard Deviation for 8 Subjects at ±20 deg/s Peak Velocity (after Benson, 1972)

a) Eye Movement Control System. As shown in Figure 2.5.22, the eye can be thought of as being a gimballed sensor whose directional commands are accomplished by a multiport servo system. Signals for providing the primary control of the eye gimbal are: (1) the deviation of the visual field on the retina (as modified by the central nervous system); (2) rotational movement of the head in space and relative to the body; and (3) vehicle rotation in space. The rotation of the head or vehicle in space or both provide additional inputs to control the system as shown. Some aspects of this servo system have been discussed previously, such as the tracking behaviour or pursuit reflex of the eye and associated nonvoluntary eye movements, such as the physiological and optokinetic nystagmus. For the tracking response, the input signals for directing the eyes are derived from the retina. This

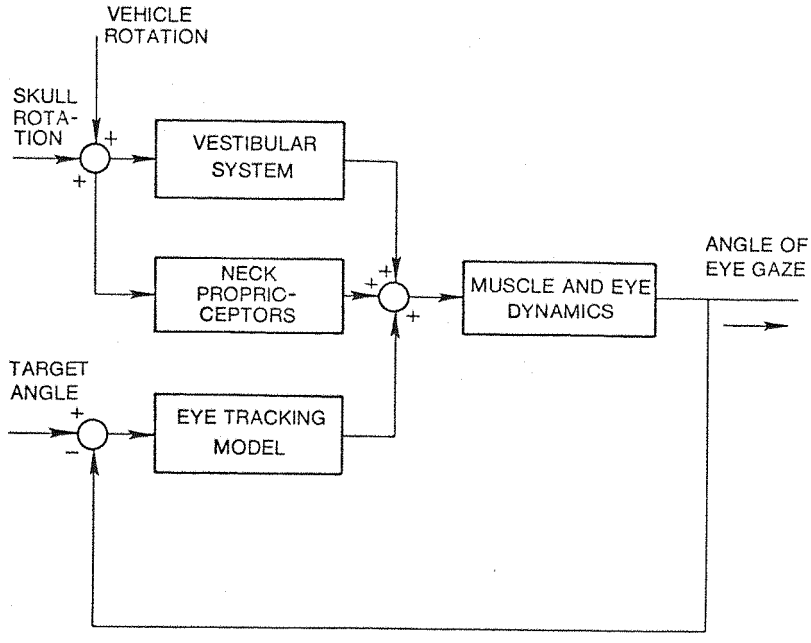

Figure 2.5.22. Block Diagram of Eye Movement Central System (after Meiry, 1971)

tracking mode is performed during both active and passive functioning of the eyes when targets and/or visual field are moving. When there is no movement of the head in space or relative to the body, this mode completely dominates the control of eye movement (along with the centrally-mediated saccadic eye movements). However, when the observer undergoes some rotational movement in space or is required to move his head to track a target, or when head movements are induced passively or involuntarily as in the case of whole-body vibration, the rotational movements of the head cause a stimulation of the semicircular canals which act as highly-damped rotational accelerometers in approximately the pitch, roll, and yaw axes of the head. The afferent signals from the receptors in the vestibular end organs are coded to represent head velocity and are modified by a neurointegrator and other response modification sites to become efferents for control of the extra-ocular muscles which, in turn, gimbal the eye to maintain line-of-sight in inertial space. The resulting response of the eyes to the vestibular stimulation is termed the vestibular nystagmus or vestibulo-ocular reflex. The anatomical and neurophysiological aspects of the vestibular control of eye movements have been treated in depth by Robinson (1968), Cohen (1971), Jones (1971, 1976), and Barnes (1976).

b) The Vestibulo-Ocular Reflex. Vestibular nystagmus exhibits both "slow phase" and "fast phase" movements similar to the optokinetic nystagmus discussed previously. In this case, the "slow phase" movement compensates for the movement of the head, stabilizing on the retina the image of an object located in inertial space. The "fast phase" movement resets the fixation position of the eye after the object has moved off-center of the eye by some amount. Barnes (1976, 1979a) has shown that the fast phase component of the vestibulo-ocular function is extremely important also in coordinating the voluntary movements of the head and eye to acquire visual targets. The slow phase frequency response of the vestibular nystagmus was shown by Meiry (1965) to extend from at least .03 Hz to 1.6 Hz, with approximately a -6 dB gain of the eye relative to the rotational input (in the yaw axis). Benson

(1974) was able to show that, between 0.5 Hz and 5 Hz, the phase between head and eye movement remained at 180 degrees (eye rotation exactly antiphase of head rotation) while the mean gain increased from -3 dB at 0.5 Hz to approximately +1.2 dB at 5 Hz (Figure 2.5.23). Barnes (1976) indicated that, since the output of the vestibular system is coded for a measurement velocity, it is thereby phase advanced on head position; and during periodic stimulation, this phase lead can give the eye a predictive estimation of future head position.

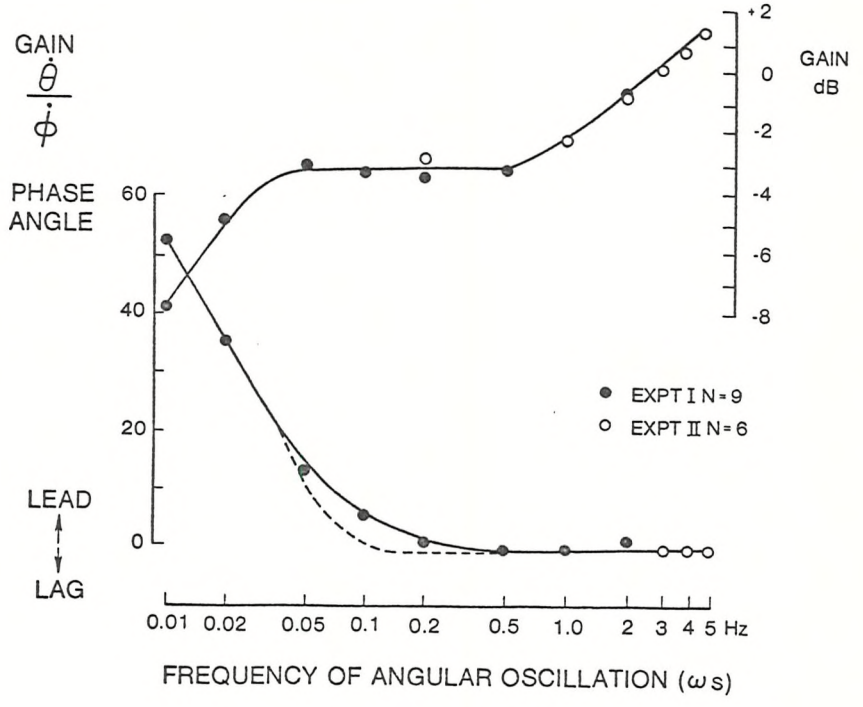

Figure 2.5.23. Amplitude Ratio and Phase Angle of Slow Phase Eye Velocity ($\dot{\theta}$) With Respect to Head Velocity ($\dot{\phi}$) During Rotational Oscillation of the Lateral Semicircular Canals (from Benson, 1974; after Barnes, 1976)

When the head is allowed to move relative to the body, proprioceptors in the head also elicit compensatory movements of the eyes which is termed in colliculo-ocular reflex. Meiry (1965) has shown that the colliculo-ocular reflex exhibits slow phase and fast phase components as the vestibular nystagmus. He asserts that the main purpose of the reflex is to extend the low

frequency response of the overall stabilization reflex, especially at frequencies less than 0.2 Hz; but above 1.0 Hz, the reflex probably has little influence on the control of eye movements.

Meiry (1971) showed that the gain of the eye angle to the input angle increased to one (i.e., 0 dB) when subjects were required to track an inertial reference line (earth-fixation point), while undergoing rotational stimulation in the yaw axis (at least up to 2 Hz). Either the tracking response (pursuit reflex) of the eye (as shown in Figure 2.3.19) or the vestibulo-ocular reflex (shown in Figure 2.5.23) alone could not account for this behaviour. Therefore, it can be assumed that the tracking reflex can aid the vestibular nystagmus, assuming that both are attempting to maintain stabilization of the same target reference point on the retina. This behaviour is desirable for most normal visual situations in the natural world. It also follows that, if the visual environment is not fixed relative to inertial space while the subject is receiving rotational stimulation of the semicircular canals, then a perceptual conflict will result. Such a situation would exist, for example, within the artificial viewing environment created by the helmet-mounted display during the rotational oscillation of the head. Compensating eye movements elicited by the vestibular reflex would be contrary to the retinally-derived tracking response needed to maintain fixation of the display which is moving with the head.

The results of Benson (1972) indicated that the useful bandwidth of the vestibulo-ocular reflex can extend up to 8 Hz. Griffin (1976b) also observed that at 7 Hz, a ±12.8 minutes-of-arc rotational displacement of the head in the pitch axis was required to perceive a blur of a point source of light located at 6 m, whereas, at 15 Hz a blur was perceived with a head pitch displacement of only ±0.9 minutes-of-arc. Griffin concluded that, at 7 Hz, the large rotational head movements were probably accompanied by smaller rotational movements of the eye, implying that an ocular stabilization of the eyes was present. Benson and

Barnes (1978) and Barnes et al. (1978) later elucidated the interaction of the visual and vestibular mechanisms for controlling the movements of the eye. They found that the suppression of the slow phase vestibular reflex when a tracking conflict was present (e.g., for the helmet-mounted display), followed the same general form as the inverse of the frequency response of the pursuit reflex. In this regard, Benson and Barnes (1978) observed a decrease in gain for the tracking response in the presence of a vestibular stimulation relative to the overall gain of the pursuit reflex between 0.2 and 0.5 Hz. This result implied that a conflict of the vestibulo-ocular reflex and the pursuit reflex tended to hasten the onset of vestibular-stabilized eye movements which could not be suppressed at frequencies greater than about 1.0 Hz.

c) Interaction of the Optokinetic Nystagmus and Vestibulo-Ocular Reflex. Normally, the optokinetic nystagmus and the vestibulo-ocular reflex (vestibular nystagmus) will be complimentary when viewing earth-fixed targets while the head is undergoing rotational oscillation. This fact may help to extend the useful bandwidth of the vestibulo-ocular reflex. Guedry et al. (1978) found that the peripheral optokinetic nystagmus also promoted visual suppression of the vestibulo-ocular reflex when viewing targets moving with the head (while undergoing whole-body rotational acceleration in the yaw axis), even though there was relative movement between the foveal field fixated on the target versus a peripheral field viewing an earth-referenced vertical grating. When there was a discordant movement between the earth reference and the peripheral visual field (due to decelerating the motion platform), the ability of subjects to suppress vestibular nystagmus was degraded significantly.

d) Eye Resonance. It is reasonable to assume that as the vestibulo-ocular reflex reaches its bandwidth limitation at 8 to 10 Hz, the eye will begin to follow the rotational motion of the head, that is, until the mechanical properties of the eyes, such as extra-ocular structures and support tissues, reach their resonance

frequencies. Other factors which may influence the rotational displacement of the eye are vibration displacement of the scalp and facial tissues. Although evidence for eye resonances between 18 Hz to 90 Hz has been presented by Coermann (1940), Thomas (1965), and Ohlbaum (1976), there are no consistent findings for a single eye resonant frequency in the literature. Intra-ocular resonances of the basic eye structures (e.g., retina and lens) may also be possible within this frequency range. Griffin (1975b) concluded that, over a frequency range of 15 Hz to 75 Hz, the mean effective transmissibility of vibration from the head to the retina was proportional to the square of the vibration frequency. He reasoned that, since vertical seat-to-head transmissibility had been shown to be approximately inversely proportional to frequency, the mean vibration levels of the seat that would cause blurring of the visual image would take the form (generally) of a constant velocity curve (even though there would be different local regions of maximum sensitivity due to eye resonances, etc. for the different subjects). Regardless of the high frequency behaviour of the eye, the attenuation of the body to the transmission of vertical vibration to the head will probably reduce the overall effect of whole-body vibration on vision above 20 Hz.

2.5.5.3 Factors Affecting Visual Performance During Whole-Body Vibration

Since an interrelationship between the oscillatory rotational movement of the head and eyes (as mediated by combined tracking and vestibular modes) has been established, it is now possible to make some assumptions about the factors which will affect vision during whole-body vibration. The biodynamic factors which have been shown to affect the transmissibility of vibration to the head causing both translation and rotation of the head (and eyes as given by the vestibulo-ocular reflex) can also be expected to affect vision during whole-body vibration. These factors include the direction, frequency, amplitude of vibration, and the seating condition and other postural variables. Characteristics of the visual material which have been shown to affect

perception during static and object vibration conditions (e.g., target size, luminance and contrast), can be expected also to influence vision during whole-body vibration. The viewing distance of visual material can be expected to be sensitive to the translational movement of the eyes, but not to the rotational movement. The influence of these factors has been reaffirmed by Griffin and Lewis (1978) in their recent review of the literature.

a) Frequency and Amplitude of Whole-Body Vibration. Lewis (1977) used a numerical reading task presented on a static display to determine the effect of whole-body vibration frequency and level upon reading accuracy and reading time. He used vertical Z axis vibration over a frequency range of 2.8 Hz to 63 Hz at vibration levels at 0.5 to 8.0 m/s^2 rms, depending upon the frequency. To reduce to the effects of postural variables, the author used a five-point restraint harness in conjunction with a hard-surfaced helicopter seat. Lewis found that the main effects of vibration level, vibration frequency, and frequency x level interactions on reading time and error rates were highly significant ($p<.01$). Tests for simple main effects for vibration level on reading errors were significant ($p<.05$) at all frequencies except for 45 Hz and 63 Hz. There were also significant linear trends of vibration level on error rate at all frequencies. From the mean data, the author constructed linear regression models and computed contours of equal performance degradation as shown in Figure 2.5.24. The similarity of the accuracy and reading time contours indicated their sensitivity to task difficulty. Although Lewis noted that the greatest sensitivity of visual performance occurred in the frequency range of 8 Hz to 16 Hz, he made no attempt to explain the reasons for this behaviour. He commented, however, that there was a large intersubject variability in performance and presented contours of equal performance for each subject that were similar in form across frequencies, but varied greatly in vibration level required to produce a given percentage reading error. Some of the variation was correlated with static reading performance.

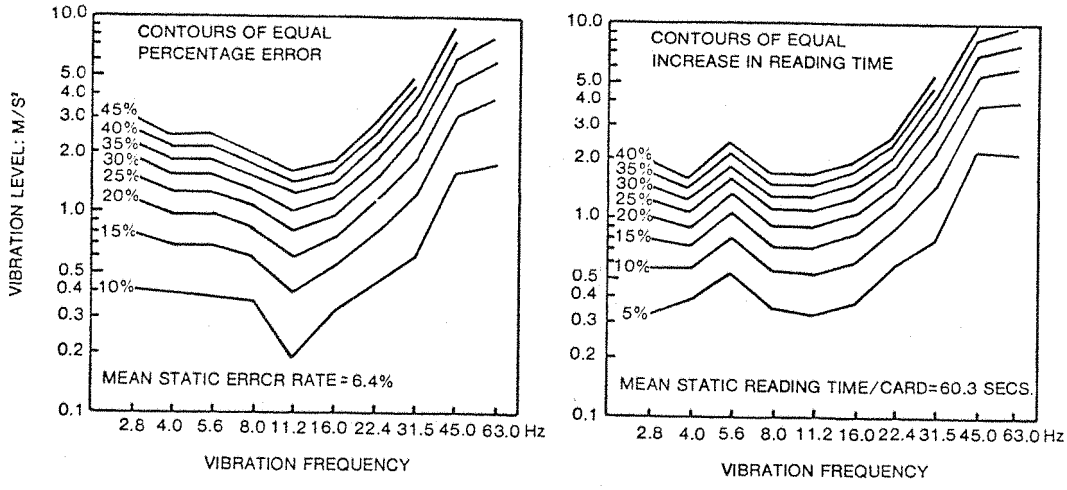

Figure 2.5.24. Mean Contours of Vibration Levels Required to Produce Equal Percentage Reading Errors and Equal Percentage Increases in Reading Time, 10 Subjects (after Lewis, 1977)

In a later study using a similar task, Lewis (1979b) attempted to relate mean contours of equal reading performance that he obtained for different seating conditions (i.e., flat seat versus helicopter seat) to the mean head vertical Z axis and pitch head dynamic responses of the subjects. The results of his analysis for the two seating conditions are shown in Figure 2.5.25. It can be seen that there was a general decrease in the sensitivity in reading error to head pitch and head Z axis motion as frequency increased. As would be expected, the correlation between the curves showing sensitivity due to head pitch was greatest above 8 Hz to 10 Hz where the vestibulo-ocular reflex was inoperative, but head Z axis motion correlates well for the vibration conditions at frequencies below 10 Hz when translation of the head relative to the display was the primary factor degrading visibility. (Note: Perhaps it can also be inferred that the rapid increase of sensitivity to head pitch between 8 Hz to 15 Hz is due to the bandwidth limitation of the vestibulo-ocular reflex as the eyes begin to rotate with the head. The further roll-off beyond 20 Hz may be due to inertial stabilization of the eyes, and possibly eye and head resonance effects.) Lewis indicated

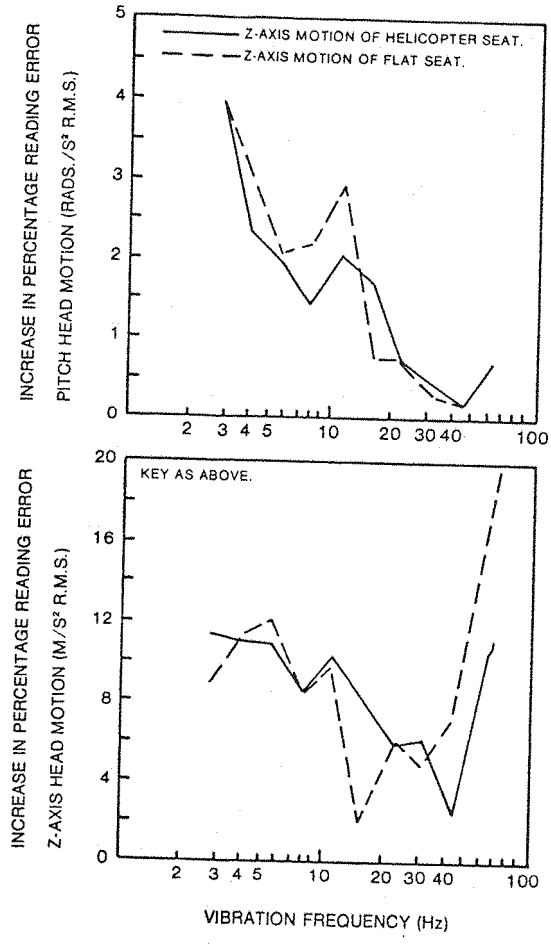

Figure 2.5.25. Comparison of the Ratios of the Slopes of Regression Models for Reading Performance to Head Pitch Axis and Vertical Seat Z Axis Motion for Two Seating Conditions (after Lewis, 1979)

that linear correlation between the curves for head pitch and for the two seating conditions was 0.912, whereas the correlation for the head Z axis motion was 0.513. These correlations, however, were computed across the entire frequency range. It was emphasized by the author that the general agreement between the curves was obtained under drastically different biodynamic response conditions (e.g., Figure 2.5.9) and using mean data from experimental conditions wherein individual variability in reading performance and vibration transmissibility were high.

While Lewis used a static display and vertical Z axis seat vibration, Barnes et al. (1978) observed effects of frequency and amplitude of oscillatory rotational motion in the yaw and pitch axis while viewing a display that moved with the subjects' head. As shown in Figure 2.5.26, the form of the reading performance was similar for the 12 minute-of-arc target size for the yaw and pitch conditions. Statistically significant decrements in performance ($p<.01$) occurred for yaw rotational acceleration of 2.2 rad/s^2 (peak) at 4 Hz and pitch angular accelerations of approximately 1.1 rad/s^2 (peak) at 2 Hz. The subjects reported that the formation of nodal images facilitated the reading of visual material at the higher frequencies. (Note: In this case, the nodal image was formed due to the motion of the eye rather than the motion of the display.) The authors observed that subjects employed two different strategies in the reading task: one group read the visual material at a slow rate, making fewer errors whereas the other group read at a faster rate producing more errors. While Lewis (1977) observed very large variations in reading performance across subjects, Barnes et al. commented that their between subject differences in reading performance were remarkably small (one standard deviation equaled approximately 10 percent of the mean value). It is conjectured by the present author that this difference in the variability of visual performance was due to the individual biodynamic properties which were manifested during Lewis' experiment, but practically eliminated by the body and head restraints used by Barnes et al. The differing biodynamic properties of subjects may be the greatest factor causing variation in subject visual performance. It follows that this factor will be important at the low vibration frequencies in the range of 3 Hz to 8 Hz where large variations in the biodynamic response (due to resonances) have been observed.

b) Viewing Distance. Using vertical Z axis vibration at 3.15 Hz and 16 Hz and static numeric characters presented at 0.75 m, 1.5 m, and 3.0 m (with character sizes adjusted to give constant 4.5 minutes-of-arc subtended angle), Lewis and Griffin (1979b)

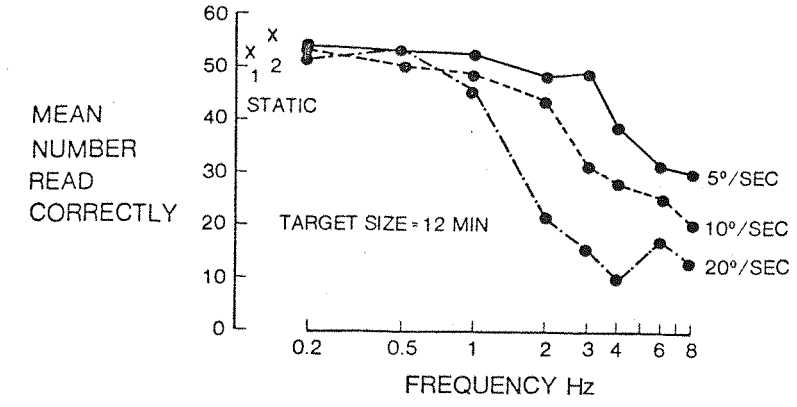

A) YAW AXIS MOTION

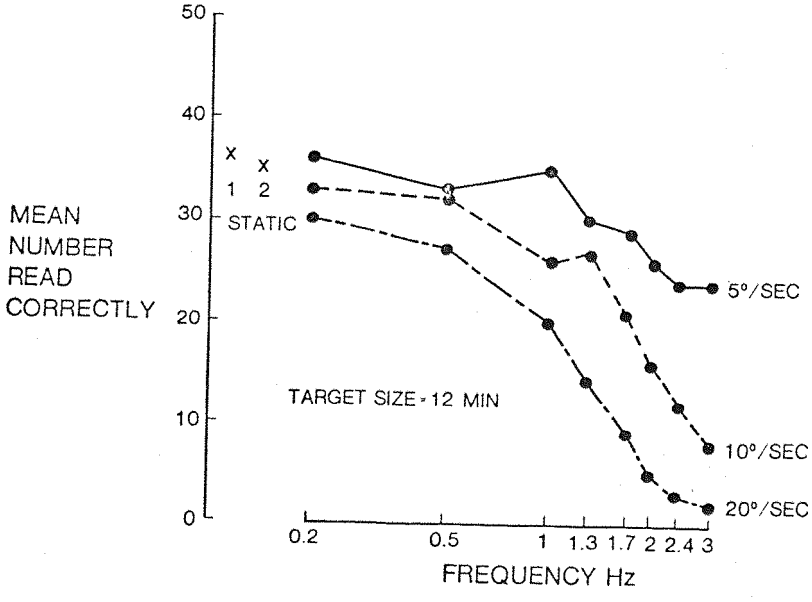

B) PITCH AXIS MOTION

Figure 2.5.26. Mean Reading Performance of a Head-Fixed Display During Rotational Oscillation of the Head in the Yaw and Pitch Axis at Three Levels of Peak Rotational Velocity, 8 Subjects (after Barnes et al., 1978)

found a significant effect of viewing distance and interactions between level/frequency and level/viewing distance on reading performance. At either frequency, there was little difference in performance between the 1.5 m and 3.0 m viewing distances, but a large affect at 0.75 m. At the 3.15 Hz frequency, there was no

consistent effect of vibration level on reading performance when the targets were presented at a distance of 1.5 m or 3.0 m; however, reading errors at the 0.75 m viewing distance increased with increasing vibration level. At the 16 Hz vibration frequency, there was an overall increase in reading error with increasing vibration level at all viewing distances. Lewis concluded, from the mean data, that at 3.15 Hz the rotational movement of the eye was minimal (due to the vestibulo-ocular reflex), and reading errors were caused by translational movements of the eye which, in turn, had their greatest effect at the closest viewing distance. The performance degradation at 16 Hz was due primarily to rotational movements of the eyes, although the translational movement tended to increase errors at the highest vibration levels and closest viewing distance. The Lewis and Griffin results were thereby consistent with the thesis proposed by Rowlands and Allen (1969) and observed by Griffin (1976) that rotational movements of the eyes (as well as translational) caused visual performance to degrade during vertical Z axis whole-body vibration.

This behaviour of the eyes probably accounted for the findings of Wilson (1974) involving the use of collimated displays. Wilson found that if a collimation lens were placed in front of a static zero indicator display, the performance of the subjects in a compensatory tracking task improved significantly over a condition without collimation up to a vibration frequency of approximately 8 Hz.

c) Complex Vibration. In the same series of experiments reported above, Lewis and Griffin (1979b) also compared the reading performance of subjects under combinations of single sinusoidal frequencies. They found that the majority of the subjects produced fewer reading errors under the multiple frequency or complex vibration conditions than under the largest single sinusoidal component alone. The nature of his results were similar to those observed by Alexander (1972) for object vibration. Lewis and Griffin showed that a model of the data based on the

most sensitive component method had the greatest fidelity in predicting reading performance over the other methods using root-mean-square, root-mean-quartic, or arithmetic sum of the components.

d) Vibration in Other Axes. In addition to the literature reviewed by Griffin and Lewis (1978) for the effects of whole-body vibration in other axes, Lewis (1979b) determined the effects of vertical, fore-and-aft, and lateral vibration on the visibility of numeric characters presented on a static CRT display. Shown in Figure 2.5.27 is a comparison of the 10 percent equal error contours computed from the mean data for the helicopter seating condition. As can be seen, the fore-and-aft (X axis) vibration level must be approximately twice the vertical (Z axis) vibration level to produce the same number of reading errors. Lewis found that lateral (Y axis) vibration did not produce reading errors that were statistically significantly different from the zero vibration condition.

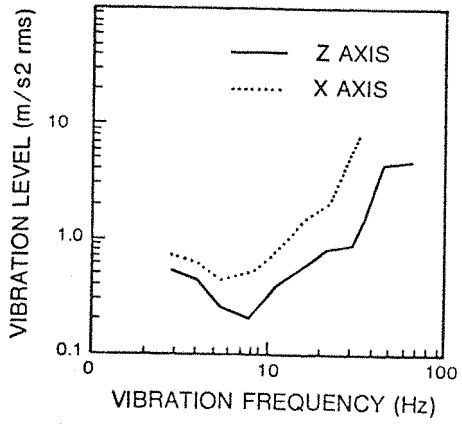

Figure 2.5.27. Mean Contours of Levels of Vertical (Z Axis) and Fore/Aft (X Axis) Vibration Required to Produce 10 Percent Reading Errors, 10 Subjects (after Lewis and Griffin, 1979b)

e) Stimulus Material. A variety of visual stimulus materials and visual tasks have been used by experimenters to assess visual perception during whole-body vibration (e.g., Snellen letters,

Landolt "C", alphanumeric reading material, cockpit-type indicators). Rubenstein and Taub (1967) measured acuity indirectly by having subjects adjust the contrast of a target until they could detect a fixed target separation. Recently, Evans (1980) measured threshold contrast sensitivity function during whole-body vibration by having subjects adjust the contrast of sinusoidal gratings of various spatial frequencies until the grating could be detected by the subject. Performance measures using the variety of visual materials above usually have been reading accuracy, reading time, target detection, and recognition performance. Unfortunately, the diversity of visual stimulus material has caused some difficulty comparing the results of the several experiments which have been reported.

It has been observed in many experiments reported in the literature that visual performance under whole-body vibration can be improved by increasing the visual angle subtended by the visual material and/or increasing its brightness or contrast with the background. These factors, of course, are the same factors which also increased visibility under static and object vibration conditions. The recent studies reported by Benson and Barnes (1978) and Barnes et al. (1978) have shown that increasing subtended angle of the target from 12 minutes-of-arc to 18 minutes-of-arc increased the minimum rotational acceleration in yaw required to produce a statistically significant level of errors from 2.2 rad/s^2 (peak) to 4.4 rad/s^2 (at 2 Hz). Also, Lewis (1979a), using vertical Z axis vibration at 4 Hz and 11.2 Hz, showed that increasing the subtended visual angle of numeric characters on a panel-mounted display from 4.58 to 9.17 minutes-of-arc caused concommitant decreases in reading errors. Linear regression models of the reading errors as a function of vibration level and character size are shown in Figure 2.5.28. The sensitivity or propensity of subjects to produce reading errors, as a function of vibration level, decreases linearly with increasing character size, but tends to asymptote at the larger character sizes. The increase in error rate as a function of

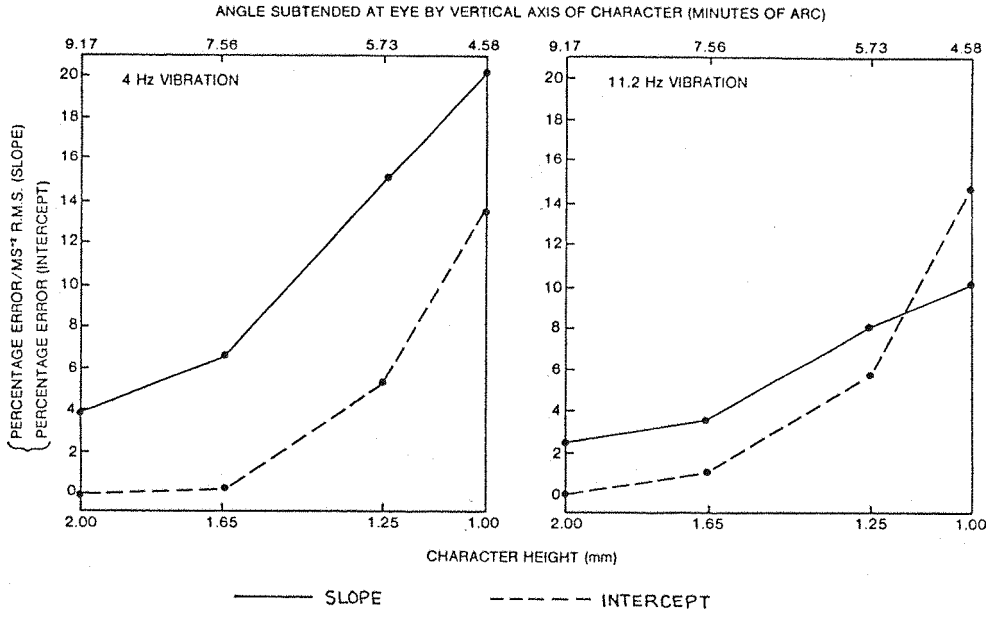

Figure 2.5.28. Slope and Intercept of Least Squares Linear Regression Models of Mean Percentage Reading Errors for 10 Subjects as a Function of Character Size at 4 Hz and 11.2 Hz Vibration Frequencies (After Lewis and Griffin, 1979a)

vibration level at 11.2 Hz is about one-half of that at 4.0 Hz. From these data and those of other investigators, Lewis recommended that the character height be adjusted in operational use, based upon the maximum weighted level of the vibration. (The weighting is to be performed using the recommended procedure of the ISO 2631.) If the weighted vibration levels are less than 0.4 m/s^2 rms, then the minimum character height should be at least 15 minutes-of-arc; however, if the weighted level is greater than 1.6 m/s^2 rms, the minimum character height should be increased to 34 minutes-of-arc. Lewis continued that these recommended character heights were conditional upon good illumination and contrast.

Morris (1966) found that, with adequate illumination (at least 3.4 cd/m^2), painted numerals on digital counters subtending 15 minutes-of-arc could be read under 6 Hz, 16 Hz, and random whole-body vibration conditions, even at acceleration levels up

to 6 m/s^2 rms. However, when the luminance was reduced to 0.34 cd/m^2 and again to .034 cd/m^2, substantial decrements in performance occurred, even when character size was increased to 24 minutes-of-arc. Morris also found a significant interaction between vibration frequency and illumination.

As observed by Meddick and Griffin (1976) for object vibration, Lewis (1977) also found that some of his 5 by 7 matrix numerals produced more errors than others. Most of the errors appeared to be produced by confusion between characters rather than because of total illegibility. Lewis also found that some characters, such as number 1, produced up to 14 times more errors at 16 Hz (2.0 m/s^2 rms) than at 4.0 Hz (2.0 m/s^2 rms). He attributed this finding to the possible introduction of lateral (yaw) movement of the head at the higher frequencies, even though the seat motion was vertical.

2.5.5.4 Vision During Aircraft Vibration

Very few studies have been reported in the open literature dealing with the effects of fixed or rotary-wing aircraft vibration on visual acuity or display legibility (viz. Dean et al., 1964; Hurt, 1963; Griffin, 1974). Griffin (1975c) measured the acuity of pilots during flight in Sioux and Scout helicopters against dark wire targets on the ground. The helicopters were flown in a hover maneouvre. For a viewing condition when the target was presented against a 86 cd/m^2 background, Griffin measured visual acuity during flight that was about 10 percent poorer than under static conditions. However, this difference disappeared when the background luminance of the target was increased to 686 cd/m^2. Griffin noted that these overall differences were small when compared to the individual differences shown by subjects in the experiment.

2.5.6 Perception of the Helmet-Mounted Display During Whole-Body Vibration

The research findings discussed in Section 2.5.5 have shown that the rotational oscillation of the head at frequencies greater than 1.5 to 2.0 Hz will induce compensatory movements of the eye which cannot be suppressed regardless of the nature of the visual input. The implications of this finding on the visibility of a display which moves with the head is obvious. Based upon the laboratory data reported above, aircraft vibration which is transmitted to the body via the seat (and other parts) can be expected to produce rotational motions of the head. The head motions (in the pitch and yaw axes) which occur within a frequency range of 2.0 Hz to 8.0 Hz probably will elicit a compensatory reflex which will tend to maintain stabilization of the eyes in space. If there is good coupling between the helmet and the head; that is, the helmet follows movement of the head with little relative motion, then the optical axis of the helmet-mounted display affixed to the helmet will exhibit rotational motion in space different than that of the line-of-sight of the eyes. The display image which is projected on the retina will have some relative motion and consequently, the perception of the head-coupled display can be expected to degrade in a way similar to the condition wherein the object alone is vibrating (Section 2.5.4). It can be seen that some of the typical vibration levels for aircraft (both fixed-wing and rotary-wing) (Section 2.5.2) and the biodynamic response of the observer reported in the literature (Section 2.5.3), will produce the conditions which can be deleterious to visual perception of a head-coupled display. Other factors which may interact are the display characteristics (character size, brightness, contrast) and individual dynamic characteristics as well as head-to-helmet movement dynamics. Very likely the factors which have been shown to increase the visibility of the display under static and object vibration conditions will also increase the visibility of head-coupled displays under whole-body vibration.

For a true helmet-mounted display, the optical axis of the display/helmet combination will probably have some relative motion with the

head (Section 2.5.3.12); consequently, the degradation in performance due to the vestibulo-ocular reflex may, under some conditions, be increased or decreased depending upon the angular movement of the helmet on the head relative to the eyes. Unfortunately, the literature contains very little data to allow an assessment of the relative helmet display to eye motion which may be expected during actual aircraft vibration conditions. The experiment reported by Tatham (1976) can offer some insight into this problem. If it is assumed that, while a subject's eyes remain stabilized on a target while attempting to aim a helmet-mounted reticle at the target, then the data reported by Tatham provides an estimated measure of the displacement between the optical axis of the eye and the helmet-mounted display. As shown in Section 2.5.3.12, the rms rotational displacements of the helmet relative to a target fixed in space were shown to vary with vibration level, but had power spectral characteristics influenced by the input aircraft vibration. From these data (i.e., Table 2.5.1), the angular displacement between the eye and display can be estimated to be 0.77 degree rms in the pitch axis and .31 degree rms in the yaw axis at a frequency of 1.7 Hz. Based upon the results reported in the literature for object vibration with these angular displacements and frequencies, the whole-body vibration produced by the Canberra aircraft flown at low altitude and high speed can be expected to degrade significantly the information presented on the helmet-mounted display.

There is only one study in the open literature wherein the visibility of the helmet-mounted display has been investigated under conditions of whole-body vibration (Laycock, 1978). Laycock reproduced the vibration conditions of a Canberra aircraft in a two-axis vibrator using the same facility and vibration spectra as reported by Tatham (1976) and Jarrett (1978). Subjects read numeric characters presented on a prototype helmet-mounted display while experiencing vertical and lateral vibration conditions reproduced from a Canberra aircraft. As shown in Figure 2.5.29, Laycock found that there was a significant increase in the number of reading errors during vibration conditions. The percentage errors decreased with increasing character size and

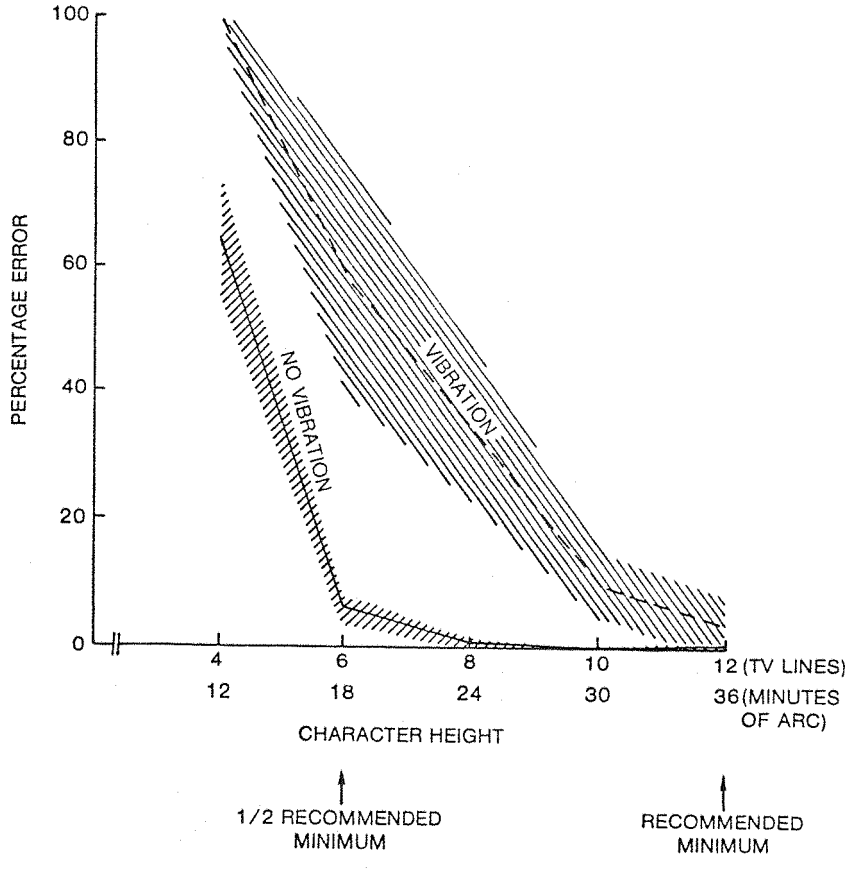

Figure 2.5.29. Mean and ±1 Standard Deviation of Percentage Reading Error as a Function of Character Size on a Helmet-Mounted Display Under Simulated Aircraft Vibration Conditions, 4 Subjects, (after Laycock, 1978)

resolution on the display during both vibration and static conditions. The difference in the static and dynamic conditions was greatest when the character sizes subtended 18 minutes-of-arc. At this size, the vibration caused an 11 to 1 increase in the mean percentage reading error. Although Laycock considered his study as only "preliminary," his findings confirmed that whole-body vibration can affect perception of helmet-mounted displays.

2.6 SUMMARY

The objective of this review has been to identify the factors reported in the open literature which may affect the visual perception of

helmet-mounted displays by observers in airborne vibration environments. The review has explored the operator/display interface from a sensory and cognitive processing standpoint and has shown that the design of the helmet-mounted display can cause special perceptual problems which must be overcome, or at least controlled, in the experimental process.

The operational vibration environment in which the observer must ultimately use the helmet-mounted display has been shown to vary with aircraft type and flight conditions, as well as with the primary and secondary paths which transmit the aircraft vibration to the body. The biodynamic properties of the operator also vary widely and must be controlled by postural and seating restraints. The dynamic visual acuity, pursuit tracking reflex of the eyes, and visibility of vibrating objects have been shown to interact. During whole-body vibration, the angular movements of the head can elicit the vestibulo-ocular reflex which will stabilize the eyes in space over a wide vibration frequency range. The vestibulo-ocular reflex can degrade the visibility of a helmet-mounted display, but many other factors, such as helmet to head dynamics and display characteristics, must be considered.

Table 2.6.1 summarizes some of the factors identifed in this literature review which may influence the way that whole-body vibration will affect the perception of helmet-mounted displays. The central finding of this review supports the hypothesis that whole-body vibration will, under some circumstances, degrade the performance of helmet-mounted displays, however, the nature and extent of this degradation has not been systematically investigated.

TABLE 2.6.1. FACTORS WHICH MAY AFFECT THE PERCEPTION OF HEAD-COUPLED DISPLAYS UNDER AIRCRAFT VIBRATION CONDITIONS

- DISPLAY FACTORS (2.2)

  CRT Characteristics

    luminance
    modulation transfer function
    phosphor color
    phosphor persistance
    refresh rate
    bandwidth

  Optical Characteristics

    field-of-view (magnification)
    viewing distance (collimation)
    modulation transfer function
    combiner
      transmittance
      reflectance
      spectral characteristics
    visor
      transmittance
      spectral characteristics
    exit pupil size

  Mechanical Characteristics

    helmet height
    helmet center-of-gravity
    helmet suspension technique

- VISUAL FACTORS (2.3/2.4/2.5)

  Observer Characteristics

    eye dominance
    visual acuity
      contrast sensitivity function
      Snellen acuity
    learning proficiency
    experience

  Stimulus Characteristics

    type of presentation
      simple reticle
      complex symbols
      pictorial images
    stimulus meaning
    subtended visual angle
    luminance
      target
      background
    contrast
      target to background
    spatial properties } of stimulus
    temporal properties } of stimulus
    spectral properties } of stimulus
    interocular luminance

  Ambient Characteristics

    luminance of surround
    complexity of background scene
    spatial properties

  Other

    training

- BIODYNAMIC FACTORS (2.5)

  Intrinsic

    body weight
    body height
    hip circumference
    body, head, eye resonances
    posture
    muscle tension
    head position

  Extrinsic

    seating conditions
    restraint mechanisms
    secondary paths of vibration conduction

- VIBRATION FACTORS (2.5)

  General Characteristics

    deterministic
      simple harmonic
      complex harmonic
    random
    deterministic and random
    frequency spectra
    amplitude
    direction

  Aircraft

    aircraft type
      fixed wing
      rotary wing
    flight conditions
      velocity
      altitude
      fuel load
    terrain features
    weather
    piloting characteristics

Chapter 3
INTRODUCTION TO EXPERIMENTATION

3.1 OVERVIEW OF EXPERIMENTATION

The central premise of this thesis is that whole-body vibration will affect the perception of visual information presented on the helmet-mounted display. Based upon the review of the literature in Chapter 2, the effects of vibration probably will be a function of the individual subject characteristics, the nature of the vibration input, task variables, and display factors. The purpose of this chapter is to introduce the experimental programme which was conducted to investigate how these factors may affect the perception of a representative helmet-mounted display.

An outline of the research programme is shown in Figure 3.1.1. A total of seventeen experiments were conducted and are reported in this thesis. The experiments were grouped into five categories: character legibility experiments, biodynamic experiments, subjective image displacement experiments, helicopter field trials, and an imagery/stabilization experiment. The organization of these experiments and factors investigated in each of these categories are discussed below, and are listed in Table 3.1.1 for the reading performance experiments and in Table 3.1.2 for the dynamic experiments.

3.1.1 Laboratory Character Legibility Experiments (LG)

Four laboratory experiments were conducted to determine the nature of vertical Z axis sinusoidal whole-body vibration on the legibility of numeric characters presented on the helmet-mounted display. Vibration factors and display factors were dependent variables in these experiments. Vibration factors were the frequency and acceleration level of the vertical seat vibration. Display factors were format of the visual material, character size, character to background contrast, and background luminance. The accuracy of reading the visual material was a dependent variable in all four experiments. The types of reading errors which occurred (i.e., the confusion between numeric characters)

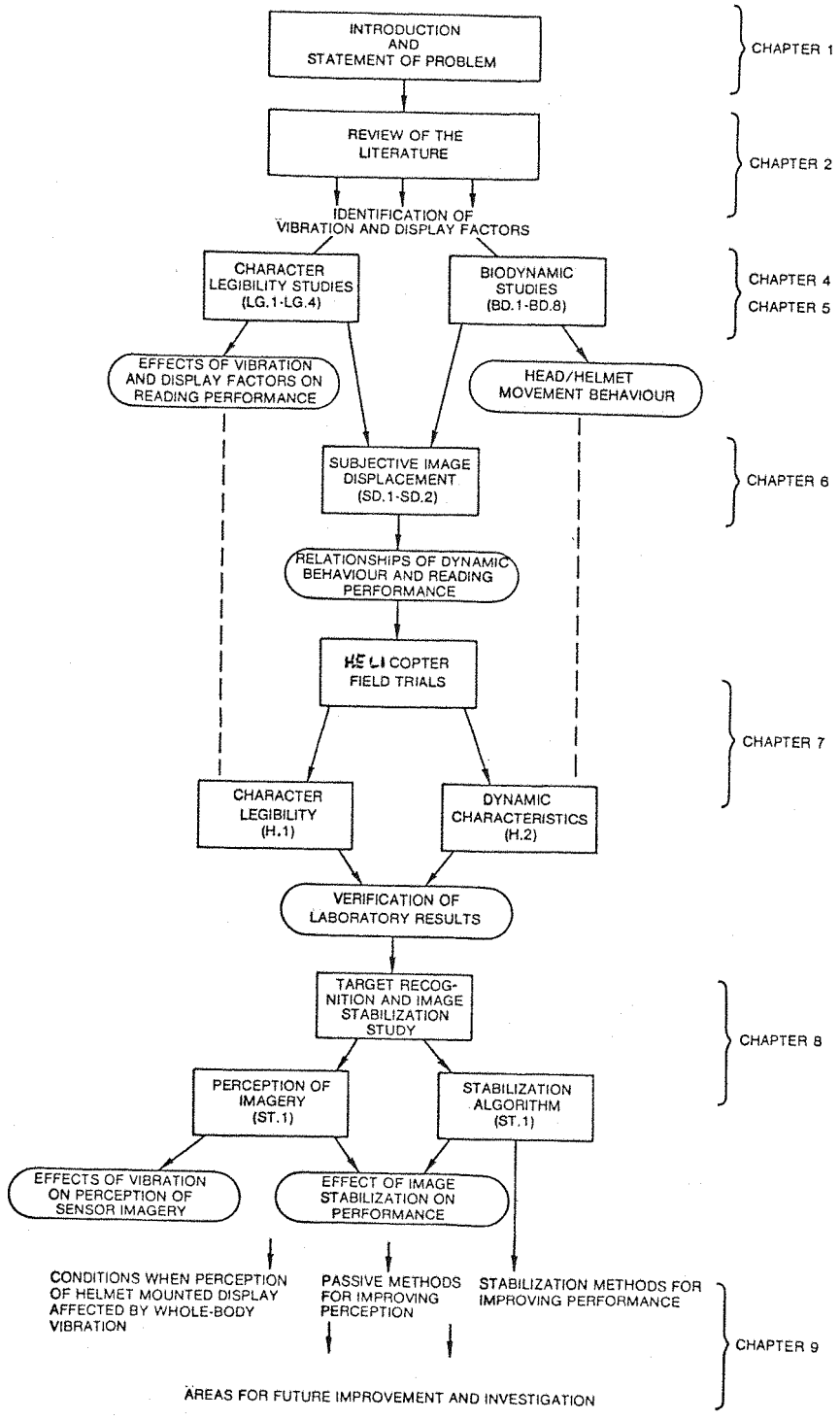

Figure 3.1.1. Outline of Research Programme

were also dependent variables in two legibility experiments. Table 3.1.1 lists the laboratory legibility experiments and the dependent and independent variables which were investigated. These experiments are reported in Chapter 4.

TABLE 3.1.1. FACTORS STUDIED IN CHARACTER LEGIBILITY AND TARGET RECOGNITION PERFORMANCE EXPERIMENTS

Experiment		Section	Independent Variables: Visual Material: Character Array	Visual Material: Character Line	Visual Material: Target Imagery	Display: Format	Display: Image Size	Display: Contrast	Display: Background Luminance	Display: Image Stabilization	Vibration: Frequency	Vibration: Level	Dependent Variables: Accuracy	Dependent Variables: Types of Errors	Dependent Variables: Visual Angle at Recognition
LG.1	Effect of vibration frequency and level on display legibility	4.2	X								X	X	X	X	
LG.2	Effect of display format	4.3	X	X		X					X	X	X		
LG.3	Effect of character size	4.4		X			X		X		1	1	X	X	
LG.4	Effect of contrast and background luminance	4.5		X			X	X	X		2	2	X	X	
H.1	Helicopter field trial - effect of character size	7.2	X				X	3	3		4	4	X		
ST.1	Effect of vibration and image stabilization on target recognition	8.0			X		5			X	2	2	X	X	5

[1]Levels were no vibration (static) and vibration of 1.0 m/s^2 rms at 4.0 Hz and 16.0 Hz.

[2]Levels were no vibration (static) and vibration of 1.0 m/s^2 rms at 4.0 Hz.

[3]Display factors based upon ambient luminance conditions in field trial.

[4]Vibration factors based upon dynamic environment of helicopter during six flight conditions.

[5]Dependent variable was subtended visual angle at target recognition (i.e., target size increased until recognized).

TABLE 3.1.2. FACTORS STUDIED IN DYNAMIC PERFORMANCE

Experiment	Section	Vibration Input: Discrete Frequency	Vibration Input: Swept Frequency	Vibration Input: Helicopter	Independent Variables: Frequency	Independent Variables: Level	Independent Variables: Head Orientation	Independent Variables: Helmet	Independent Variables: Image Displ. on Retina	Independent Variables: Flight Condition	Independent Variables: Stabilization	Dependent Variables: Seat: Seat Z	Seat: Seat X	Seat: Seat Back Z	Seat: Seat Back X	Dependent Variables: Head: Head Z	Head: Head Pitch	Head: Head Roll	Dependent Variables: Helmet: Helmet Pitch	Helmet: Helmet Yaw	Helmet: Helmet/Head Pitch	Image Displ. in Space	Feedback Gain
BD.1 Characteristics & seat Z vibration	5.2	X			X							X											
BD.2 Characteristics of seat back vibration	5.2		X		X									X	X								
BD.3 Single frequency ⅓ octave rms transmissibilities	5.3	X			X												X		X	X	X		
BD.4 Linearity of helmet pitch	5.4	X			X	X													X				
BD.5 Helmet and head transfer function	5.5		X														X	X		X			
BD.6 Head roll to seat Z transfer function	5.6		X		X	X												X					
BD.7 Effect of head orientation	5.7		X		X		X										X			X	X		
BD.8 Effect of flight helmet	5.8		X		X	X			X								X	X					
SD.1 Displacement of display image in space	6.2	X			X	X																X	
SD.2 Displacement of display image on retina	6.3	X			X	1			1			1											
H.2 Head and helmet movement in helicopter field trial	7.3			X	2	2				2		X	X				X	X		X			
ST.1 Image stabilization	8.0	X									X												X

[1]Seat Z acceleration level adjusted by subject to cause specified displacement of nodal images.

[2]Helicopter vibration was varied by the flight conditions.

3.1.2 Biodynamic Experiments (BD)

The purpose of the biodynamic experiments was to determine the nature of the transmission of the vertical sinusoidal vibration of the seat to the head and helmet of seated subjects. Eight experiments were conducted. Independent variables in these experiments were frequency and level of seat vibration and measuring site of the vibration motion. In one experiment, helmet-mounted display orientation in space was also an independent variable (i.e., Experiment BD.7). Dependent variables were the motion behaviour of the head, helmet, and display expressed in terms of the input seat vibration (and head orientation).

The variables investigated in the biodynamic experiments are given in Table 3.1.2. These experiments are reported in Chapter 5.

3.1.3 Subjective Image Displacement Experiments (SD)

The purpose of these experiments was to determine the relationships of the dynamic movements of the head, helmet-mounted display, and eye to the reading performance observed in the character legibility experiments. Since the movements of the eye relative to the helmet-mounted display could not be measured directly, these experiments were conducted to measure these motions using subjective techniques. Both the movement of the helmet-mounted display image in space (i.e., Experiment SD.1) and the relative movement of the display image on the retina of the eye (i.e., Experiment SD.2) were measured this way. Table 3.1.2 lists the variables studied in the subjective displacement experiments. These experiments are reported in Chapter 6.

3.1.4 Helicopter Field Trials (H)

Two field trials were conducted to measure display legibility and dynamic behaviour of the head and helmet due to whole-body vibration in a representative helicopter. In the first study (H.1), the accuracy of reading numeric characters was measured as a function of the subtended angle of the character and the helicopter flight condition

(Table 3.1.1). In the second experiment (H.2), the dynamic nature of the transmission of whole-body vibration to the head and helmet was investigated (Table 3.1.2). These results were used also to verify the results of the laboratory experiments. The helicopter experiments are reported in Chapter 7.

3.1.5 Imagery/Stabilization Experiment (ST)

The purpose of this experiment (ST.1) was twofold: the first, to determine the effect of whole-body vibration on target identification using simulated sensor images presented on the helmet-mounted display; and the second, to define the effect on target identification when the image on the helmet-mounted display was being stabilized in space. The variables studied in this experiment are given in Table 3.1.1. The experiment is reported in Chapter 8.

3.1.6 Implications of Experimental Results

A summary of the experimental results of the research program described above is given in Chapter 9. The implications of results are also discussed in terms of their impact on the design and operation of helmet-mounted displays.

3.2 EXPERIMENTAL HELMET-MOUNTED DISPLAY SYSTEM

3.2.1 General Requirements

The research program outlined above required a helmet-mounted display system which could be used in both laboratory studies and field trials. The display system also had to provide some flexibility to study image and display variables.

Some of the required features were: (1) variable adjustment of the visual angle subtended by the display image; (2) adjustment of the amount of background luminance; (3) adjustment of the amount of image "see-through" so that the virtual image from the display could be superimposed upon outside objects; (4) ability for presenting reticle

or cross-wires independent of video source inputs. Another feature which was especially important for Experiment ST.1 (Chapter 8) was the use of linear deflection amplifiers which facilitated the displacement of the display image to achieve image stabilization. Because of its ability to meet these requirements, the Hughes Aircraft Company Helmet-Mounted Display System (Model 212) was selected for use in this experiment. The system was originally developed by the United States Air Force, Aerospace Medical Research Laboratory, to study the utility and effectiveness of the head-coupled display concept for a variety of military airborne applications (Birt and Furness, 1974). This system was provided to the author by the Flight Systems Department of the Royal Aircraft Establishment, Farnborough.

3.2.2 Description

The helmet-mounted display system (i.e., Hughes Aircraft Company, Model 212) consisted of three units or subsystems: a display electronics unit, a helmet-mounted unit, and a control panel unit. Figure 3.2.1 shows the functional interface of the three units. The display electronics unit received video and composite synchronization signals from a video source and generated the necessary modulation and deflection signals to produce an appropriate image on the cathode-ray tube which was located in the helmet-mounted unit. The helmet-mounted unit also contained a monocular optics assembly which magnified, collimated, and projected the image from the CRT into the right eye of the subject. The optics assembly incorporated a variable density filter which the adjusted transmission of external ambient light through display combiner to the right eye. The control panel unit provided controls for the adjustment of luminous intensity and video gain (i.e., contrast) of the displayed image. For this research programme, the helmet-mounted unit was attached to and used in conjunction with a modified United States Air Force flying helmet (Model HGU 2A/P). The helmet-mounted unit is attached to the flying helmet with a rapid release latch mechanism. Figure 3.2.2 shows a photograph of the three units comprising the helmet-mounted display system. Figure 3.2.3 shows a subject wearing the helmet with the attached helmet-mounted unit. The helmet-mounted unit shown can be

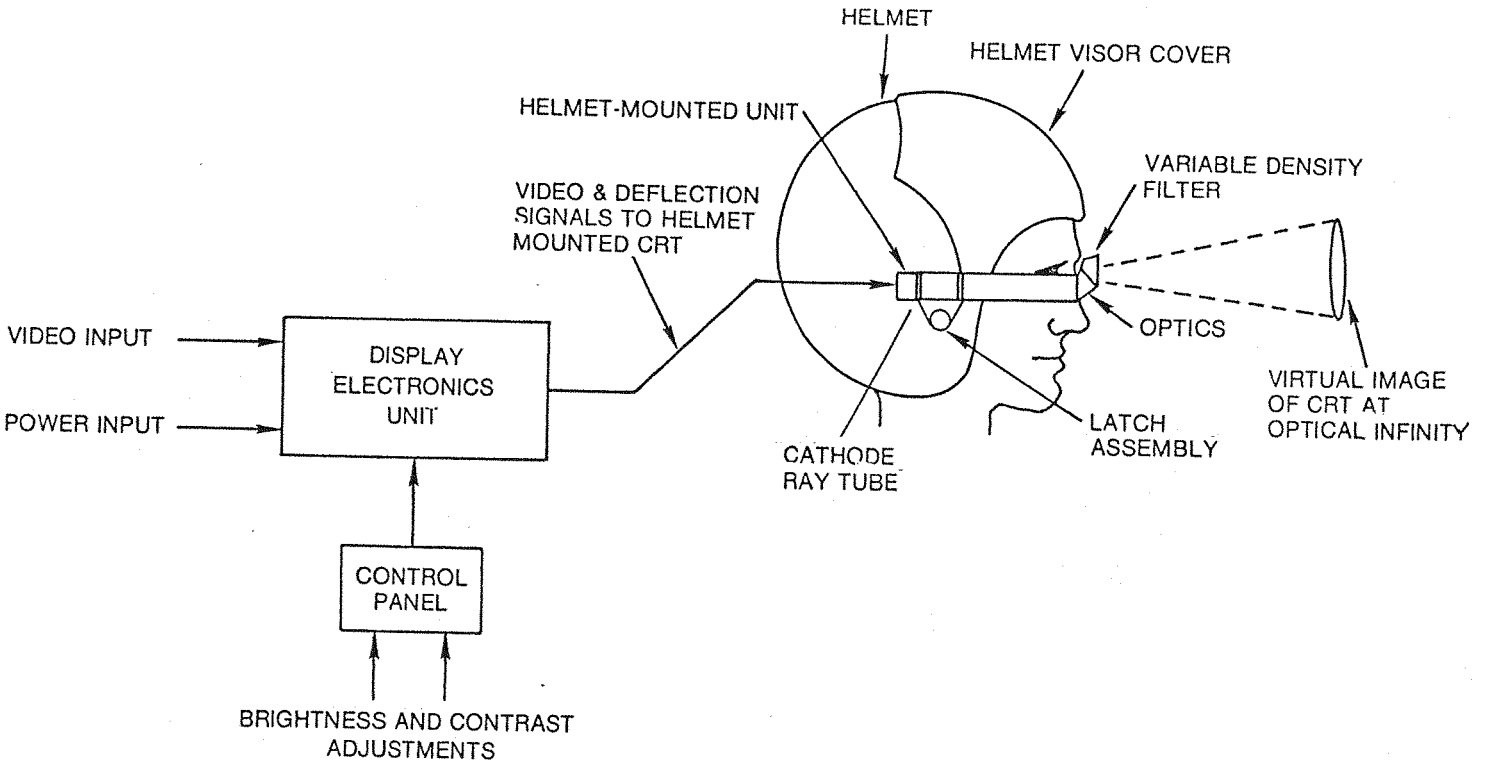

Figure 3.2.1. Functional Interface of Helmet-Mounted Display Components

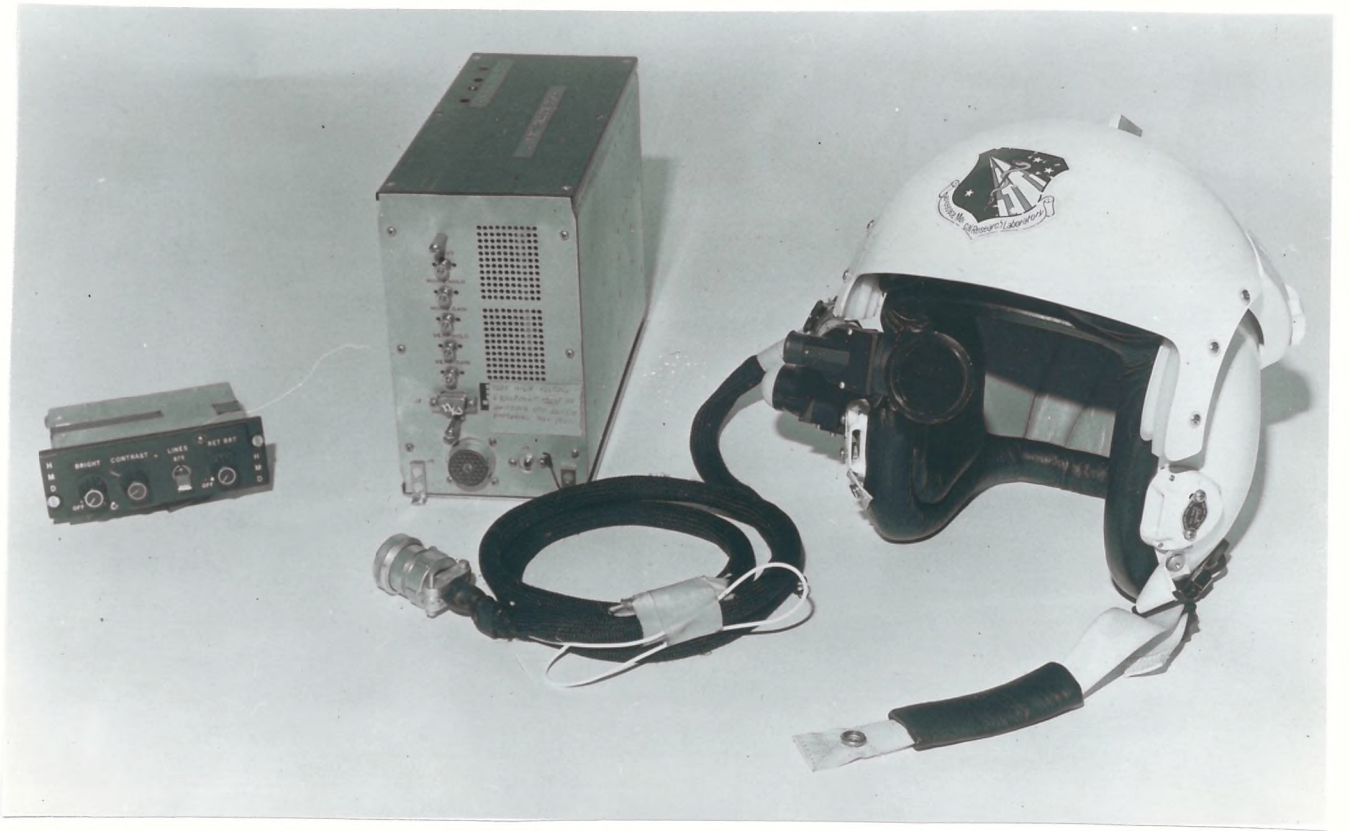

Figure 3.2.2. Units Comprising Helmet-Mounted Display System (Hughes Model HMD 212) Used in Experimental Program. Units are (Left to Right): Control Panel, Display Electronics Unit, Cable and Helmet-Mounted Unit Attached to Flight Helmet (HGU 2A/P)

Figure 3.2.3. Subject Wearing Flight Helmet with Helmet-Mounted Display Unit Attached

operated with the flight visor so that a 15 percent transmittance neutral density filter could be positioned in front of both the right eye with the display and the left eye. Table 3.2.1 gives a summary of the physical and electro-optical characteristics of the helmet-mounted display. A more detailed description of the helmet-mounted display system and its theory of operation is given in Appendix A.3.1. A discussion of the imaging performance of the helmet-mounted display is given in Appendix A.3.2.

TABLE 3.2.1. HELMET-MOUNTED DISPLAY PERFORMANCE CHARACTERISTICS

Optical Characteristics	
Monocular eye piece, either eye operation	
Maximum visual field-of-view	30°
Exit pupil diameter	15 mm
Optical magnification	1 mm on CRT subtends visual angle of 1.58°
Collimation	optical infinity
Combiner transmission	
without filter	.14
with variable transmission filter	.056 - .00066
CRT Raster Characteristics	
Phosphor screen diameter	19 mm
Phosphor type	P-1
Luminance	0-1000 cd/m^2
Total number of scan lines/raster	625
Active scan lines	~588
Interlace	2:1
Frame rate	25 Hz
Useful video bandwidth	>20 MHz
Image Quality*	
Vertical resolution (across scan lines)	
at 50% modulation	6.4 cycles/degree
at 10% modulation	9.4 cycles/degree
Horizontal resolution (along scan lines)	
at 50% modulation	9.0 cycles/degree
at 10% modulation	16.2 cycles/degree
Physical Characteristics	
Additional mass to helmet (including optics, CRT, latch and .25 m of cable)	520 gm
Total helmet mass with display	2255 gm
Center of gravity shift due to helmet-mounted display	32.4 mm**

*Based upon theoretical calculation of modulation transfer functions using laboratory spot size measurements (Appendix A.3.2).

**Estimated shift of center of combined masses of helmet-mounted unit and helmet based upon a center of mass of the helmet-mounted unit located at 190 mm from the helmet center of mass.

3.3 VIBRATION AND CONTROL EQUIPMENT

3.3.1 General Considerations

Single-axis whole-body sinusoidal vibration was used in all laboratory experiments. The vibration was applied to seated subjects in the Z axis. The vibration was restricted to these conditions in order to simplify analyses of the legibility and biodynamic behaviour of the subjects and to facilitate the identification of specific vibration frequencies and levels wherein vibration had the greatest effect on performance. This approach, although not completely realistic in representing the types of vibration environments in aerospace vehicles, did yield results which provided a better understanding of the mechanisms involved in the perception of head-coupled displays under general vibration conditions. Furthermore, the results obtained could be more easily related to laboratory experiments by other investigators. The field tests (i.e., Experiment H.1 and H.2 reported in Chapter 7) provided the means of associating the laboratory data obtained under the sinusoidal single-axis conditions with a real-world multiaxis, complex motion environment. The vertical (Z axis) vibration was considered to be most relevant to use in this research program because there is a preponderance of vertical vibration motion in both rotary and fixed wing aircraft wherein the crew are seated. Also from Chapter 2, the vertical Z axis of vibration appears to have the greatest effects on performance.

3.3.2 Vibration Apparatus

3.3.2.1 Seating Configuration

Subjects were seated on a special helicopter-type seat constructed of wooden plyboard affixed to reinforced aluminium tubing. The seat had a backrest and integral footrest. The geometry of the seat and the position of the feet on the footrest were similar to the seating configuration in the Westland Sea King helicopter. The position of the footrest was adjusted so that the upper legs of the subjects remained horizontal. During the course of the laboratory experimental program,

the seat underwent some modification. Figure 3.3.1 shows a diagram of the seat before modification. This configuration was used for Experiment LG.1, and Experiment SD.1. Figure 3.3.2 shows the seat configuration after modification.

3.3.2.2 Restraint System

The subjects were restrained in the seat by a five point harness system consisting of two shoulder straps, two lap straps, and a strap attached to the horizontal platform of the seat, and routed between the legs to the lap. All straps were connected at the waist by a quick-release buckle. The lap straps and strap between the legs were tightened by adjusting the length of the straps. The shoulder straps were tightened via a reel and ratchet assembly located behind the backrest of the seat.

The purpose of the restraint system was to restrict subject movement and minimize postural variations during the experiment runs. Both of these factors have been shown to have large effects on the transmission of vibration to the head (as discussed in Section 2.5.3.4).

3.3.2.3 Vibrator

The seat and restraint system were mounted on a Derritorn VP180LS electrodynamic vibrator. The vibrator is shown in Figure 3.3.3 with the attached seat. The vibrator was driven by a Derritron 1500 W solid state power amplifier. Figure 3.3.4 shows a subject seated on the helicopter seat, wearing the restraint system and helmet-mounted display.

3.3.2.4 Vibrator Control System

A special purpose control system provided the excitation signals to the power amplifier driving the vibrator. Figure 3.3.5 is a schematic diagram of the control system. The input signal source was derived from either a sine-wave oscillator (Farnell Type LFM 2) or a sine-wave

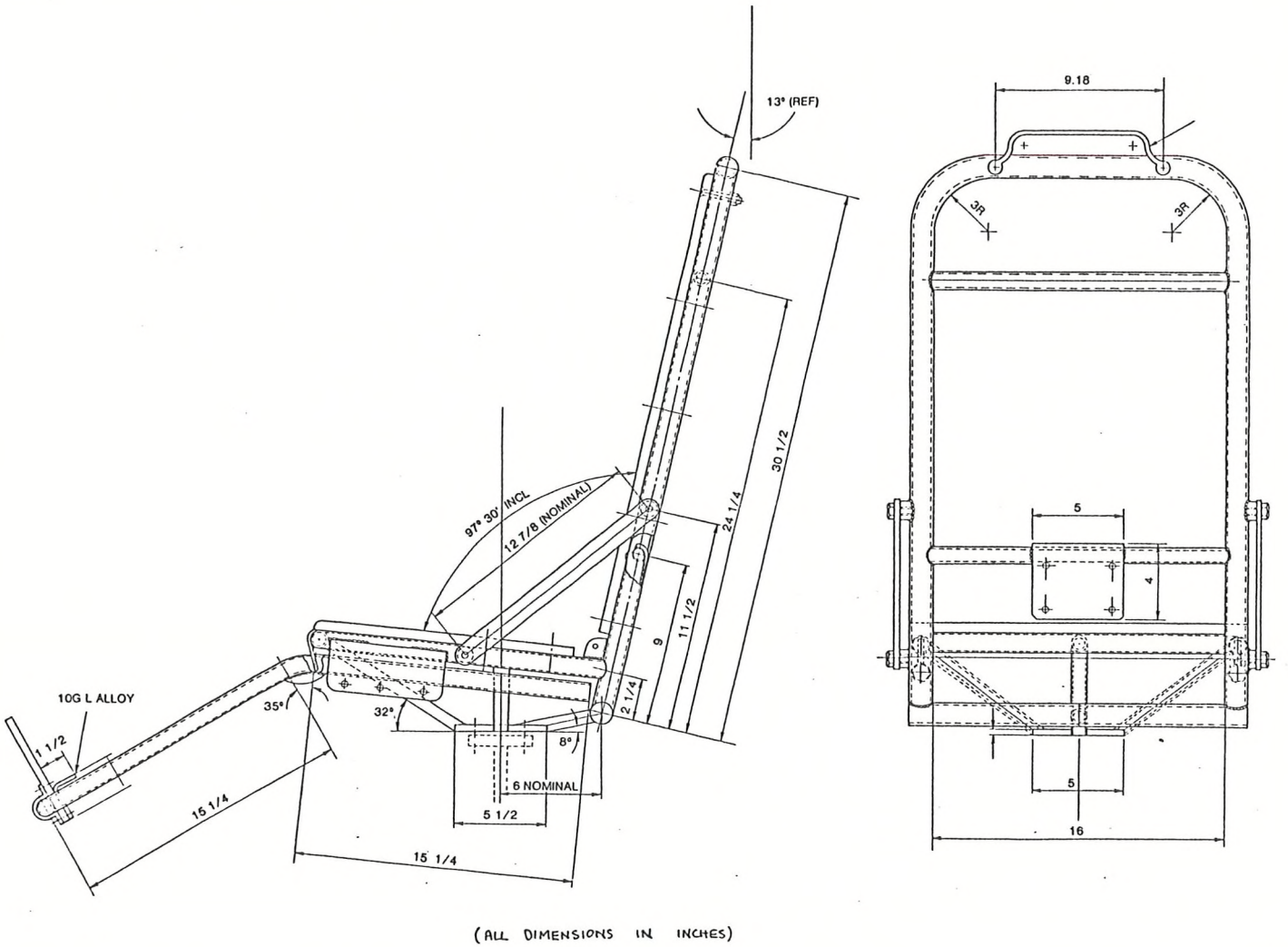

Figure 3.3.1. Configuration of Unmodified Helicopter-Type Seat Used in Research Program

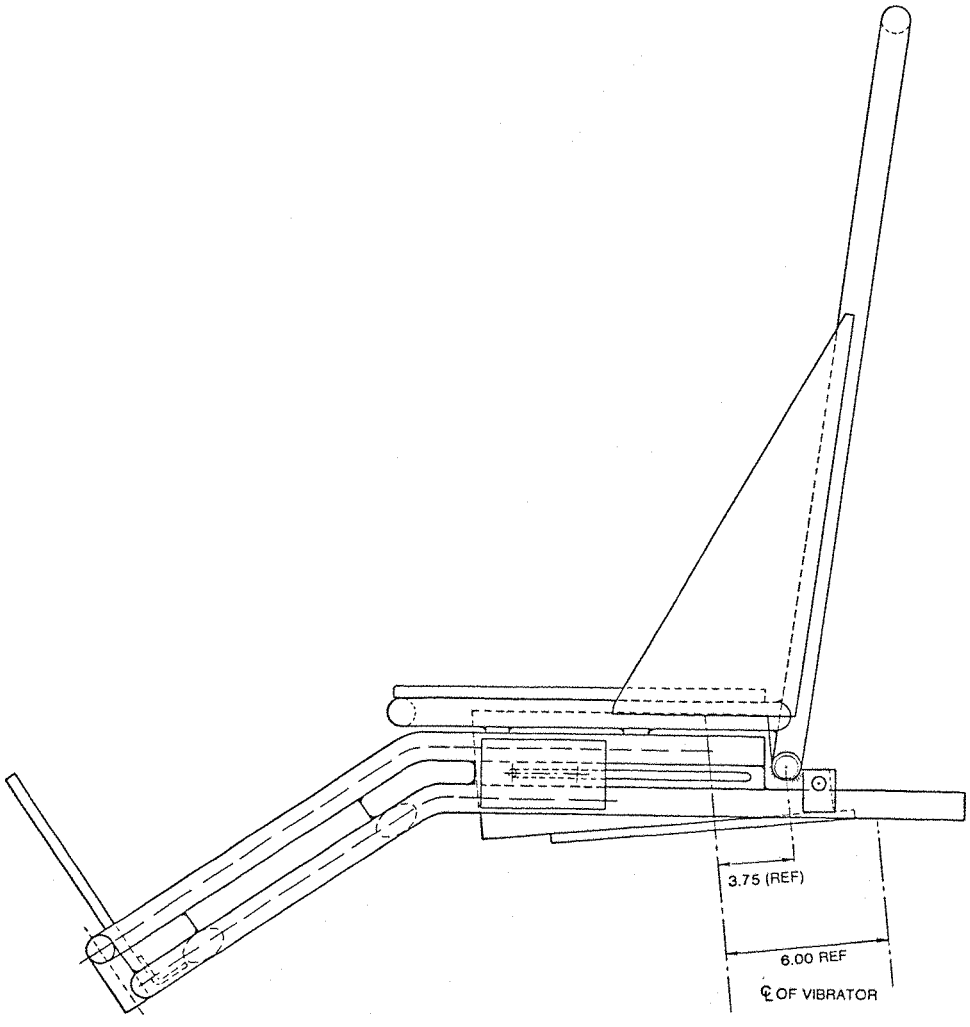

Figure 3.3.2. Configuration of Helicopter Seat After Modification (Major Dimensions Same as Figure 3.3.1)

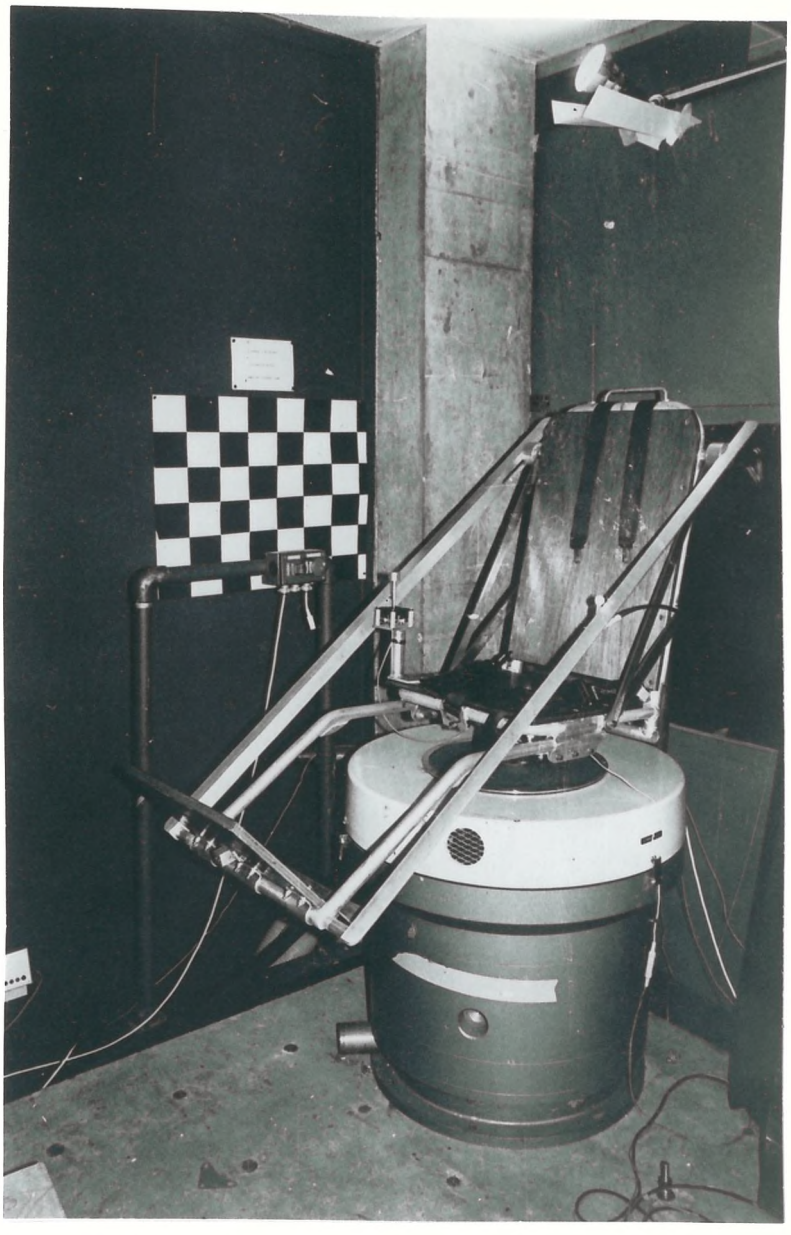

Figure 3.3.3. Electrodynamic Vibrator and Attached Seat Used in Vibration Experiments

Figure 3.3.4. Subject Seated on Vibrator Wearing Restraint System and Helmet-Mounted Display

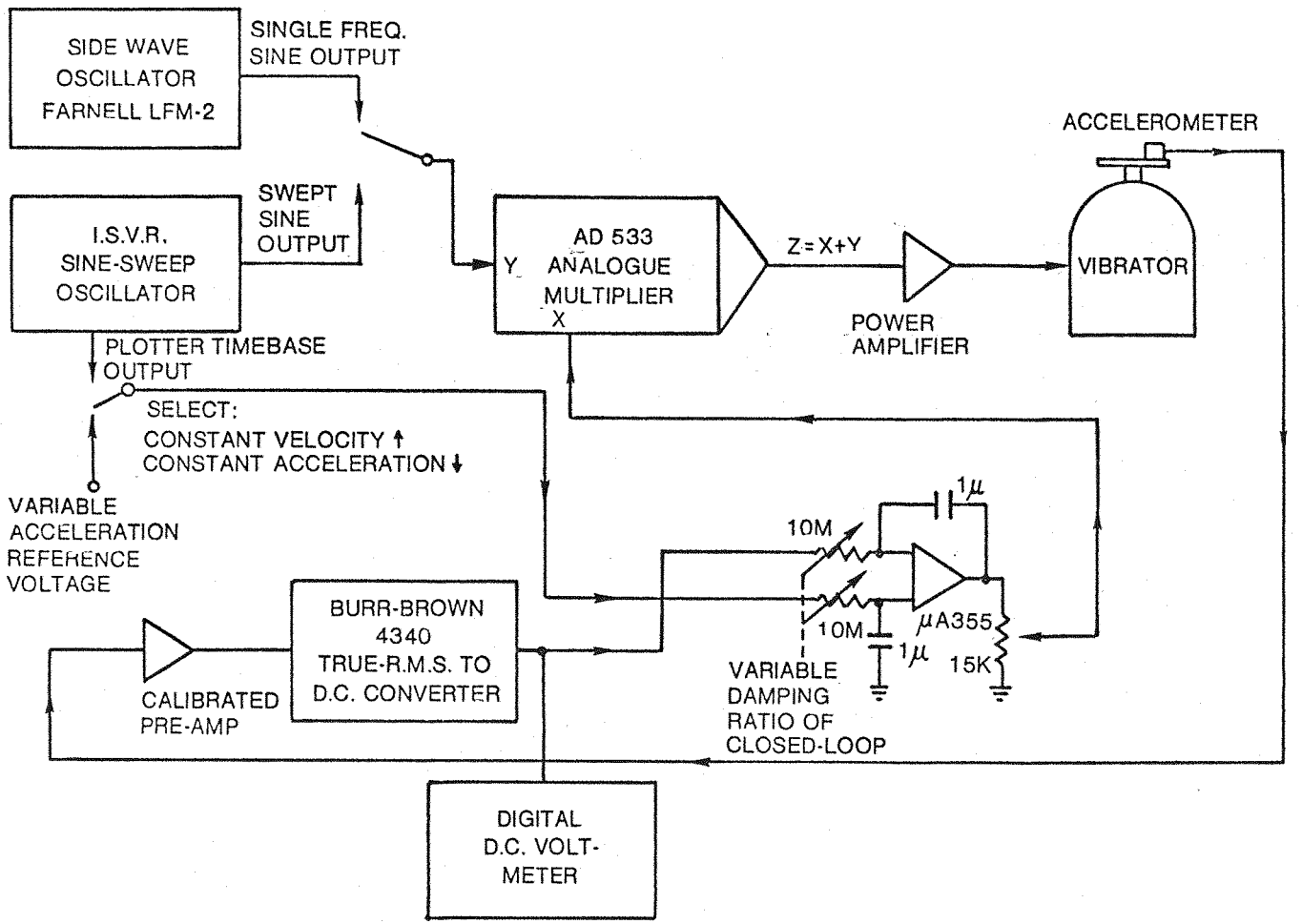

Figure 3.3.5. Schematic Diagram of Vibration Control System

sweep oscillator (ISVR) depending upon the experimental conditions. The desired frequency of oscillation of the vibrator was set on the oscillator (or frequency sweep range and duration in the sine-sweep oscillator). The output of the oscillator was input into an analogue multiplier which performed as a variable gain amplifier. The desired seat acceleration level was set as a reference voltage into an integrating differential amplifier. The vertical vibration acceleration level of the seat was measured continuously by a piezoresistive accelerometer (Endevco Type 2265-20) which was firmly attached to the base of the seat. The output of the accelerometer was preamplified and converted to a voltage representing the root-mean square (RMS) acceleration level in units of m/s^2 rms/volt. This level was monitored during each experiment run by a digital voltmeter (Sinclair Model DM2). The seat acceleration level was also input into the integrating differential amplifier and compared with the reference voltage. The output of this amplifier was then input to the analogue multiplier to control the output level of the oscillator signal to the vibrator amplifier maintaining the seat acceleration at the reference level. As can be seen from Figure 3.3.5, possible fluctuations in the seat acceleration level due to the physical characteristics of subjects (i.e., the loading of the vibrator) or other signal fluctuations (assuming a constant reference voltage) would be compensated automatically. The time constants in the differential integrator were adjusted to provide a reasonable "on-set" and "off-set" of vibration at the beginning and end of the vibration run.

3.3.2.5 Vibrator Performance--Harmonic Distortion

The harmonic distortion of the acceleration motion of the vibrator varied as a function of frequency and vibration level. In general, the distortion was the greatest at frequencies below 2.0 Hz. but decreased with increasing frequency. In Experiment BD.1 (Section 5.2), an empirical analysis of the vibrator distortion is reported over a range of frequencies and vibration levels.

3.3.3 Vibration Conditions

The vibration frequencies and levels used in the experiments described in this thesis were based upon four criteria:

a. The capability of the electrodynamic vibrator;

b. Vibration frequencies and levels deemed nonhazardous by the ISO Standard 2631-1978(E);

c. Pilot studies to determine the frequencies and levels which affected performance;

d. Vibration frequencies and levels most likely to occur in aircraft.

Because the displacement of the vibrator was limited to ±2.5 cm and the output current of the drive amplifier was limited to 100A, sufficient acceleration levels could not be produced by the vibrator at frequencies below 1.4 Hz. Harmonic distortion also increased at the lower frequencies. In general, discrete frequencies separated by ½ octaves over a range of 1.42 Hz to 63 Hz were used for the legibility experiments (i.e., LG.1, LG.2, LG.3, LG.4). The seat Z acceleration levels for each experiment were varied, depending upon the results of pilot studies and the experimental parameters to be investigated.

Some of the biodynamic experiments (i.e., BD.2, BD.5, BD.6, BD.7, BD.8) involved the use of swept sinusoidal frequencies from 1 Hz to 80 Hz or less over a period of up to 100 s. Under all experimental conditions, the exposure of the subjects to vibration was kept to a minimum. At no time did the levels exceed the 1 hour fatigue decreased proficiency curve for vertical Z axis vibration in ISO Standard 2631-1978(E). The average time per experimental run in the legibility experiments was 60 s. The maximum run times for the biodynamic experiments was 200 s.

3.3.4 Safety Precautions

Located at all times within easy reach of both the subject and experimenter was a large red coded "panic" button which, when pressed, would immediately remove all input power and drive signals to the vibrator. The subjects were instructed how to use of this switch before each experiment. In addition, the vibrator contained a mechanical trip switch which was activated when the displacement limits had been exceeded. An adjustable current trip was included in the power amplifier should the output current exceed a specified limit.

3.4 SUBJECTS

3.4.1 Selection of Subjects

A pool of 14 male adults were chosen as subjects for the laboratory experiments. The subjects participated on a volunteer basis, but were paid for their participation. With one exception, all subjects were members of the research staff at the Institute of Sound and Vibration Research, University of Southampton. The subject which was the exception was a skilled craftsman employed outside the university. Prior to participating in each experiment, the nature of the tasks and vibration conditions involved in the experiment were explained to potential subjects. Also, potential subjects were required to read a list of medical conditions which would render them unfit for the experiment (as shown in Appendix A.3.3). If the candidate subject was satisfied that he was medically fit for the experiment (i.e., did not have any of the medical contraindications), then he could volunteer for the experiment by signing an application/declaration form which was also signed by the experimenter (shown in Appendix A.3.4).

3.4.2 Vision Tests

Prior to being selected for participation in the experiments, the subjects were administered a visual acuity test using a Snellen letter test (Overington, 1976). Candidate subjects with unaided visual acuity less than 6/6 in either eye were rejected from participation in

the experiments. In addition, the eye dominance of the subjects was determined using a sighting preference test.

3.4.3 Subject Data

The subjects who participated in the laboratory experiments are listed in Table 3.4.1 with age, height, weight, and results of vision tests. Also given in this table are the specific experiments in which each subject particpated. The characteristics of the two pilots who participated in the flight trials are given in Chapter 7 (Table 7.2.3).

3.5 DATA ANALYSES

3.5.1 Types of Analyses

The analyses performed on the data from the reading performance and dynamic experiments are summarized in Table 3.5.1. A majority of these analyses were performed using the facilities of the Data Analysis Center within the Institute of Sound and Vibration Research, University of Southampton.

3.5.2 Data Analysis Center

The Data Analysis Center operates and maintains a DEC PDP 11/50 digital computer system. A unique software system has been developed by the ISVR staff for acquisition and analyses of time series data using this computer. The foundation of the system is the DEC RSX-11M operating system. The system is a "user-oriented" time-shared system which allows the user to assemble "JOBs" from various software modules. Included in the system are: (1) peripheral transfer modules which perform digitization and storage of time history data using two 14 bit analogue to digital converters (with multiplexing up to 4 channels); (2) arithmetic and general manipulation modules for performing numerical operations on the files in preparation for analysis; (3) data analysis and processing modules which compute Fast Fourier transforms, correlation analysis, power spectral distributions, cross spectral distributions, probability densities, and various statistical

TABLE 3.4.1. CHARACTERISTICS OF SUBJECTS PARTICIPATING IN LABORATORY EXPERIMENTS

Subject	Age (yr)*	Height (cm)	Weight (kg)	Eye Dominance	Visual Acuity Left Eye	Visual Acuity Right Eye	Experiments
1 (JM)	18	185	85	R	6/4	6/4	LG.1, LG.2, LG.3, LG.4, BD.1, BD.2, BD.3, BD.4, BD.5, BD.6, BD.8, SD.1, SD.2, ST.1
2 (ML)	28	181	67	R	6/4	6/4	LG.1, BD.8, SD.1, SD.2
3 (RK)	31	176	75	R	6/4	6/4	LG.1, LG.2, LG.3, LG.4, BD.5, BD.7, BD.8, SD.1, ST.1
4 (TG)	31	181	75	L	6/4	6/4	LG.1, LG.2, LG.3, LG.4, BD.5, BD.8, SD.1, SD.2, ST.1
5 (JL)	31	178	70	L	6/5	6/5	LG.1, LG.2, LG.3, LG.4, BD.5, BD.8, ST.1
6 (IF)	28	169	65	R	6/4	6/4	LG.1, BD.6, BD.8, SD.1
7 (RR)	41	180	77.5	R	6/4	6/5	LG.1, LG.2, LG.3, LG.4, BD.5, BD.8, SD.1, SD.2, ST.1
8 (PH)	25	182	70	L	6/5	6/5	LG.1, LG.2, LG.3, LG.4, BD.5, BD.7, BD.8, SD.1, SD.2, ST.1
9 (SW)	27	180	82	R	6/4	6/4	LG.1, BD.5, BD.8, SD.1
10 (PS)	27	163	55	L	6/5	6/5	LG.1, BD.8, SD.1
11 (RH)	41	176	73.5	L	6/4	6/5	LG.3, LG.4, BD.5, SD.2, ST.1
12 (CL)	29	176	72	L	6/4	6/4	LG.3, LG.4, BD.5, SD.2, ST.1
13 (KP)	26	181	66	L	6/4	6/5	LG.3, LG.4, BD.5, ST.1
14 (MW)	24	181	77	L	6/5	6/4	LG.3, LG.4, ST.1

*Age as of participation in first experiment.

TABLE 3.5.1. DATA ANALYSES PERFORMED ON EXPERIMENTAL DATA

Statistical Analyses (reading performance data)

- Parametric
  - 2 factor analysis-of-variance (ANOVA)
  - 3 factor ANOVA } mixed effect modules
  - split-plot ANOVA } mixed effect modules
  - simple main effects (partition of sums of squares)
  - trend analysis (orthogonal contrasts)
  - regression analysis--equal performance contours
  - chi-square goodness-of-fit
  - paired-t statistical test
  - cumulative probability
  - Dunn's multiple comparison procedure
  - Duncan's new multiple range test
- Nonparametric
  - Friedman two-way analysis of variance
  - Wilcoxon matched-pairs signed ranks test
  - Spearman rank order correlation test

Time Series Analysis (dynamic data)

- Running RMS level
  - power spectral density
  - cross spectral density
  - coherence function
  - transfer function (modulus and phase)
  - confidence intervals
  - transfer function (mean and standard deviation)

analyses; and (4) graphics modules which allow an interactive display of analyzed data and/or plotting of data. The data analysis system above supports multiple user in a time-shared mode using Tektronix 4010 graphics terminals, Newbury VDV terminals, and/or DEC LA36 hard-copy terminals.

3.5.3 Special Programs

In addition to the time series data analysis modules above, several statistical analysis programs were used including two and three factor analysis of variance, split plot analysis of variance, analysis of simple main effects, trend analysis, and computation of equal performance contours. These programs were developed (in Fortran IV plus) and reported by Lewis (1978). In addition, the present author in collaboration with Dr. C. Lewis, ISVR, developed another program for performing the analysis of the transfer functions. Several of these programs are listed for reference purposes in Appendix A.4.1.

Chapter 4
LABORATORY LEGIBILITY EXPERIMENTS

4.1 INTRODUCTION TO LEGIBILITY EXPERIMENTS

The review of the literature (Chapter 2) identified several vibration and stimulus characteristics as having a possible impact upon the perception of a helmet-mounted display during whole-body vibration (e.g., Table 2.6.1). In order to investigate the influence of some of these factors on display perception, four laboratory studies were conducted and are reported in this chapter (i.e., Experiments LG.1, LG.2, LG.3, LG.4; Table 3.1.1). In these studies, display perception was evaluated using a character reading task. This task was selected because it offered the advantages of being easy to score and required minimum subject training. Also, empirical results from these experiments could be related easily to other investigations of the effects of vibration on vision using similar reading tasks.

4.1.1 Visual Material

Numeric characters were used for the reading tasks in these experiments. The characters consisted of the Arabic numerals "zero" through "nine." The numerals were formed in a dot matrix format using 5 elements in the horizontal dimension and 7 elements in the vertical dimension. Figure 4.1.1 shows the character fonts used.

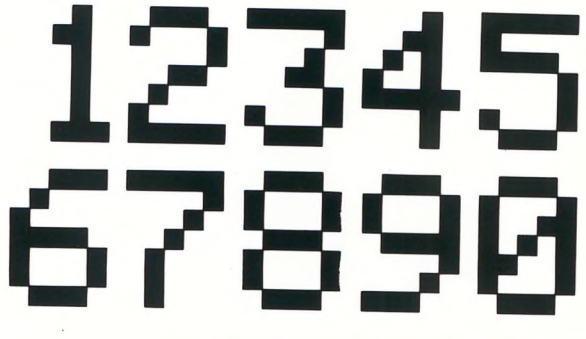

Figure 4.1.1. Examples of Numeric Characters Used in the Legibility Experiments

The numeric characters were generated by a Z axis modulated scanning raster in a computer terminal (Newbury Model 7001) and output as composite video signals to the displays used in the experiments. The numerals were presented as single digits within either an array or line format. The array format contained fifty numerals arranged in five rows by ten columns. The line format consisted of a single row of five or ten numerals, depending upon the particular experiment being conducted. Each format was produced by recalling a data file from either a DEC PDP-11/50 or PDP-11/10 computer.

A total of ten data files were stored in computer memory. Each file contained five lines of ten numbers (0-9) randomly distributed but balanced across positions within all ten files. Each experimental run involved the presentation of fifty numbers from a different file presented either as the array (i.e., 5 rows by 10 columns), five separate lines of ten numbers (10 number-line format), or ten separate lines of five numbers (5 number-line format). Typical array and line formats are shown in Figure 4.1.2. During the experiment runs, the presentation of the formats was monitored by the experimenter using the computer terminal.

4.1.2 Reading Task

In all of the legibility experiments, the subjects were instructed to read aloud each format of numerals presented on the display while being subjected to the various vibration and display conditions. Each line in the format was to be read from left to right, beginning with the top row (array format), and each number was to be read as accurately as possible. The subjects were also asked to pace their reading of each number in cadence with an external tone generator adjusted to produce a 2600 Hz modulated tone burst of 0.2 s duration occurring once each second. The main reason for pacing the reading task was to remove the confounding influence of individual subject reading rate from the accuracy of reading. Pacing also facilitated the scoring of the data. During the presentation of each experimental

a) ARRAY FORMAT

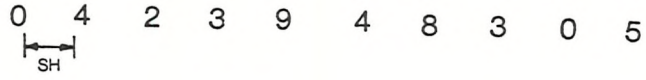

b) LINE FORMAT (10 CHARACTERS)

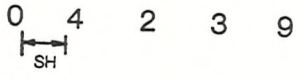

c) LINE FORMAT (5 CHARACTERS)

SH = HORIZONTAL SEPARATION DISTANCE = 5 CHARACTER SPACES *

SV = VERTICAL SEPARATION DISTANCE = 3 CHARACTER SPACES**

* NOTE: CHARACTER HEIGHT OCCUPIES 1/2 OF VERTICAL CHARACTER SPACE

** NOTE: CHARACTER WIDTH OCCUPIES 2/3 OF HORIZONTAL CHARACTER SPACE

Figure 4.1.2. Formats of Visual Material used in Character Legibility Experiments

condition and display file, the subject responses were recorded by the experimenter. Between runs, a new format of numerals was selected by the experimenter. During this time, the display presentation was blanked. The display was unblanked after the next vibration condition had been initiated.

The responses of subjects in performing the reading task were scored to determine both the accuracy of reading (i.e., number of errors committed), and the types of confusions between numbers. Statistical methods were used to test hypotheses concerning the effect of experimental condition on legibility. Because the number of characters presented during each experiment run was large, the error rate was assumed to be a continuous measure exhibiting the properties of a ratio scale (Siegel, 1956). Also, the distributions of the subjects' error scores assumed approximately a normal distribution. Because of these factors, and the assumption that the subjects and samples were drawn from a population that was normally distributed, parametric statistical models were used in the analysis of reading accuracy. Analysis of variance, analysis of simple main effects, tests for trends, and tests for differences in means were assessed by the F distribution and t distribution. Tests for comparing the types of errors committed across experimental conditons were performed with the chi-square distribution. The specific nature of these tests as they apply to the experimental results is discussed for each experiment. Descriptive statistics were used to relate measures of central tendency, dispersion, and correlation in the error scores to the levels of experimental variables such as vibration frequency, level, character size, etc. Several of the computer programs used to analyze the reading performance data are listed in Appendix A.4.1.

4.1.3 Helmet-Mounted Display Operation

The character formats generated on the computer terminal were presented on the helmet-mounted display described in Section 3.2 and Appendix A.3.1, and other panel-mounted displays (described in Experiment LG.1, Section 4.2.2).

Special aspects of adjusting and operating the helmet-mounted display for the laboratory experiments are discussed below.

4.1.3.1 Monocular Viewing

Even though the helmet-mounted unit of the helmet-mounted display system can be used with either the left or right eye of the subject, operation was restricted to right eye only for the experiments reported herein. In order to preclude the effects of binocular rivalry discussed in Section 2.4.7, the ambient illumination and/or outside scene was prevented from entering the left eye by masking the visor of the helmet or, in the case of contrast/background luminance experiment (Experiment LG.4, Section 4.5), by placing a patch over the left eye. In the legibility experiments reported below, the ambient illumination was also eliminated from being transmitted through the combiner of the display on the right eye, except during the contrast/background luminance experiment when the ambient illumination was an experimental variable (Experiment LG.4, Section 4.5).[1] In all of the experiments, the subjects were instructed to keep both eyes open and not to squint while viewing at the helmet-mounted display presentation.

4.1.3.2 Helmet Fit

Prior to each experimental session, the helmet was fitted to the subject in order to minimize slippage of the helmet on the head. The helmet was fitted by inserting foam rubber pads of various thicknesses into the fiberglass shell of the helmet. The foam rubber pads were covered with a soft pliable leather liner and fastened to the inside of the helmet shell with VELCRO strips. Movement of the helmet was restricted further by securing the helmet to the head with a chin strap. This procedure was similar to that followed in the operational flight testing of the helmet-mounted display.[2]

---

[1] The see-through aspect of the helmet-mounted display optical combiner was used in later experiments (SD.1 and ST.1) reported in this thesis wherein subjects were required to superimpose the virtual image generated by the helmet display over an external object.

[2] Later versions of this display employed a "foam in place" helmet liner which consisted of leather covered foam inserts which were formed by using the operator's head as a mold.

4.1.3.3 Adjustment of Display Exit Pupil

The optics assembly of the helmet-mounted display was adjusted for each subject prior to an experimental session to position the exit pupil of the display optics over the pupil of the eye. The diameter of the exit pupil through which the total 30 degree field of view could be viewed was 15 mm. The size of the entrance pupil of the eye (depending upon the light adaptation state) is from 1.5 mm to 8 mm. Nominally, a pupil diameter of 4 mm to 5 mm can be expected for a light adapted eye with an adapting field of 0.1 to 100 cd/m^2 (Overington, 1976). The mechanisms for adjusting the exit pupil are described in Appendix A.3.1. Because the exit pupil is larger than the entrance pupil of the eye, precision adjustment of exit pupil position was not necessary; however, it was desirable to center (approximately) the exit pupil over the entrance pupil of the eye, because image quality was greatest at this position. Another reason was to provide a margin of allowable displacement between the eye and the display optics which could be tolerated should the helmet slip on the head due to vibration transmitted from the seat to the head.

4.1.3.4 Display Focus

In order to insure that the same image quality was being presented to each subject and experimental session, the display focus was inspected prior to each session and any necessary adjustments made to the optical and electronic focus. The collimation of the optics assembly was adjusted to infinity visually by superimposing a displayed character on the helmet-mounted display onto a distant object (i.e., >30 m) and then adjusting the position of the CRT in the barrel of the optics assembly until both the distant object and character were in focus simultaneously.

4.1.3.5 Display Luminance/Contrast

The luminance of the display image and the contrast of the character or target to its background were adjusted via the contrast and brightness controls on the control panel. These controls were calibrated to give precise display output luminances commensurate with the levels of the video input. Because the helmet-mounted display produced a virtual image of the CRT faceplate, there was an inherent difficulty in measuring the brightness characteristics of the images as perceived by the subject. (Note here that the term "luminance" is used to describe the intensity of emitted light from the CRT whereas "brightness" is the apparent luminance intensity as perceived by the subject.) A procedure for measuring the brightness of the virtual image was developed using a brightness matching technique. The details of this technique are reported in Appendix A.4.2. The specific display luminances and contrasts are described in each experiment.

4.1.3.6 Subtended Visual Angle of Display Image

The size of the scanning raster on the CRT and hence the subtended visual angles of the characters, targets, etc. were set by the adjusting the gain of the horizontal and vertical deflection amplifiers. Direct measurement of the dimensions of the images on the CRT faceplate was not possible due to the small sizes of the characters, which were typically less than 0.4 mm in height. Instead, visual angles subtended by the images on the CRT were measured by superimposing the display image on external objects of known size. The procedures for adjusting image size using this approach are described in Appendix A.4.3. Specific dimensions of the display images are described in each experiment.

4.1.3.7 Cable Support

In order to minimize the asymmetrical load of the helmet-mounted unit on the helmet and head, the cable leading from the display electronics unit to the helmet-mounted unit was supported by an attaching it to

the seat structure approximately 250 mm from the helmet-mounted unit. Although the cable was supported in this way, because of its flexibility, there was little or no transmission of vibration from the seat to the helmet via the cable nor was there any restriction (or stiffening) of the head and helmet movements which occurred during the whole-body conditions.

4.1.4 Vibration Conditions

In the legibility experiments, vertical Z axis sinusoidal vibration was presented to subjects seated in the helicopter seat mounted on the Derritron VP-180LS electrodynamic vibrator. The characteristics of the vibrator and its associated control equipment are described in Chapter 3. After Experiment LG.1, the helicopter seat was modified to provide additional stiffening of the seat backs and footrest; however, later studies (Lewis, 1979a) indicated that this modification had little effect on the transmission of vibration to the body. The configuration of the two seats are shown in Section 3.3.2. The specific vibration frequencies and acceleration levels used in the legibility experiments are reported separately for each experiment.

4.1.5 Other Experimental Considerations

4.1.5.1 Duration of Experiments

The duration of a typical experiment run, during which a specific display and/or vibration condition was presented, was from 50 s to 60 s. The durations of the experimental sessions ranged from 1 hour to 1.5 hours including the set-up and adjustment times for the display and practice runs. Subjects were given frequent rest periods during the experiments and at least a 5 minute break approximately half-way through each experimental session.

4.1.5.2 Noise

The influx of cooling air into the vibrator caused a constant broadband noise which was 55 dBA when measured at the subject's head. When the helmet-mounted display was operated, the rotary cooling fan and

motor caused an additional high pitched noise which was added to that above. The total noise from both systems was 58 dBA at the subject's head. These sound levels were measured with a precision sound level meter (B&K Model 2203) operated with a slow time constant.

4.2 EXPERIMENT LG.1: EFFECT OF VIBRATION FREQUENCY AND LEVEL ON HELMET-MOUNTED DISPLAY LEGIBILITY

4.2.1 Introduction and Background

The review of the literature in Chapter 2 has led to the thesis that whole-body vibration will degrade the visibility of head-coupled displays, especially when the input vibration causes rotational motion of the head in either the pitch or yaw axis. The purpose of the first experiment was to determine the nature and extent that whole-body sinusoidal vibration in the vertical Z axis affected the legibility of numeric characters presented on a helmet-mounted display system. The independent variables in the experiment were seat vibration frequency and acceleration, while the performance measure, or dependent variable, was the accuracy of reading visual material consisting of numeric characters (as discussed in Section 4.1).

Prior to conducting this experiment, a pilot study was conducted with three subjects (who did not participate in the main experiment), during which the subtended visual angles of the characters on the helmet-mounted display and the vibration frequencies and levels were manipulated. From the results of the pilot study, a specific character size and a range of vibration conditions were selected so that the performance measure would be sensitive to the various vibration conditions. It was also decided that several vibration levels would be used at each vibration frequency so that regression analyses could be performed for relating reading accuracy to vibration level at each frequency.

In addition to the experiments with the helmet-mounted display, two panel-mounted displays were used as control conditions. The character

size, viewing distances, and vibration conditions used in the experiment for the panel displays were the same as those used by Lewis (1977) in an earlier experiment, wherein photographic visual material was presented. The use of the panel displays thereby provided a possible comparison of this experiment to other experiments where hard copy stimulus material was used (e.g., Crook et al., 1950; Alexander, 1971; O'Hanlon and Griffin, 1971; Meddick and Griffin, 1976; and Lewis, 1977).

4.2.2 Method

4.2.2.1 Displays

The helmet-mounted display equipment used in this experiment is described in Sections 3.2, 4.1.3, and Appendix A.3.1. For comparison, two conventional cathode-ray tube television monitors were used as panel displays. The large panel-mounted display was a video monitor (Phillips Model EL 8111) with a 28 cm diagonal picture tube. The small panel-mounted display was a video monitor (National Model WV 760) with a 15 cm diagonal picture tube.

4.2.2.2 Visual Material

The visual material used in the experiment was a five row by ten column array of fifty random numbers consisting of single digit numerals 0 through 9. Specific aspects of the format of the array, character front, and method of generation are contained in Section 4.1.1.

4.2.2.3 Display Conditions

a) Helmet-Mounted Display

The characters were presented on the helmet-mounted display with a luminance of 19.2 cd/m^2 on an almost totally dark background. The external light was effectively reduced to zero by placing an opaque mask over the helmet-mounted display visor. The visual field from the

helmet-mounted display was viewed only with the right eye of the subject. The raster size of the helmet-mounted display was adjusted so that each character subtended a vertical visual angle of 13 minutes-of-arc and a horizontal visual angle of 9.5 minutes-of-arc. The visual angles separating adjacent numbers in the matrix were 91 minutes-of-arc in the vertical axis and 83 minutes-of-arc in the horizontal axis.

b) Panel-Mounted Displays

The raster size of the small panel-mounted display was adjusted for a character height of 1.1 mm and viewed at a distance of 0.75 m causing each character to subtend a visual angle of 5.0 minutes-of-arc. The raster size on the large panel-mounted display was adjusted for a character height of 2.2 mm and viewed at 1.5 m also producing a subtended angle of 5.0 minutes-of-arc. For both panel-mounted displays, the visual angles separating adjacent numbers in the array were 35 minutes-of-arc in the vertical axis and 32 minutes-of-arc in the horizontal axis. The characters was presented on the panel-mounted displays at a luminance of approximately 3.4 cd/m^2 on a background of approximately 0.3 cd/m^2. The luminance of the overall visual surround in the experimental room was less than the display background luminance. Subjects viewed the two panel-mounted displays with both eyes and did not wear any headgear during the experimental sessions using these displays.

4.2.2.4 Subjects/Task

Ten subjects (S1, S2, S3, S4, S5, S6, S7, S8, S9, S10) were used in the experiment. The individual characteristics of these subjects are noted in Table 3.4.1. The task given the subjects is described in Section 4.1.2. Subjects were given written instructions to read prior to each experimental session. (These instructions are reproduced in Appendix A.4.4.)

The subjects attended three experimental sessions, one for each display type. The duration of each session was approximately 1.25 hours

including the set-up time for the helmet-mounted display. Subjects were given a 7 minute break at the half-way point of each session.

4.2.2.5 Vibration Conditions

During each experimental session, the subjects were presented fifty whole-body vibration conditions consisting of five vibration levels at each of ten sinusoidal frequencies. Details of the vibration conditions used for the two panel-mounted displays are given in Table 4.2.1 and for the helmet-mounted display in Table 4.2.2. The order of presentation of the display type (i.e., helmet-mounted display, small panel-mounted display, large panel-mounted) were randomized across subjects. The order of presentation of the vibration conditions (i.e., frequencies and levels) within each display type were balanced across subjects. A control condition with no vibration was also administered at the beginning and the end of each experimental session. A summary of the experimental conditions is given in Table 4.2.3.

TABLE 4.2.1. VIBRATION CONDITIONS FOR THE TWO PANEL-MOUNTED DISPLAYS

Frequency (Hz)		Vibration Levels (m/s^2 rms)				
		V1	V2	V3	V4	V5
F1	2.8	0.50	1.00	1.50	2.00	2.50
F2	4.0	0.40	0.80	1.20	1.60	2.00
F3	5.6	0.40	0.80	1.20	1.60	2.00
F4	8.0	0.40	0.80	1.20	1.60	2.00
F5	11.2	0.40	0.80	1.20	1.60	2.00
F6	16.0	0.40	0.80	1.20	1.60	2.00
F7	22.4	0.56	1.12	1.68	2.24	2.80
F8	31.5	0.80	1.60	2.40	3.20	4.00
F9	45.0	1.12	2.24	3.36	4.48	5.60
F10	63.0	1.60	3.20	4.80	6.40	8.00

TABLE 4.2.2. VIBRATION CONDITIONS FOR THE HELMET-MOUNTED DISPLAY

Frequency (Hz)		Vibration Levels (m/s^2 rms)				
		V1	V2	V3	V4	V5
F1	1.42	0.28	0.56	0.84	1.12	1.40
F2	2.0	0.28	0.56	0.84	1.12	1.40
F3	2.8	0.24	0.48	0.72	0.96	1.20
F4	4.0	0.20	0.40	0.60	0.80	1.00
F5	5.6	0.20	0.40	0.60	0.80	1.00
F6	8.0	0.20	0.40	0.60	0.80	1.00
F7	11.2	0.28	0.56	0.84	1.12	1.40
F8	16.0	0.40	0.80	1.20	1.60	2.00
F9	22.4	0.56	1.12	1.68	2.24	2.80
F10	45.0	1.12	2.24	3.36	4.48	5.60

4.2.3 Results

4.2.3.1 Analysis of Variance

An analysis of the number of reading errors was carried out for the helmet-mounted display using a mixed effects, 5 by 10 factorial analysis of variance, with subjects as randomized blocks (Kirk, 1968). A summary of this analysis is given in Table 4.2.4. The analysis of variance indicated that the main effects of vibration acceleration level, frequency, and the frequency and level interaction were all highly significant ($p<.001$). Tests of simple main effects of vibration levels were carried out for each frequency showing that the effect of vibration level on reading errors was significant ($p<.01$) for the lower frequencies (1.42 Hz, 2.0 Hz, 2.8 Hz, 4.0 Hz, 5.6 Hz, 8.0 Hz, 11.2 Hz). A test for trends in these data with orthogonal contrasts indicated a highly significant ($p<.001$) linear trend as a function of vibration level for the same frequencies. There were no significant quadratic trends or other departures from linearity in any of the data. A summary of the levels of statistical significance resulting from these analyses is given in Table 4.2.5.

TABLE 4.2.3. EXPERIMENT LG.1: EFFECT OF VIBRATION FREQUENCY AND LEVEL ON HELMET-MOUNTED DISPLAY LEGIBILITY

Purpose: To determine the nature and extent that whole-body vibration affects reading performance of the helmet-mounted display.

Method: Accuracy of reading numeric characters presented on the helmet-mounted display and two panel-mounted displays.

Subjects: 10S (S1, S2, S3, S4, S5, S6, S7, S8, S9, S10).

Viewing Conditions: 5 by 10 array of numeric characters

	Small Panel-Mounted Display	Large Panel-Mounted Display	Helmet-Mounted Display
Display Size	15 cm	28 cm	--
Viewing Distance	0.75 m	1.5 m	optical infinity
Visual Angle of Characters (vertical)	5 min-of-arc	5 min-of-arc	13 min-of-arc
Luminance of Character	19.2 cd/m^2	3.4 cd/m^2	3.4 cd/m^2
Luminance of Background	~0	0.3 cd/m^2	0.3 cd/m^2

Vibration Conditions:
Vertical, Z axis, sinusoidal
Helicopter seat (unmodified)
10 frequencies by 1/2 octaves:
- 2.8 Hz to 63 Hz (panel-mounted displays)
- 1.42 Hz to 45 Hz (helmet-mounted display)

5 levels per frequency
- Table 4.3.1 (panel-mounted displays)
- Table 4.3.2 (helmet-mounted display)

TABLE 4.2.4. ANALYSIS OF VARIANCE SUMMARY TABLE FOR READING ERRORS ON THE HELMET-MOUNTED DISPLAY (EXPERIMENT LG.1)

Treatments: S = Subjects
A = Vibration Levels
B = Vibration Frequency

Source	SS	DF	MS	F Ratio	p
Subjects	16031.78152	9	1781.30911	30.77658	<.001
Treatments	23702.69586	49	483.72849	8.35762	<.001
A	13168.84402	4	3292.21100	39.46881	<.001
B	8310.81277	9	923.42360	5.27649	<.001
A × B	2223.03913	36	61.75108	2.39722	<.001
Residual	25524.51616	441	57.87872		
A × S	3002.86726	36	83.41298		
B × S	14175.59402	81	175.00733		
A × B × S	8346.04713	324	25.75940		
Total	65258.99328	499	130.77955		

For the two panel-mounted displays, a mixed effects, 5 × 10 × 2 factorial analysis of variance, with subjects as randomized blocks, was carried out for the number of reading errors. A summary of this analysis is contained in Table 4.2.6. The analysis of variance indicated that the effects of vibration acceleration level, frequency, and interactions of level and frequency, level and display, and frequency and display were all highly significant ($p<.001$). The main effect of display type (small versus large panel-mounted display) was also significant ($p<.01$). For each of the two panel-mounted displays, tests of simple main effects of vibration level on error rate and analyses of trends were carried out at each frequency. Summaries of these analyses are contained in Tables 4.2.7 and 4.2.8. For the small panel display condition, the effect of vibration level upon reading performance was significant ($p<.05$) at frequencies of 5.6 Hz, 8.0 Hz, 11.2 Hz, and 22.4 Hz. Tests for trends with orthagonal contrasts indicated significant linear trends ($p<.05$) for all frequencies with the exception of 45 Hz and 63 Hz. For the large panel display, the test for simple main

effects of vibration level on reading performance indicated that there was no significant effect of vibration level upon reading performance at any frequency; however, significant linear trends ($p<.05$) were observed in the data at 5.6 Hz, 8.0 Hz, 11.2 Hz, 22.4 Hz, and 31.5 Hz. For both the small and large panel displays, there were no significant quadratic trends or departures from linearity in any of the data.

TABLE 4.2.5. LEVELS OF SIGNIFICANCE FOR THE ANALYSIS OF SIMPLE MAIN EFFECTS AND TESTS FOR TRENDS FOR THE HELMET-MOUNTED DISPLAY (EXPERIMENT LG.1)

Vibration Frequency f (Hz)	Analysis of Simple Main Effects of Level at f	Tests for Trends		
		Linear	Quadratic	Nonlinear
	p	p	p	p
1.42	<.01	<.001	ns	ns
2.0	<.001	<.001	ns	ns
2.8	<.001	<.001	ns	ns
4.0	<.001	<.001	ns	ns
5.6	<.001	<.001	ns	ns
8.0	<.01	<.001	ns	ns
11.2	<.01	<.001	ns	ns
16.0	ns	<.05	ns	ns
22.5	ns	<.01	ns	ns
45.0	ns	ns	ns	ns

TABLE 4.2.6. ANALYSIS OF VARIANCE SUMMARY TABLE FOR READING ERRORS ON THE PANEL-MOUNTED DISPLAY (EXPERIMENT LG.1)

Treatments: S = Subjects
A = Vibration Levels
B = Vibration Frequency
C = Display Type

Source	SS	DF	MS	F Ratio	p
S	20036.57086	9	2226.28571	82.01131	< .001
A	9983.05496	4	2495.76373	26.43217	< .001
B	4207.00795	9	467.44532	5.22511	< .001
C	7535.02357	1	7535.02356	20.04593	< .01
A × B	1539.42191	36	42.76172	3.41173	< .001
A × C	1043.47660	4	260.86915	14.96229	< .001
B × C	1300.43753	9	144.49306	4.56899	< .001
A × B × C	397.88282	36	11.05230	1.23123	ns
Residual	24187.15679	891	27.14608		
A × S	3399.17194	36	94.42144		
B × S	7246.37513	81	89.46142		
C × S	3382.99225	9	375.88804		
A × B × S	4060.92975	324	12.53373		
A × C × S	627.66408	36	17.43511		
B × C × S	2561.60163	81	31.62471		
A × B × C × S	2908.42194	324	8.97661		
Total	70230.03906	999	70.30034		

TABLE 4.2.7. LEVELS OF SIGNIFICANCE FOR THE ANALYSIS OF SIMPLE MAIN EFFECTS AND TESTS FOR TRENDS FOR THE SMALL PANEL-MOUNTED DISPLAY (EXPERIMENT LG.1)

Vibration Frequency f (Hz)	Analysis of Simple Main Effects of Level at f p	Tests for Trends		
		Linear p	Quadratic p	Nonlinear p
2.8	ns	<.01	ns	ns
4.0	ns	<.05	ns	ns
5.6	<.01	<.001	ns	ns
8.0	<.05	<.001	ns	ns
11.2	<.05	<.001	ns	ns
16.0	ns	<.01	ns	ns
22.4	<.05	<.01	ns	ns
31.5	ns	<.01	ns	ns
45.0	ns	ns	ns	ns
63.0	ns	ns	ns	ns

TABLE 4.2.8. LEVELS OF SIGNIFICANCE FOR THE ANALYSIS OF SIMPLE MAIN EFFECTS AND TESTS FOR TRENDS FOR THE LARGE PANEL-MOUNTED DISPLAY (EXPERIMENT LG.1)

Vibration Frequency f (Hz)	Analysis of Simple Main Effects of Level at f p	Tests for Trends		
		Linear p	Quadratic p	Nonlinear p
2.8	ns	ns	ns	ns
4.0	ns	ns	ns	ns
5.6	ns	<.05	ns	ns
8.0	ns	<.01	ns	ns
11.2	ns	<.05	ns	ns
16.0	ns	ns	ns	ns
22.4	ns	<.05	ns	ns
31.5	ns	<.05	ns	ns
45.0	ns	ns	ns	ns
63.0	ns	ns	ns	ns

4.2.3.2 Equal Performance Contours

The performance of subjects in each display reading task can be represented as constant error rate contours of vibration level across frequencies. This form of data presentation allows the frequencies of greatest vibration sensitivity to be clearly indicated. In order to calculate equal performance (error rate) contours, the regression equation

$$e(f) = A_0 + A_1 \cdot v(f)$$

was calculated for each vibration frequency (f), where e(f) is the mean percentage reading error due to vibration level (v). The linear regression values for A_0 and A_1 and the coefficients of correlation are shown for the three displays in Table 4.2.9. Mean static error rates were included in the regression calculation in order to allow extrapolation below the lowest vibration levels actually presented in the experiment. This did not affect the validity of the linear model, as evidenced by the linear correlation coefficients which, for the helmet-mounted display, exceeded 0.96 with the exception of the two highest frequencies, 22.4 Hz and 45.0 Hz, where the correlation coefficients were approximately 0.92. All of the linear correlations for the small panel-mounted display exceeded 0.94 and for the large panel-mounted display exceeded 0.90. All of these coefficients are significantly larger than zero. The vibration level (v) which would result in a given percentage of reading errors (E) was then estimated from the equation

$$V_E(f) = \frac{E - A_0(f)}{A_1(f)}$$

Using this equation, contours of estimated vibration acceleration levels required to produce equal percentage mean reading errors of 10, 20, 30, and 40 percent were computed, and are illustrated in Figure 4.2.1 for the small panel-mounted display, in Figure 4.2.2 for the large panel-mounted display, and in Figure 4.2.3 for the helmet-mounted display. Figure 4.2.4 compares the equal performance contours of the three display conditions for a 10 percent mean reading error.

TABLE 4.2.9. LINEAR REGRESSION EQUATIONS AND COEFFICIENTS OF CORRELATION BETWEEN READING ERROR AND VIBRATION LEVEL AT EACH FREQUENCY OF VIBRATION

Frequency	r_0	A_0	A_1
	A. Helmet-Mounted Display		
1.42	.984	0.729	12.888
2.0	.991	0.548	15.051
2.8	.986	0.633	20.000
4.0	.994	3.100	25.000
5.6	.984	-0.038	22.143
8.0	.965	2.490	19.986
11.2	.987	1.562	12.531
16.0	.976	1.410	5.007
22.4	.924	0.052	3.724
45.0	.920	2.138	0.742
	B. Small Panel-Mounted Display		
2.8	.988	1.500	5.520
4.0	.981	1.248	6.236
5.6	.992	0.852	10.664
8.0	.982	2.352	9.564
11.2	.976	2.862	9.921
16.0	.989	1.138	7.029
22.4	.990	0.610	5.719
31.5	.971	2.424	3.646
45.0	.948	2.019	0.878
63.0	.981	1.986	1.229
	C. Large Panel-Mounted Display		
2.8	.901	1.050	1.700
4.0	.938	1.026	1.582
5.6	.963	0.560	3.482
8.0	.969	0.245	6.346
11.2	.969	0.507	4.468

TABLE 4.2.9. LINEAR REGRESSION EQUATIONS AND COEFFICIENTS OF CORRELATION BETWEEN READING ERROR AND VIBRATION LEVEL AT EACH FREQUENCY OF VIBRATION (continued)

Frequency	r_0	A_0	A_1
16.0	.959	0.931	2.661
22.4	.989	1.017	3.625
31.5	.990	1.012	2.498
45.0	.940	1.312	0.499
63.0	.946	2.217	0.506

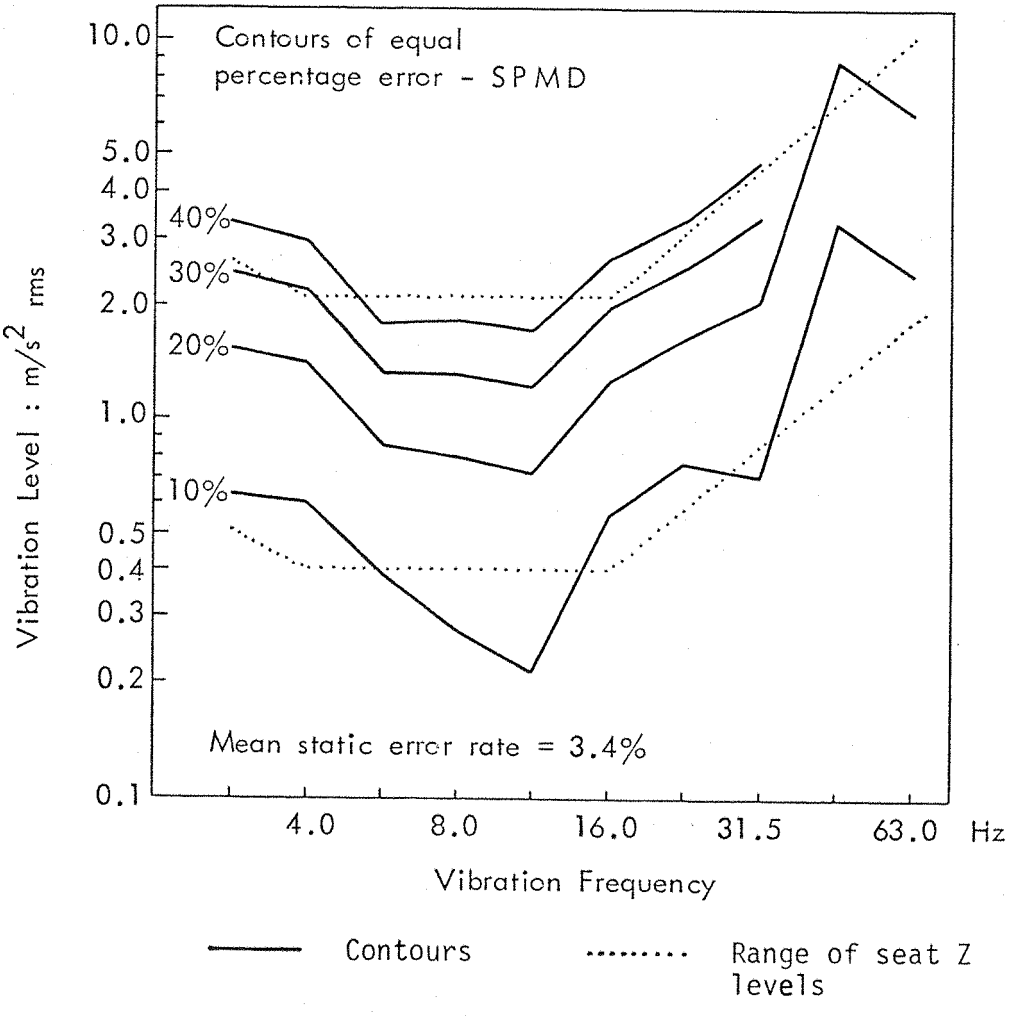

Figure 4.2.1. Mean Contours of Vibration Levels Required to Produce Equal Percentage Reading Errors on the Small Panel-Mounted Display

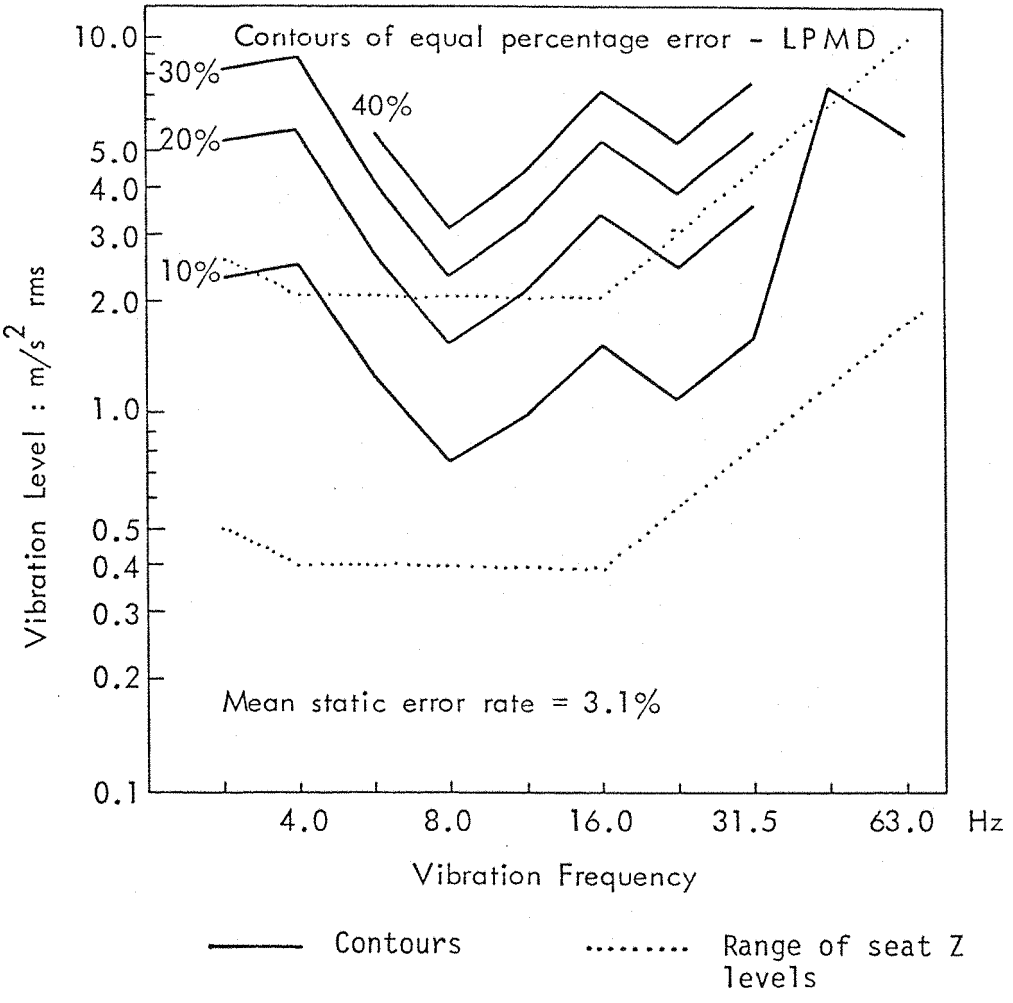

Figure 4.2.2. Mean Contours of Vibration Levels Required to Produce Equal Percentage Reading Errors on the Large Panel-Mounted Display

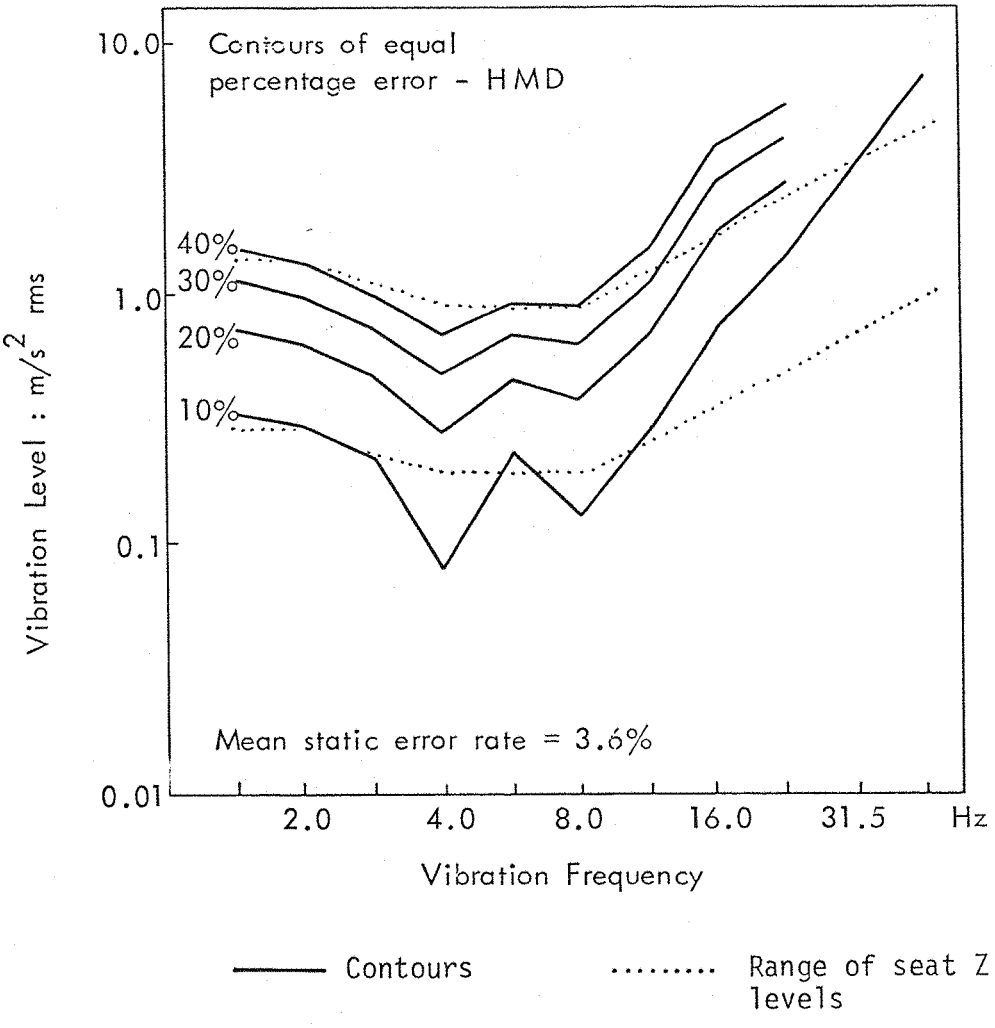

Figure 4.2.3. Mean Contours of Vibration Levels Required to Produce Equal Percentage Reading Errors on the Helmet-Mounted Display

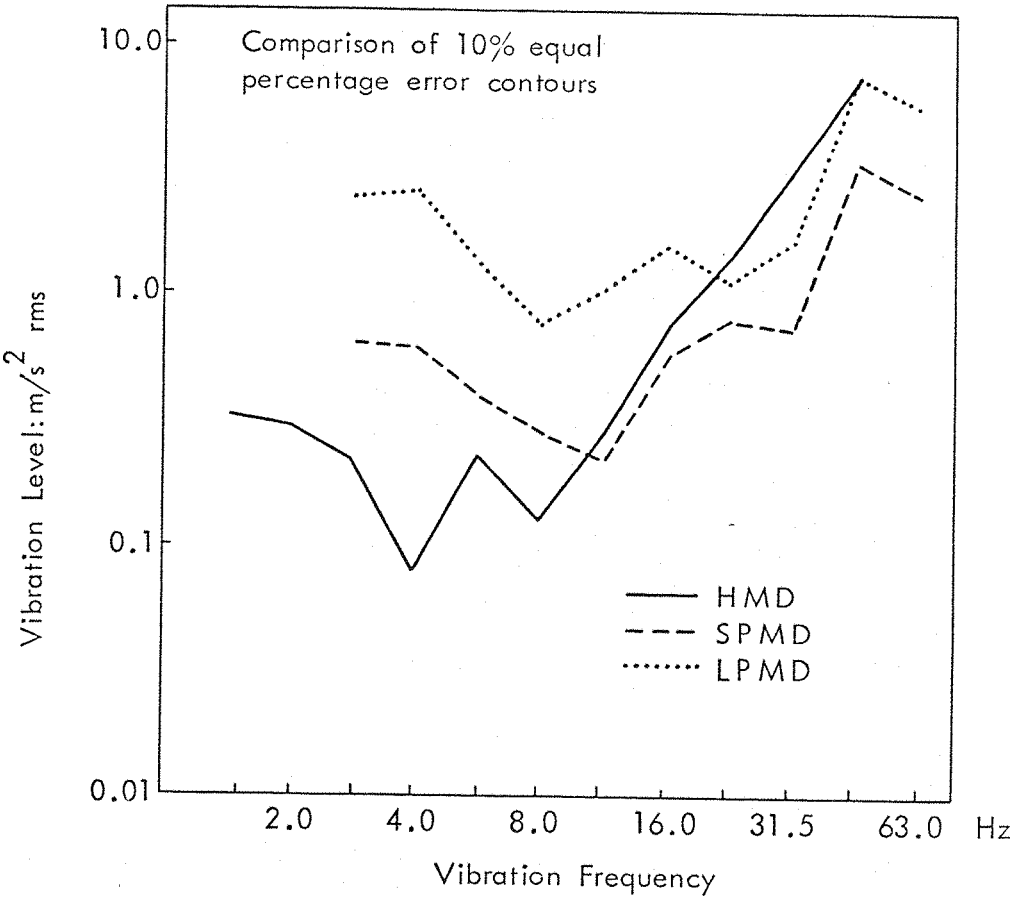

Figure 4.2.4. Comparison of 10 Percent Mean Reading Errors for the Helmet-Mounted Display (HMD), Small (SPMD), and Large (LPMD) Panel-Mounted Displays

It can be seen from Figure 4.2.3 that, while using the helmet-mounted display, subjects were most sensitive to vibration at 4.0 Hz where the regression model predicted that only a 0.08 m/s^2 rms vibration level would produce a 10 percent mean reading error. In fact, at 4.0 Hz the lowest vibration level actually used in the experiment for the helmet-mounted display was 0.20 m/s^2 rms, during which a 18.2 percent mean error rate was observed. By comparison, in Figure 4.2.4, below 11.2 Hz the subjects were less sensitive to vibration while using the two panel-mounted displays, even though the mean reading errors for all three displays under static conditions were approximately equal (i.e., about 3 percent).

4.2.3.3 Comparisons with Photographic Visual Material

The data for the small panel-mounted display is consistent with the results of an experiment by Lewis (1977) using similar character reading material reproduced and presented photographically and viewed under the same vibration conditions. A comparison of the photographic versus electronic display presentations can be made using the equal performance contours. Shown in Figure 4.2.5 are the 95 percent confidence intervals about the 20 percent error equal performance contours for both the photographic data obtained by Lewis (1977) and the small panel-mounted display data from the present experiment. A "paired t" statistical test showed that the equal performance contours derived from performance on the photographic and the small panel-mounted display were not significantly different ($p<.05$). The overlap of the areas between the confidence limits for each type of presentation and the results of the statistical test indicate that the data have been drawn from the same population; therefore, the null hypothesis that there is no significant difference in the photographic hard copy and electronic display presentations is accepted.

4.2.3.4 Individual Variability

The results above were derived from linear regression models of the mean data (in order to obtain the equal performance contours) and as such, do not reflect the large variability in the response observed across individual subjects. For example, Figure 4.2.6 presents the equal performance contours for a 20 percent reading error on the helmet-mounted display for individual subjects. The discontinuities noted in the contours for Subjects S2 and S7 at the 4.0 Hz and 5.6 Hz frequencies are due to the very high error rates produced by these subjects at these frequencies. The greatest intersubject difference in actual error scores occurred at 2.8 Hz and at a vibration level of 0.96 m/s^2 rms when Subject S4 made one error while Subject S6 made 43 errors. Most subjects exhibited a high sensitivity to vibration in the frequency region of 2.8 Hz to 5.6 Hz with the exception of Subjects S4, S5, S8, and S10 whose performance seemed to be affected most at 8.0 Hz and 11.2 Hz. The performance of most subjects improved

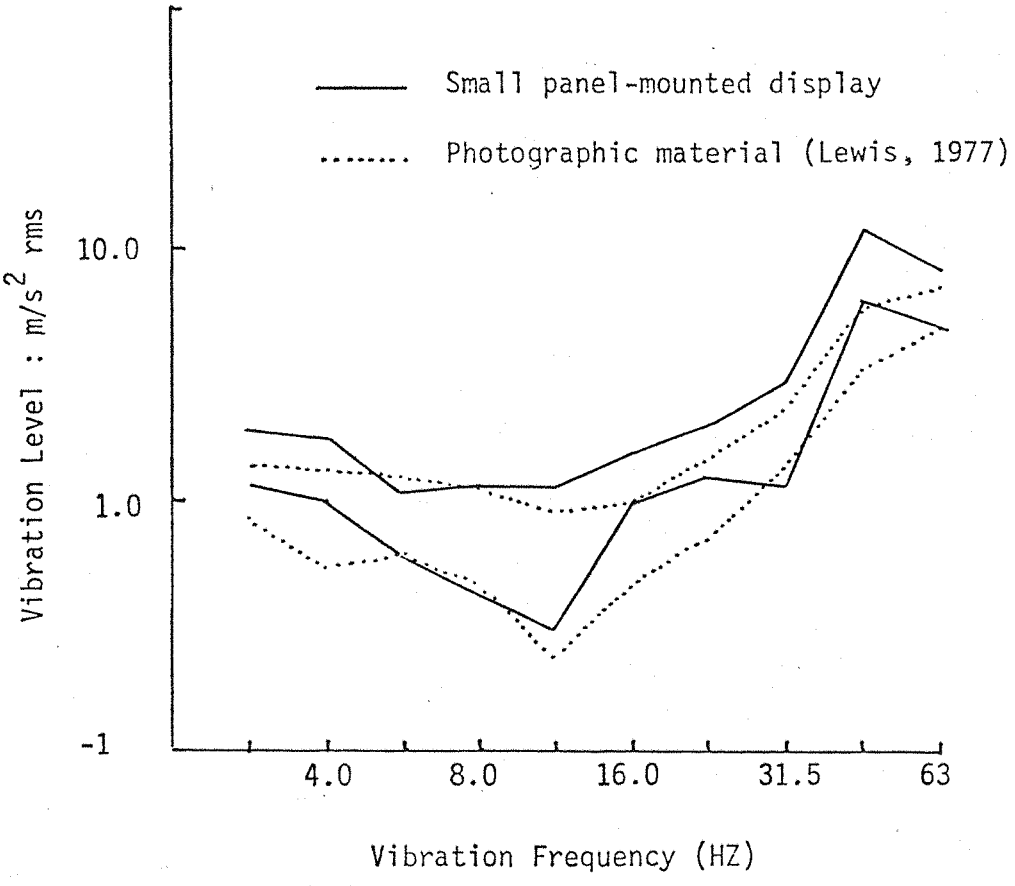

Figure 4.2.5. Overlay of the 95 Percent Confidence Intervals About the 20 Percent Equal Performance Contours for the Photographic Data from Lewis (1977) and the Small Panel-Mounted Display (Experiment LG.1)

above 8 Hz except Subject S10 whose performance improved above 11.2 Hz and Subject S7 whose performance inproved above 16.0 Hz. As expected from the analysis of simple main effects, all subjects showed little effect of vibration level on error rate at 45 Hz.

The variability in the performance of subjects as a function of vibration frequency can be represented by the confidence intervals for the computed values of A_1 in the regression equations in Table 4.2.9. For a given mean reading error rate and frequency, the estimated interval of vibration levels which will produce that error at a particular statistical significance level was computed. Figure 4.2.7 shows the 95 percent confidence interval about the 20 percent mean equal performance contour for the helmet-mounted display. This figure shows that

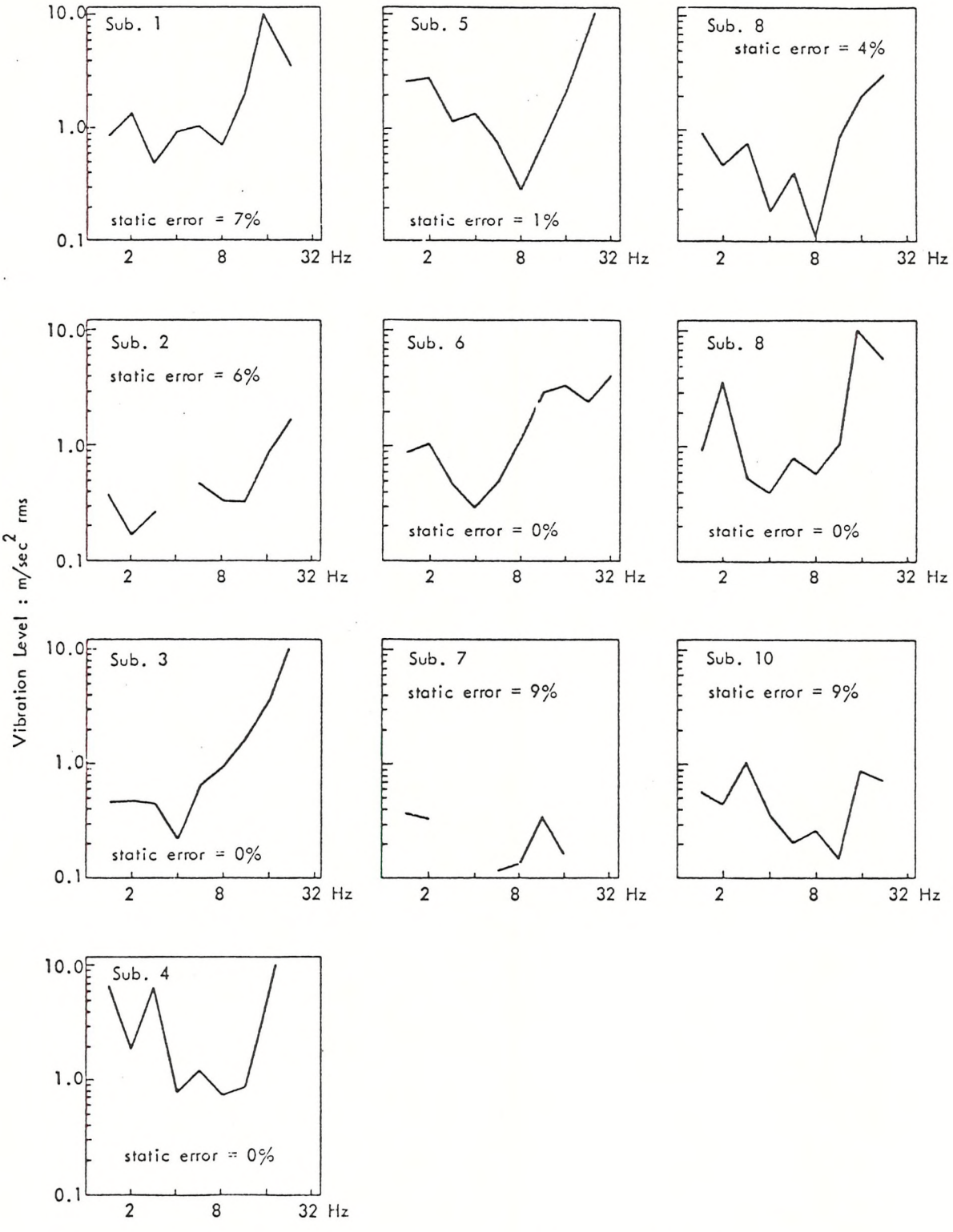

Figure 4.2.6. Contours of Vibration Levels Required to Produce 20 Percent Reading Errors on the Helmet-Mounted Display by Individual Subjects (Experiment LG.1)

although the frequency of greatest sensitivity was 4.0 Hz, the frequency of greatest variability was 8.0 Hz. A possible explanation of this finding will be given later.

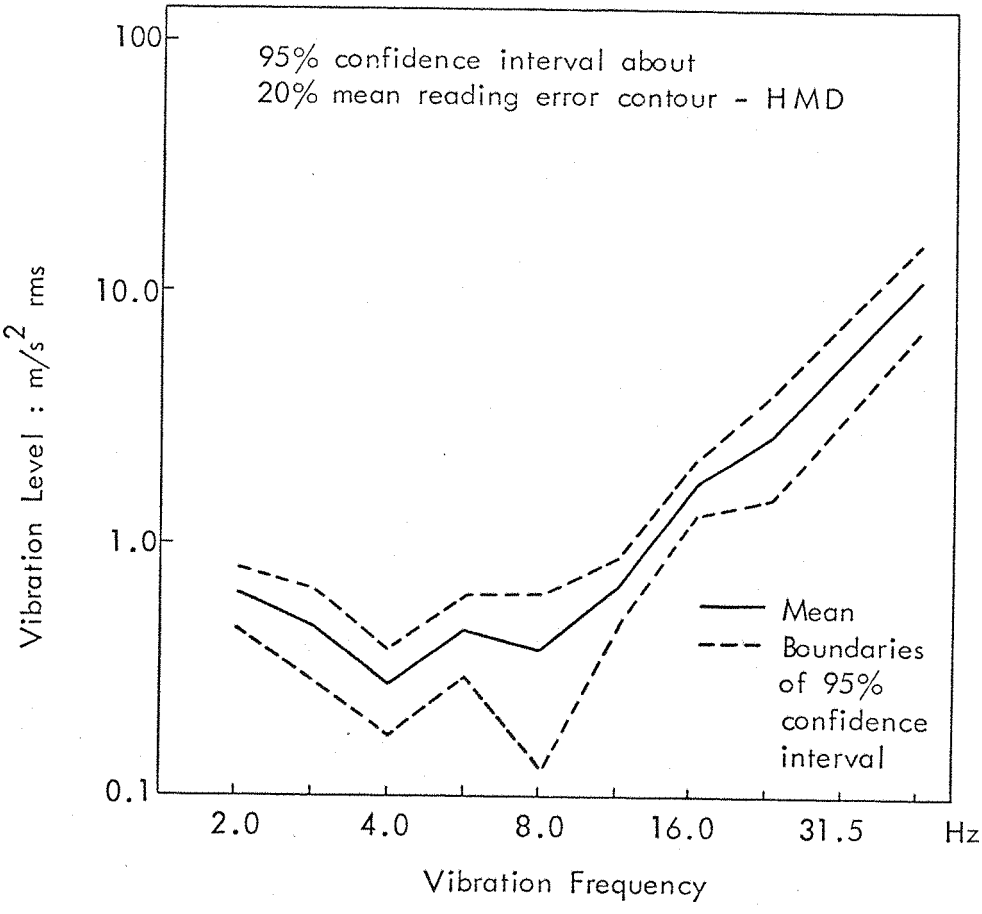

Figure 4.2.7. 95 Percent Mean Confidence Interval About the 20 Percent Equal Performance Contour for the Helmet-Mounted Display (Experiment LG.1)

4.2.3.5 Effect of Character Type

An analysis of the mean error rate for each character type presented on the helmet-mounted display as a function of vibration level at 4.0 Hz and 16.0 Hz is shown in Figure 4.2.8. This figure indicates that the effect of vibration on reading accuracy varied for the different characters being presented. The numeral "8" was most sensitive to vibration whereas the numeral "1" was least affected. The difference in the effects of the two vibration frequencies was very large

and was reflected in the general form of the equal performance contours (Figure 4.2.3). At the 16.0 Hz frequency, the accuracy of reading the numerals "1," "4," and "7" was not affected greatly by vibration until levels greater than 1.2 m/s^2 rms. Note that the linear regression equations shown in Table 4.2.9 for the helmet-mounted display at 4.0 Hz and 16.0 Hz frequencies closely approximates the data shown in Figure 4.2.8.

An analysis of the types of reading errors made by subjects using the helmet-mounted display is shown in Table 4.2.10 for static and vibration conditions of 4.0 Hz and 16.0 Hz. For all of the vibration conditions analyzed, the greatest number of errors was made with the numeral "8." Out of a total of 100 presentations of "8" under static conditions, "8" was read as "0" 11 times accounting for 20 percent of all the errors made under static conditions. The confusion of "8" continued for all vibration conditions even though the errors became more distributed over the other characters as shown. For example, at 4.0 Hz (1.0 m/s^2 rms), "8" was confused in 42 out of 50 presentations being read primarily as "0," "2," "5," or "6." At 16.0 Hz (2.0 m/s^2 rms), "8" was confused with "0" and "6."

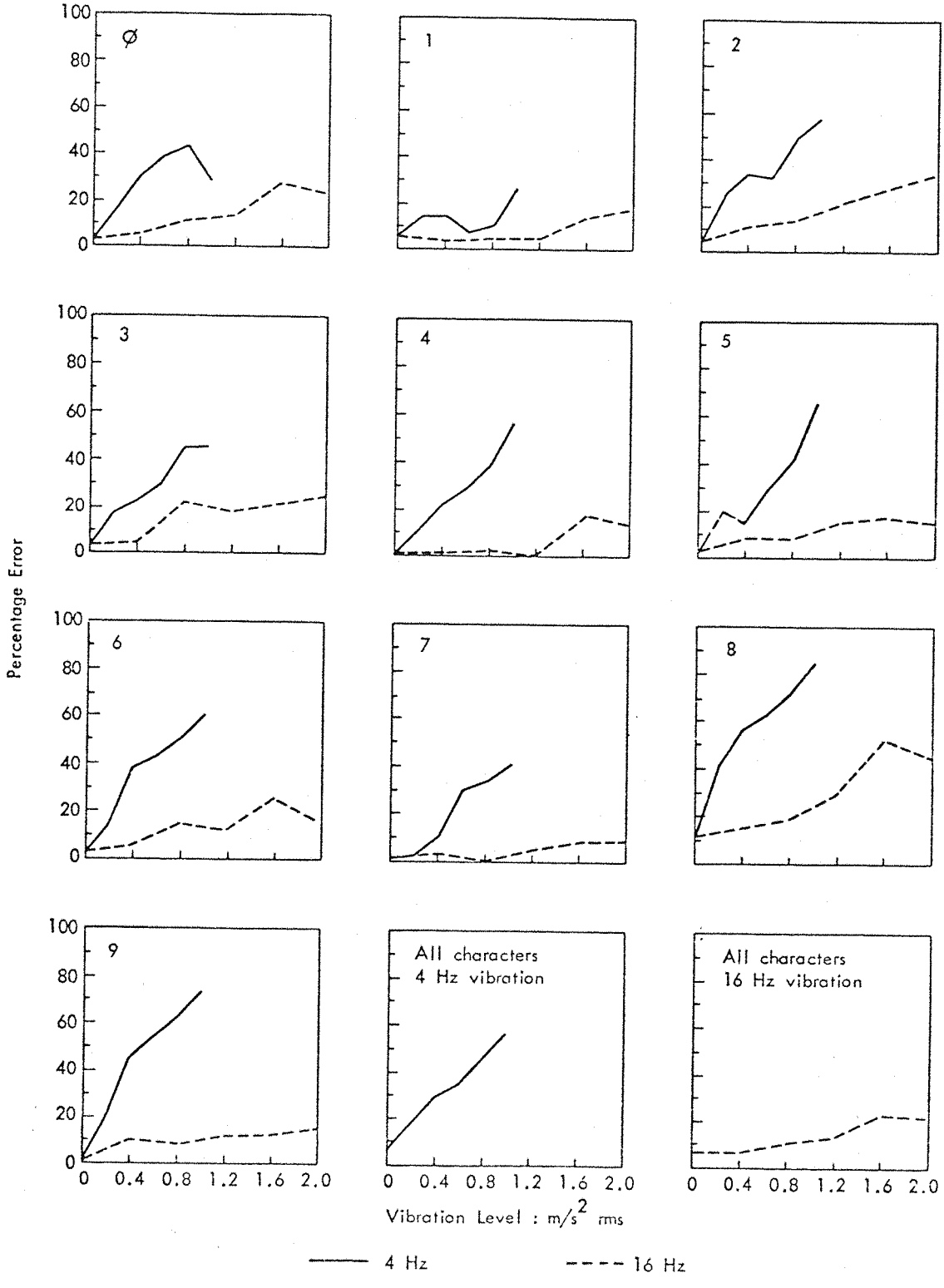

Figure 4.2.8. Increase in Error with Vibration for Each Character Presented on the Helmet-Mounted Display (Experiment LG.1)

TABLE 4.2.10. TOTAL INCIDENCE OF CONFUSIONS BETWEEN INDIVIDUAL CHARACTERS BY 10 SUBJECTS FOR THE HELMET-MOUNTED DISPLAY (EXPERIMENT LG.1)

Error Type	Correct Characters									
	0	1	2	3	4	5	6	7	8	9
	Static Conditions									
0	0	0	0	0	0	0	0	0	6	0
1	1	0	0	0	0	0	0	0	1	0
2	0	3	0	0	0	1	0	0	0	0
3	0	0	3	0	0	1	0	0	1	0
4	0	0	2	0	0	0	1	0	0	0
5	0	1	0	0	0	0	1	0	0	0
6	0	0	0	0	0	0	0	0	1	0
7	0	0	0	3	0	0	0	0	0	0
8	1	0	0	0	0	0	1	0	0	0
9	0	0	0	0	0	0	0	0	2	0
Total	2	4	5	3	0	2	3	0	11	0

N = 30

Error Type	Correct Characters									
	0	1	2	3	4	5	6	7	8	9
	4 Hz Whole-Body Vibration at 1.0 m/s^2 rms									
0	0	1	6	2	7	5	5	5	7	6
1	1	0	2	3	4	1	1	3	2	2
2	0	3	0	0	2	2	0	3	7	1
3	3	1	5	0	4	7	2	1	3	6
4	3	2	3	1	0	3	4	2	2	1
5	3	1	2	5	2	0	5	3	6	8
6	2	2	6	0	1	3	0	1	8	3
7	0	0	0	6	6	4	6	0	4	4
8	5	2	3	2	1	2	3	1	0	5
9	7	1	2	4	1	6	4	1	3	0
Total	24	13	29	23	28	33	30	20	42	36

N = 278

TABLE 4.2.10. TOTAL INCIDENCE OF CONFUSIONS BETWEEN INDIVIDUAL CHARACTERS BY 10 SUBJECTS FOR THE HELMET-MOUNTED DISPLAY (EXPERIMENT LG.1) (continued)

Error Type	Correct Characters									
	0	1	2	3	4	5	6	7	8	9
	16 Hz Whole-Body Vibration at 2.0 m/s^2 rms									
0	0	0	1	1	0	0	4	0	7	1
1	0	0	1	0	1	0	0	0	3	0
2	1	4	0	1	0	0	0	0	2	0
3	0	0	4	0	1	2	0	0	1	2
4	1	0	6	0	0	0	1	0	1	0
5	0	3	2	3	1	0	2	1	0	0
6	4	0	1	1	2	2	0	1	8	1
7	1	0	0	7	1	1	0	0	0	1
8	3	0	1	0	0	2	1	0	0	2
9	2	2	1	0	1	1	0	2	1	0
Total	12	9	17	13	7	8	8	4	23	7

N = 108

A chi-square test of significance was performed comparing the number of errors made for each character at 1.42 Hz, 4.0 Hz, and 16.0 Hz to determine if significant differences existed (Siegel, 1956). The types of errors made at 16.0 Hz were found to be significantly different from those at 1.42 Hz and 4.0 Hz ($p<.05$); however, the types of errors made at 1.42 Hz and 4.0 Hz were similar. All distributions of errors across characters were significantly different from chance ($p<.01$). A further analysis of errors across the vibration levels within each frequency above indicated that the types of errors made were similar ($p<.05$); that is, for an individual frequency, the same types of confusions were made regardless of the vibration level.

4.2.4 Discussion

The experiment was conducted to determine the effects of vibration on the ability of subjects to read visual information on a helmet-mounted display and two panel-mounted displays. The results show that for the character sizes used, the helmet-mounted display was more sensitive to

vibration at frequencies below 11.2 Hz than the two panel-mounted displays. The legibility of all displays was shown to be a function of vibration frequency and amplitude.

The very high error rates observed during this experiment during only moderate levels of vibration indicated the high level of difficulty of the visual task. This task difficulty can be related to the small character sizes. Even the static error rates of 3 percent would be unacceptable for operational applications; but it was necessary to use small characters to insure that errors occurred, even with very low vibration levels, so that the shape of the equal performance contours could be defined over a wide range of vibration levels. The increase in reading errors due to whole-body vibration probably can be attributed to displacements of the display image on the retina due to a relative movement between the optical axis of the eye and the display. If movements of the eye under whole-body vibration were mediated by pursuit and compensatory reflexes, then the unique viewing conditions of each display may have caused the differences in reading performance observed across the three displays.

4.2.4.1 Comparison of Displays

The differences in the effect of vibration on reading performanace across the three displays can be seen by the shape and level of the equal performance contours in Figure 4.2.4. The large panel-mounted display was the simplest case. Here, the longer viewing distance of 1.5 m reduced the relative angular movement of the display due to the linear displacement of the eye resulting from the vertical Z axis vibration input; therefore, motion of the eye relative to this display was due primarily to eye rotation rather than eye displacement. Eye rotation, in turn, resulted from involuntary head motion, due to the vertical, Z axis vibration transmitted through the body to the head. Griffin (1976b) concluded that it was angular motion of the eye rather than linear motion which produced a perceptible blur when subjects viewed stationary point sources of light from a distance of 1.2 m while experiencing whole-body vertical Z axis vibration at frequencies of 7 Hz, 15 Hz, 30 Hz, and 60 Hz. Lewis (1977) also observed in a

numeric reading task similar to the present experiment that for constant subtended visual angles of 4.58 minutes-of-arc and at vertical Z axis vibration frequencies of 3.15 Hz and 16.0 Hz, there was no significant effect upon mean reading errors when the viewing distance was increased from 1.5 m to 3.0 m. This finding again suggests that angular movements of the eye were mostly responsible for the observed decrement in visual acuity of the large panel-mounted display in the present experiment. In this case, the large panel-mounted display was effectively "space-stabilized" relative to the subject. Since the vestibulo-ocular compensatory mechanism seeks to space-stabilize the eye, the pursuit and compensatory reflexes complemented each other, giving rise to the performance contours for the large panel-mounted display shown in Figure 4.2.2. The frequency dependence of these curves was partly due to the nature of the transmission of vertical seat motion to the head, causing the head to move in the pitch axis. Below 4.0 Hz, the error rate was probably reduced due to small displacements of the display image on the retina. This condition would exist if the eyes were being effectively space stabilized by the vestibulo-ocular reflex (VOR) which began at 1 to 2 Hz (Benson and Barnes, 1978). The failure of the VOR to compensate for eye display movement between 4.0 Hz and 11.2 Hz may have been due to the roll-off in gain of the VOR. In addition, large head pitch motions have been shown to occur in this frequency range with a maximum amplitude at approximately 8.0 Hz (Rance, 1978). Improvement in performance above 11.2 Hz may have been due in part to the attenuation of vibration transmitted to the head at the higher frequencies.

The performance of the helmet-mounted display was the most severe departure from the large panel-mounted display. Assuming there was little displacement of the helmet-mounted display on the head, movement of the display image relative to the eye was due to eye rotation. Instead of being effectively stabilized in space, as was the case with the panel-mounted display, the helmet-mounted display was "head-stabilized" except for any slippages of the helmet on the head. Again, below a seat vibration frequency of 1 Hz to 2 Hz, the pursuit reflex would probably have allowed the image to remain stabilized on the retina maintaining the reading performance as shown in Figure 4.2.3;

however, above this frequency, as shown by Benson and Barnes (1978), the subject's ability to suppress the compensatory mechanism failed and the VOR was operative. In this case, the VOR probably stabilized the eye in space not relative to the moving display, causing a movement of the eye relative to the display. Indeed, at frequencies where the VOR was operative, the helmet-mounted display appeared to behave as if the display was vibrating and not the subject. [Huddleston (1970) also found the objects vibrating with a 4 degree double amplitude were most difficult to see at frequencies between 3 Hz and 5 Hz.] It appears from Figure 4.2.3 that above 4.0 Hz the effect of the compensatory reflex may have begun to decrease, causing a slight improvement in the reading performance of the helmet-mounted display. The discontinuity in this trend at 8.0 Hz may have been due to large head rotational displacements stated earlier, or perhaps relative movements of the helmet on the head.

The performance of the small panel-mounted display was probably affected both by translational and rotational motions of the display relative to the subject's eye. Since the subtended angle and the luminances of the characters were the same for both panel-mounted displays, the differences in performance as shown in Figure 4.2.4 were primarily due to viewing distance. The viewing distance of the small panel-mounted display was one-half that of the large panel-mounted display (0.75 m versus 1.5 m) causing the linear displacement of the display relative to the subject to be twice that for the large panel-mounted display, whereas the rotational components of movement were the same. The reading performance of the small panel-mounted display can be attributed, therefore, to both linear and rotational vibration components of the head and eye.

It is interesting to note that the performance of all three displays approached each other at the frequencies above 16.0 Hz (Figure 4.2.4). Since the rotational movements of the eye have been shown to dominate at the higher frequencies (e.g., Griffin, 1976), the effect of eye linear motion on the small panel-mounted display reading task was reduced, causing performance to approach that of the large panel-mounted display. Rance (1978) has shown also that the amplitude of

head pitch motion resulting from vertical Z axis seat vibration is also greatly attenuated at the higher frequencies. This factor may account for the improvement of helmet-mounted display performance at the higher frequencies.

4.2.4.2 Subject Variability

The large variability in display reading performance across subjects shown in this experiment was a factor also noted by Griffin (1975b) which he found to be largely due to differences in the transmission of vibration to the head. As shown in Figure 4.2.6, there were similarities in the shape of the equal performance contours for individual subjects reading the helmet-mounted display, but there were also large differences in the overall vibration levels required to produce a given error rate. Part of the intersubject variability may have been associated with differences in the difficulty of the reading task experienced by individual subjects under static conditions. From Figure 4.2.6, there does appear to be some correlation between the overall level of equal performance contours and the number of errors made during static conditions. Another factor which affected variability in these data was posture. Griffin (1975b) noted large effects of voluntary changes in posture upon vibration transmitted to the head, thereby altering considerably the threshold of visual blur. In the present experiment, however, major changes in sitting posture were prevented by a restraining harness, even though minor postural changes and increased muscle tension may have affected performance. The frequency dependence of the variability of certain results may relate to the differing biodynamic responses of the subjects. Resonances and the absorption of vibration by the upper torso may vary greatly across subjects and affect the amount of vibration transmitted to the head.

Another factor affecting performance was the level of effort each subject applied to the reading task. Several subjects were observed to "give up" when higher vibration levels were encountered while others remained diligent, even though they complained about the difficulty of the task. All subjects were instructed to keep trying. In general,

the subjects consistently underestimated their accuracy in the reading task under all conditions.

4.2.4.3 Character Confusions

The distribution of errors as shown in Table 4.2.10 and the chi-square tests for significance indicate that for the helmet-mounted display different visual mechanisms may have been present at the 4.0 Hz and 16.0 Hz frequencies. One possible explanation for this finding is that the characteristics of the vibration transmitted to the head may have been different for these frequencies. Subjects indicated that at seat vibration frequencies of 16 Hz and above, the characters appeared to move in lateral, circular, or elliptical directions rather than strictly vertical (as observed at frequencies of 1.42 Hz to 4.0 Hz). Griffin (1975b) also found that his subjects observed a change in the motion of the characters in the visual field as a function of frequency. Meddick and Griffin (1976) noted that when reading numerals which were vibrating in a frequency range of 3 to 10 Hz, the errors due to confusions between numerals depended upon the vertical, horizontal, or circular motion of the numbers. A possible reason for these observations is that at 16 Hz, a greater level of yaw and roll motion of the eye and head may have existed than at 4.0 Hz. The asymmetrical shift in the center of gravity of the head/helmet mass due to the extra mass of the helmet-mounted unit on the right-hand side of the helmet may have contributed to the introduction of yaw and roll motion of the display under some vibration conditions. This possibility will be discussed in more detail in Chapter 5.

The large number of "8s" which were misread under static conditions was a trend observed throughout all of the data. A close inspection of the character fonts shown in Figure 4.1.1 shows that perhaps the similarity of the "8" and "0" due to the diagonal line through the zero may explain this high error rate. Meddick and Griffin (1976) also found a high incidence of error with the numeral "8" in their experiment using character fonts conforming to British Standard 3693A.

4.2.4.4 Dyanmic Behaviour and Reading Performance

It is evident that a more rigorous explanation of the findings of this experiment and an understanding of the effects of vibration on head-coupled display performance cannot be obtained until the nature of eye, head, and helmet movement behaviour present under these vibration conditions have been investigated. The dynamic response of the subjects' head and helmet to whole-body vibration will be reported in Chapter 5. Further treatment of the relationships between biomechanical factors and display visibility in light of the biodynamic experiments is deferred until Chapter 6.

4.2.5 Summary

The objective of this experiment was to determine the nature and extent of the effects of vibration on the perception of information presented of the helmet-mounted display. The principal findings of the experiment were as follows:

1. Vertical sinusoidal Z axis whole-body vibration significantly degraded helmet-mounted display legibility with the 4.0 Hz frequency causing the greatest number of reading errors.

2. Linear relationships were observed between mean error rates and vibration levels for most frequencies. Equal performance contours were computed from linear models of mean error rates.

3. A large variability in reading performance was observed across subjects with 8 Hz being the frequency of greatest variability.

4. The effects of vibration on display legibility were different for the helmet-mounted display and the two panel-mounted displays.

5. Data from the experiment for the small panel-mounted display were similar to that of other experiments using photographic visual material.

6. The types of reading errors varied with vibration frequency, but not at different levels within a vibration frequency.

7. The sensitivity of reading performance to vibration level varied with character type, the number "8" being the most sensitive and the number "1" being the least sensitive.

The sensitivity of the helmet-mounted display to vibration was enhanced by using a small character size; nevertheless, the degradation in performance as a function of vibration was real and could be measured as a result of the reading errors committed by the subjects. Because of the small character size, the absolute levels of vibration to produce a given error rate is not meaningful from a practical design standpoint; however, the shape of the equal performance contour curve (as a function of frequency) and the linear relationship with level is significant (at least for the range of vibration conditions and character sizes used). The influence of the character size on reading is investigated in Experiments LG.3 and LG.4 reported in Section 4.4 and 4.5.

There are many implications of the results of this experiment with regard to operational use of the helmet-mounted display. Under some conditions, the degradation may be so severe as to require stabilization of the display image relative to the eye. The treatment of these operational aspects of the research findings of this experiment as well as other related visibility and biodynamic experiments will be deferred until Chapter 9.

4.3 EXPERIMENT LG.2: LINE VERSUS ARRAY DISPLAY FORMAT

4.3.1 Background

The results of Experiment LG.1 clearly indicated that whole-body vibration affected the legibility of symbolic visual material presented on the helmet-mounted display. In that experiment, the 13 minutes-of-arc visual angle subtended by the characters presented on the helmet-mounted display was chosen as being sufficiently small to cause some residual error under a no vibration condition. This aspect of the visual presentation caused the reading accuracy measure to be sensitive to very low levels of vibration. However, the magnitude of the spacing between characters in the vertical dimension of the array was a factor which was not addressed in either the pilot study or main study of Experiment LG.1. During the conduct of that experiment, several subjects indicated that under some extreme vibration levels, they had observed overlapping of the nodal images between the adjacent rows in the array, but that they could not judge if this overlap had affected their performance. It was noted by the experimenter that some subjects, during some vibration conditions, seemed to lose place while reading the matrix; that is, they would reread a row of numbers or even skip an entire row. The subjects stated that the array appeared to have 10 rows instead of 5. This phenomena was due to the formation of nodal images on the retina caused by the relative pitch axis angular motion of the helmet display, head, and eyes during the vertical Z axis whole-body vibration. The profusion of nodal images alone may have caused some degradation in reading performance and, consequently, would have to be considered an artifact which may have confounded the results of the experiment.

Experiment LG.2 described in this section was conducted to investigate the possible artifacts of the array format. The purpose of the experiment was to compare the reading performance of the array format with a single line format under vibration conditions similar to Experiment LG.1. The central null hypothesis for this experiment was that there is no significant difference in reading performance between the two display formats.

4.3.2 Method

This experiment was conducted using helmet-mounted display and vibration experimental apparatus as described for Experiment LG.1. The modified helicopter seat was used instead of the original seat (Section 3.3). The subtended angle of the characters was set at 15 minutes-of-arc and the display luminance adjusted to approximately 19 cd/m^2.

The visual material for each data run consisted of 50 random numbers. As an experimental condition, the numbers were arranged either in an array format (5 rows by 10 columns) as in the previous experiment or in five single rows of 10 numbers which were presented a row at a time in the display (e.g., Table 4.1.2). The vibration conditions consisted of six sinusoidal frequencies (2.8 Hz, 4.0 Hz, 5.6 Hz, 8.0 Hz, 11.2 Hz, 16.0 Hz) presented at three seat Z axis acceleration levels (0.6, 1.0, 1.4 m/s^2 rms). Other conditions were the same as Experiment LG.1.

Six subjects were used in this experiment. These subjects were drawn from the original ten subjects used in Experiment LG.1 (S1, S3, S4, S5, S7, and S8) having the physical characteristics described in Table 3.4.1. The subjects were given similar written instructions as in the first experiment. Appendix A.4.5 contains a copy of the instructions to subjects for the array and line formats. For the line format, the subjects were instructed to read from left to right a line of 10 numerals after which the experimenter would cause the next line to appear on the display and so on until the subject had read 5 lines of 10 numbers each for that condition. The order of presentation of the display formats and vibration frequencies and levels were randomized and balanced across subjects. Reading scores were taken under static (no vibration) conditions at the beginning and end of each display format condition. Subjects were given a practice run before each display format condition. A summary of the conditions for the experiment are given in Table 4.3.1.

TABLE 4.3.1. EXPERIMENT LG.2: LINE VERSUS ARRAY DISPLAY FORMAT

Purpose:	To determine presence of artifacts in reading performance due to an array format presented on the helmet-mounted display.
Method:	Compare reading accuracy of helmet-mounted display visual material arranged in a line versus an array format.
Subjects:	6S (S1, S3, S4, S5, S7, S8)
Visual Material:	Visual angle of characters (15 minutes-of-arc) Character luminance (19 cd/m^2) Line format (5 separate lines of 10 characters each) Array format (1 array of 5 rows by 10 columns)
Vibration:	Vertical, Z axis, sinusoidal Helicopter seat (modified) 6 Frequencies (2.8, 4.0, 5.6, 8.0, 11.2, 16 Hz) 3 Levels (0.6, 1.0, 1.4 m/s^2 rms)

4.3.3 Results and Discussion

4.3.3.1 Central Tendency of Reading Accuracy

The mean and standard deviation of the number of reading errors categorized by display format and vibration condition are shown in Table 4.3.2. The mean data are plotted in terms of percentage reading error in Figure 4.3.1 for the array format data and Figure 4.3.2 for the line format data.

Both sets of curves show a consistent effect of vibration level at most frequencies (the exception being 8.0 Hz).

TABLE 4.3.2. MEAN AND STANDARD DEVIATION OF THE NUMBER OF READING ERRORS FOR THE LINE AND ARRAY DISPLAY FORMATS (EXPERIMENT LG.2)

Vibration Frequency (Hz)	Seat Z Axis Acceleration					
	Level 0.6 m/s^2 rms		Level 1.0 m/s^2 rms		Level 1.4 m/s^2 rms	
	Line	Array	Line	Array	Line	Array
2.8	3.83 (6.01)*	2.67 (3.44)	7.33 (11.08)	6.00 (5.76)	12.33 (11.64)	10.50 (9.69)
4.0	6.83 (5.78)	7.17 (7.91)	10.67 (7.34)	9.00 (6.29)	15.17 (13.99)	18.00 (10.60)
5.6	5.17 (3.06)	5.17 (5.53)	9.83 (6.59)	10.33 (8.71)	15.17 (9.95)	13.17 (11.81)
8.0	6.33 (5.01)	5.00 (6.57)	7.67 (6.86)	5.33 (6.50)	6.67 (5.65)	6.50 (8.17)
11.2	2.67 (3.44)	2.83 (3.76)	4.17 (4.62)	2.67 (2.94)	5.83 (4.96)	4.17 (3.60)
16.0	1.50 (3.21)	0.83 (1.17)	2.33 (2.66)	2.83 (2.93)	4.00 (3.90)	3.83 (4.45)
Static (line) = 0.75			Static (array) = 1.00			

*Standard deviation shown in brackets

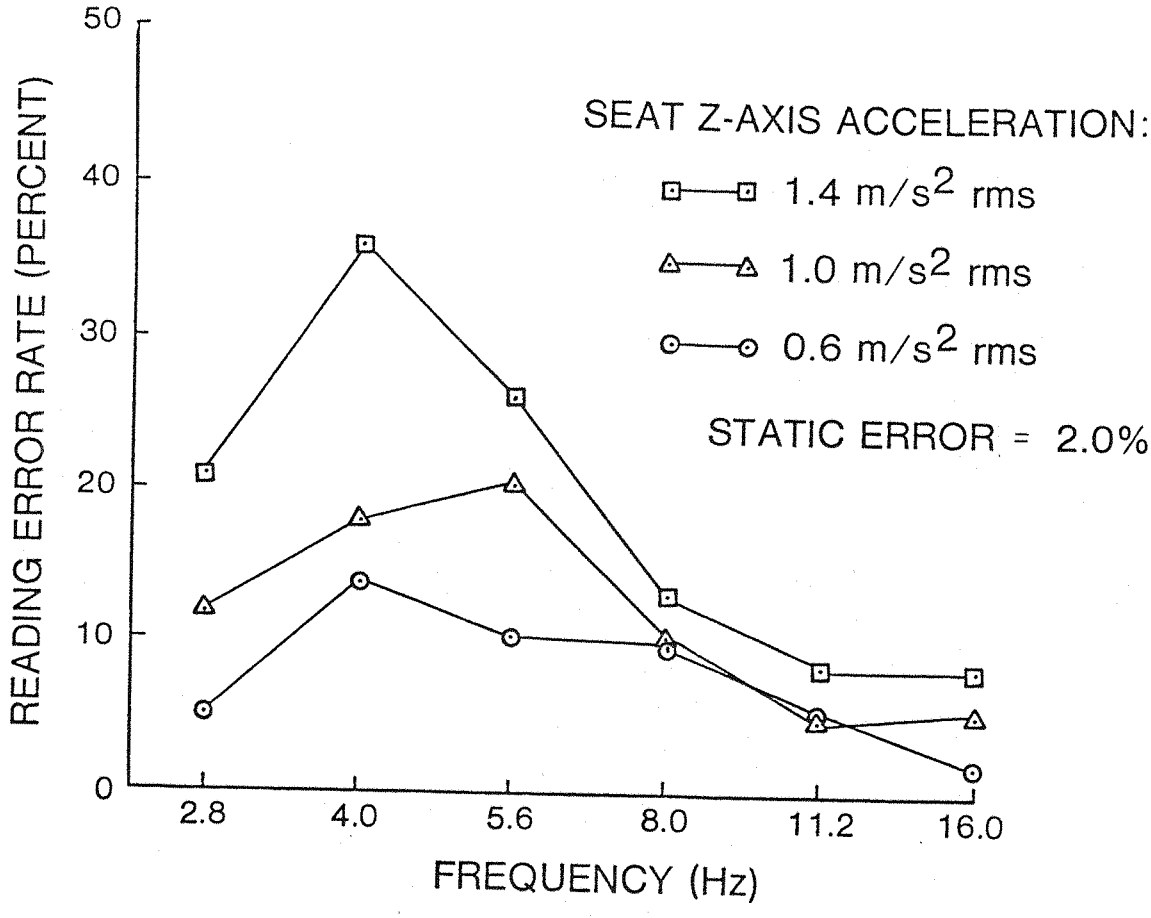

Figure 4.3.1. Mean Percentage Reading Errors for Array Format Presentation at Three Seat Z Axis Acceleration Levels (Experiment LG.2)

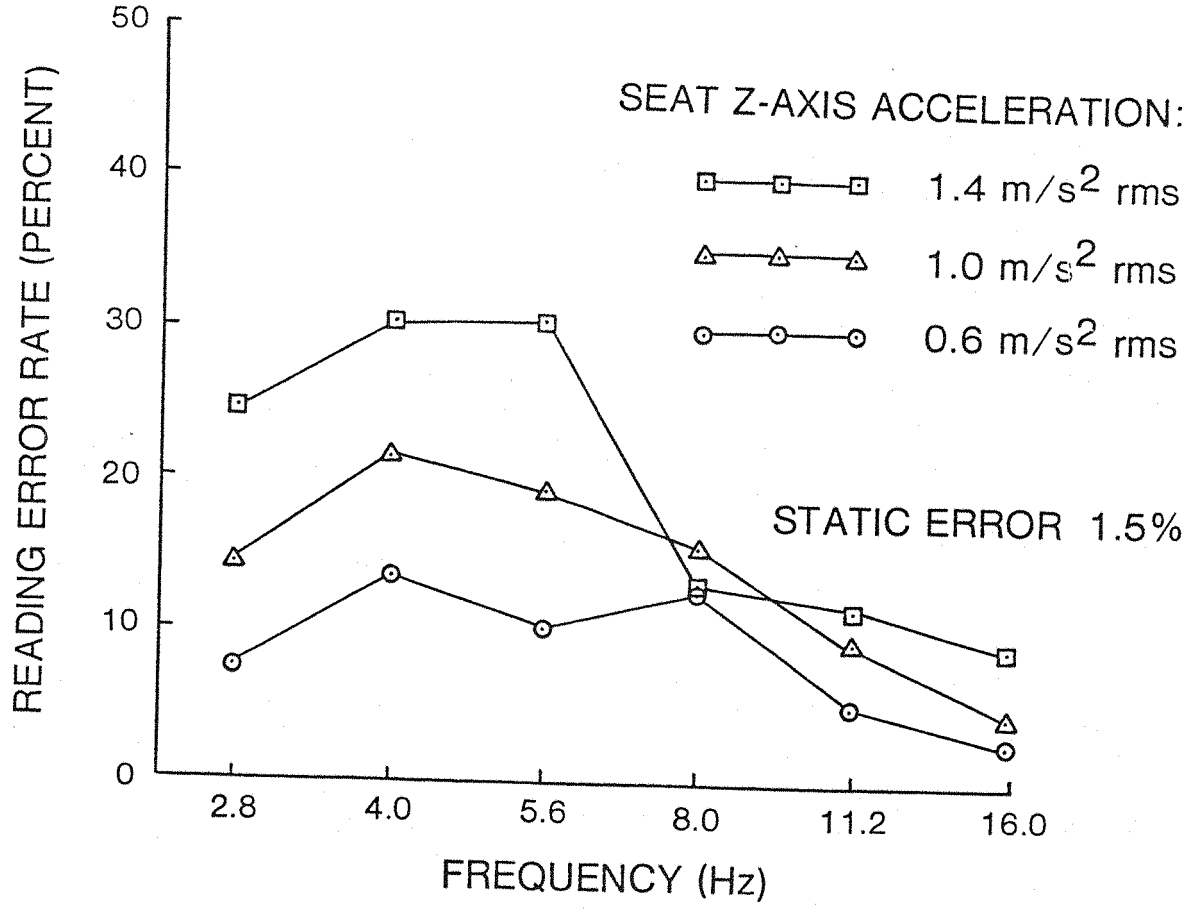

Figure 4.3.2. Mean Percentage Reading Errors for Line Format Presentation at Three Seat Z Axis Acceleration Levels (Experiment LG.2)

4.3.3.2 Analysis of Variance

An analysis of the number of reading errors was performed using a mixed effects three factor analysis of variance with subjects as randomized blocks (Kirk, 1968). The factors were display format (2 levels), vibration frequency (6 levels), and vibration level (3 levels). A summary of the results of the analysis of variance is given in Table 4.3.3. The main effects of vibration level ($p<.001$) and frequency ($p<.05$) and the interaction of these factors ($p<.01$) were all statistically significant. This result was expected based upon the results of Experiment LG.1. There was, however, no significant effect of display format in the data.

TABLE 4.3.3. ANALYSIS OF VARIANCE SUMMARY TABLE FOR READING ERRORS IN EXPERIMENT LG.2

Treatments: S = Subjects
A = Vibration Levels
B = Vibration Frequency
C = Display Format

Source	SS	DF	MS	F Ratio	p
S	3208.82031	5	641.76404	20.71730	<.001
A	1073.86133	2	536.93066	20.60946	<.001
B	2006.59668	5	401.31934	3.09021	<.05
C	22.04199	1	22.04199	0.36103	ns
A × B	482.58301	10	48.25830	3.19860	<.01
A × C	3.02734	2	1.51367	0.27731	ns
B × C	25.04199	5	5.00840	0.29040	ns
A × B × C	53.97461	10	5.39746	0.73256	ns
Residual	5421.01074	175	30.97720		
A × S	260.52637	10	26.05264		
B × S	3246.70312	25	129.86812		
C × S	305.26270	5	61.05254		
A × B × S	754.36621	50	15.08732		
A × C × S	54.58496	10	5.45850		
B × C × S	431.16797	25	17.24672		
A × B × C × S	368.39941	50	7.36799		
Total	12296.95801	215	57.19515		

In addition, the mean number of reading errors between the two display formats were compared using a paired-t statistical evaluation for each vibration level across all the vibration frequencies. No significant difference in error due to display format was found in any of these tests. From these results, it can be concluded that even if nodal image overlap did occur, there was no significant effect upon actual reading performance; therefore, the null hypothesis is accepted.

4.3.3.3 Subject Opinion

At the conclusion of the experiment, subjects were asked which format (i.e., the array or line) they preferred. Five out of the six subjects indicated that they preferred the line format. S4, however, indicated that he preferred the array format, because it provided a technique for improving his performance. He stated that he used the adjacent nodal images of the rows in the array to make comparisons regarding each character he was reading. If he were unsure about the identity of a particular character, he would compare it with the adjacent nodal images to determine if it were similar or dissimilar to the other characters of whose identity he was certain. Although this approach sounds bizarre, S4 consistently made fewer errors than all the other subjects in most of the experiments discussed in this thesis.

4.3.3.4 Comparisons with Experiment LG.1

Inspection of the percentage reading error curves in Figure 4.3.1 for the array format indicates that the general shape of the curve (i.e., sensitivity of reading performance to vibration frequency) was similar to the results in Experiment LG.1. The magnitudes of the errors, however, were dissimilar.

Subjects consistently made fewer errors (under the same vibration conditions) in this experiment than they made in Experiment LG.1. For example, mean reading errors for a seat vibration level of 1.0 m/s^2 and the array format are compared for Experiments LG.1 and LG.2 in Table 4.3.4. The values for Experiment LG.1 were estimated from the regression equations in Table 4.2.9. It is apparent that the reading accuracy and, hence, legibility of the reading material in Experiment LG.2 was consistently better than that of Experiment LG.1. A paired-t statistical evaluation of these data showed that the differences were statistically significant ($p<.01$). An inspection of the data of individual subjects participating in both experiments also indicated a large consistent difference in the reading error rate.

TABLE 4.3.4. COMPARISON OF MEAN NUMBER OF READING ERRORS FOR EXPERIMENTS LG.1 AND LG.2 AT A 1.0 m/s^2 SEAT Z AXIS VIBRATION LEVEL

Vibration Frequency	Mean No. of Reading Errors at Seat Z Vibration Level 1.0 m/s^2 rms	
	Experiment LG.1*	Experiment LG.2
2.8	20.63	6.0
4.0	28.10	9.0
5.6	22.10	10.33
8.0	22.48	5.33
11.2	14.09	2.67
16.0	6.42	2.83

*estimated from regression equations

There are several possible explanations for the dichotomy in these data. The first may be related to the differences in the seat configuration between the two experiments. As indicated in Section 3.3 and Section 4.1.4, several mechanical modifications were made to the seat; however, the contour and seating configuration, harnesses, and footrest remained unchanged. Lewis (1979a) measured differences in the dynamic behaviour of the modified seat but these were not apparent until vibration frequencies above 11.2 Hz and then there were only minor changes in the seat back vibration transmissibility. Furthermore, Lewis found no differences between the two seats in similar character reading tasks using panel-mounted displays. In the present experiment, it is unlikely that difference in the seat configuration could have had any significant influence on reading performance at frequencies below 11.2 Hz, yet the actual differences in error rate were found across all frequencies.

Another factor that may have affected reading performance between experiments was the proficiency of subjects. Experiment LG.2 was conducted approximately 9 months after Experiment LG.1; and during the intervening period, these subjects participated in other character reading studies using the helmet-mounted display. It was likely that

there were some improvements in reading performance due to increased familiarity and practice.

A third factor which may have affected reading performance between LG.1 and LG.2 was the slight difference in the subtended visual angle of the characters (i.e., 13 minutes-of-arc for LG.1 versus 15 minutes-of-arc for LG.2).[1] Several investigators have found very large differences in reading performance with only small changes in character size during object and whole-body vibration (e.g., Sections 2.5.4.4, 2.5.5.3, and 2.5.6). As will be shown later in Experiments LG.3 and LG.4, helmet-mounted display legibility is also highly sensitive to visual angle subtended by the characters.

It is concluded from the discussion above that perhaps a combination of factors contributed to the differences in performance between LG.1 and LG.2. It is likely, however, that the larger character size in LG.2 was the most significant factor in reducing the number of reading errors in contrast to Experiment LG.1.

4.3.4 Summary

The purpose of this experiment was to measure the effect of the line versus array display format on the legibility of the helmet-mounted display. The principal results of the experiment were as follows:

1. No significant effect of display format on display reading performance was observed.

2. The main effects of vibration frequency and level on reading performance were statistically significant.

---

[1] Originally, it was intended by the experimenter that character sizes be equal for the two experiments. However, the differences in reading error in these experiments served as an impetus to recheck the character size using procedures detailed in Appendix A.4.3. The outcome of this investigation was that the original gain settings of the horizontal and vertical deflection amplifiers in Experiment LG.1 produced a character visual angle of 13 minutes-of-arc instead of 15 minutes-of-arc. (This corrected value is given in Experiment LG.1.)

3. The effect of vibration frequency on mean reading error with the array format was similar in form between Experiments LG.1 and Experiment LG.2.

4. The magnitudes of the mean reading errors for the array format between Experiments LG.1 and LG.2 were significantly different.

4.3.5 Interpretation of Results

From the results above, it is concluded that the results of Experiment LG.1 are valid to the extent that artifacts due to the array format were not a significant source of reading error. Because of the discrepancy between the magnitudes of the errors between the two experiments, the absolute level of the vibration amplitude required to produce a given error rate is questionable and is probably a function of the character size. Since the data in Experiment LG.1 is to be used only in a relative sense, that is, to show the relative effects vibration level and frequency, this discrepancy does not compromise the usefulness of the results.

4.4 EXPERIMENT LG.3: EFFECT OF CHARACTER SIZE ON HELMET-MOUNTED DISPLAY LEGIBILITY

4.4.1 Introduction and Background

4.4.1.1 Character Size Considerations

Experiments LG.1 and LG.2 reported in Sections 4.2 and 4.3 have shown that vertical, Z axis sinusoidal vibration of the seat degraded the legibility of numeric characters displayed on the helmet-mounted display. The extent of this reduction in display visibility was a function of vibration frequency and amplitude as well as the type of character (number) presented. In these experiments, the visual angles subtended by the numeric characters were made small to cause reading performance to be sensitive to the vibration condition. Consequently, these character sizes did not represent a realistic display

presentation which would be used operationally. As discussed in Chapter 1, the head-coupled virtual image display has an advantage of presenting symbolic information and imagery at subtended angles greater than that possible with conventional cockpit panel-mounted displays. The effect of character size on reading performance should, therefore, be considered as a design dimension in the operational use of the helmet-mounted display.

Laycock (1978) investigated the effects of character size on reading performance using a helmet-mounted display and simulated aircraft vibration conditions (Section 2.5.6). He found that reading errors decreased as the subtended angle and resolution (i.e., number of discrete elements forming the character) increased under both static and vibration conditions. Laycock compared his data with other research studies pertaining to the legibility of reading material and concluded that, at least in the absence of vibration, the primary factor limiting legibility was resolution (i.e., number of discrete elements or television scan limits forming the character), and not the size of the character alone.

4.4.1.2 Contrast/Background Luminance Considerations

Contrast and/or background luminance are other display quality parameters which have been shown to affect reading performance of vibrating material. Crook et al. (1950) found that when they increased the luminance of reading material from 0.02 fL to 15 fL, the minimum vibration amplitude (peak-to-peak) at which reading performance significantly degraded increased from 0.25 mm to 0.5 mm. The authors also noted significant first order interactions between vibration amplitude and character luminances and between character size and luminance. A significant higher order interaction between character size, luminance, and vibration amplitude was also found.

4.4.1.3 Pilot Studies

From these and other research findings reported in the literature, both character size and background luminance can be expected to affect

the legibility of characters presented on the helmet-mounted display. In order to investigate the general nature of these factors, several pilot studies were conducted as a prelude to the more extensive studies reported as Experiments LG.3 and LG.4 to follow. The main purpose of the pilot studies was to investigate the general range and influence that character size (i.e., subtended visual angle of character presented on the helmet), background luminance, and display format had on helmet-mounted display reading performance during whole-body vibration. From these preliminary studies, large systematic trends emerged (across the four subjects used: S1, S3, S4, S8), in that both character size (range of 11 to 35 minutes-of-arc) and background luminance had large effects on reading accuracy.

From the pilot studies, the ranges of the character size and background luminance variances were selected for further investigation of the effects of these variable on reading performance in Experiments LG.3 and LG.4.

4.4.2 Method

The display conditions for Experiment LG.3 consisted of six character sizes presented on backgrounds at two luminance levels. The six character sizes were 9, 12, 15, 19, 23, and 27 minutes-of-arc (MOA). These sizes were determined from the pilot experiment to cover the range of interest from the smallest size producing the very large errors to the larger size providing about zero errors. In the "dark background" luminance condition, the characters were presented on the helmet-mounted display with a luminance of 19.2 cd/m^2 on a "totally dark" background for a character to background contrast of 100 percent.[1] For the "raster background" luminance condition, the

[1] Luminance contrast (percent) for the presentation of characters on the helmet-mounted display is computed using the equation below (McCormick, 1976).

$$\text{Luminance Contrast} = \frac{L_C - L_B}{L_C} \times 100\%$$

where L_C = luminance of the character and L_B = luminance of the background.

characters were presented with a luminance of 15.3 cd/m^2 on a raster background of 0.7 cd/m^2 for a character to contrast of 97 percent. The characters were presented in a line format with ten numeric characters per line (e.g., Figure 4.1.2). During each display presentation condition (i.e., character size and background), the subjects were presented with one static (no vibration) and two vibration conditions. The vibration conditions consisted of vertical, Z axis sinusoidal motion of the seat at 4.0 Hz and 16.0 Hz frequencies at an acceleration level of 1.0 m/s^2 rms. These conditions were chosen a priori as representing the "worst case" vibration frequency (i.e., 4.0 Hz from Experiments LG.1 and LG.2) and a vibration frequency (i.e., 16 Hz) which is representative of the rotor passage frequency of some helicopter aircraft (Section 2.5.2). The order of presentation of the vibration frequencies, background luminance conditions, and character sizes were randomized across subjects. The vibration and display equipment used in the experiment is described in Sections 3.2 and 3.3. Ten subjects were used in the experiment (S1, S3, S4, S5, S7, S8, S11, S12, S13, and S14). Six of these subjects also participated in Experiments LG.1 and LG.2. The four subjects in the pilot study (i.e., S1, S3, S4, and S8) also took part in this experiment. Physical characteristics of the subjects are given in Table 3.4.1. The written instructions to subjects are shown in Appendix A.4.6. A summary of the conditions in this experiment is given in Table 4.4.1.

4.4.3 Results

4.4.3.1 Analysis of Variance

A three factor analysis of variance was performed on the number of reading errors for each experimental condition using a mixed effects model and with subjects as randomized blocks. The factors consisted of character size (6 levels), vibration condition (2 levels), and background luminance (2 levels). A summary of the results of the analysis of variance is given in Table 4.4.2. The analysis indicated that main effects of all three factors were highly significant

TABLE 4.4.1. EXPERIMENT LG.3: EFFECT OF CHARACTER SIZE ON HELMET-MOUNTED DISPLAY LEGIBILITY

Purpose:	To determine the effects of characters size on the perception of the helmet-mounted display under whole-body vibration conditions.
Method:	Measure reading accuracy with a range of character subtended visual angles presented with two levels of background luminance.
Subjects:	10S (S1, S3, S4, S5, S7, S8, S11, S12, S13, S14)
Visual Material:	6 character sizes (9-27 minutes-of-arc) 2 character-background luminance conditions:

	No. 1	No. 2
Character	19.2 cd/m^2	15.3 cd/m^2
Background	0	0.7 cd/m^2

Display format: line of 10 numeric characters

Vibration Conditions:	2 Frequencies (4.0, 16.0 Hz) 1 Level (1.0 m/s^2 rms) 1 Static Condition Helicopter Seat (modified)

($p<.001$). In addition, the interactions of size and vibration condition and size and background luminance were highly significant ($p<.001$). The interaction of vibration frequency and background luminance was also significant ($p<.05$). The interaction of all three factors was not significant. The main effects of treatments and their interactions accounted for approximately 80 percent of the variance of the error scores in the experiment.

TABLE 4.4.2. ANALYSIS OF VARIANCE SUMMARY TABLE FOR READING ERRORS IN EXPERIMENT LG.3

Treatments: S = Subjects
A = Character Size
B = Vibration Frequency
C = Background Luminance

Source	SS	DF	MS	F Ratio	p
S	1311.23633	9	145.69293	11.56158	<.001
A	12228.65820	5	2445.73169	65.74686	<.001
B	2161.11719	2	1080.55859	50.94685	<.001
C	1050.62500	1	1050.62500	69.46331	<.001
A × B	2673.55273	10	267.35529	40.81246	<.001
A × C	1549.05469	5	309.81094	33.64193	<.001
B × C	85.31641	2	42.65820	4.54290	<.05
A × B × C	114.35156	10	11.53516	1.70223	ns
Residual	3969.46289	315	12.60147		
A × S	1673.96484	45	37.19922		
B × S	381.77148	18	21.20953		
C × S	136.12402	9	15.12489		
A × B × S	589.57422	90	6.55082		
A × C × S	414.40820	45	9.20907		
B × C × S	169.02148	18	9.39008		
A × B × C × S	604.59863	90	6.71776		
Total	25143.37500	359	70.03775		

4.4.3.2 Measures of Central Tendency

The mean and standard deviation of the reading errors across the ten subjects are given in Table 4.4.3 as a function of the display and vibration conditions. The mean scores converted to percentage reading errors are plotted for the dark background condition in Figure 4.4.1 and raster background condition in Figure 4.4.2. Figure 4.4.3 shows a comparison of the reading performance at the two background luminance levels and the 4.0 Hz vibration condition. In all of the display background and vibration conditions, the data show that a decrease in

character size causes a decrease in the legibility of the characters as indicated by the increase in the number of errors committed by the subjects. Mean error rates ranged from 32 percent for a 9 minute-of-arc character to about 0 percent for a 27 minutes-of-arc character (dark background at 4.0 Hz). For the same vibration conditions, the number of errors for the dark background condition were from 2 to 9 times greater than for the raster background condition depending upon the subtended angle of the character. Reading errors for the 4.0 Hz vibration frequency were always greater than for the 16.0 Hz condition.

TABLE 4.4.3. MEAN AND STANDARD DEVIATION OF READING ERRORS (EXPERIMENT LG.3)

Display Background	Frequency of Vibration	Mean (SD)* Number of Reading Errors**					
		Character Height (minutes-of-arc)					
		9	12	15	19	23	27
Dark	Static	12.9	2.1	0.4	0.1	0.1	0.0
		(6.3)	(3.3)	(0.7)	(0.3)	(0.3)	(0.0)
	4.0 Hz	32.0	16.0	5.1	2.8	1.5	0.8
		(4.7)	(8.7)	(5.1)	(3.5)	(1.2)	(1.6)
	16.0 Hz	22.3	6.6	1.8	0.2	0.2	0.1
		(9.0)	(8.1)	(1.9)	(0.4)	(0.4)	(0.3)
Raster	Static	1.9	0.1	0.1	0.0	0.1	0.0
		(2.2)	(0.3)	(0.3)	(0.0)	(0.3)	(0.0)
	4.0 Hz	20.7	6.1	2.2	0.6	0.6	0.2
		(11.6)	(6.4)	(2.4)	(1.3)	(1.1)	(0.4)
	16.0 Hz	9.5	1.4	0.2	0.0	0.1	0.0
		(7.2)	(2.1)	(0.4)	(0.0)	(0.3)	(0.0)

*Numbers in brackets are standard deviation.

**Out of a presentation of 50 numbers.

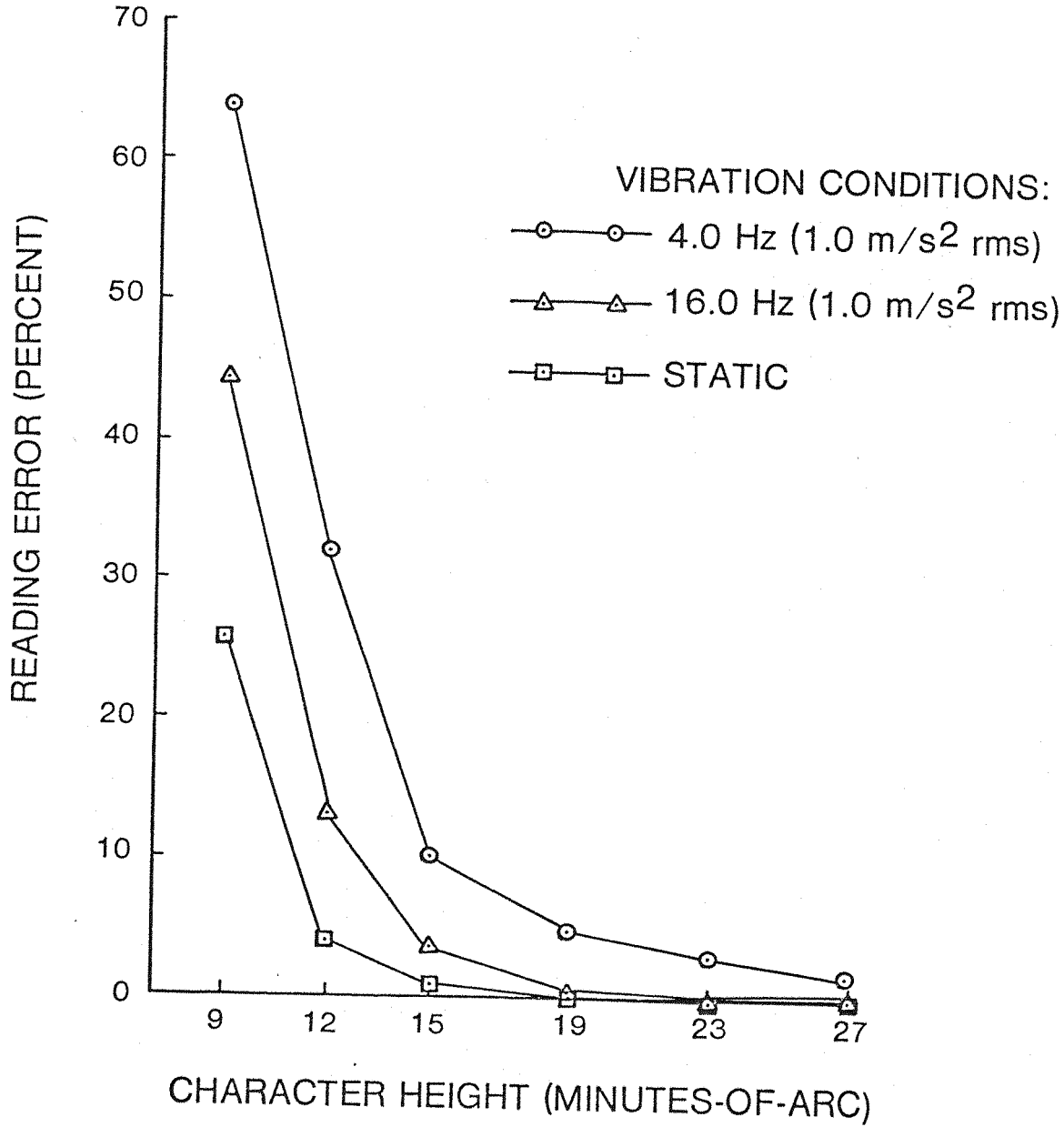

Figure 4.4.1. Mean Percentage Reading Errors as a Function of Character Size and Vibration Frequency for the Dark Background Display Condition (Experiment LG.3)

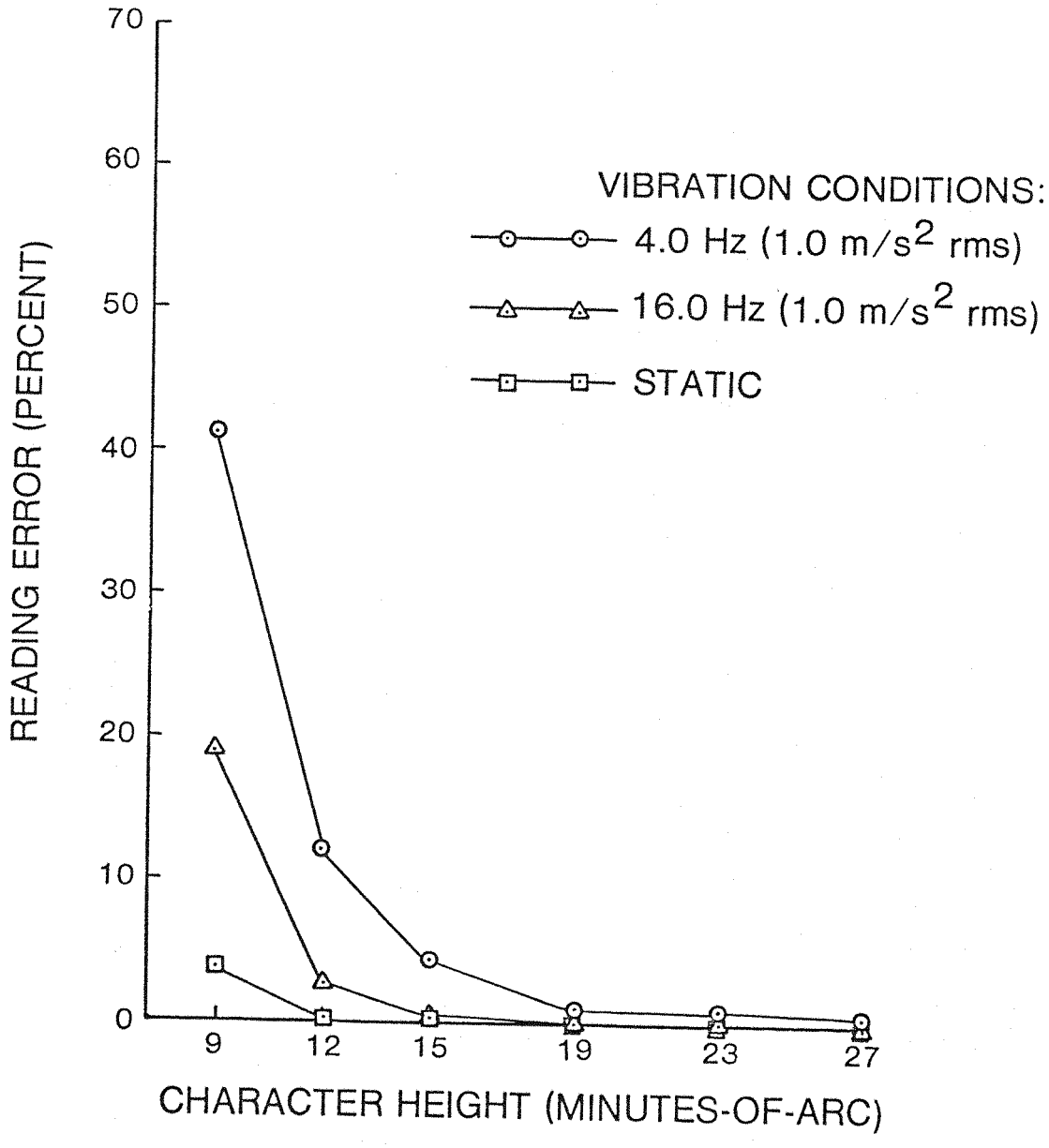

Figure 4.4.2. Mean Percentage Reading Errors as a Function of Character Size and Vibration Frequency for the Raster Background Display Condition (Experiment LG.3)

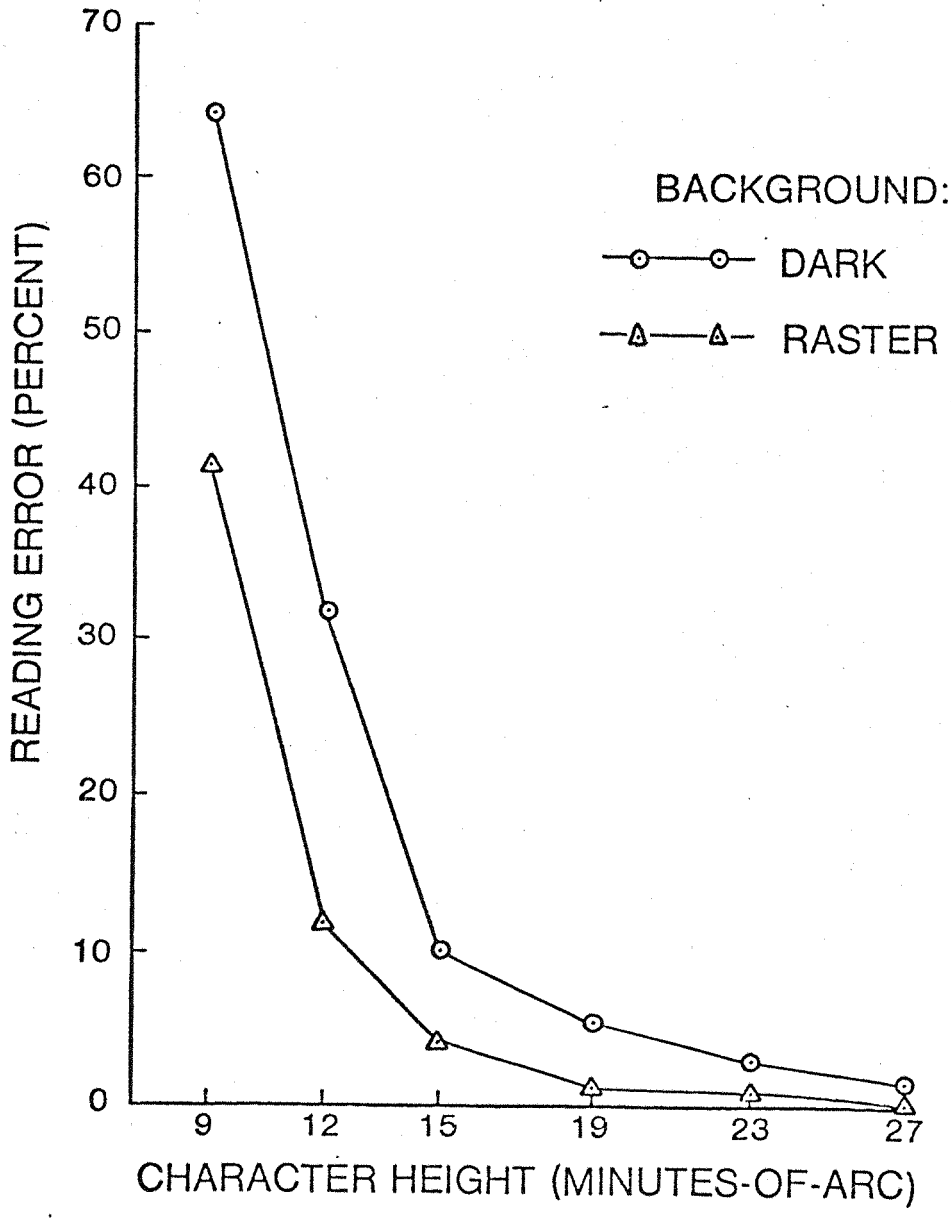

Figure 4.4.3. Comparison of Mean Percentage Reading Errors as a Function of Character Size Display Background Conditions at a 4.0 Hz Vibration Frequency (Experiment LG.3)

4.4.3.3 Analysis of Confusions

An analysis of the types of errors was performed to determine the nature of the errors and the extent to which individual characters were confused with different character types. Table 4.4.4 gives the distribution of reading errors by character type for the 9 and 12 minutes-of-arc character sizes and the dark background. Table 4.4.5 gives similar data for the raster background condition. The most noticeable trend in the type of reading errors was again the confusion between the "8" and "0." The "8" was more often interpreted as a "0" rather than the "0" as "8." This was probably due to the predisposition of subjects to identify characters as "0," when they were difficult to discern. This behaviour would account for the large number of confusions of all characters to "0," when the overall error rate was high. Other notable confusions were between the "5" and "3" and "5" and "9." The least number of confusions were observed for the "1" and "7" across all conditions.

A series of chi-square goodness-of-fit tests (Siegel, 1956) were performed on the data in Tables 4.4.4 and 4.4.5 for the 9 and 12 minutes-of-arc character size. The purpose of these tests was to determine the degree to which the distribution of errors agreed with each other (across experimental conditions) or differed significantly from chance. The chi-square values and their levels of statistical significance are given in Table 4.4.6. The goodness-of-fit tests could only be applied under those conditions where there was a sufficient number of reading errors distributed across character types.[1] For the conditions tested, all of the distributions of errors were significantly different from chance. The distributions of errors for the 9 minutes-of-arc character size and dark background were significantly different between each of the static, 4.0 Hz and 16.0 Hz vibration conditions;

[1]Siegel (1956) recommended that the chi-square test should not be used for the one sample case if either there were more than 20 percent of the expected frequencies less than 5 or if any expected frequency were less than 1.

TABLE 4.4.4. DISTRIBUTIONS OF READING ERRORS BY CHARACTER TYPE FOR 9 MINUTES-OF-ARC (SIZE 1) AND 12 MINUTES-OF-ARC (SIZE 2) CHARACTERS PRESENTED WITH A DARK BACKGROUND

SIZE 1 STATIC DARK

ERROR MATRIX

ERROR	CORRECT CHARACTER 0	1	2	3	4	5	6	7	8	9	
0	0	0	0	0	1	2	1	0	13	2	
1	1	0	10	1	0	1	0	1	1	0	
2	2	4	0	1	0	2	0	0	2	0	
3	0	1	4	0	0	1	0	0	1	0	
4	0	2	3	0	0	0	4	0	1	0	
5	0	2	0	4	0	0	0	0	0	0	
6	1	1	0	0	9	0	0	0	2	0	
7	0	1	0	1	0	1	0	0	2	1	
8	10	0	3	1	0	4	2	0	0	2	
9	2	0	0	2	0	10	0	1	2	0	
TOTAL	16	11	20	10	10	21	7	2	24	5	N= 126

SIZE 2 STATIC DARK

ERROR MATRIX

ERROR	CORRECT CHARACTER 0	1	2	3	4	5	6	7	8	9	
0	0	0	0	0	0	0	2	0	3	1	
1	0	0	0	0	0	0	0	0	0	0	
2	0	1	0	0	0	0	0	0	0	0	
3	0	0	7	0	0	0	0	0	0	1	
4	0	0	0	0	0	0	0	0	0	0	
5	0	0	1	2	0	0	1	0	0	0	
6	0	0	0	0	0	0	0	0	0	1	
7	0	0	0	1	0	0	0	0	0	0	
8	1	0	0	0	0	0	0	0	0	0	
9	0	0	0	0	0	0	0	0	0	0	
TOTAL	1	1	8	3	0	0	3	0	3	3	N= 22

SIZE 1 4.0 HZ DARK

ERROR MATRIX

ERROR	CORRECT CHARACTER 0	1	2	3	4	5	6	7	8	9	
0	0	4	13	4	8	10	9	1	14	12	
1	0	0	4	2	4	2	1	1	2	1	
2	2	4	0	4	0	2	1	2	0	0	
3	2	0	2	0	2	3	1	1	4	0	
4	4	4	5	2	0	3	11	3	7	8	
5	1	3	5	12	3	0	1	2	4	3	
6	9	1	4	1	1	3	0	1	6	4	
7	2	1	2	1	1	1	5	0	1	4	
8	7	0	5	2	1	1	0	0	0	4	
9	5	0	0	7	1	10	1	9	5	0	
TOTAL	32	17	40	35	21	35	30	20	43	36	N= 309

SIZE 2 4.0 HZ DARK

ERROR MATRIX

ERROR	CORRECT CHARACTER 0	1	2	3	4	5	6	7	8	9	
0	0	2	3	3	4	3	4	1	18	8	
1	1	0	4	0	2	1	0	0	1	1	
2	1	2	0	2	0	3	1	1	0	2	
3	0	2	9	0	0	0	2	0	2	1	
4	0	2	3	1	0	1	7	1	4	5	
5	0	1	2	7	0	0	3	0	4	2	
6	4	1	1	0	2	1	0	0	2	1	
7	0	0	1	3	1	1	0	0	0	0	
8	5	1	1	2	1	1	2	0	0	3	
9	0	0	1	3	0	4	1	1	3	0	
TOTAL	11	11	25	21	10	15	20	4	34	23	N= 174

SIZE 1 16.0 HZ DARK

ERROR MATRIX

ERROR	CORRECT CHARACTER 0	1	2	3	4	5	6	7	8	9	
0	0	4	6	3	4	7	7	2	22	5	
1	0	0	3	0	2	1	0	3	2	2	
2	0	2	0	4	3	0	0	2	0	0	
3	0	4	13	0	0	0	0	0	0	0	
4	0	2	1	2	0	3	9	3	2	0	
5	0	3	1	3	0	0	1	0	0	1	
6	3	0	2	0	8	3	0	0	10	2	
7	0	0	0	3	0	1	0	0	1	1	
8	13	1	2	2	1	2	1	0	0	0	
9	4	3	1	9	0	9	0	6	4	0	
TOTAL	20	19	29	26	18	26	18	16	41	11	N= 224

SIZE 2 16.0 HZ DARK

ERROR MATRIX

ERROR	CORRECT CHARACTER 0	1	2	3	4	5	6	7	8	9	
0	0	0	1	0	1	0	0	0	11	0	
1	0	0	2	0	0	0	0	0	2	0	
2	0	2	0	0	0	0	0	0	0	0	
3	0	1	2	0	0	0	0	0	0	0	
4	0	1	1	0	0	0	3	0	0	0	
5	0	1	2	3	0	0	0	0	1	0	
6	0	0	0	0	0	2	0	0	1	0	
7	0	0	0	6	0	0	0	0	0	4	
8	3	0	0	0	0	1	0	0	0	0	
9	0	1	3	1	0	5	0	0	3	0	
TOTAL	3	6	11	10	1	8	3	0	18	4	N= 64

TABLE 4.4.5. DISTRIBUTIONS OF READING ERRORS BY CHARACTER TYPE FOR 9 MINUTES-OF-ARC (SIZE 1) AND 12 MINUTES-OF-ARC (SIZE 2) CHARACTERS PRESENTED WITH A RASTER BACKGROUND

SIZE 1 STATIC RASTER

ERROR MATRIX

ERROR	CORRECT CHARACTER 0	1	2	3	4	5	6	7	8	9	
0	0	0	0	0	0	1	0	0	10	0	
1	0	0	0	0	0	0	0	0	0	0	
2	0	0	0	0	0	0	0	0	0	0	
3	0	0	0	0	0	0	0	0	0	0	
4	0	0	0	0	0	0	1	0	0	0	
5	0	1	0	0	0	0	0	0	0	0	
6	0	0	0	0	0	0	0	0	0	0	
7	0	0	0	0	0	0	0	0	0	0	
8	5	0	0	0	0	1	0	0	0	0	
9	1	0	0	1	0	1	0	0	0	0	
TOTAL	6	1	0	1	0	3	1	0	10	0	N= 22

SIZE 2 STATIC RASTER

ERROR MATRIX

ERROR	CORRECT CHARACTER 0	1	2	3	4	5	6	7	8	9	
0	0	0	0	0	0	0	0	0	1	0	
1	0	0	0	0	0	0	0	0	0	0	
2	0	0	0	0	0	0	0	0	0	0	
3	0	0	0	0	0	0	0	0	0	0	
4	0	0	0	0	0	0	0	0	0	0	
5	0	0	0	0	0	0	0	0	0	0	
6	0	0	0	0	0	0	0	0	0	0	
7	0	0	0	0	0	0	0	0	0	0	
8	0	0	0	0	0	0	0	0	0	0	
9	0	0	0	0	0	0	0	0	0	0	
TOTAL	0	0	0	0	0	0	0	0	1	0	N= 1

SIZE 1 4.0 HZ RASTER

ERROR MATRIX

ERROR	CORRECT CHARACTER 0	1	2	3	4	5	6	7	8	9	
0	0	4	8	4	7	9	9	2	26	14	
1	2	0	0	1	2	0	0	1	0	0	
2	1	3	0	6	0	2	0	2	0	0	
3	0	2	7	0	1	5	0	0	0	0	
4	1	1	0	2	0	1	6	0	1	0	
5	0	1	3	3	0	0	2	0	2	3	
6	3	0	2	0	4	0	0	2	6	3	
7	1	0	0	1	0	0	1	0	0	1	
8	8	0	2	0	0	5	0	0	0	1	
9	4	1	1	5	0	6	0	1	4	0	
TOTAL	20	12	23	22	14	28	18	8	39	22	N= 206

SIZE 2 4.0 HZ RASTER

ERROR MATRIX

ERROR	CORRECT CHARACTER 0	1	2	3	4	5	6	7	8	9	
0	0	0	1	0	0	1	1	0	16	1	
1	0	0	0	0	0	0	0	0	1	0	
2	1	2	0	2	0	0	1	0	0	1	
3	0	0	0	0	0	2	0	0	1	1	
4	1	0	0	0	0	0	1	0	0	0	
5	0	1	0	4	0	0	0	0	0	2	
6	0	0	0	0	2	0	0	0	1	0	
7	0	0	0	0	0	0	0	0	2	0	
8	3	0	0	1	0	1	0	0	0	1	
9	1	1	0	2	0	3	0	0	2	0	
TOTAL	6	4	1	9	2	7	3	0	23	6	N= 61

SIZE 1 16.0 HZ RASTER

ERROR MATRIX

ERROR	CORRECT CHARACTER 0	1	2	3	4	5	6	7	8	9	
0	0	0	0	0	3	1	2	0	22	0	
1	0	0	1	0	1	0	0	0	0	0	
2	0	0	0	1	0	0	0	0	0	0	
3	1	1	4	0	0	0	0	1	1	0	
4	0	0	0	0	0	0	3	0	0	0	
5	0	2	0	1	0	0	1	0	0	1	
6	2	0	1	0	4	0	0	0	8	0	
7	0	0	0	5	1	0	0	0	0	2	
8	11	0	0	0	0	1	0	0	0	0	
9	0	0	1	3	0	7	0	2	3	0	
TOTAL	14	3	7	10	9	9	6	3	34	3	N= 98

SIZE 2 16.0 HZ RASTER

ERROR MATRIX

ERROR	CORRECT CHARACTER 0	1	2	3	4	5	6	7	8	9	
0	0	0	0	0	0	0	1	0	11	0	
1	0	0	0	0	0	0	0	0	0	0	
2	0	1	0	0	0	0	0	0	0	0	
3	0	0	0	0	0	0	0	0	0	0	
4	0	0	0	0	0	0	0	0	0	0	
5	0	0	0	0	0	0	0	0	0	0	
6	0	0	0	0	0	0	0	0	0	0	
7	0	0	0	0	0	0	0	0	0	0	
8	0	0	0	0	0	0	0	0	0	0	
9	0	0	0	0	0	0	0	0	1	0	
TOTAL	0	1	0	0	0	0	1	0	12	0	N= 14

TABLE 4.4.6. SUMMARY OF CHI-SQUARE GOODNESS-OF-FIT TESTS FOR CONFUSIONS BETWEEN CHARACTERS (EXPERIMENT LG.3)

	Observed Values											
	Size 1 (9 minutes-of-arc)						Size 2 (12 minutes-of-arc)					
	Dark Background			Raster Background			Dark Background			Raster Background		
Expected Values	Static	4.0	16.0	Static	4.0	16.0	Static	4.0	16.0	Static	4.0	16.0
Size 1 Static Dark	X	123.2***	57.6***	ISE	N/A	N/A						
Size 1 4.0 Dark		X	17.2*	N/A	7.9	N/A		14.3				
Size 1 16.0 Dark			X	N/A	N/A	27.7**						
Size 1 Static Raster				X	ISE	ISE						
Size 1 4.0 Raster					X	26.2**		11.2				
Size 1 16.0 Raster						X						
Size 2 Static Dark							X					
Size 2 4.0 Dark								X				
Size 2 16.0 Dark									X			
Size 2 Static Raster										X		
Size 2 4.0 Raster											X	
Size 2 16.0 Raster												X
Chance	38.4***	26.7**	28.7***	ISE	33.3***	78.1***	ISE	40.6***	ISE	ISE	ISE	ISE
LG.1 4.0 Dark		11.5	--					20.6*				
LG.1 16.0 Dark		--	17.3*									

ISE = insufficient errors

*p<.05

**p<.01

***p<.001

however, the distribution of errors between the raster background and dark background for 9 minutes-of-arc at 16.0 Hz was significantly different, while at 4.0 Hz the differences were not significant. There was also a lack of a significant difference between the distribution of errors for the 9 minutes-of-arc and 12 minutes-of-arc characters for the 4.0 Hz vibration condition with dark background. When compared with the data from Experiment LG.1, the distributions of errors were found to be significantly different for the 16.0 Hz case, but not significantly different for the 4.0 Hz condition. (It may be recalled that the character size in Experiment LG.1 was 13 minutes-of-arc and presented in an array format rather than a line format.)

4.4.3.5 Subject Comments

Although no comments were solicited by the experimenter, several subjects did comment about the quality of the images presented on the display. This was also true in the pilot experiment which preceded this experiment. In both of these studies, three or four subjects mentioned that the characters in the dark background condition appeared too bright and were not well defined. These and other subjects also noted that the characters (with dark background) appeared to alternate in and out of focus, although frequency checks of the equipment verified that the helmet-mounted display was functioning properly. Several subjects commented that the raster background presentation was much easier to view, and the characters appeared to be better defined and clearer than in the dark background conditions.

4.4.4 Discussion

4.4.4.1 Effect of Character Size on Reading Performance Under Static Conditions

Figure 4.4.4 shows the reading error for the static (no vibration) data from Table 4.4.3 plotted as a function of character size for the two background luminance conditions. For the dark background and no vibration condition, reading errors were approximately zero for the character sizes between 19 and 27 minutes-of-arc (i.e., one error was

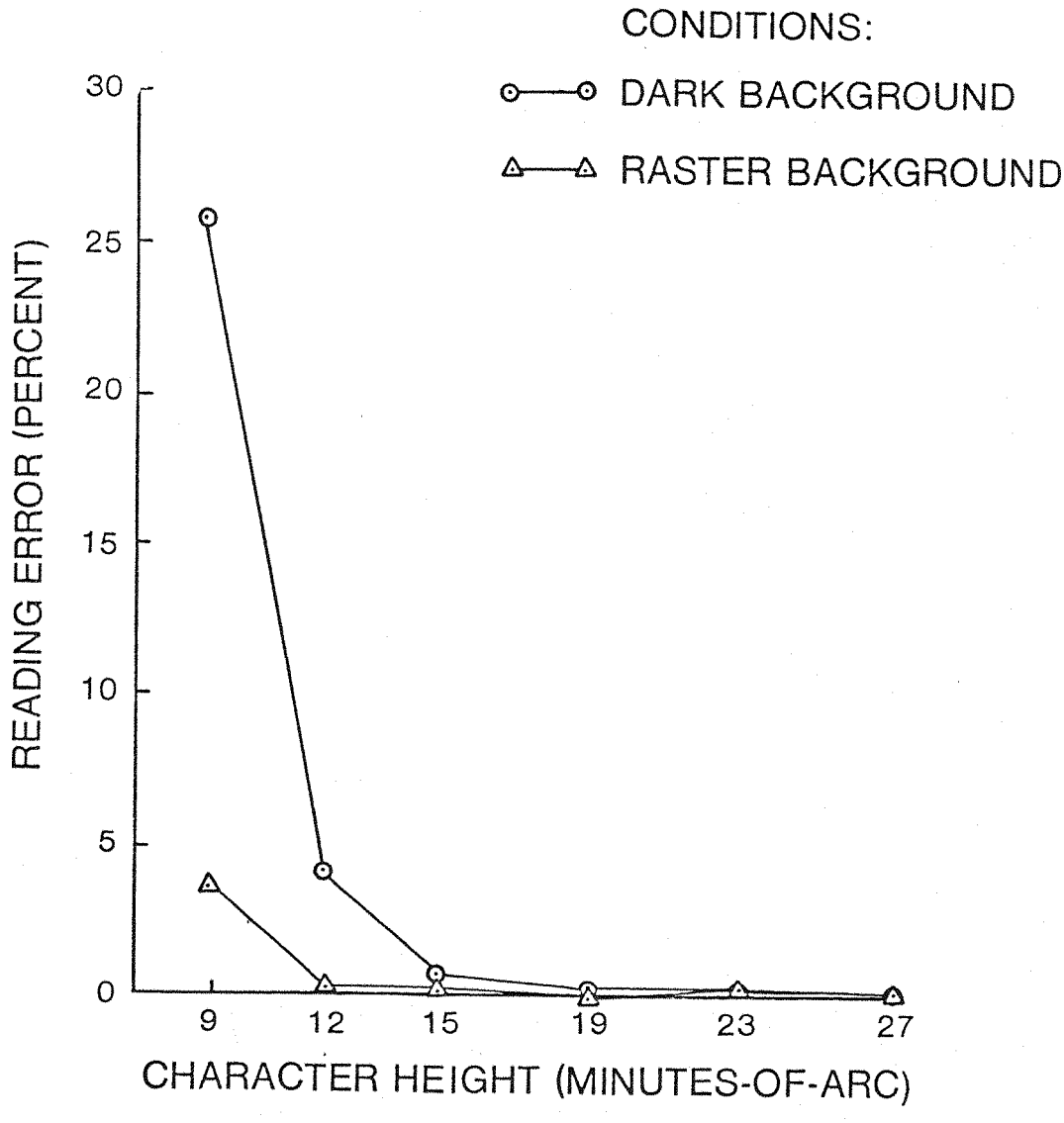

Figure 4.4.4. Comparison of Mean Percentage Reading Errors Under Static Conditions for Dark and Raster Display Backgrounds (Experiment LG.3)

made by one subject at each of the 19 and 23 minutes-of-arc character sizes), and errors did not begin to increase significantly until characters subtended less than 15 minutes-of-arc. Between 12 minutes-of-arc and 9 minutes-of-arc, reading accuracy became severely impaired, causing error rate to rise sharply from 4.2 percent to 29.8 percent. In contrast to the dark background conditions, static reading performance did not degrade for the raster background until the character size was reduced to 9 minutes-of-arc, and then the mean reading error increased to only 3.8 percent. Two questions are incited by these findings; the first is the reason for the decrease in reading errors for "moderately large"[1] character sizes, and the second is the reason for the large differences in reading performance for the two background luminance conditions.

a) Character Size Considerations

The resolution limitation of the helmet-mounted display was the most likely cause of the increased reading difficulty at the smaller character sizes, since the limiting visual acuity of subjects was appreciably better than that of the display.

Figure 4.4.5 shows the theoretical horizontal and vertical modulation transfer function of the helmet-mounted display from Appendix A.3.2 for a CRT spot size of $\sigma = 12$ μm. (This spot size was typical for the helmet-mounted display model used in these experiments.) These curves depict modulation contrast which the display produces as a function of the spatial frequency at the operator's eye.

Figure 4.4.5 also shows a typical visual demand function (i.e., reciprocal visual contrast sensitivity function) for a cathode-ray tube display. Rogers and Carel (1973) obtained these data for the visual demand curve by measuring the modulation threshold of subjects viewing

[1] It may be recalled from Experiment LG.1 that characters subtending visual angles of 13 minutes-of-arc on the helmet-mounted display produced about the same reading error (under static conditions) as a 5 minutes-of-arc character size on the panel-mounted displays.

a sine wave grating stimulus pattern presented on a panel-mounted display. The pattern subtended a visual angle of 1 degree and had an average luminance of 17 cd/m^2 on a background surround of 1.7 cd/m^2. Although these conditions were somewhat different from the helmet-mounted display viewing conditions in this experiment, the data do reflect a general level of subject sensitivity to contrast modulation at luminance levels approximating the luminance condition of the present experiment. (The visual demand curve shown in Figure 4.4.5 was corrected by the authors for field viewing situations by multiplying the 100 percent threshold values by a factor of 3.2. This figure was also established from empirical studies.) Based upon the findings of Campbell and Green (1965), an addition factor of 1.414 was applied to the Rogers and Carel data to correct for monocular rather than binocular viewing of the display. This curve is also shown in Figure 4.4.5.

The theoretical limiting resolution of the display-observer interface can now be derived from Figure 4.4.5. It is the spatial frequency wherein the demand for scene modulation exceeds the display's capability of providing that modulation and is, therefore, the point where the display MTF curve intersects the modified visual demand curve. For the vertical dimension, this point occurs at a spatial frequency of approximately 10 cycles/degree and modulation of 7.0 percent. For the horizontal dimension, the intersection occurs at a spatial frequency of approximately 15 cycles/degree and modulation of 12 percent. These limiting resolutions correspond to subtended visual angles of 6.0 minutes-of-arc/cycle (vertical) and 4.0 minutes-of-arc/cycle (horizontal). Since a cycle of information in the vertical dimension consists of two scan lines, the limiting resolution of adjacent scan lines occurs when their separation becomes less than a subtended visual angle of 3.0 minutes-of-arc. At this point the scan lines cannot be resolved as separate lines. For the characters formed by a dot matrix pattern, a visual angle of 3.0 minutes-of-arc is the smallest separation distance of the elements in the matrix before adjacent dots merge and cannot be distinguished as separate elements. Under these conditions, the vertical subtended angle of the 5 × 7 element character would be 21 minutes-of-arc. Similarly, the minimum

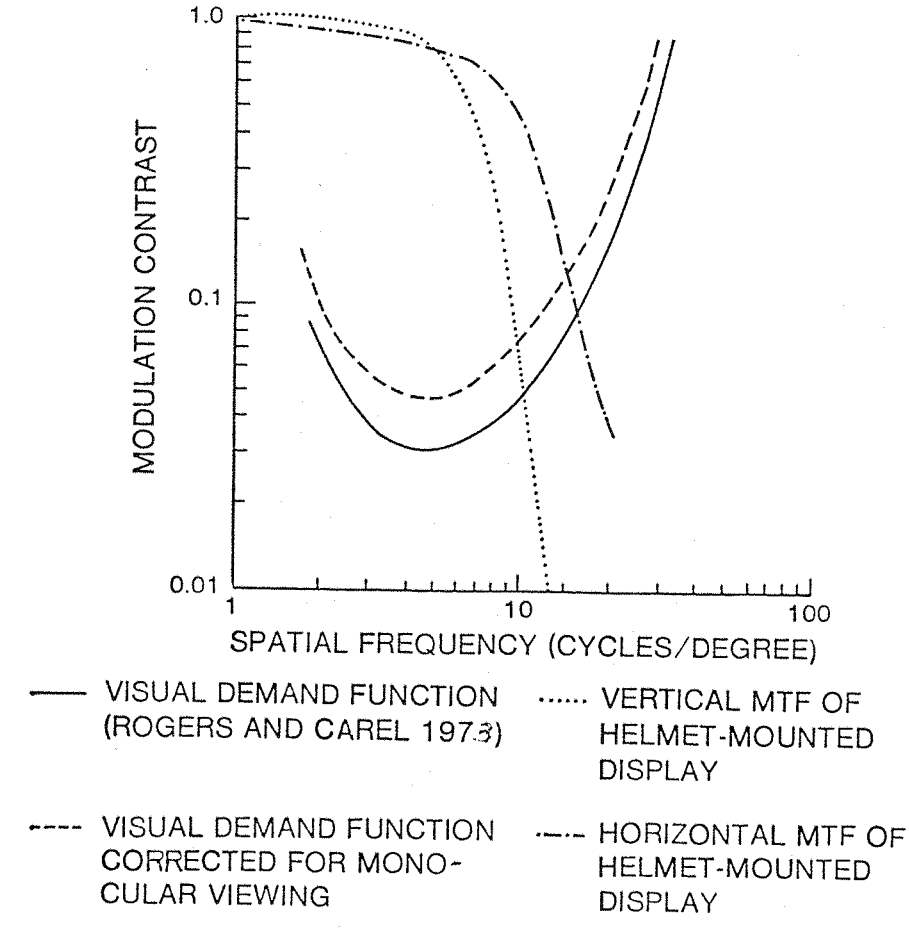

Figure 4.4.5. Determination of the Limiting Resolution of the Helmet-Mounted Display Based Upon Display Modulation Transfer Functions and Visual Demand Functions

visual angle, when individual horizontal elements would become indistinguishable, would be 4.0 minutes-of-arc corresponding to an angular character width of 20 minutes-of-arc. Therefore, at least in theory, the individual elements forming the dot matrix character cannot be resolved in both horizontal and vertical dimensions until the character height exceeds 28 minutes-of-arc (i.e., causing the character width to exceed 20 minutes-of-arc).

By inspection of Figure 4.1.1, some loss of the vertical spaces between elements may be desirable to provide for the continuous linking of elements as shown. [Note: This feature corresponds to 100 percent active area of emitters in solid static matrix element displays (Scanlin, 1976).] The overlapping of adjacent elements becomes undesirable when a space between two active elements becomes obscured (e.g., the vertical separation of the top line and loop in the numeral "5"). This would occur in the vertical dimension on helmet-mounted display for 5 x 7 character heights of less than 12 minutes-of-arc and in the horizontal dimension for character widths of less than 10 minutes-of-arc. From this analysis, apparently the definition of the 5 x 7 dot matrix character would begin to degrade significantly at character heights less than 14 minutes-of-arc (i.e., character widths less than 10 minutes-of-arc). At character heights between 14 and 12 minutes-of-arc the degradation would primarily be in the horizontal dimension until the total obscuration of its spaces between vertical elements occurred at approximately 12 minutes-of-arc. Two vertical spaces (e.g., the loop in the "8") would become totally obscured at approximately 9 minutes-of-arc.

It follows also from the analysis above that the gradual loss of either vertical and/or horizontal resolution will not affect each numeral equally. Decreasing resolution with decreasing character size should not become a problem until the unique distinguishing features of each character became obscured (e.g., when the shape of the "0" approaches that of the "8" and the upper gaps or loops in the "5" and "9" begin to disappear). The data in Table 4.4.4 also show that the effects of character size on the type of reading errors were different for the 9 and 12 minutes-of-arc character sizes. Most of the errors

at 12 minutes-of-arc occurred with the "2" being read as a "3" (7 errors) and the "8" being read as a "0" (3 errors). At 9 minutes-of-arc, "8" was read as a "0" (13 errors), "0" as an "8" (10 errors), "2" as a "1" (10 errors), "9" as a "5" (10 errors), and "4" as a "6" (9 errors). Most of these errors can be explained given the obscuration of distinguishing features of the character provided by the dot matrix elements and spaces.

The analysis of the theoretical limiting resolution of the display-operator interface agrees with the trends in reading accuracy and character confusions observed for the static conditions in this experiment. Reading accuracy of characters viewed against a dark background began to depreciate at angular character heights less than 15 minutes-of-arc, and became severely impaired at less than 12 minutes-of-arc. Reading errors also increased for the raster background condition at 9 minutes-of-arc. These subtended visual angles corresponded to the image viewing situation discussed above wherein either horizontal and/or vertical element separations were expected to be obscured. A hypothesis of reading accuracy based upon theoretical display-operator limiting resolution is supported, therefore, by the experimental results.

b) Background Luminance Considerations

The background luminance of the display presentation had a profound effect on character legiblity even during static conditions. This finding proposes a conundrum. Ostensibly, reducing the luminance of the character (i.e., from 19.2 cd/m^2 to 15.3 cd/m^2) and increasing the luminance of this background (i.e., from 0 to 0.7 cd/m^2) would reduce the modulation of the elements forming the character on the display. It would follow then, from the previous discussion, that the apparent resolution and, hence, reading accuracy should have <u>decreased</u> instead of increased. In their comments, the subjects have given some clues which may aid in explaining this reading behaviour. The first clue was that the characters presented against a dark background appeared to be very bright and, for some subjects, were difficult to read. Also, under these same viewing conditions, subjects often complained

of the characters appearing to drift "in and out of focus," although frequent checks verified that the display equipment was operating properly. A third comment was that the characters presented against a raster background appeared to be "more defined" and "easier to read." Using these comments, the following explanations for the effect of background luminance on reading performance can be postulated:

1. The maximum luminance level of the dark background characters was slightly greater than that of the raster background condition (i.e., 19.2 versus 15.3 cd/m^2). It was likely that the slight increase in the beam current to produce the higher luminance also caused some growth in the diameter of the CRT spot. It would follow, therefore, that limiting resolution of the helmet-mounted display relative to the visual demand function of the observer may have occurred at a slightly lower spatial frequency for the greater luminance condition. Based upon the performance characteristics of the CRT used in the experiment (Appendix A.3.1), a change in luminance of the magnitude above would cause a change in CRT spot diameter of less than 2 percent. It is unlikely, therefore, that spot size alone had any appreciable effect on limiting resolution and reading performance.

2. It is possible that the raster background condition produced a dot-matrix element which appeared to be smaller and more well defined than without the background. This effect is illustrated in Figure 4.4.6. The top portion of the figure shows the hypothetical spatial distribution of luminances across the CRT spot. (It is assumed here that the current density of the CRT beam producing the spot has a Gaussian distribution.) The horizontal dimension of a dot-matrix element is formed as the beam scans along the raster line and is modulated in the Z axis. Because the distribution of luminance across the spot is Gaussian (resulting from Gaussian current density across the beam), the perceived width of the element will be a function of the visual threshold. Under the dark background viewing conditions in the

current experiment, this threshold can be expected to be approximately 0.5 percent of the maximum luminance of the character (derived from Teichner and Krebs, 1972, for a threshold luminance of a 2 minute-of-arc target.) For a Gaussian spot, the subtended angle of the diameter of the perceived spot on the helmet-mounted display would equal approximately 7 minutes-of-arc. (This size is not to be confused with the element separation distance wherein the contrast modulation of the adjacent elements and element spaces falls below threshold.) Similarly, for the raster background condition, the luminance of the background was fixed at 0.7 cd/m^2 or approximately 5 percent of the maximum character luminance of 15.3 cd/m^2. Under these conditions, the perceived diameter of the CRT spot would equal about 5.6 minutes-of-arc or a decrease of about 20 percent from the dark background spot size. Therefore, under the raster background condition, the elements forming the characters should appear to have boundaries against the background and along the scan line which are better defined (i.e., smaller size and sharp edges) than during the dark background condition (i.e., $d'' < d'$ in Figure 4.4.6). Although the raster background characters should have a more distinct appearance, this factor above probably had little effect on the legibility of the very small characters because the overlapping of the luminances of adjacent elements and spaces would have not been affected by the raster background. This aspect is also illustrated in Figure 4.4.6 (e) and (f). Furthermore, the raster background probably had a slight degrading effect for the vertical dimension. When the luminances of adjacent scan lines overlapped by one or two spaces, the luminances of the background raster located in the element spaces contributed to the build up of luminances between the elements, thereby reducing the contrast modulation of the element to element space. However, the magnitude of this contrast loss was probably no greater than about 5 percent of the normal contrast loss due to the overlapping of element luminances. (This value is based

upon the ratio of the background luminance to the maximum luminance of the elements.)

3. A third factor which may have caused the background luminance to affect reading performance was that the raster background also served as an adapting field for the right eye (i.e., the eye viewing the helmet-mounted display). This eye became more light-adapted than under the dark background condition. A possible effect of this adaptation may have been to moderate a "stopping down" of the entrance pupil of the eye (Overington, 1976, page 10). Likewise, Campbell and Gubish (1966) along with other investigators have shown that the modulation transfer function of the optics of the human eye is a function of the pupil diameter. Likewise, there can be a large effect on the contrast sensitivity function of the eye (e.g., Campbell and Green, 1965a). Using the findings of the investigators above, an adapting field provided by the raster background could decrease the modulation threshold by a factor of 10 percent for the spatial frequencies equivalent to subtended angles of about 2 to 4 minutes-of-arc per cycle.

4. Another aspect of the pupil diameter is that the larger pupil diameter under the dark background conditions is likely to provoke blurring of the image due to the spherical aberrations of the eye (Graham, 1965). These aberrations would not be present under the higher luminance background conditions.

   Similarly, the raster background may have obscured optical aberrations in the helmet-mounted display optics and other spurious phosphor blooming and haloing phenomena which were perceived in the dark background condition.

5. In order for the helmet-mounted display image to be focused on the retina of the eye, the eye must be accommodated to optical infinity (i.e., the depth of focus of the eye should

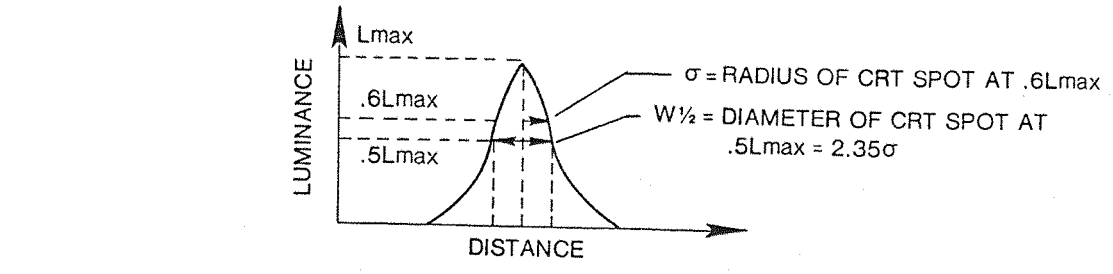

A) LUMINANCE DISTRIBUTION — TYPICAL CRT SPOT.

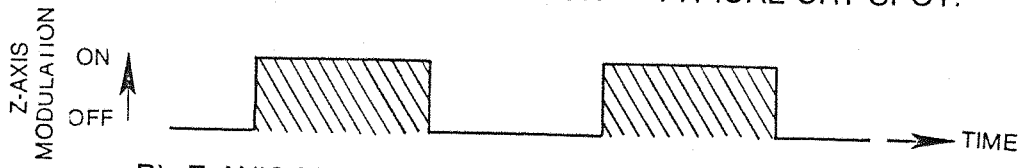

B) Z-AXIS MODULATION OF CRT BEAM TO PRODUCE TWO HORIZONTAL CHARACTER ELEMENTS.

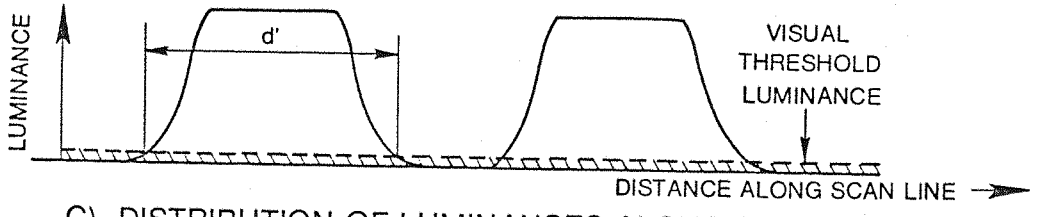

C) DISTRIBUTION OF LUMINANCES ALONG SCAN LINE DUE TO Z-AXIS MODULATION ABOVE, d' = PERCEIVED ELEMENT WIDTH.

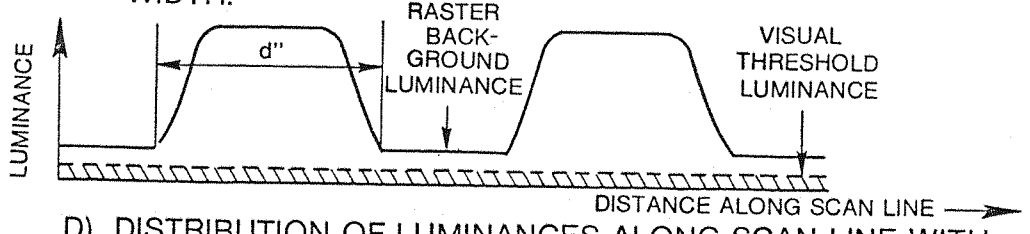

D) DISTRIBUTION OF LUMINANCES ALONG SCAN LINE WITH RASTER BACKGROUND, d'' PERCEIVED ELEMENT WIDTH.

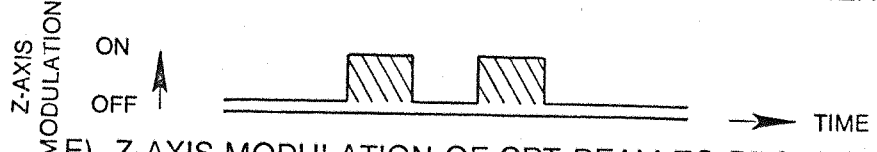

E) Z-AXIS MODULATION OF CRT BEAM TO PRODUCE TWO HORIZONTAL CHARACTER ELEMENTS OF REDUCED SIZE.

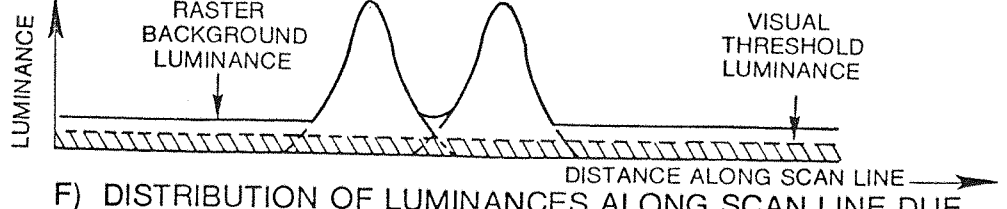

F) DISTRIBUTION OF LUMINANCES ALONG SCAN LINE DUE TO Z-AXIS MODULATION ABOVE.

Figure 4.4.6. Viewing Conditions of Character Elements Along CRT Scan Line

allow a collimated image to be focused on the retina). Several subjects complained that under the dark background viewing condition, the characters often appeared to go out of focus. As discussed in Section 2.3.2.7, Campbell and Westheimer (1959) have found that the lens accommodation reflex of the eye is mediated by chromatic and spherical aberrations of the eye. They noted that several subjects had difficulty focusing on visual targets which were monochromatic. Those subjects who were successful under the monochromatic viewing situation were then unsuccessful when spherical aberrations were removed. Based upon a spatial frequency channel model for the human visual system (e.g., Ginsburg, 1978), it can be postulated that the accommodation reflex may be based upon a spatial frequency maximization process within the retinal-cortical visual system. In this process, channels associated with high spatial frequencies (i.e., greater than 20 cycles/degree) may constantly monitor the high frequency spatial content of the image impressed on the retina and through a feedback loop to the muscles of accommodation, maintain an optimum focus of the image on the retina. This mechanism would depend, of course, on having high spatial frequencies present in the display image initially.

Since the helmet-mounted display scene was almost monochromatic, an accommodative response mediated by chromatic aberrations in the eye would have been disabled from focusing the display image on the retina. Also, the structure of the visual field under the dark background condition was devoid of high spatial frequencies because of the blurring or perceived spread of the CRT spot. (It also will be recalled that the display scene was the only viewing object within the visual field since objects outside the display were occluded from view.) This factor may have reduced the spatial frequency content of the scene necessary to maintain accommodation. In contrast to the dark background condition, the raster background produced sharp boundaries

between the character and background (as discussed above) and thereby contained higher spatial frequencies than the dark background. Also the total raster structure present in the visual field may have promoted better focusing of the display image on the retina. (It may be recalled that there were no complaints of image defocusing during the raster background conditions.) It is surmised, therefore, that improper focusing of the display image on the retina may have caused some loss in reading performance. Similarly, Campbell and Green (1965a) found large effects of even slight image defocus on the contrast sensitivity to various spatial frequencies. For example, they found that a defocusing of the image on the retina by only one diopter can cause a loss in contrast sensitivity by a factor of 4 for a spatial frequency of 2.72 minutes-of-arc/cycle.

In summary, the presence of the raster background in the display scene may have affected both the image performance of the helmet-mounted display and the optical quality attributes of the eye. Probably a combination of the factors, working together, contributed to the total effects of the background luminance on reading performance under static conditions. This aspect of the display presentation will be addressed in more depth in Experiment LG.4.

4.4.4.2 Effect of Character Size (Vibration Conditions)

In the previous section, it was shown that both character size and background luminance affected the legibility of characters under static conditons. Figures 4.4.7 and 4.4.8 show the mean reading errors for the 4.0 Hz and 16.0 Hz vibration conditions with the static errors of Figure 4.4.4 subtracted. These figures show that both character size and background luminance also affected reading performance during whole-body vibration. The difficulty of the reading task under static conditions seemed to have a multiplying effect on errors produced during whole-body vibration.

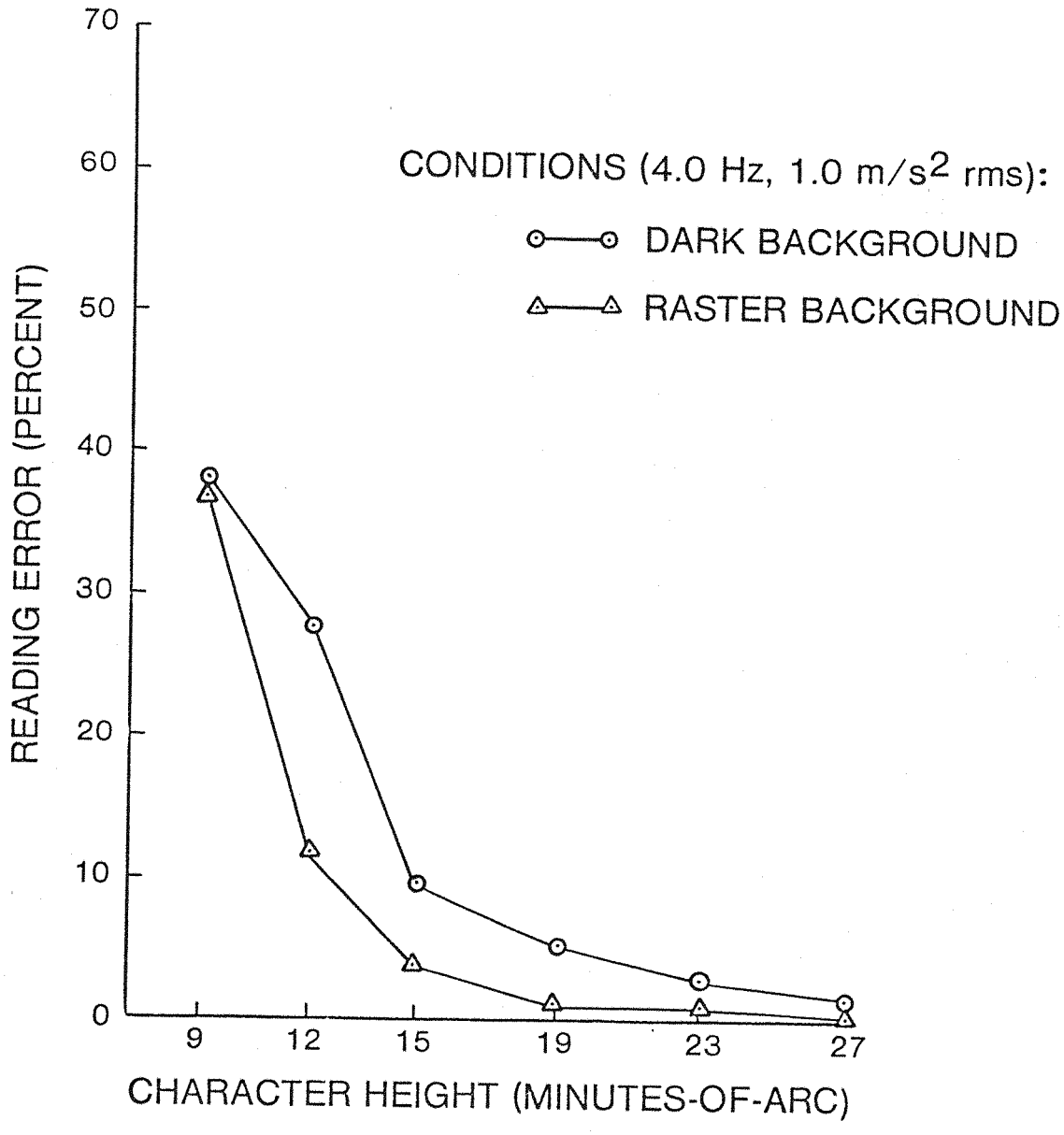

Figure 4.4.7. Comparison of Mean Percentage Reading Errors due to 4.0 Hz (1.0 m/s^2 rms) Vibration (with Static Errors Removed) for Dark and Raster Backgrounds (Experiment LG.3)

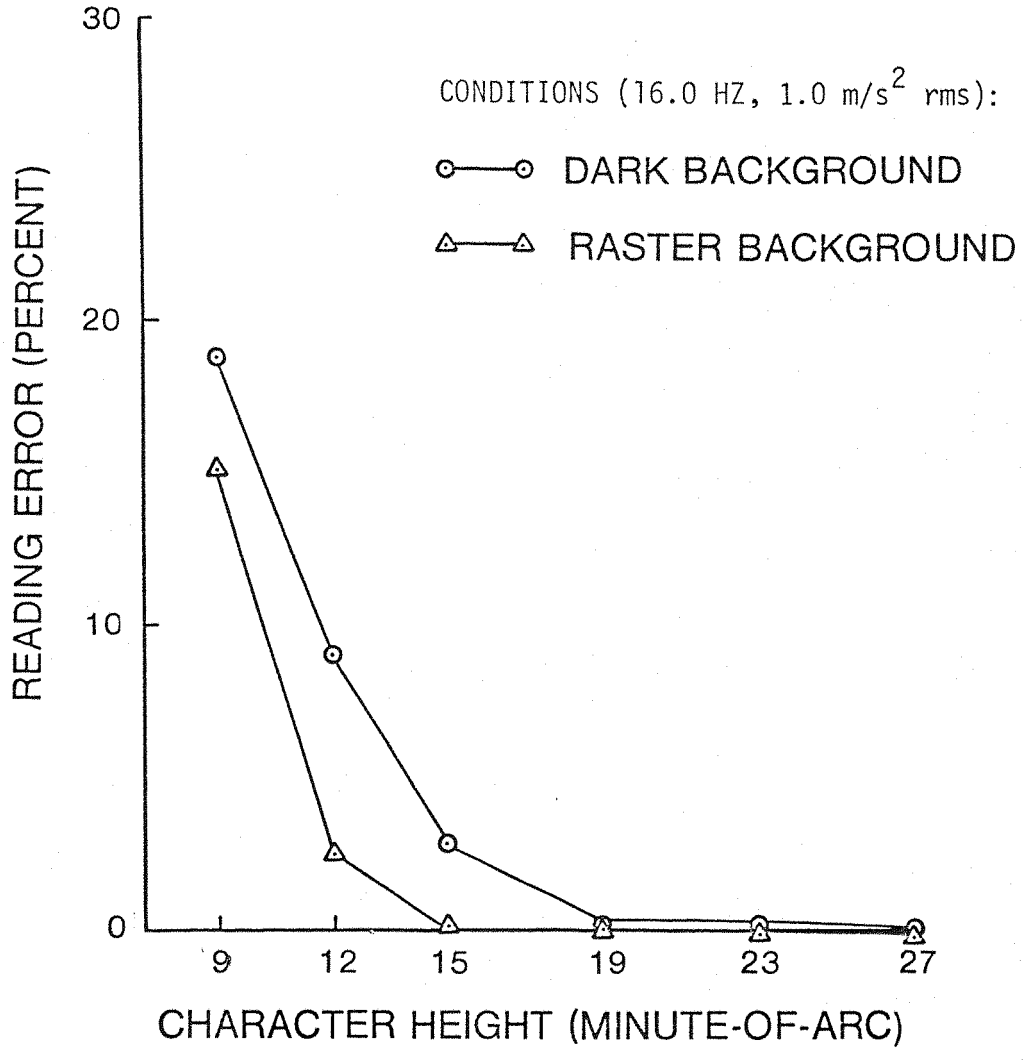

Figure 4.4.8. Comparison of Mean Percentage Reading Errors due to 16.0 Hz (1.0 m/s^2 rms) Vibration (with Static Errors Removed) for Dark and Raster Backgrounds (Experiment LG.3)

The effect of character size on reading performance during whole-body vibration can be understood if it is assumed that the vertical movement of the body induced rotational motions of the head and, in turn, sinusoidal movements of the display image on the retina. Such a situation would cause nodal images of the reading material to be formed at or near the zero velocity points of the image movement across the retina. O'Hanlon and Griffin (1971) have shown that the visibility of a vibrating "Landolt C" character can be associated with the period of time the distinguishing feature of the character (i.e.,

the gap) remains over a small area of receptors on the retina. A finite amount of time is required for the receptors to integrate the light quanta to produce the sensation of the character feature (i.e., contrast modulation). For a fixed area in the field of receptors, this time is a function of the frequency and amplitude of the vibration.

It follows that this time also will be a function of the area that the distinguishing feature impresses upon the retina. Indeed, O'Hanlon and Griffin found that increases in the size of the "Landolt C" by as little as 25 percent decreased by 30 to 50 percent the number of errors in detecting the correct position of the gap. In the case of the helmet-mounted display presentation, this problem was exacerbated by the decreased contrast modulation due to the overlapping of the dot matrix elements for the smaller character sizes. For example, Figure 4.4.9 shows how the contrast modulation of adjacent vertical scan lines is affected by the spacing between the scan lines. The combined effect of reducing the area of distinguishing features on the receptor field and the decreased modulation of the dot matrix elements would cause a greatly increased sensitivity to movement of the display image on the retina, independent of static errors.

Inspection of the curves in Figures 4.4.7 and 4.4.8 for the two background luminance conditions indicates that the raster background condition caused a consistently lower reading error across most character sizes under both vibration frequencies. This result can be ascribed to the higher image quality engendered by the raster background (as discussed in the previous section). Accordingly, nodal images of the raster background characters also exhibited higher contrast modulations over the distinguishing features of the character. It should be noted, however, that the positive effect of the raster background on reading performance diminished as the character size approached 9 minutes-of-arc.

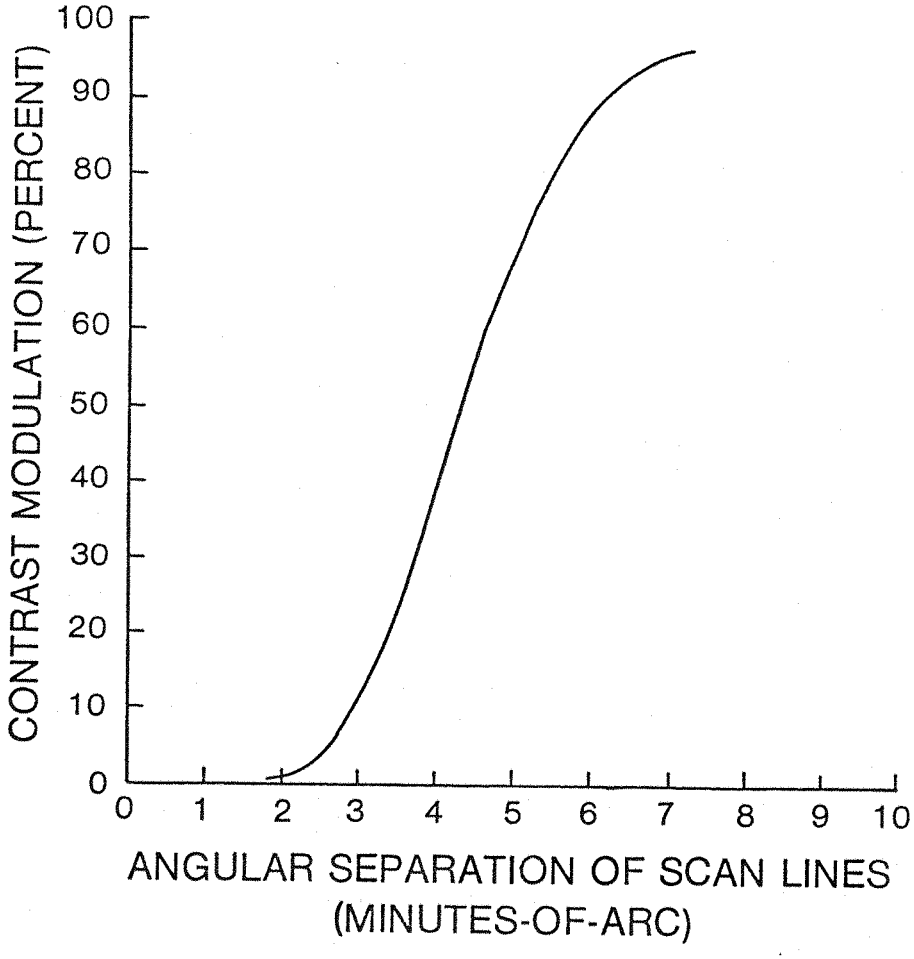

Figure 4.4.9. Theoretical Effect of Vertical Angular Separation of Scan Lines on Contrast Modulation for a CRT Spot Size of σ = 12μm

4.4.4.3 Effect of Character Size and Vibration Frequency

Comparison of Figures 4.4.7 and 4.4.8 indicates that the mean number of reading errors at 16 Hz (with static errors removed) was less than one-half of those at 4.0 Hz for all character sizes and both background luminances. A decrease in reading errors at the 16.0 Hz frequency (1.0 m/s^2 rms) relative to the 4.0 Hz frequency (1.0 m/s^2 rms) was anticipated, based upon the results of Experiments LG.1 and LG.2. Table 4.4.7 compares the mean number of reading error for selected conditions across the three experiments. In each experiment, there was a consistent difference in reading errors between 4.0 Hz and 16.0 Hz. In Experiment LG.2, the ratio of 4.0 Hz to 16.0 Hz errors

was as great as 4.58 to 1 (line format). (It may be recalled that in the current experiment, the 4.0 Hz vibration frequency was selected because it represented the "worst case" based upon the previous experiments.) From the findings reported in the literature (Section 2.5.5.3), it is likely that the characteristics of the transmissibility of seat vibration to head, eyes, and helmet-mounted display and the bandwidth of the vestibulo-ocular reflex were the primary factors causing the differences in reading performance between the 4.0 Hz and 16.0 Hz vibration frequencies.

TABLE 4.4.7. COMPARISON OF MEAN NUMBER OF READING ERRORS IN EXPERIMENTS LG.1, LG.2, AND LG.3

Experiment:	LG.1	LG.2	LG.2	LG.3	LG.3
Character Size: (minutes-of-arc)	13	15	15	12	15
Character Format:	array	array	line	line	line
Character Background:	dark	dark	dark	dark	dark
No. of Subjects:	10	6	6	10	10
Mean No. of Reading Errors					
Static	1.55	1.00	0.75	2.10	0.40
4.0 Hz ($1.0\ m/s^2$ rms)	28.10	9.00	10.67	16.00	5.10
16.0 Hz ($1.0\ m/s^2$ rms)	6.40	2.83	2.33	6.60	1.80

4.4.4.4 Comparison with Laycock (1978)

Figure 4.4.10 compares the mean reading errors from Experiment LG.3 (dark background condition only) with the results of Laycock (1978). Substantially fewer reading errors were produced in Experiment LG.3 than in Laycock's experiment for equivalent subtended visual angles of the characters. These differences in reading performance may be ascribed to the experimental methods by which the results were obtained. Table 4.4.8 summarizes the conditions for the two experiments. The two factors in Laycock's experiment which may have had the

greatest bearing on producing greater reading errors were the image quality of the characters and the nature of the vibration input to the subject.

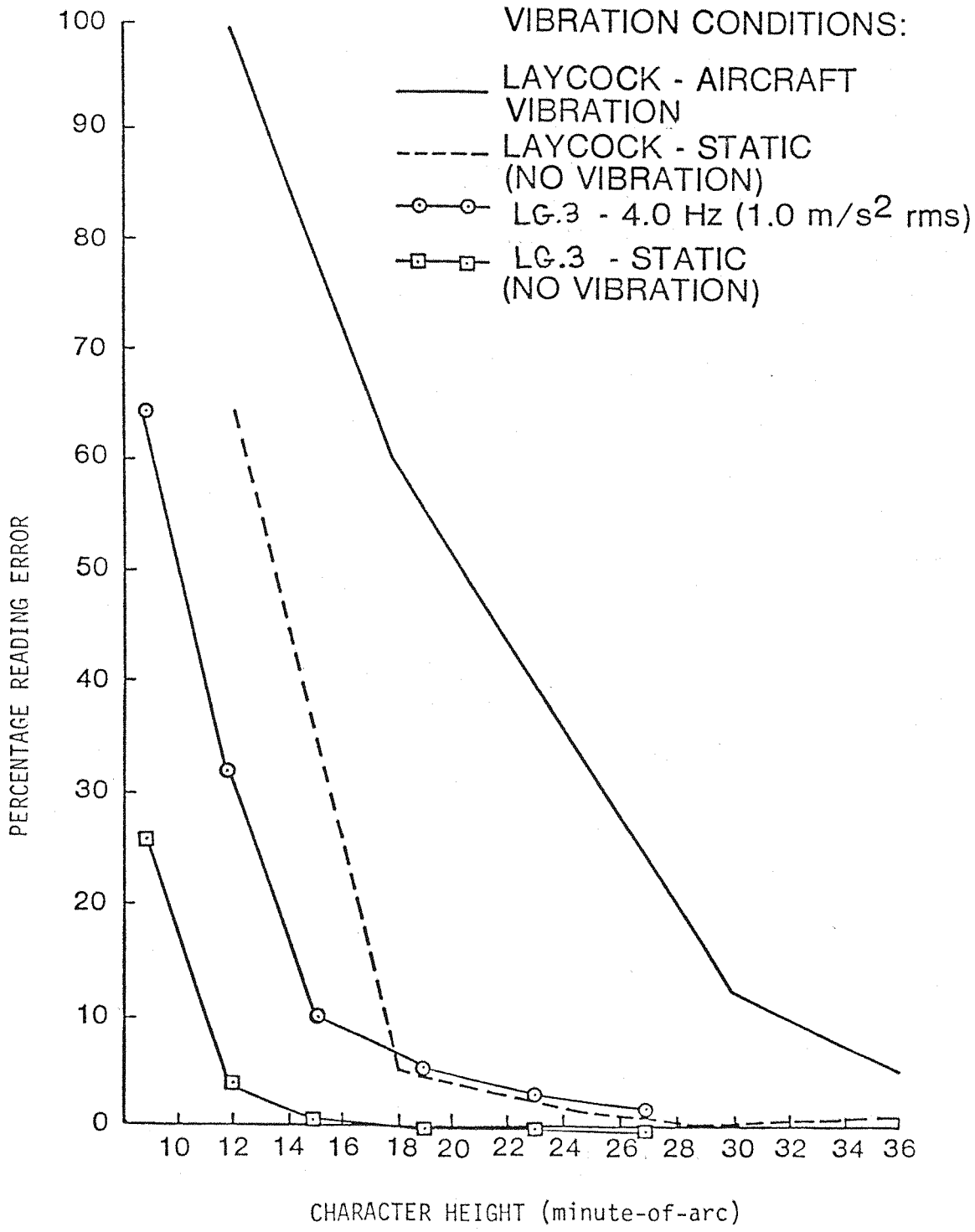

Figure 4.4.10. Comparison of Mean Percentage Reading Errors Between Experiments LG.3 and the Results of Laycock (1978)

TABLE 4.4.8. COMPARISON OF CHARACTER SIZE EXPERIMENTS

	Laycock (1978)	Experiment LG.3
Characters	numerals (0-9)	numerals (0-9)
Font	5 x 7 LED matrix	5 x 7 dot matrix
Method Generated	Video tape replay of TV camera aimed at LED characters	On-line computer terminal
How Presented (per run)	100 presentations of sets of 3 numbers	5 lines of 10 numbers presented line at a time
Character Size (subtended visual angles)	12, 18, 24, 30, 36 (minutes-of-arc)	9, 12, 15, 19, 23, 27 (minutes-of-arc)
Resolution	4, 6, 8, 10, 12 TV lines, respectively	7 TV lines-constant for all character sizes
Ambient Illumination	"room dimmed"	black background
Subjects	4	10
Vibration Used	2 axes (Z and Y axes) Vibration time history from Canberra Aircraft	Vertical Z axis sinusoidal 4.0 Hz/16.0 Hz

First, the materials used to generate the characters were different. Laycock generated the visual material on the helmet-mounted display by replaying video tape recordings of characters of different sizes. The characters were originally recorded by viewing a row of three light emitting diode characters with a television camera using a variable focal length lens. The focal length of the lens was adjusted to provide characters of various sizes on the television screen. Since the size of the scanning raster in the television camera and helmet-mounted display was not changed, then the characters were presented with different resolutions as well as subtended visual angles (i.e., the number of scan lines varied with the character height). In Laycock's experiment, each scan line subtended a visual angle of 3 minutes-of-arc regardless of the character height. Since the original visual material was generated by a television camera and then recorded, the quality of the characters was affected by the combined

modulation transfer functions of the television camera and video tape recorder. It is likely that the resulting image quality was less than the direct computer terminal video source used in the present experiment. Image quality between the two experiments can be compared under static conditions at character sizes of about 18 to 19 minutes-of-arc. Under these conditions, Laycock experienced a reading error rate of about 5 percent whereas reading error rate for Experiment LG.1 was almost zero. The substantial increase in Laycock's error rate at character heights less than 18 minutes-of-arc was probably due to the insufficient resolution of the scan lines which formed the distinguishing features of the characters. This factor did not occur in Experiment LG.3 until character sizes were less than 12 minutes-of-arc. In this regard, it is interesting to note that shifting the static error curve for Experiment LG.3 to the right by approximately 6 minutes-of-arc causes these data to coincide with Laycock's. This factor may reflect the differences in the image quality of the characters.

The aircraft vibration input used by Laycock also may have been a reason for the large differences in reading performance. The vibration input was not sinusoidal and was presented in the Z axis and Y axis. According to the power spectral densities of the vibration input, the vibration acceleration at a 4.0 Hz frequency in the vertical Z axis was approximately 0.45 m/s^2 rms and at 16.0 Hz was approximately 0.045 m/s^2 rms. Although these vibration acceleration levels were not as great as those used in Experiment LG.3, more reading errors were produced. In Laycock's experiment the subtended visual angle producing a given error rate was approximately twice the subtended angle as in Experiment LG.3. Indeed, Laycock observed a substantial onset of error at subtended angles less than 30 minutes-of-arc!

In spite of these large differences of reading error between Laycock's experiment and Experiment LG.3, there is a remarkable similarity in the relationships of the mean reading errors under vibration to those under no vibration. For example, for a character size of 14 minutes-of-arc, Laycock found a mean reading error rate under vibration (i.e.,

60 percent) which was 12 times the static error (i.e., 5 percent). Similarly, in the present experiment at 15 minutes-of-arc, the mean reading error under 4.0 Hz vibration and dark background (i.e., 10 percent) was approximately 12 times the static error (i.e., 0.8 percent). This aspect of the two experiments indicates that image quality is an important factor is determining reading performance under vibration. In comparing these two experiments, differences in image quality seems to have had more effect on performance than differences in the nature of the vibration.

4.4.5 Summary

The main findings of this experiment have been to show that in addition to the factors of vibration frequency and level, the characteristics of the display image also have a large effect on the reading performance of the helmet-mounted display during whole-body vibration. Reading accuracy was directly related to the visual angle subtended by the numeric characters. Under static conditions, reading performance was related to the theoretical limiting resolution relationships between the subject's visual capabilities and the imaging quality of the display. Under dynamic conditions, reading errors increased in proportion to the errors under static conditions. Reading errors at 4.0 Hz (1.0 m/s^2 rms) were consistently greater than those at 16.0 Hz. The presentation of a raster background with the characters significantly improved reading accuracy during both static and dynamic conditions. This effect was attributed to the improved optical characteristics of the eye and better image quality of the display due to the raster field. The reading accuracy results of the experiment were shown to differ in magnitude but remain similar in form to those of Laycock (1978). The performance differences of these experiments were ascribed mainly to image quality.

It is clear from the present experiment that the deleterious effects of whole-body vibration on the reading performance of the helmet-mounted display which was observed in Experiments LG.1 and LG.2 can be reduced by manipulating display factors such as character size and background luminance. Even under the "worst case" condition of the present experiment (i.e., 4.0 Hz vibration and dark background), the

32 percent reading rate observed with 9 minutes-of-arc characters could be reduced to about zero by increasing character size to 15 minutes-of-arc and adding a 0.7 cd/m^2 background raster luminance. Further treatment of these aspects of helmet-mounted display operation will be deferred to Section 4.5.4 after the nature of the background luminance and character subtended angle are investigated in Experiment LG.4.

4.5 EXPERIMENT LG.4: EFFECT OF BACKGROUND LUMINANCE AND CONTRAST ON READING PERFORMANCE

4.5.1 Introduction to Experiment

In Experiment LG.3, both character size and background luminance had a significant effect on helmet-mounted display legibility. A background luminance of only 0.7 cd/m^2 significantly reduced reading errors relative to a dark display background during both static and vibration conditions. Since only two background luminance conditions were used, the results of Experiment LG.3 cannot be generalized to changes in background luminance over a wide range. Because the scanning raster provided the background luminance in Experiment LG.3, the question arises as to whether the differences in observed performance were caused by changes in the perceptual characteristics of the subjects or artifacts in the helmet-mounted display. Furthermore, is there an optimum background luminance and/or contrast upon which the characters should be viewed to minimize the effects of whole-body vibration?

The literature suggests that two mechanisms may be involved when background luminance is manipulated over a wide range. Since the eyes tend to adapt to the average luminance of the visual field (Section 2.3.2.3), very low background luminance levels would cause the photochemical gain of the retina to increase, reducing the time constant for light integration. This behaviour of the retina would increase the susceptibility of the subject to perceive blur when an image moved across the retina; therefore, in the case of the HMD, characters presented on a completely dark background may be more susceptible to blur because of the resulting adaptation state of the

eye. Likewise, a nominal background luminance on the helmet-mounted display may serve as an adapting field to lower the photochemical gain and thereby reduce the likelihood of image blur should an image move on the retina. In this way, increasing background luminance may reduce the effects of whole-body vibration. Conversely, if the luminance of the character generated on the CRT is maintained at a constant level, increasing the background luminance (from an external source) would also reduce the character to background contrast. At some point, the contrast would reach a level wherein the characters would be difficult to see and reading accuracy would decrease. The interaction and combination of these two mechanisms would most likely produce a "U shaped" (nonmonotonic) curve for error rate as a function of background luminance. The purpose of Experiment LG.4 was to test this hypothesis and to determine the levels of background luminance and character size wherein the effects of vibration on character legibility were minimized. A secondary purpose of the experiment was to measure differences in reading performance due to background luminances provided by the raster versus external light sources.

4.5.2 Method

4.5.2.1 Visual Material

The paced random number reading task described in Section 4.1 was used in this experiment. Each visual presentation consisted of a line of five numbers presented in ten successive lines for a total presentation per run of fifty numeric characters (e.g., Figure 4.1.2). In the main experiment, three character sizes were presented at six background luminance levels and under static and whole-body vibration conditions.

4.5.2.2 Character Size/Format

The visual angles subtended by the three character heights were 9, 15, and 23 minutes-of-arc which corresponded to three of the character sizes used in Experiment LG.3. The visual angle separating adjacent horizontal characters in the line was 3.6 times the visual angle of

the character height or 32.4, 54.0, and 82.8 minutes-of-arc, respectively. Because subjects experienced some difficulty in seeing the characters under certain background luminance conditions, special crosswires/reticle symbol was placed above the line of five numbers as shown in Figure 4.5.1. The width of the horizontal line was equal to the width of the line of 5 numbers. The vertical line in the crosswires was located above the center number in the line as shown in the figure. The relative dimension of the visual presentations are shown in Figure 4.5.1 in terms of the subtended visual angle as a function of the subtended angle of the character height. The size of the characters was set by adjusting the gain of the horizontal and vertical deflection amplifiers in the helmet-mounted display electronics unit (Appendix 4.3).

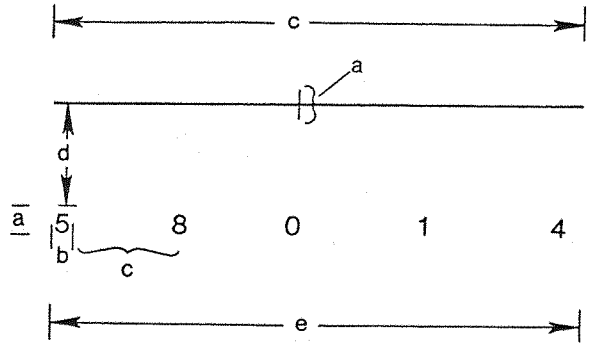

a = CHARACTER HEIGHT (9 MOA, 15 MOA, 23 MOA)
b = CHARACTER WIDTH = 5/7 x a
c = HORIZONTAL SEPARATE DISTANCE = 3.6 x a
d = HEIGHT OF HORIZONTAL CROSS WIRES ABOVE CHARACTERS = 12a
e = WIDTH OF LINE = 18 x a

Figure 4.5.1. Configuration and Relative Dimensions of the Visual Presentation Consisting of Characters and Crosswires (Experiment LG.4)

4.5.2.3 Character Luminance

Because the beam current in the CRT remained constant, independent of the deflection gain, the luminance of the characters varied somewhat with the different character sizes. The second column in Table 4.5.1

shows the luminance of the characters for each character size. The luminance of the crosswires was set at a level 20 percent greater than that of each character size.

TABLE 4.5.1. LUMINANCE OF CHARACTERS AND BACKGROUNDS AND CHARACTER TO BACKGROUND CONTRASTS FOR EXPERIMENT LG.4

Character Height (minutes-of-arc)	Character Luminance (cd/m^2)	Contrast (percent)					
		Background Luminance (cd/m^2)					
		48.0	19.2	1.9	0.9	0.2	0.0
9	48.3	50	72	96	98	99	100
15	19.2	29	50	91	96	99	100
23	12.7	21	40	87	94	98	100

4.5.2.4 Background Luminance

The luminance of the display field on which the characters were presented was varied using the apparatus shown in Figure 4.5.2. A translucent PERPLEX® screen was illuminated from the rear by a 500 watt slide projector. The distance of the projector to the screen was adjusted to give a uniform area source of light with dimensions of 0.5 m by 0.5 m and with a luminance of 343 cd/m^2 from the observer side of the screen. The distribution of luminance within the illuminated area did not vary more than 5 percent. The subject was located approximately 150 mm from the screen with the right eye centered within the illuminated area making the subtended visual angle of the rear illuminated position of the screen equal to 118 degrees (i.e., ±59 degrees in the vertical axis and horizontal axis from an axis from the right eye perpendicular to the rear projection screen). An eye patch was placed over the left eye of the subjects to exclude any light from entering the left eye. The luminance of the background visual field was set by adjusting the variable density filter attached in front of the combiner of the helmet-mounted unit. The six background luminances used in the experiment are shown in Table 4.5.1. The completely dark (~0.0 cd/m^2) background condition was achieved by

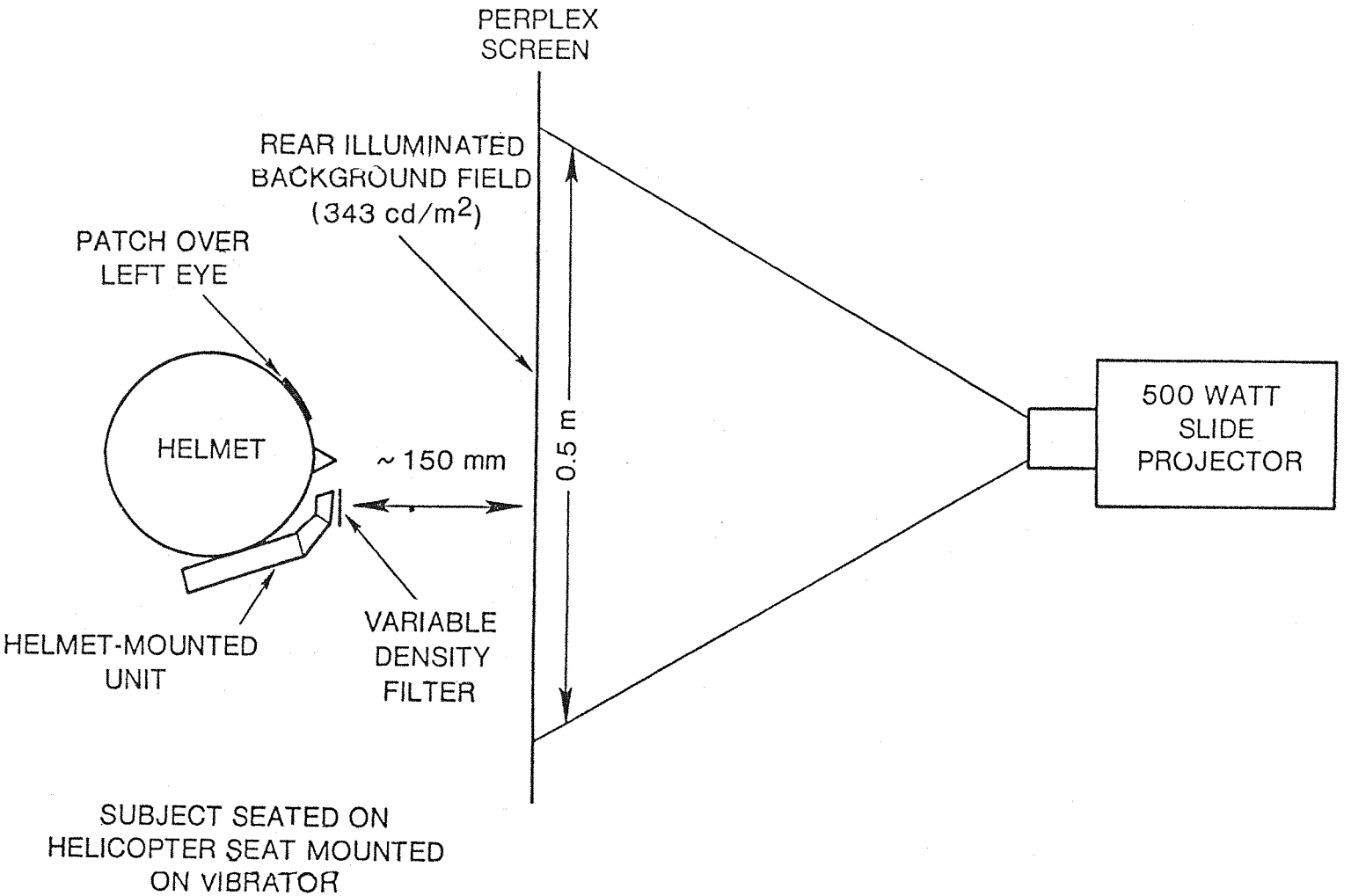

Figure 4.5.2. Plan View of Apparatus to Generate Background Luminance in Experiment LG.4

switching off the projector and placing an opaque visor over the helmet-mounted display to exclude external light from entering the display over the right eye of the subject.

The luminance levels for this experiment were selected following a short pilot study wherein 4 subjects were given similar random number reading tasks. The maximum luminance level selected was that level which tended to produce a 50 percent or greater reading error rate. The other levels were selected to span the range from the dark background (used in Experiments LG.1, LG.2, and LG.3) and the bright background above. The background luminance levels shown in Table 4.5.1 were calculated from the luminance of the background screen and the transmittances of the optical combiner and variable density filter determined previously by the author. The character luminance levels shown in Table 4.5.1 were measured directly using the methods described in Appendix A.4.2.

4.5.2.5 Contrast

The contrast of the characters on the helmet-mounted display varied as a function of both the luminance of the character and the luminance of the background visual field. Since the characters were presented as virtual images "superimposed" on the background visual field via the optical combiner in the helmet-mounted unit, the luminance of the character was the sum of the luminance generated on the CRT and transmitted through the optics and the luminance transmitted through the variable density filter and combiner from the external source of light on the rear projection screen. The values for the luminance contrast of the characters to the background was calculated using the relationship below (McCormick, 1976):

$$\text{Luminance Contrast} = \frac{L_1 - L_2}{L_1} \times 100 \text{ percent}$$

where

L_1 = total luminance of the character
L_2 = total luminance of the background

In this case, the brighter areas were the characters and the darker areas were the visual level in which the characters are presented; therefore,

L_1 = character luminance (L_C) + background luminace (L_B)

and L_2 = background luminance (L_B)

Substituting in the equation above, luminance contrast can now be expressed in terms of the character and background luminances:

$$\text{Luminance Contrast} = \frac{L_C}{L_C + L_B}$$

Using this equation and levels for the character and background luminances, the luminance contrasts were computed and shown in Table 4.5.1 for the various character and display background luminance conditions. These data are also plotted in Figure 4.5.3.

4.5.2.6 Vibration

During each combination of display background luminance and character size, subjects were presented with a static (no vibration) and a vertical Z axis sinusoidal vibration condition. The vibration frequency was 4.0 Hz and level 1.0 m/s^2 rms in order to duplicate the "worst case" vibration conditions observed in Experiments LG.1 and LG.2.

4.5.2.7 Subjects and Procedure

Ten subjects were used in the experiment (S1, S3, S4, S5, S7, S8, S11, S12, S13, and S14). The physical characteristics of the subjects are given in Table 3.4.1. The subjects were divided into two groups of five subjects. To one group of subjects, the characters were presented with increasing background luminance levels and to the other a decreasing order of background luminances. The order of presentation of the character size and vibration conditions was randomized within each group. At least 5 minutes was allowed between each background luminance condition to allow the subject's eyes to adapt to the new

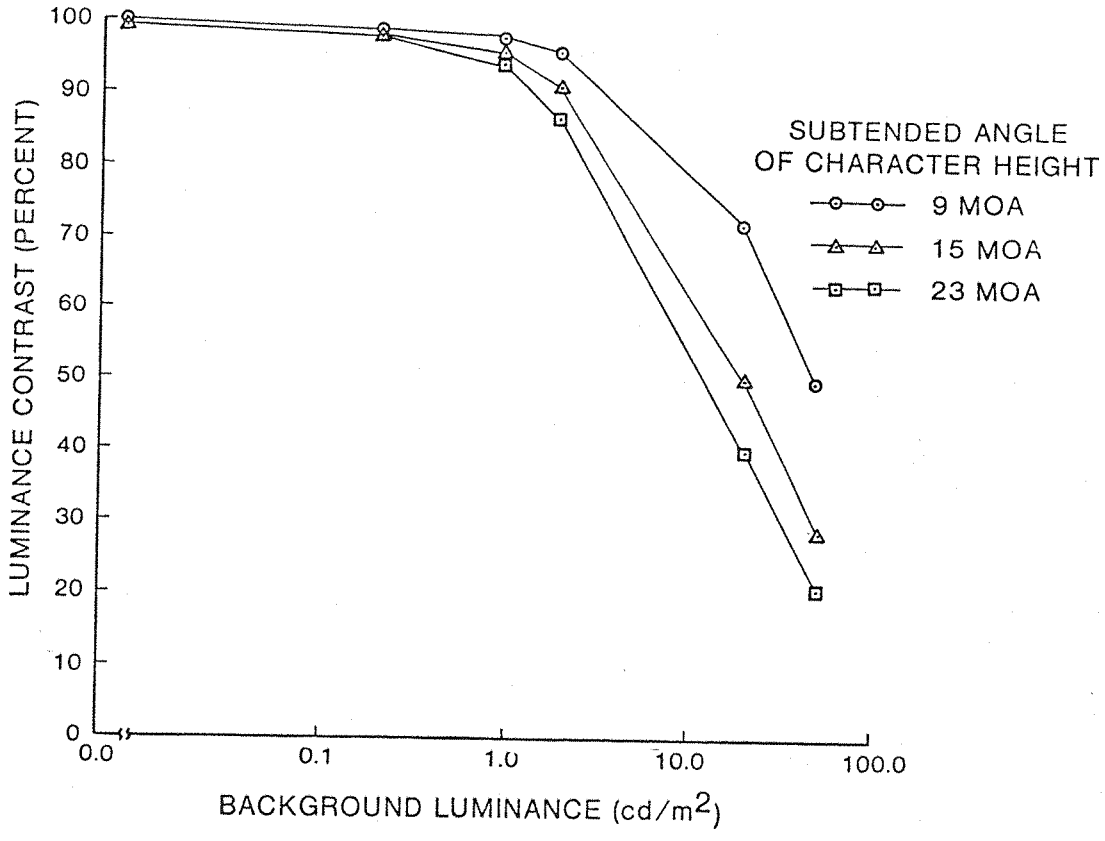

Figure 4.5.3. Effect of Display Background Luminance and Character Size on Character to Background Luminance Contrast Presented on the Helmet-Mounted Display

background luminance level (Section 2.3.2.3). The subjects were given verbal instructions by the experimenter similar to the written instructions in Experiment LG.3. In addition, subjects were instructed to use the crosswires as a visual cue to locate the numbers written on the visual field, should the characters become difficult to see during some display conditions.

4.5.2.8 Raster Background Ancillary Experiment

In addition to the main experiment, display conditions using a raster background condition similar to Experiment LG.3 were presented to the subjects. The purpose of this ancillary experiment was to provide

data for comparing the white neutral density character backgrounds manipulated with the variable density filter described above, with the adjustment of the green background luminance from the display raster. The three character sizes (i.e., 9, 15, and 23 minutes-of-arc) were presented with the luminances, background luminances, and contrasts as shown in Table 4.5.2. The raster background display conditions were also presented under static and the 4.0 Hz (1.0 m/s^2 rms) vertical Z axis vibration conditions. The ancillary experiment was administered to one-half of the subjects before the main experiment and to the other half after the main experiment. The time at which the ancillary experiment was administered was made independent of the assignment of the subjects to groups for the main experiment. The order of presentation of the character size and vibration conditions was randomized across the subjects. A summary of the conditions in the main and ancillary experiments is given in Table 4.5.3.

TABLE 4.5.2. BACKGROUND LUMINANCES AND CHARACTER-TO-BACKGROUND CONTRASTS FOR THE RASTER BACKGROUND CONDITION (EXPERIMENT LG.4)

Character Size (minutes-of-arc)	Character Luminance (cd/m^2)	Raster Background Luminance (cd/m^2)	Contrast (percent)
9	42.8	1.1	98
15	15.3	0.5	97
23	10.1	0.3	97

TABLE 4.5.3. EXPERIMENT LG.4: EFFECT OF BACKGROUND LUMINANCE AND CONTRAST ON READING PERFORMANCE

Purpose:	To determine the effects of background luminance and character-to-background contrast on the perception of the helmet-mounted display under whole-body vibration conditions.
Method:	Measure reading accuracy of characters of three sizes viewed against a range of background luminances.
Subjects:	10S (S1, S3, S4, S5, S7, S8, S11, S12, S13, S14)
Visual Material:	6* background luminances (0-48 cd/m^2) 3** character sizes (9, 15, 23 minutes-of-arc) 2 orders of presentation (ascending/descending luminances)
Vibration Conditions:	1 static condition 1 vibration condition (4.0 Hz at 1.0 m/s^2 rms) helicopter seat (modified)

*plus one raster background luminance condition

**character luminances vary with size (Table 4.5.1)

4.5.3 Results

4.5.3.1 Measures of Central Tendency

The mean and standard deviation of the number of reading errors as a function of the character size and background luminance for the vibration and static conditions are given in Table 4.5.4. The data shown are pooled scores across the two sets of subjects wherein the order of presentation was also a variable. The mean scores are plotted for the static and vibration conditons in Figures 4.5.4 and 4.5.5, respectively. The mean error scores were greater for the vibration than for the static conditions for all display presentations. Generally, error rates were greatest when the background luminance was maximum. Also,

during vibration, the minimum error rates tended to occur at background luminances in the middle of the luminance range (e.g., 18.9 mean errors at 9 minutes-of-arc character height and 1.9 cd/m^2 luminance level, 2.7 mean errors at 15 minutes-of-arc and 0.2 cd/m^2, and 0.7 mean error at 23 minutes-of-arc and 0.2 cd/m^2). Also shown in Table 4.5.4 and Figures 4.5.4 and 4.5.5 are the data for the raster background luminance condition. These data show good agreement with the external background luminance conditions for those values of background luminance interpolated from the experimental data.

4.5.3.2 Analysis of Variance

A split plot factorial repeated measures design was used to perform an analysis of variance on the number of reading errors. The subjects were randomized blocks. The analysis following the computational procedures given by Kirk (1968) for a SPR 2.236 design where the order of presentation of the background luminance levels (i.e., ascending or descending) was the between block treatment (two levels), and the three within block treatments were vibration condition (two levels, i.e., static and vibration), character size (three levels), and background luminance (six levels). The ancillary experiment using a raster background was not considered in this analysis. The analysis of variance summarized in Table 4.5.5 indicates that the order of presentation did not have any consistent effect on the reading errors, nor were any interactions of this factor and other treatments statistically significant. The main effects of all three within block treatments (i.e., vibration condition, character size, and background luminance) were highly significant ($p<.001$). Interactions of these factors individually and together were also statistically significant.

TABLE 4.5.4. MEAN AND STANDARD DEVIATION OF READING ERRORS AS A FUNCTION OF BACKGROUND LUMINANCE, CHARACTER SIZE, AND VIBRATION CONDITIONS IN EXPERIMENT LG.4

Vibration Condition	Character Size (minutes-of-arc)	Mean (Standard Deviation)* of Reading Errors**						
		Background Luminance (cd/m^2)						
		48.0	19.2	1.9	0.8	0.2	0.0	Raster
Static	9	10.1	7.8	4.8	6.0	4.3	9.0	4.2
	C_1	(10.5)	(8.7)	(6.1)	(6.6)	(4.9)	(5.9)	(3.1)
	15	4.8	5.0	0.4	0.1	0.1	0.1	0.2
	C_2	(8.6)	(12.4)	(0.8)	(0.3)	(0.3)	(0.3)	(0.4)
	23	15.6	4.6	0.1	0.1	0.0	0.0	0.0
B_1	C_3	(18.2)	(9.5)	(0.3)	(0.3)	(0.0)	(0.0)	(0.0)
Vibration	9	30.9	25.1	18.9	21.4	22.9	29.9	22.1
4.0 Hz	C_1	(11.1)	(10.3)	(11.9)	(11.1)	(10.8)	(8.2)	(11.5)
(1.0 m/s^2 rms)	15	25.4	11.6	4.4	2.9	2.7	5.7	4.2
	C_2	(13.9)	(11.5)	(6.7)	(4.0)	(3.6)	(6.9)	(5.3)
	23	39.7	11.6	1.2	1.1	0.7	2.1	0.8
B_2	C_3	(7.9)	(14.0)	(2.0)	(1.9)	(1.0)	(3.4)	(1.6)
		d_1	d_2	d_3	d_4	d_5	d_6	

*numbers in brackets are standard deviations

**out of a presentation of 50 numbers

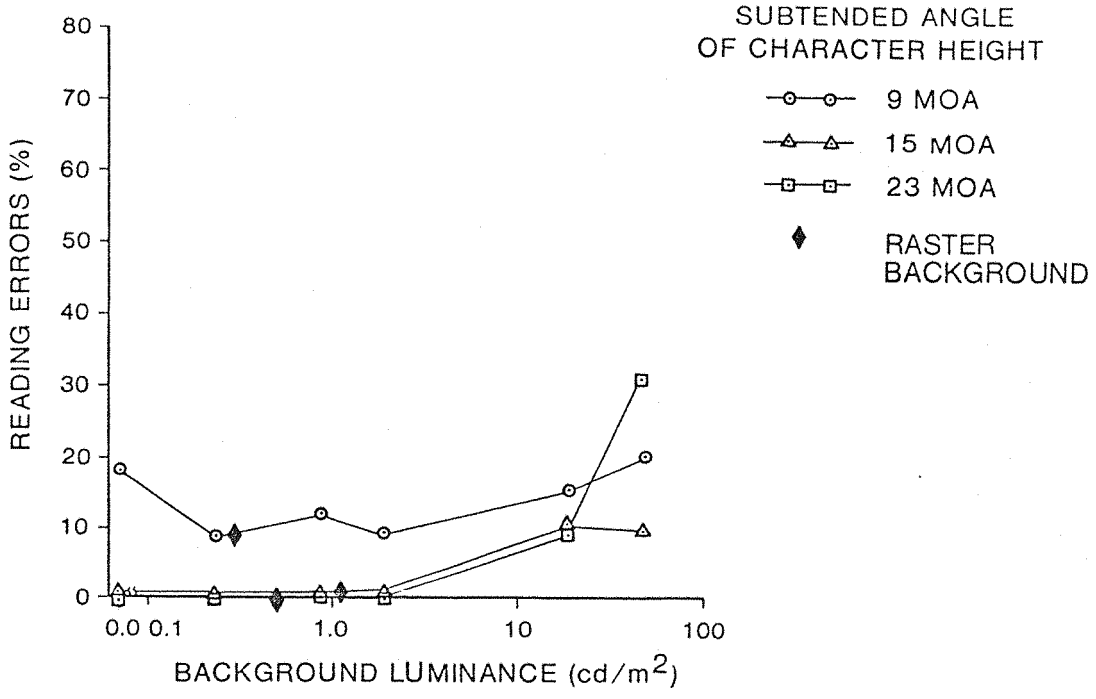

Figure 4.5.4. Effect of Display Background Luminance and Character Size on HMD Reading Background Under Static Conditions

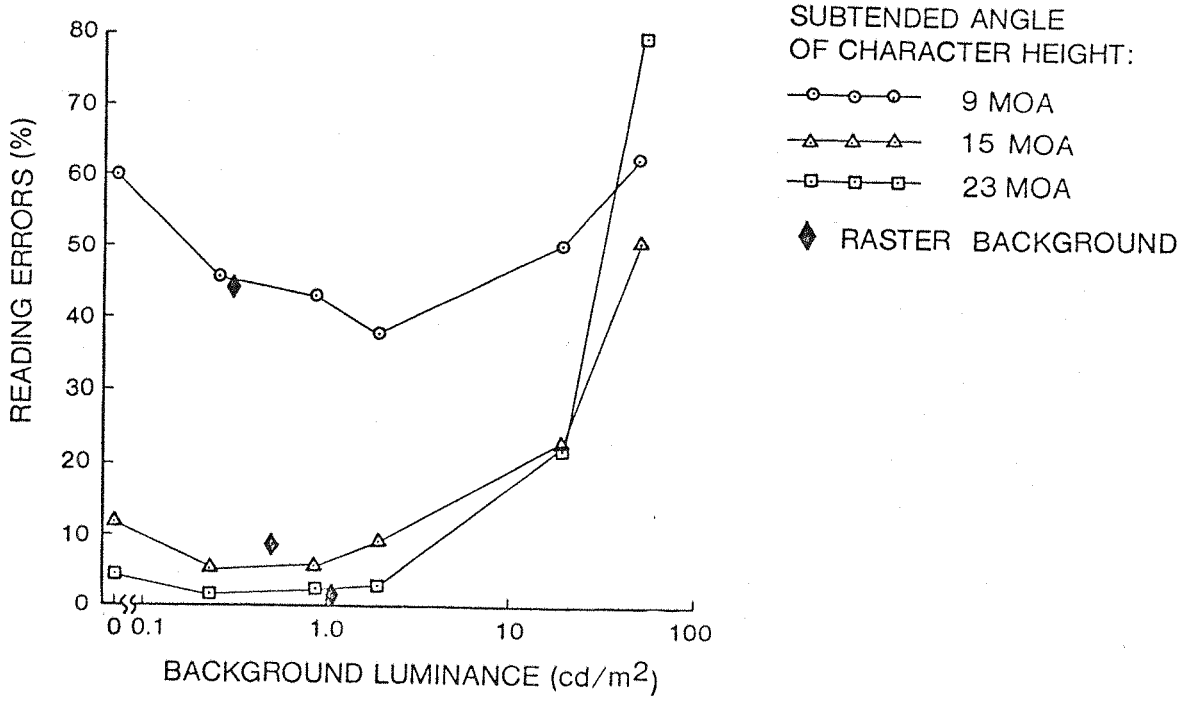

Figure 4.5.5. Effect of Display Background Luminance and Character Size on HMD Reading Performance Under Vertical Z Axis Whole Body Vibration (4.0 Hz at 1.0 m/s^2)

TABLE 4.5.5. ANALYSIS OF VARIANCE SUMMARY TABLE FOR READING ERRORS IN EXPERIMENT LG.4

Treatments:
S = Subjects
A = Order of Presentation
B = Vibration Condition
C = Character Size
D = Background Luminance

Source	SS	DF	MS	F Ratio	p
S	6971.37	9	774.60		
A	97.14	1	97.14	0.11	ns
A × S	6874.23	8	859.28		
Within S	54085.63	350	154.53		
B	9537.80	1	9537.80	55.38	<.001
C	8224.41	2	4112.21	38.55	<.001
D	11778.13	5	2355.63	18.87	<.001
A × B	1.74	1	1.74	0.01	ns
A × C	23.57	2	11.79	0.11	ns
A × D	344.83	5	68.97	0.55	ns
B × C	2584.91	2	1292.46	69.41	<.001
B × D	2685.37	5(1)*	537.07	14.20	<(.01)
C × D	4138.41	10(1)*	413.84	12.13	<(.01)
A × B × C	65.33	2	32.67	2.92	ns
A × B × D	106.39	5	21.28	0.56	ns
A × C × D	225.61	10	22.56	0.66	ns
B × C × D	869.27	10	86.93	7.78	<.001
A × B × C × D	77.29	10	7.73	0.69	ns
B × S	1377.81	8	172.23		
C × S	1706.90	16	106.68		
D × S	4993.50	40	124.84		
B × C × S	297.99	16	18.62		
B × D × S	1512.73	40(8)*	37.82		
C × D × S	2729.77	80(8)*	34.12		
B × C × D × S	893.87	80	11.17		
Total	61057.00	359	170.08		

*denotes modified number of degrees of freedom (Geisser-Greenhouse Conservative F-test)

It should be noted that the split plot analysis of variance above required the pooling of the sums of squares of the subjects within groups error terms for the two between block groups of subjects. In order for the F ratio shown to follow an F distribution, the sources of variation in the two error terms must be homogenous. Again, following the procedure described by Kirk (1968), the subject's within groups sums of squares were tested for homogenity by means of the F_{max} test. These tests showed that, with two exceptions, the variances estimated by the mean squares of the subjects within groups and three interactions were homogeneous for the two groups. The exceptions were for the B x D x S and C x D x S interactions wherein the differences in the error terms were significant ($p<.05$). F ratio comparisons using these two error terms (i.e., B x D and C x D) were made using the Geisser-Greenhouse conservative F test (Kirk, 1968, page 262) wherein the degrees of freedom were modified as shown in Table 4.5.5.

4.5.3.3 Analysis of Simple Interaction Effects

Because the interactions of the main effects of vibration condition, character size, and background luminance were significant, a further analysis was conducted of the effects of size and background luminance on the sums of squares for the vibration condition. This analysis was applied to answer the question: "under which combination of character size and background luminance conditions did vibration significantly effect performance?" In order to maintain an overall level of significance of $p<.05$ for this family of tests, the individual simple interaction effect ratios were tested at $\frac{p}{18}<.0034$ (where 18 was the number of tests). A summary of this analysis, shown in Table 4.5.6, indicates that for the 9 minutes-of-arc character size, vibration had a significant effect on reading performance regardless of the background luminance level ($p<.001$). When the character size was increased to 15 minutes-of-arc, the significant effect of vibration was confined to the three highest background luminances (and three lowest contrast levels) and the lowest background luminance. For the 23 minutes-of-arc character size, vibration had a significant effect on reading performance only at the two highest background luminance conditions. The analysis of variance and simple interaction effects support the

reliability of the mean data in Figures 4.5.4 and 4.5.5. The "U-shaped" nature of the curves show the tendency for the reading performance to be affected least by vibration when background luminances were between the extremes of dark and light values.

TABLE 4.5.6. ANALYSIS OF VARIANCE FOR SIMPLE EFFECTS OF VIBRATION (B) AT COMBINATIONS OF CHARACTER SIZE (C) AND BACKGROUND LUMINANCE (D) (EXPERIMENT LG.4)

Source*	SS	DF	MS	F Ratio	p**
Between B at cd_{11}	10547.70	1		373.63	<.001
cd_{12}	6892.05	1		244.14	<.001
cd_{13}	3970.65	1		140.65	<.001
cd_{14}	4925.90	1		174.49	<.001
cd_{15}	5415.40	1		191.83	<.001
cd_{16}	9730.65	1		344.69	<.001
cd_{21}	6666.90	1		236.16	<.001
cd_{22}	1587.30	1		56.23	<.001
cd_{23}	192.80	1		6.83	<.05
cd_{24}	82.70	1		2.93	ns
cd_{25}	71.60	1		2.54	ns
cd_{26}	322.10	1		11.41	<.01
cd_{31}	18166.85	1		643.53	<.001
cd_{32}	1549.10	1		54.87	<.001
cd_{33}	13.85	1		0.49	ns
cd_{34}	11.60	1		0.16	ns
cd_{35}	4.55	1		0.16	ns
cd_{36}	43.05	1		1.52	ns
Pooled error term	4082.40	144	28.23		

*For designation of levels of character size (C) and background luminance (D), see Table 4.5.4

**Levels of significance shown for family of tests; individual tests performed at p/18 [i.e., p<.001 (p<.000056), p<.01 (p<.00056), p<.05 (p<.0034)]

4.5.3.4 Trend Analysis

Because the main effects of character size, background luminance, and their interactions were determined to be statistically significant, some trends were present in the data. Tests using orthagonal contrasts were conducted to determine the linear, quadratic, cubic, etc. components of the trends in these main effects and their interactions. The results of the tests on the main effects are shown in Table 4.5.7. Both the linear and quadratic trend components for character size and background luminance were statistically significant. These same trend components were also found in the analysis of trends for the character size x background luminance (C x D) interaction shown in Table 4.5.8.

Since the C x D interaction was found to be statistically significant in the original analysis of variance, the profiles (i.e., curves of mean data) for the character size treatment (C) at the six levels of background luminance (D) are not parallel and, conversely, the profiles for D at three levels of C are not parallel. Indeed, the analysis of trend components in the C x D interaction indicated that 71.9 percent of the C x D interaction sums of squares was due to the linear (C) x linear (D) interaction of the two factors. In addition, a linear (C) x quadratic (D) interaction component contributed 11.3 percent of the total sums of squares for the C x D interactions. (The power of the tests of trend components has been increased by computing the F ratio using mean squares for error terms which have also been partitioned across the interaction trends.)

4.5.3.5 Model Fitting

Because the background luminance treatment exhibited a highly significant quadratic trend component, an equation of the form

$$E = a_0 + a_1 \log L_B + a_2 (\log L_B)^2$$

TABLE 4.5.7. SUMMARY OF ANALYSIS OF TRENDS IN READING ERROR FOR LEVELS OF CHARACTER SIZE AND BACKGROUND LUMINANCE (EXPERIMENT LG.4)

Source	SS	df	MS	F Ratio	p*
Character Size (C)	8224.41	2	4112.21	38.547	<.001
linear trend	5443.54	1	5443.54	29.257	<.01
quadratic trend	2780.86	1	2780.86	101.841	<.001
Background Luminance (D)	11778.13	5	2355.63	18.869	<.001
linear trend	5992.93	1	5992.93	15.322	<.05
quadratic trend	5458.34	1	5458.34	51.060	<.001
cubic trend	239.12	1	239.12	5.693	ns
quartic trend	2.83	1	2.83	.045	ns
higher level trends	84.91	1	84.91	4.118	ns
C × D	4138.41	10	413.84	12.129	<.001
C × S	1706.90	16	106.68		
C × S (linear)	1488.466	8	186.058		
C × S (quadratic)	218.444	8	27.306		
D × S	4993.5	40	124.84		
D × S (linear)	3129.13	8	391.141		
D × S (quadratic)	855.211	8	106.901		
D × S (cubic)	336.051	8	42.006		
D × S (quartic)	508.167	8	63.521		
D × S (higher level)	164.941	8	20.618		
C × D × S	2729.77	80	34.12		

*Levels of significance shown for family of tests, individual trend tests performed at p/2 for character size and p/5 for background luminance.

TABLE 4.5.8. TESTS OF SIGNIFICANCE OF TREND COMPONENTS FOR CHARACTER SIZE (C) AND BACKGROUND LUMINANCE (D) INTERACTIONS (EXPERIMENT LG.4)

Source	SS	df	MS	F Ratio	p*
C × D Total	4138.41	10	413.841	12.128	<.001
C × D (lin × lin)	2976.703	1	2976.703	60.003	<.001
C × D (lin × quad)	465.774	1	465.774	21.993	<.05
C × D (lin × cubic)	409.457	1	409.457	8.171	ns
C × D (lin × quartic)	8.751	1	8.751	.142	ns
C × D (quad × lin)	.443	1	.443	.021	ns
C × D (quad × quad)	184.302	1	184.302	6.319	ns
C × D (quad × cubic)	52.117	1	52.117	2.279	ns
C × D (quad × quartic)	21.217	1	21.217	1.010	ns
C × D (lin/quad × higher)	19.646	2	19.646	.554	ns
C × D × S Total	2729.77	80	34.122		
C × D × S (lin × lin)	396.874	8	49.609		
C × D × S (lin × quad)	169.420	8	21.178		
C × D × S (lin × cubic)	400.876	8	50.110		
C × D × S (lin × quartic)	494.196	8	61.775		
C × D × S (quad × lin)	166.356	8	20.795		
C × D × S (quad × quad)	233.333	8	29.167		
C × D × S (quad × cubic)	182.951	8	22.869		
C × D × S (quad × quartic)	167.994	8	20.999		
C × D × S (lin/quad × higher)	567.77	16	35.486		

*Levels of significance shown in family of tests, individual tests for trends performed at p/9.

where

E = estimated number of mean reading errors and
$\log L_B$ = log luminance of background

was fitted using multiple regression procedures to the mean reading error data for the vibration condition. Table 4.5.9 gives the values of the constants a_0, a_1, and a_2 and the coefficient of correlation (r_0) between the model and the empirical data for the three character sizes. In all three size conditions, the coefficients were statistically significant. A comparison of the predicted value for reading error using the model versus the observed value is shown in Figure 4.5.6 for the 15 minutes-of-arc and 9 minutes-of-arc character sizes.

TABLE 4.5.9. MULTIPLE REGRESSION MODELS OF MEAN READING ERRORS (E) AS A FUNCTION OF LOG BACKGROUND LUMINANCE ($\log L_B$) (EXPERIMENT LG.4)

$$E = a_0 + a_1 \log L_B + a_2 (\log L_B)^2$$

Character Size	a_0	a_1	a_2	r_0
9	19.942	-1.913	4.886	.987**
15	2.299	3.391	5.284	.971**
21	-1.29	6.18	8.59	.938*

E = estimated number of mean reading errors
$\log L_B$ = log background luminance (log cd/m^2)

*$p<.01$ **$p<.001$

4.5.3.6 Types of Character Errors

A comprehensive analysis of the types of character errors was not performed for this experiment. A brief inspection of the individual subject reading errors revealed that the types of errors committed by

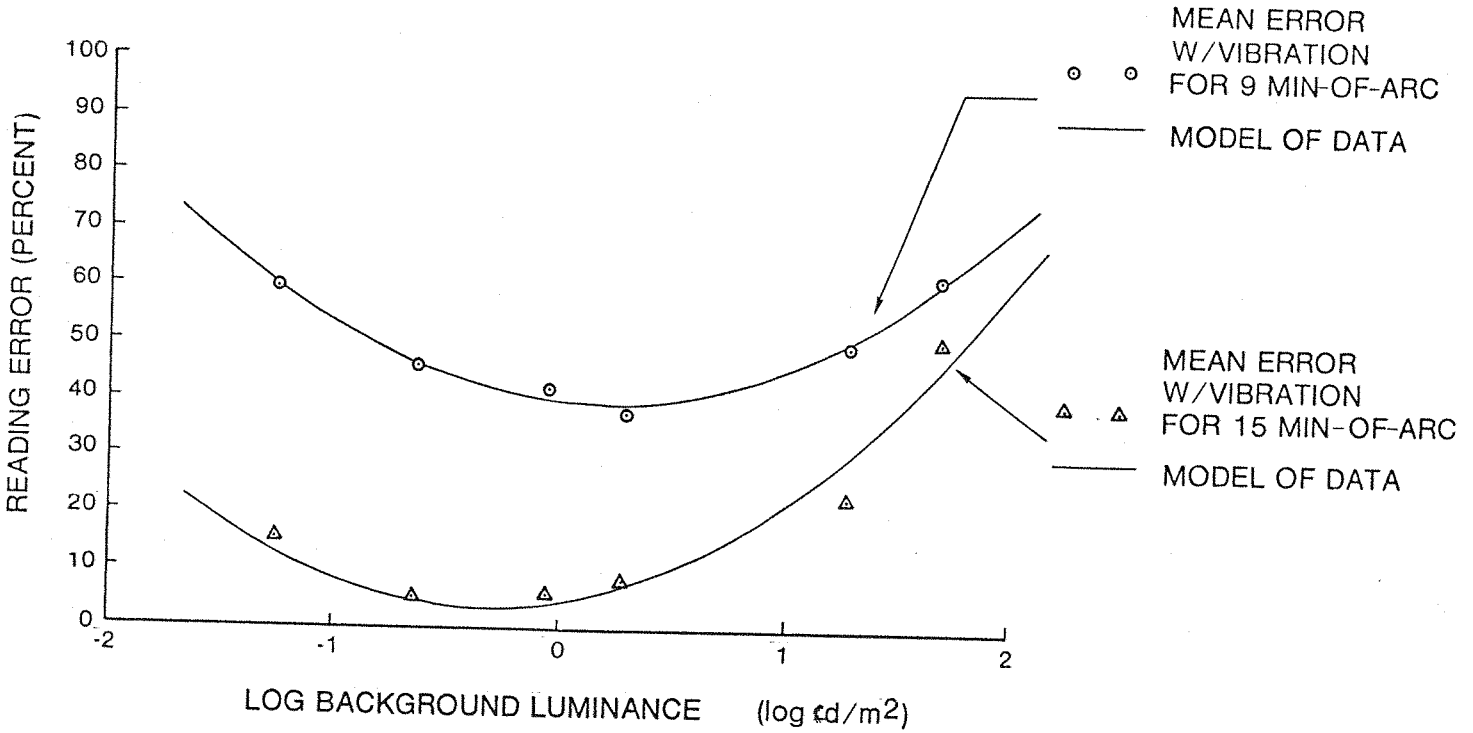

Figure 4.5.6. Comparison of Mean Reading Error (Percent) with Models of Data for 9 and 15 Minutes-of-Arc Character Sizes and Vibration at 4.0 Hz (1.0 m/s^2 rms)

subjects during the low to middle background luminance condition of the experiment were similar to each other and to the error observed in Experiments LG.1 and LG.3 during equivalent conditions. This comparison was not true for the high background luminance conditions wherein the types of errors tended to be more evenly distributed across all of the character types. This result implies that the subjects were guessing character identity rather than confusing a character with another. Clearly, the visual phenomena affecting performance at the two extremes of background luminance were different.

4.5.4 Discussion

4.5.4.1 Effect of Background Luminance

The shapes of the family of curves for the vibration conditions shown in Figure 4.5.5 support the hypothesis presented in the introduction (Section 4.5.1) that the behaviour of reading performance would most likely be a "U shaped" distribution of error as a function of background luminance. The significant quadratic trend component in background luminance (Table 4.5.7) and the significant coefficient of correlation for the quadratic model of the data provide additional proof of this hypothesis. The nature of subject reading performance can be illustrated by examination of Figure 4.5.7 where the reading errors using the 15 minutes-of-arc character size are compared for the static and vibration conditions. Here the nature of the effect of vibration, relative to the static condition, is different for the low, middle, and high levels of background luminance. Indeed, at the middle levels of background luminance, there was no statistically reliable difference between the vibration and static condition as shown by the analysis of simple interaction effects reported in Table 4.5.6. Even though the mean static error rate remained unchanged at the very low background luminance level condition, vibration did provide a significant increase in reading errors (again from Table 4.5.6). This increase in susceptibility to vibration at the low versus middle levels of background luminance can be attributed to the increased photochemical gain of the receptors in the retina due to the dark background serving as an adapting field. When the background

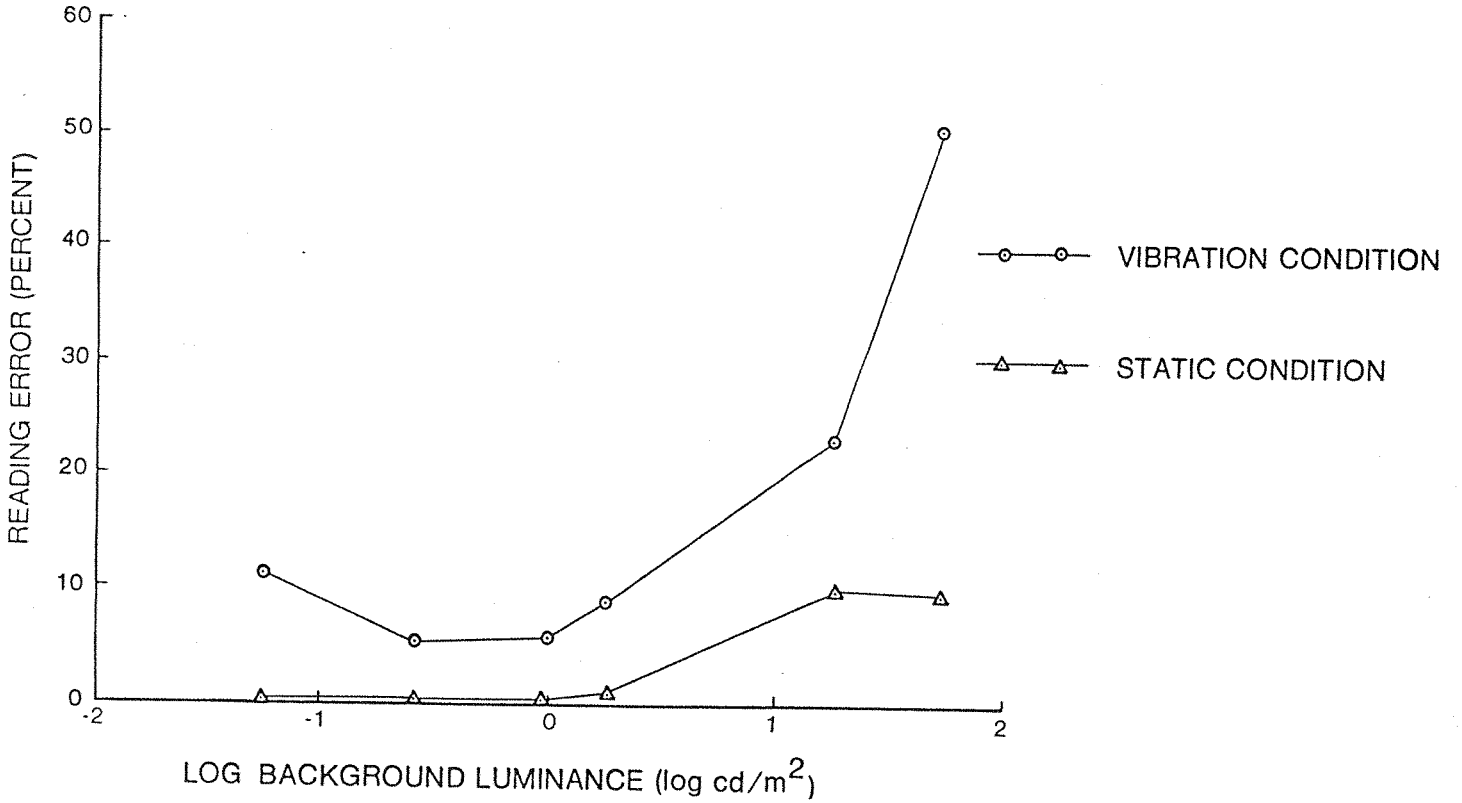

Figure 4.5.7. Comparison of Percent Reading Error as a Function of Background Luminance for a 15 Minutes-of-Arc Character Size Under Static and Vibration Conditions

luminance was increased to the highest levels, reading errors under static condition began to increase, probably due to the lower character to background contrasts produced by the external background. The display presentation of the characters became "washed out" as the contrast dropped to 50 percent and below. Subjects often indicated an extreme hardship in just "finding" the characters on the display under these conditions. And, as shown in Figures 4.5.5 and 4.5.6, whole-body vibration accentuated the difficulty of reading the characters against the high luminance background. The best reading performance was achieved, therefore, at a midpoint between the dark background extreme where the eye was very sensitive to small changes in the retinal image displacement (i.e., creating blur of the image and reducing contrast modulation of the elements forming the characters) and the bright background luminance extreme wherein the character to background contrast modulation also approached visual threshold.

4.5.4.2 Effect of Character Size

Varying the subtended angle of the characters also had a significant effect on reading performance. This result was anticipated based upon the findings of Experiment LG.3. The interaction of character size and background luminance was statistically significant (Table 4.5.5) and was shown to be largely due to a linear by linear trend component and to a lesser extent by a linear by quadratic trend component. The trend influences of character size on reading error can be seen in response surface for the mean data (for vibration) illustrated in Figure 4.5.8. As can be seen, the interaction of character size and background luminance was very weak at the lower background luminance levels, where the main effect of decreasing character size caused a uniform increase in reading errors (i.e., the lines are approximately parallel). The interaction effect at the higher luminance levels became more dramatic when the influence of character size on the number of reading errors changed into a nonmonotonic relationship, and there was a crossover in the errors produced by the largest character size. The interaction at the three highest background luminance levels probably accounted for most of the background luminance and

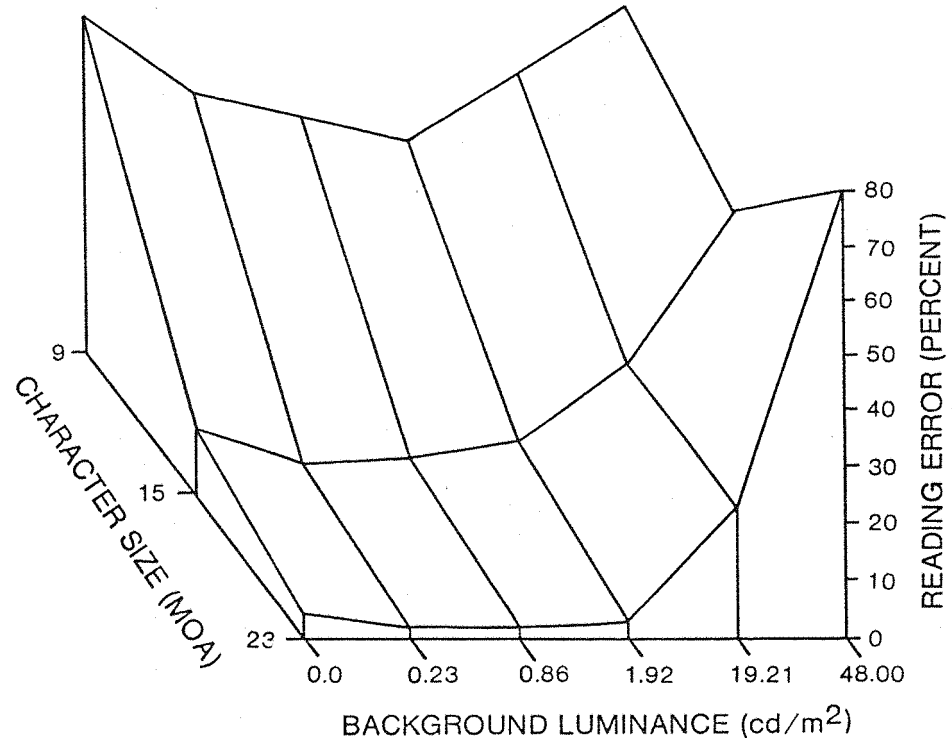

Figure 4.5.8. Mean Percentage Reading Error Surface Showing Interactions of Character Size and Background Luminance for the 4.0 Hz (1.0 m/s^2 rms) Vibration Condition (Experiment LG.4)

character size interaction sums of squares. The reason for the dramatic change in behaviour was due to the difference in character luminances for the three character sizes and the interaction of the character to background luminances in changing contrast.

Figure 4.5.9 shows the mean percentage reading error plotted as a function of character to background contrast for three character sizes. Here, the influence of contrast on reading performance can be seen. It is postulated that these curves would approach some limiting condition (as represented by the dotted line) if the character size continued to increase.

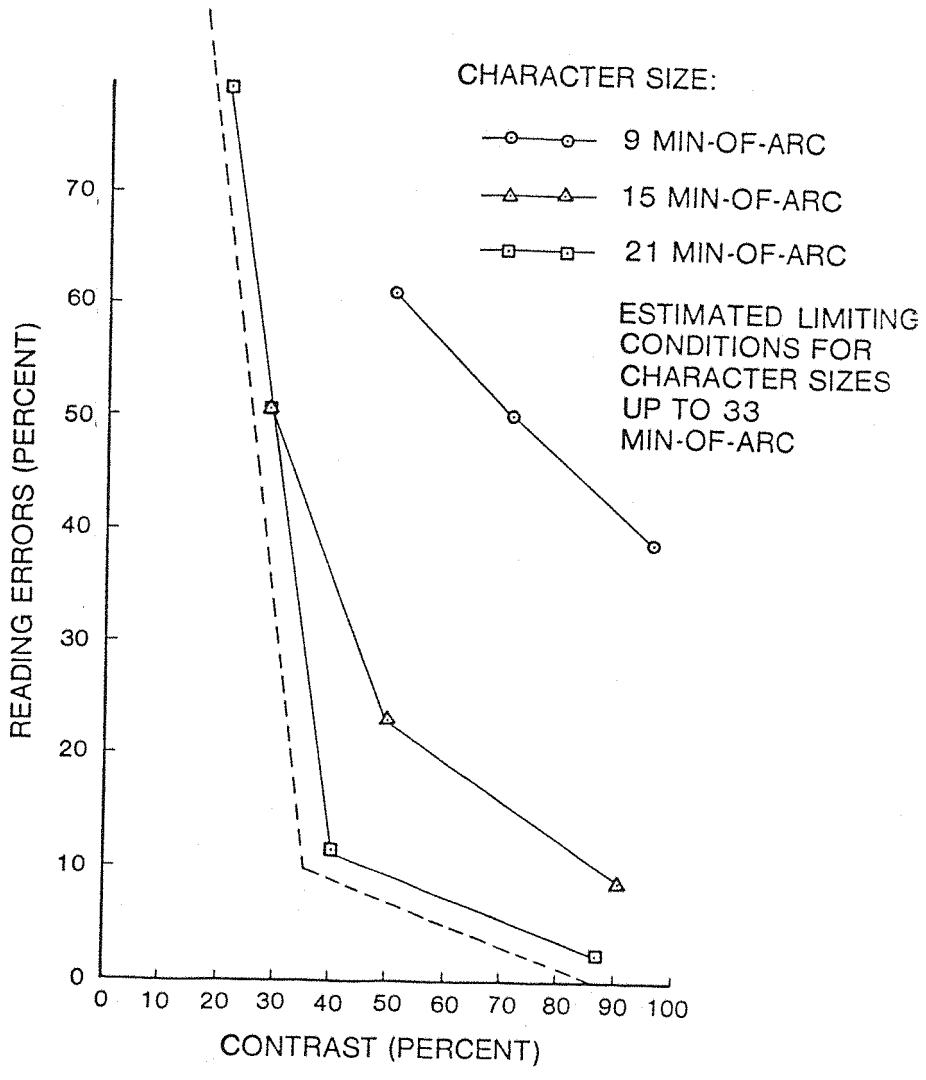

Figure 4.5.9. Relationship of Mean Reading Error to Character/ Background Contrast for Three Character Sizes Under Vibration Conditions

4.5.4.3 Models of Mean Data

The models for mean reading error in Table 4.5.9 and plotted in Figure 4.5.6 appear to be good predictors of mean reading error during the vibration condition. The influence of character size can be seen in the relative values of a_0, a_1, and a_2. The noninteraction influence of character size on mean error as a function of background luminance is contained in a_0, whereas the linear and quadratic interactions are exhibited by a_1 and a_2, respectively. The first

derivative of the model equation is useful for predicting, for each character size, the background luminance when mean reading error should be minimim (E_{min}):

$$\frac{dE}{d(\log L_B)} = a_1 + 2a_2 \log L_B$$

For the minimum error rate, the derivative is set equal to 0:

$$\frac{dE}{d(\log L_B)} = 0 = a_1 + 2a_2 \log L_B$$

and

$$\log L_B = -\frac{a_1}{2a_2} \text{ (for } E_{min})$$

Substituting the values for a_1 and a_2 in the equation above for the three character sizes, the predicted values for L_B causing minimum errors were obtained and are summarized in Table 4.5.10.

TABLE 4.5.10. PREDICTED BACKGROUND LUMINANCE TO PRODUCE MINIMUM MEAN READING ERROR AT THREE CHARACTER SIZES UNDER BACKGROUND CONDITIONS

Character Size (minutes-of-arc)	a_1	a_2	$-\frac{a_1}{2a_2}$	L_B at E_{min} (cd/m^2)
9	-1.913	4.886	.196	1.57
15	3.391	5.284	-.321	.48
23	6.18	8.59	-.359	.44

Again, the difference in the background luminance required to produce minimum reading errors can be attributed to the differences in the luminance of the characters. The "ideal" background luminances above correspond to equal character-to-background contrasts of approximately 96 percent. Had the character luminances contrasts remained equal to 42.8 cd/m^2 across the three character sizes, then the "ideal" background luminance probably would have been equal to approximately 1.5 cd/m^2.

4.5.4.4 External Versus Raster Backgrounds

Inspection of Figures 4.5.4 and 4.5.5 shows that there was good agreement between the mean errors produced by the raster background condition versus the equivalent external background luminance levels. A paired-t comparison test failed to show any reliable difference of mean reading errors between the raster and external background conditions. This finding connotes that the reading errors will be approximately equivalent if background luminances are adjusted either by intensity of the raster or transmitted light from external sources. The implication of this finding is that the background luminance mainly serves as an adapting field for the eye of the operator. With an ideal adjustment of this background, the modulation and luminance thresholds become optimum for viewing characters presented on the helmet-mounted display during static conditions as well as viewing the nodal images of these characters during whole-body vibration.

4.5.5 Summary

This experiment has shown that display factors, such as character size, contrast, and background luminance, can have a substantial influence on helmet-mounted display visibility during static and vibration conditions. Likewise, an adjustment of the character and background luminance and the subtended angle of the characters can substantially reduce the effects of vibration (i.e., at 4.0 Hz and 1.0 m/s^2 rms) on the reading of numeric characters. The findings of this experiment are in agreement with the hypothesis advanced at the beginning of the experiment (Section 4.5.1) that a nominal background luminance would provide an adapting field for the eyes. This adapting field, in turn, would minimize the degrading effects of a helmet-mounted display image vibrating relative to the retina of the eye. The implication of this finding is that not only can the helmet-mounted display be used as a medium for displaying information to the operator, but it can also be used as an adapting field to optimize the visual properties of the operator for viewing the display. The data from the experiment show that a background luminance of at least 0.5 to 1.5 cd/m^2 should be provided for the characters regardless of

the helmet-mounted display at 4.0 Hz and 16.0 Hz vibration frequencies. In most conditions, the reading errors were due to confusions between the "8" and "0" (LG.1, LG.3).

4. The reading performance of a small panel-mounted display was equivalent to the results of a previous study by Lewis (1977) using photographic reading material (LG.1).

5. There was no significant effect of a line versus an array format of numerical characters on helmet-mounted reading performance (LG.2).

6. Reading accuracy increased when the visual angle subtending the character also increased (LG.3).

7. Error rates versus character size was shown to be related to the limiting resolution of the display-observer interface (LG.3).

8. Characters presented against a raster background produced fewer reading errors than when presented against a dark background (LG.3, LG.4).

9. Character contrast and background luminance were shown to interact with character size in producing different reading errors (LG.4).

10. Optimum adjustment of character size, contrast, and background luminance was shown to decrease significantly the number of reading errors during static and vibration conditions (LG.3, LG.4).

11. Intersubject and intrasubject performance was shown to vary widely across experiments (LG.1, LG.2, LG.3, LG.4).

It is clear that there are many aspects of these results which can impact the design and operation of the helmet-mounted display. Further consideration of the implications of these results and those of the other experiments to follow will be addressed in Chapter 9.